

Note: The Errata/Addenda are
affixed to the end of the thesis.

FOAM GRANULATION

A thesis submitted in fulfilment of the requirement for
the degree of Doctor of Philosophy

by

Melvin X.L. Tan

Bachelor of Engineering (Hons.)

Department of Chemical Engineering

Monash University

Clayton Victoria 3800 Australia

November 2010

Copyright Notices

Notice 1

Under the Copyright Act 1968, this thesis must be used only under the normal conditions of scholarly fair dealing. In particular no results or conclusions should be extracted from it, nor should it be copied or closely paraphrased in whole or in part without the written consent of the author. Proper written acknowledgement should be made for any assistance obtained from this thesis.

Notice 2

I certify that I have made all reasonable efforts to secure copyright permissions for third-party content included in this thesis and have not knowingly added copyright content to my work without the owner's permission.

DECLARATION

**Monash University
Monash Research Graduate School**

Declaration for thesis based or partially based on conjointly published or unpublished work

In accordance with Monash University Doctorate Regulation 17 / Doctor of Philosophy regulations the following declarations are made:

I hereby declare that this thesis contains no material which has been accepted for the award of any other degree or diploma at any university or equivalent institution and that, to the best of my knowledge and belief, this thesis contains no material previously published or written by another person, except where due reference is made in the text of the thesis.

The core theme of the thesis is FOAM GRANULATION. The ideas, development and writing up of all the papers in the thesis were the principal responsibility of Melvin X.L. Tan, the candidate, working within the Department of Chemical Engineering under the supervision of Dr. Karen P. Hapgood.

The inclusion of co-authors reflects the fact that the work came from active collaboration between researchers and acknowledges input into team-based research.

Signed:



Date:

29/11/2010
.....

ACKNOWLEDGEMENTS

My humble thanks go to my *Lord Jesus Christ* for what he hath promised: “strength for the day, light for the way, rest for the labour, comfort for the tears, grace for the trials, help from above and love which undying”.

My greatest thanks go to my supervisor, Dr. Karen Hapgood, who provided far more encouragement, guidance, opportunities than I ever expected. I am truly honoured, fortunate and grateful for being part of her MAPEL research team.

My appreciation also goes to many friends, research colleagues and general/technical staffs from the Monash Chemical Engineering Department, including Steven Ho, Thanh Nguyen, Waithira Kariuki, Dr. Rachel Smith, Dr. Jenny Ho, Dr. Michael Danquah, Dr. Ali Akhavan, Dr. Meng Wai Woo, Dr. Nipen Shah, Ronald Halim, Harvey Huang, Lawrence Quek, Nyomi Uduman, Anushi Rajapaksa, Yuan Fang, Jill Crisfield, Lilyanne Price, Garry Thunder, Wren Schoppe, Kate Malcolm, Ron Graham, Gamini Ganegoda and Roy Harrip for their motivation, discussion, advice, and great friendships. A big thank you also goes to Heather Emady for proof reading this thesis.

Special appreciation also goes to my brothers and sisters in Christ, including Pastor Dorcas, Pastor Caleb, Dr. Yeng Kwang Tay, Hui Ting Eng, Dr. Lawrence Tay, Wuan Theng Law, Dr. Clement Lau, Nancy Chiew, Dr. Joseph Sia, Jia Yin Tay, Hui Voon Tan, Rou Min Chok and Guo Guang Chao for their prayer, encouragement and support.

I would also like to sincerely acknowledge The Dow Wolff Cellulosics (Midland, MI, USA) and Australian Postgraduate Award for the financial support for the project and scholarship.

Finally, yet importantly, my sincere gratitude goes to my beloved father, mother, brother, sister, wife and all of my family members, for their moral support, love and prayer during times of frustration in the often seemingly never ending saga of experiments and writing up.

THESIS SUMMARY

Wet granulation is a process of particle size enlargement whereby a liquid binder is added onto agitated powder beds to facilitate granule formation. This PhD thesis studies the foam granulation process, where the liquid binder is added as an aqueous foam.

The investigation into foam granulation technology begins with a literature review on both the foam and wet granulation disciplines, followed by a series of experimental studies. The experimental studies are divided into a few different stages, starting with small scale experiments investigating single nucleus formation on static powder beds, followed by nuclei formation by a nucleation-only mechanism on real moving powder beds, foam granulation at a wide range of material and process conditions, and case studies investigating moisture and drug distribution in granules, with the primary aim to develop understanding of the mechanisms controlling (foam) binder dispersion and nucleation during foam granulation.

It was discovered that the liquid drainage rate is the rate limiting step during foam penetration. Large binder concentration and/or fine powder particles are associated with a slow foam penetration process, which also give rise to the formation of fine nuclei. Nucleation via foam penetration on static powder beds was shown to provide better liquid usage and improve liquid distribution efficiency compared to the nucleation via drops on lactose powder.

From the study of nuclei formation on a real moving powder bed, it was proposed that wetting and nucleation during foam granulation involves “foam drainage” and “mechanical dispersion” controlled mechanisms. Foam granulation limited to a nucleation-only mechanism was demonstrated to be able to create nuclei with uniform, narrow size distributions.

The proposition of “foam drainage” and “mechanical dispersion” controlled mechanisms was verified in a series of foam granulation experiments using a wide range of material and process properties, which showed that the mechanisms can influence the initial nuclei size distribution as well as the final granule size distribution. It was discovered that increasing the liquid to solid ratio, decreasing the foam quality, increasing the primary particle size, decreasing the binder concentration and decreasing the impeller speed all have an equivalent effect in increasing the average granule size and the spread of granule size distribution.

Two independent case studies have demonstrated the potential of foam granulation to achieve uniform moisture and drug distribution in granules. Comparison between foam and spray granulation also found the differences in the wetting and nucleation mechanisms involved, and identified the major contribution to granule heterogeneity.

Transformation and regime maps have been proposed to explain foam granulation behaviour. On the basis of the two wetting and nucleation mechanisms – “foam drainage” and mechanical dispersion” controlled mechanisms, the transformation maps summarizes the effects of material and process properties on the nuclei granule size distribution. A regime map is presented for to show the regimes of operation for the key rate processes involved in foam granulation and spray granulation. The maps should prove to be useful for foam granulation design, and act as the foundation for future study.

TABLE OF CONTENTS

DECLARATION	I
ACKNOWLEDGEMENTS.....	II
THESIS SUMMARY.....	III
TABLE OF CONTENTS.....	V
NOMENCLATURE.....	X
LIST OF FIGURES	XIII
LIST OF TABLES.....	XXI
1 INTRODUCTION AND BACKGROUND.....	1
1.1 WET GRANULATION	1
1.2 FOAM.....	2
1.3 THE UNDERSTANDING GAP IN FOAM GRANULATION	2
1.4 RESEARCH AIMS.....	3
1.5 THESIS OUTLINE.....	4
2 LITERATURE REVIEW.....	6
2.1 FOAM.....	6
2.1.1 <i>The structure of foam</i>	6
2.1.2 <i>Foam properties</i>	8
2.1.3 <i>Foam characterization</i>	11
2.1.4 <i>Foam technology</i>	15
2.1.5 <i>Foam-particle interactions</i>	18
2.1.6 <i>Foam flow in porous media</i>	20
2.2 WET GRANULATION	22
2.2.1 <i>Wetting and nucleation</i>	22
2.2.2 <i>Consolidation and growth</i>	31
2.2.3 <i>Breakage and attrition</i>	39

2.3	FOAM GRANULATION	41
2.3.1	<i>Pioneering work on foam granulation</i>	41
2.3.2	<i>Some unique challenges with the use of foam granulation</i>	46
2.4	LITERATURE SUMMARY.....	47
3	SINGLE NUCLEUS FORMATION.....	48
3.1	INTRODUCTION.....	48
3.2	EXPERIMENTAL	50
3.2.1	<i>Materials</i>	50
3.2.2	<i>Methods</i>	52
3.3	RESULTS	53
3.3.1	<i>Foam and drop specific penetration times</i>	53
3.3.2	<i>Effect of particle size on foam specific penetration time</i>	54
3.3.3	<i>Effect of binder concentration on foam specific penetration time</i>	58
3.3.4	<i>Foam and drop nucleation ratios</i>	61
3.3.5	<i>Effect of particle size on foam nucleation ratio</i>	67
3.3.6	<i>Effect of binder concentration on foam nucleation ratio</i>	68
3.3.7	<i>Nuclei morphology</i>	69
3.4	DISCUSSION	70
3.4.1	<i>Foam penetration behaviour</i>	70
3.4.2	<i>Effect of feed properties on foam wetting and nucleation</i>	74
3.5	CONCLUSIONS	76
4	BINDER DISPERSION AND NUCLEATION	78
4.1	INTRODUCTION.....	78
4.2	EXPERIMENTAL	81
4.2.1	<i>Materials</i>	81
4.2.2	<i>Methods</i>	82
4.3	RESULTS	88
4.3.1	<i>Foam drainage</i>	88

4.3.2	<i>Foam dispersion behaviour</i>	89
4.3.3	<i>Nuclei formation</i>	91
4.4	DISCUSSION	97
4.4.1	<i>Comparing nucleation by foam delivery and spray delivery</i>	97
4.4.2	<i>Proposed foam wetting and nucleation mechanisms</i>	100
4.5	CONCLUSIONS	102
5	FOAM GRANULATION	104
5.1	INTRODUCTION.....	104
5.2	EXPERIMENTAL	104
5.2.1	<i>Materials</i>	104
5.2.2	<i>Methods</i>	105
5.3	RESULTS	109
5.3.1	<i>Foam granulation profiles</i>	109
5.3.2	<i>Effect of foam quality</i>	112
5.3.3	<i>Effect of impeller speed</i>	114
5.3.4	<i>Effect of wet massing</i>	117
5.3.5	<i>Effect of primary particle size</i>	125
5.3.6	<i>Effect of binder concentration</i>	127
5.3.7	<i>Effect of foam delivery rate</i>	130
5.3.8	<i>A summary of single foam penetration, nucleation and granulation studies</i> . 131	
5.4	DISCUSSION	139
5.4.1	<i>Wetting and nucleation mechanisms</i>	139
5.4.2	<i>Relative interaction of process/material parameters</i>	141
5.5	CONCLUSIONS	144
6	A CASE STUDY OF LIQUID DISTRIBUTION	145
6.1	INTRODUCTION.....	145
6.2	EXPERIMENTAL	146

6.2.1	<i>Materials</i>	146
6.2.2	<i>Methods</i>	147
6.3	RESULTS	149
6.3.1	<i>Granule size distribution</i>	149
6.3.2	<i>Weight mean diameter</i>	153
6.3.3	<i>Moisture distribution</i>	156
6.3.4	<i>Power consumption profile</i>	161
6.4	DISCUSSION	165
6.4.1	<i>Foam versus spray granulation mechanisms</i>	165
6.4.2	<i>Moisture distribution</i>	168
6.4.3	<i>A regime map</i>	170
6.5	CONCLUSIONS	173
7	A CASE STUDY OF DRUG DISTRIBUTION	175
7.1	INTRODUCTION	175
7.2	EXPERIMENTAL	177
7.2.1	<i>Materials</i>	177
7.2.2	<i>Methods</i>	178
7.2.3	<i>Analysis</i>	180
7.3	RESULTS	182
7.3.1	<i>Foam and drop specific penetration times</i>	182
7.3.2	<i>Foam and drop nucleation ratios</i>	184
7.3.3	<i>Power consumption profile</i>	188
7.3.4	<i>Granule size distribution</i>	192
7.3.5	<i>Drug distribution</i>	194
7.4	DISCUSSION	198
7.4.1	<i>Monitoring granulation via power consumption measurement</i>	198
7.4.2	<i>Drug distribution</i>	200

7.5 CONCLUSIONS	201
8 CONCLUSIONS.....	203
8.1 A SUMMARY OF MAJOR FINDINGS	203
8.1.1 <i>Single nucleus formation</i>	203
8.1.2 <i>Binder Dispersion and Nucleation</i>	204
8.1.3 <i>Foam Granulation</i>	204
8.1.4 <i>A Case Study of Liquid Distribution</i>	205
8.1.5 <i>A Case Study of Drug Distribution</i>	205
8.2 RECOMMENDATIONS FOR FUTURE RESEARCH	206
8.3 CONCLUDING COMMENTS.....	206
REFERENCES	208

NOMENCLATURE

M_l, M_d	Interfacial mobility
μ	Bulk viscosity
μ_s	Surface shear viscosity
r	Radius of bubble curvature
D_s	Surface diffusion coefficient
E	Gibbs elasticity of the interface
D_{eff}	Diffusion coefficient
ε	Liquid volume fraction
ρ	Solution density
g	Gravity
D	Bubble diameter
V_f, V_g, V_l	Volumes of foam, gas and liquid respectively
ρ_f, ρ_g, ρ_l	Densities of foam, gas and liquid respectively
m_g, m_l	Mass of gas and liquid respectively
FQ	Foam quality
h	Penetration height
t_p	Drop penetration time
R	Radius of the capillary
γ_{LV}	Surface tension
θ	Contact angle
R_d	Radius of a spherical drop
V_o	Initial liquid volume
ε_{eff}	Effective porosity of bed
R_{eff}	Effective pore radius
ϕ	Shape factor accounted for non-spherical shapes
d_{32}	Equivalent spherical diameter with same surface to volume ratio
ε_{tap}	Tap porosity
\dot{V}	Volumetric spray rate
ψ_a	Dimensionless spray flux
\dot{A}	Powder flux traversing the spray zone

d_d	Average drop diameter
t_c	Powder circulation time (entering the spray zone)
τ_p	Dimensionless drop penetration time
S_{\max}	Maximum liquid pore saturation
w	Mass ratio of liquid to solid
ε_{\min}	Minimum porosity of the formulation
ρ_g	Granule density
Y_d	Dynamic yield stress
St_{def}	Stokes deformation number
U_c	Representative collision velocity in the granulator
U_b	Bubble velocity
d_p	Particle diameter
d_b	Bubble size
l_b	Spacing between two bubbles
ω	Drum rotational speed
D_{drum}	Drum granulator diameter
ω_i	Impeller speed
ω_c	Chopper speed
D_i	Impeller diameter
D_c	Chopper diameter
St_v	Viscous Stokes number
d_g	Granule diameter
St_v^*	Critical Stokes number
e_r	Coefficient of restitution
h_a	Height of surface asperities
h_b	Liquid layer thickness
\tilde{D}	Harmonic mean granule diameter
\tilde{m}	Harmonic mean granule mass
t_{sp}	Specific penetration time
M_n	Nuclei mass

M_f	Fluid mass
K	Nucleation mass ratio
$V_{particle}$	Volume of the particles
V_{bed}	Volume of the powder bed
HPC	Hydroxylpropyl cellulose
HPMC	Hydroxylpropyl methylcellulose
d_m	Weight mean diameter
M_i	Particle mass fraction of sieve size interval i
d_i	Mean diameter of sieve size interval i
H_f	Foam height
H_l	Liquid (drained) height
$f_{collapsed}(t)$	Dimensionless change of liquid fraction in foam
λ	Drainage constant
$V_l(t)$	Volume of liquid drained at time t
x	Particle diameter
MCC	Microcrystalline cellulose
L:S	Liquid to solid ratio
GSD	Granule size distribution
SA	Salicylic acid

LIST OF FIGURES

Figure 2-1 The structure of foam. The bubbles are separated by lamellae. Three lamellae connect to form a Plateau border.	7
Figure 2-2 A vertical draining foam. Liquid drains to the bottom while bubbles upflow to the top, forming polyhedral bubbles near the top and spherical bubbles near the base (Pugh, 2005; Saint-Jalmes, 2006).	12
Figure 2-3 Schematic of the snap-off mechanism (reproduced from Schramm 1994).	20
Figure 2-4 Schematic of the lamellae division mechanism (reproduced from Schramm 1994).	21
Figure 2-5 Schematic of the leave-behind mechanism (reproduced from Schramm, 1994).	21
Figure 2-6 The four stages of wetting and nucleation (Iveson <i>et al.</i> , 2001a).....	23
Figure 2-7 Different types of nucleation mechanisms (Hapgood <i>et al.</i> , 2007; Litster and Ennis, 2004).....	24
Figure 2-8 Nucleation regime map (Hapgood <i>et al.</i> , 2003).	30
Figure 2-9 Granule growth regime map (Iveson and Litster, 1998b; Iveson <i>et al.</i> , 2001b).	36
Figure 2-10 Equipment setup for foam generation – (right) foam generator and (left) pressure pot.....	42
Figure 2-11 Foam granulation process showing (a) initial addition of foam (b) foam dispersion after one minute of mixing (c) after two minutes, all foam has been dispersed (Sheskey <i>et al.</i> , 2003).	43
Figure 2-12 Nucleation process in foam granulation proposed by Keary and Sheskey (2004).	45
Figure 3-1 (left) Drop penetration experiment (middle) Foam penetration experiment (right) Foam dispenser.	52
Figure 3-2 Comparison of specific penetration times between HPMC foam and drop penetrations on 200 mesh lactose.....	53
Figure 3-3 Effect of glass ballotini powder particle size on specific penetration times for 10% HPMC foamed binders.	55
Figure 3-4 Effect of glass ballotini powder particle size on specific penetration times for 4% HPMC foamed binders.	56
Figure 3-5 Effect of lactose powder particle size on specific penetration times for HPC foamed binders.	56

Figure 3-6 Effect of lactose powder particle size on specific penetration times for HPMC foamed binders.....	57
Figure 3-7 Effect of binder concentration on specific penetration times for HPMC foam penetrations on AH grade glass ballotini powders.....	59
Figure 3-8 Effect of binder concentration on specific penetration times for HPMC foam penetrations on AC grade glass ballotini powders.....	60
Figure 3-9 Effect of binder concentration on specific penetration times for HPMC foam penetrations on AE grade glass ballotini powders.....	60
Figure 3-10 Comparison of HPC foam and drop nucleation ratios on AC grade glass ballotini. Gradient of graph indicates nucleation ratio, K	62
Figure 3-11 Comparison of HPC foam and drop nucleation ratios on 100 mesh lactose. Gradient of graph indicates nucleation ratio, K	62
Figure 3-12 Comparison of HPC foam and drop nucleation ratios on 200 mesh lactose. Gradient of graph indicates nucleation ratio, K	64
Figure 3-13 Comparison of nucleation via foams and drops. Filled dots indicate nucleation on lactose powder – improved nucleation efficiency with foam induced nucleation method. Unfilled dots indicate nucleation on glass ballotini – similar nucleation efficiency.	65
Figure 3-14 Effect of glass ballotini particle size on nucleation ratio, K , for HPC foamed binders.	67
Figure 3-15 Effect of lactose particle size on nucleation ratio, K , for HPC foamed binders.....	68
Figure 3-16 Foam created nuclei – (a) 3% HPC on AC grade glass ballotini. (b) 6% HPC on AC grade glass ballotini. (c) 6% HPC on AH grade glass ballotini. Scale is in millimetres.	69
Figure 3-17 Foam created nuclei – (a) 4% HPMC on 200 mesh lactose. (b) 6% HPMC on 200 mesh lactose. (c) 3% HPC on 100 mesh lactose. Scale is in millimetres.....	70
Figure 3-18 4% HPMC foam penetration on a 100 mesh lactose powder bed.	70
Figure 3-19 8% HPMC foam penetration on an AC grade glass ballotini powder bed.	71
Figure 3-20 8% HPMC foam penetration on an AC grade glass ballotini powder bed.	72
Figure 3-21 Propagation of wetting front caused by 8% HPMC foam penetration on an AC grade glass ballotini powder bed.....	73
Figure 3-22 Rate limiting step of liquid penetration – (a) foam penetration: liquid in foam undergoes a tortuous path before penetrating into powder pores and (b) liquid droplet penetration: liquid as a whole, is absorbed into powder pores.	74

Figure 3-23 Effects of feed properties on foam specific penetration time and nucleation ratio.	75
Figure 4-1 (left) Product contact area of KG-5 bowl that are exposed and come in contact with the product (right) Dimensions of three bladed impeller (Key International Inc.).....	82
Figure 4-2 Change of foam and liquid fraction in a cylindrical glass measurement tube (a) at initial time $t = 0$ (b) after time t	85
Figure 4-3 Light transmission profile of HPMC foamed binder. The right hand side legend indicates the colour key for the six profiles from $t = 0$ minutes (0:00) to $t = 18$ minutes (0:18).	86
Figure 4-4 Drainage profiles of HPMC foams at foam quality (FQ) – 97% FQ, 83% FQ and 67% FQ.....	88
Figure 4-5 Foam dispersion (shown in pink) during powder bumping flow.	89
Figure 4-6 Foam dispersion (shown in pink) during powder roping flow.....	91
Figure 4-7 Images of nuclei samples (a) $>1\text{mm}$ (b) $850\mu\text{m}$ - $425\mu\text{m}$ (c) non-granular materials $<250\mu\text{m}$. Scale is in millimetres.	92
Figure 4-8 Nuclei formation as a function of impeller speed and foam quality. The “% retained nuclei” is defined as the mass fraction of nuclei larger than $250\mu\text{m}$	92
Figure 4-9 Mass fraction of lumps (nuclei $>2\text{mm}$) as a function of impeller speed and foam quality.	94
Figure 4-10 Nuclei size distributions at 455rpm impeller speed as a function of foam quality. Note that 0% FQ indicates spray delivery.	95
Figure 4-11 Nuclei size distributions at 125rpm impeller speed as a function of foam quality. Note that 0% FQ indicates spray delivery.	96
Figure 5-1 Foam granulation experimental setup – (left) high shear mixer-granulator, (middle) liquid binder storage pot and (right) foam generator.	107
Figure 5-2 Foam granulation profile of 97% FQ foam addition on 100 mesh lactose powder: evolution of particle diameter x – fines ($0\mu\text{m}<x<180\mu\text{m}$), intermediate ($180\mu\text{m}<x<1000\mu\text{m}$) and coarse ($x>1000\mu\text{m}$) mass percentage.	110
Figure 5-3 Foam granulation profile of 91% FQ foam addition on 100 mesh lactose and microcrystalline cellulose mixture: evolution of particle diameter x – fines ($0\mu\text{m}<x<180\mu\text{m}$), intermediate ($180\mu\text{m}<x<1000\mu\text{m}$) and coarse ($x>1000\mu\text{m}$) mass percentage.	110

Figure 5-4 Foam granulation profile of 83% FQ foam addition on 200 mesh lactose and microcrystalline cellulose mixture: evolution of particle diameter x – fines ($0\mu\text{m}<x<180\mu\text{m}$), intermediate ($180\mu\text{m}<x<1000\mu\text{m}$) and coarse ($x>1000\mu\text{m}$) mass percentages.....	111
Figure 5-5 Microscopy images of (a) wetted particles and initial nuclei (b) spherical granules (c) overwetted granules and (d) cake.	112
Figure 5-6 Granule size distribution as a function of foam quality – 4% HPMC, 200 mesh lactose and microcrystalline cellulose mixture, 40% L:S, 295rpm. The dotted lines divide the granule size (x) into fine ($x<180\mu\text{m}$), intermediate ($180\mu\text{m}<x>1000\mu\text{m}$) and coarse ($x>1000\mu\text{m}$) fractions.	113
Figure 5-7 Granule size distribution as a function of foam quality – 4% HPMC, 100 mesh lactose and microcrystalline cellulose mixture, 40% L:S, 295rpm. The dotted lines divide the granule size (x) into fine ($x<180\mu\text{m}$), intermediate ($180\mu\text{m}<x>1000\mu\text{m}$) and coarse ($x>1000\mu\text{m}$) fractions.	114
Figure 5-8 Effect of impeller speed on the evolution of fine, intermediate and coarse fractions – 4% HPMC, 100 mesh lactose and microcrystalline cellulose mixture, 91% FQ.....	115
Figure 5-9 Effect of impeller speed on the evolution of fine, intermediate and coarse fractions – 4% HPMC, 100 mesh lactose and microcrystalline cellulose mixture, 83% FQ.....	116
Figure 5-10 Granule size distribution as a function of impeller speed – 4% HPMC, 100 mesh lactose, 91% FQ, 9% L:S.....	117
Figure 5-11 Granule size distribution at 91% FQ as a function of wet massing time – 4% HPMC, 200 mesh lactose, 8% L:S, 295rpm. The dotted lines divide the granule size (x) into fine ($x<180\mu\text{m}$), intermediate ($180\mu\text{m}<x>1000\mu\text{m}$) and coarse ($x>1000\mu\text{m}$) fractions.	118
Figure 5-12 Granule size distribution at 83% FQ as a function of wet massing time – 4% HPMC, 200 mesh lactose, 8% L:S, 295rpm. The dotted lines divide the granule size (x) into fine ($x<180\mu\text{m}$), intermediate ($180\mu\text{m}<x>1000\mu\text{m}$) and coarse ($x>1000\mu\text{m}$) fractions.	119
Figure 5-13 Granule mean diameter (d_{50}) as a function of wet massing time.	120
Figure 5-14 Granule size distribution at 97% FQ as a function of wet massing time – 4% HPMC, 100 mesh lactose, 10% L:S, 295rpm. The dotted lines divide the granule size (x) into fine ($x<180\mu\text{m}$), intermediate ($180\mu\text{m}<x>1000\mu\text{m}$) and coarse ($x>1000\mu\text{m}$) fractions.	122

Figure 5-15 Granule size distribution at 91% FQ as a function of wet massing time – 4% HPMC, 100 mesh lactose, 10% L:S, 295rpm. The dotted lines divide the granule size (x) into fine ($x < 180\mu\text{m}$), intermediate ($180\mu\text{m} < x < 1000\mu\text{m}$) and coarse ($x > 1000\mu\text{m}$) fractions.	123
Figure 5-16 Granule size distribution at 83% FQ as a function of wet massing time – 4% HPMC, 100 mesh lactose, 10% L:S, 295rpm. The dotted lines divide the granule size (x) into fine ($x < 180\mu\text{m}$), intermediate ($180\mu\text{m} < x < 1000\mu\text{m}$) and coarse ($x > 1000\mu\text{m}$) fractions.	124
Figure 5-17 Granule size distribution at 91% FQ as a function of primary lactose particle size – 4% HPMC, lactose and microcrystalline cellulose mixture, 50% L:S, 295rpm. The dotted lines divide the granule size (x) into fine ($x < 180\mu\text{m}$), intermediate ($180\mu\text{m} < x < 1000\mu\text{m}$) and coarse ($x > 1000\mu\text{m}$) fractions.	125
Figure 5-18 Granule size distribution at 83% FQ as a function of primary lactose particle size – 4% HPMC, lactose and microcrystalline cellulose mixture, 50% L:S, 295rpm. The dotted lines divide the granule size (x) into fine ($x < 180\mu\text{m}$), intermediate ($180\mu\text{m} < x < 1000\mu\text{m}$) and coarse ($x > 1000\mu\text{m}$) fractions.	126
Figure 5-19 Granule size distribution for 4% HPMC and 8% HPMC at 91% FQ – 100 mesh lactose and microcrystalline cellulose mixture, 50% L:S, 295rpm. The dotted lines divide the granule size (x) into fine ($x < 180\mu\text{m}$), intermediate ($180\mu\text{m} < x < 1000\mu\text{m}$) and coarse ($x > 1000\mu\text{m}$) fractions.	128
Figure 5-20 Granule size distribution for 4% HPMC and 8% HPMC at 83% FQ – 100 mesh lactose and microcrystalline cellulose mixture, 50% L:S, 295rpm. The dotted lines divide the granule size (x) into fine ($x < 180\mu\text{m}$), intermediate ($180\mu\text{m} < x < 1000\mu\text{m}$) and coarse ($x > 1000\mu\text{m}$) fractions.	128
Figure 5-21 (a) Initial granule size distribution at 3% liquid to solid ratio (b) Final granule size distribution at a 5% liquid to solid ratio – 4% HPMC, 100 mesh lactose powder, 83% FQ, 515rpm.	130
Figure 5-22 Effect of foam quality on 4% HPMC foam penetration into a 100 mesh lactose powder bed.	132
Figure 5-23 Nuclei size distribution as a function of impeller speed at 97% FQ – 4% HPMC, 100 mesh lactose powder, 1% L:S.	133
Figure 5-24 Nuclei size distribution as a function of impeller speed at 83% FQ – 4% HPMC, 100 mesh lactose powder, 1% L:S.	134

Figure 5-25 Granule size distribution as a function of foam quality at a liquid to solid ratio of (a) 3% L:S (b) 4% L:S (c) 5% L:S (d) 6% L:S (e) 8% L:S (f) 10% L:S – 4% HPMC, 100 mesh lactose powder, 295rpm. The dotted lines divide the granule size (x) into fine ($x < 180\mu\text{m}$), intermediate ($180\mu\text{m} < x < 1000\mu\text{m}$) and coarse ($x > 1000\mu\text{m}$) fractions. ...	136
Figure 5-26 Granule size distribution as a function of foam quality at a liquid to solid ratio of (a) 3% L:S (b) 4% L:S (c) 5% L:S (d) 6% L:S (e) 8% L:S (f) 10% L:S – 4% HPMC, 100 mesh lactose powder, 515rpm. The dotted lines divide the granule size (x) into fine ($x < 180\mu\text{m}$), intermediate ($180\mu\text{m} < x < 1000\mu\text{m}$) and coarse ($x > 1000\mu\text{m}$) fractions. ...	138
Figure 5-27 Dispersion and wetting coverage transformation map for foam granulation.....	140
Figure 5-28 Process parameters and material properties transformation maps for foam granulation. “GSD” indicates “Granule Size Distribution”	142
Figure 6-1 Granule size distribution as a function of foam quality at 295rpm after (a) 20% (b) 30% (c) 40% (d) 50% (e) 60% foam addition and (f) after 1min wet massing – 4% HPMC, 100 mesh lactose and microcrystalline cellulose mixture. The dotted lines divide the granule size (x) into fine ($x < 180\mu\text{m}$), intermediate ($180\mu\text{m} < x < 1000\mu\text{m}$) and coarse ($x > 1000\mu\text{m}$) fractions.	150
Figure 6-2 Granule size distribution as a function of foam quality at 515rpm after (a) 20% (b) 30% (c) 40% (d) 50% (e) 55% foam addition – 4% HPMC, 100 mesh lactose and microcrystalline cellulose mixture. The dotted lines divide the granule size (x) into fine ($x < 180\mu\text{m}$), intermediate ($180\mu\text{m} < x < 1000\mu\text{m}$) and coarse ($x > 1000\mu\text{m}$) fractions. ...	151
Figure 6-3 Weight mean diameter as a function of liquid binder level at a 295rpm impeller speed for foam (91% FQ and 83% FQ) and spray (0% FQ) granulation – 4% HPMC, 100 mesh lactose and microcrystalline cellulose. The dotted lines divide the granulation into (I) wetting and nucleation, (II) growth, (III) overwetting and (IV) caking.	154
Figure 6-4 Weight mean diameter as a function of liquid binder level at a 515rpm impeller speed for foam (91% FQ and 83% FQ) and spray (0% FQ) granulation – 4% HPMC, 100 mesh lactose and microcrystalline cellulose. The dotted lines divide the granulation into (I) wetting and nucleation, (II) growth, (III) overwetting and (IV) caking.	155
Figure 6-5 Wet (left) and dry (right) granule size distributions after (a) liquid binder addition (b) 2 minutes of wet massing for foam (91% FQ and 83% FQ) and spray (0% FQ) granulation – 4% HPMC, 100 mesh lactose and microcrystalline cellulose mixture, 50% L:S, 515rpm.	157

Figure 6-6 Moisture content after 50% liquid binder addition as a function of granule size class for foam (91% FQ and 83% FQ) and spray (0% FQ) granulation – 4% HPMC, 100 mesh lactose and microcrystalline cellulose mixture, 515rpm.....	159
Figure 6-7 Moisture content after 2 minutes of wet massing as a function of granule size class for foam (91% FQ and 83% FQ) and spray (0% FQ) granulation – 4% HPMC, 100 mesh lactose and microcrystalline cellulose mixture, 515rpm.....	160
Figure 6-8 Power consumption profiles during foam (91% FQ and 83% FQ) and spray (0% FQ) granulation of 100 mesh lactose and microcrystalline cellulose mixture – 4% HPMC, 515rpm. The processes started with dry mixing, followed by liquid binder addition and ended with wet massing.....	161
Figure 6-9 Division of a power consumption curve according to Leuenberger (1982; 2009).	162
Figure 6-10 Power consumption profiles during foam (91% FQ and 83% FQ) and spray (0% FQ) granulation of 100 mesh lactose – 4% HPMC, 295rpm. The processes started with dry mixing, followed by liquid binder addition and ended with wet massing.	163
Figure 6-11 Regime map for the granulation systems – foam versus spray. The dotted lines divide the granulation into (I) wetting and nucleation, (II) growth, (III) overwetting and (IV) caking.....	171
Figure 7-1 Schematic diagram of vacuum filtration of salicylic acid/lactose/methanol solution for filtration of lactose powder.	181
Figure 7-2 Foam and drop specific penetration times as a function of wt% hydrophobic glass ballotini.....	182
Figure 7-3 Foam and drop specific penetration times as a function of wt% salicylic acid.	183
Figure 7-4 Foam and drop nucleation ratios as a function of wt% hydrophobic glass ballotini.	185
Figure 7-5 Nuclei produced from 6wt% HPMC foam on glass ballotini powder mixtures. Scale indicates millimetres.....	185
Figure 7-6 Nuclei produced from 6wt% HPMC drops on glass ballotini powder mixtures. Scale indicates millimetres.....	186
Figure 7-7 Foam and drop nucleation ratios as a function of wt% salicylic acid.	187
Figure 7-8 Nuclei produced from 6wt% HPMC foams on powder beds containing various proportions of salicylic acid. Scale indicates millimetres.	187
Figure 7-9 Nuclei produced from 6wt% HPMC droplets and powder beds containing various proportions of salicylic acid. Scale indicates millimetres.	188

Figure 7-10 Power consumption and the slope of the profile (first derivative with respect to time) during foam and spray granulation relative to the dry mix as a function of powder composition – 4% HPMC, salicylic acid (SA) and 200 mesh lactose (L200m) powder mixtures, 285rpm.	189
Figure 7-11 Power consumption and the slope of the profile (first derivative with respect to time) during foam and spray granulation relative to the dry mix as a function of powder composition – 4% HPMC, salicylic acid (SA) and 100 mesh lactose (L100m) powder mixture, 285rpm. The processes started with dry mixing, followed by liquid binder addition and ended with wet massing.....	191
Figure 7-12 Foam (F) and spray (S) granule size distributions as a function of powder composition – 4% HPMC, salicylic acid (SA) and 200 mesh lactose (L200m) powder mixture, 285rpm.....	193
Figure 7-13 Foam (F) and spray (S) granule size distributions as a function of powder composition – 4% HPMC, salicylic acid (SA) and 100 mesh lactose (L100m) powder mixture, 285rpm.....	194
Figure 7-14 Foam granulation – % drug claim as a function of granule size for salicylic acid-200 mesh lactose formulations.....	195
Figure 7-15 Spray granulation – % drug claim as a function of granule size for salicylic acid-200 mesh lactose formulations.....	196
Figure 7-16 Foam granulation – % drug claim as a function of granule size for salicylic acid-100 mesh lactose formulations.....	197
Figure 7-17 Spray granulation – % drug claim as a function of granule size for salicylic acid-100 mesh lactose formulations.....	197

LIST OF TABLES

Table 2-1 Estimates of U_c for different types of granulators (Litster and Ennis, 2004).....	35
Table 3-1 Powder properties.	51
Table 3-2 Liquid binder properties.	52
Table 3-3 Estimated foam nucleation ratios.....	66
Table 3-4 Estimated drop nucleation ratios.....	66
Table 4-1 Powder and liquid binder properties.	82
Table 4-2 Foam drainage properties.	89
Table 4-3 Weight mean diameter of nuclei at varied impeller speed and foam quality. Note that 0% indicates spray delivery.	97
Table 5-1 Powder and liquid binder properties.	105
Table 5-2 Operating conditions for granulation experiments.	108
Table 6-1 Powder and liquid binder properties.	146
Table 6-2 Operating conditions for granulation experiments.	148
Table 7-1 Powder and liquid binder properties.	178
Table 7-2 Powder compositions and loosed packed porosity.	179

CHAPTER 1
INTRODUCTION AND BACKGROND

1 INTRODUCTION AND BACKGROUND

Wet granulation has been a topic of considerable research over the past, and great progress has been made in understanding and controlling wet granulation processes. Investigation of a broad range of wet granulation topics could be carried out in terms of a succession of length scales, which is usually termed as micro for the granules, meso for ensembles of granules and macro for whole process behaviour – establishing the general regularities, quantifying the micro and meso behaviour in terms of rates laws and producing a description of the macro behaviour (Litster and Ennis, 2004; Salman *et al.*, 2007a). These investigations have made a significant step forward over the past decade, and these developments are now at the point where they can be directly applied in many industrial processes for scale-up and formulation and process characterisation.

Foam has been a subject of scientific and technological application interest in a variety of colloid chemistry and physics disciplines, such as the subject of foam formation, stability, and properties, as well as a diverse use in various industrial processes, such as the chemical, cosmetic, food or other industries. This wide range of practical and industrial applications has precipitated a wealth of publications dedicated to foams, of which only a few are cited here (Bergeron *et al.*, 2005; Perkowitz, 2000; Prud'homme and Khan, 1996; Schramm, 1994b). Great progress has been made in the understanding of foam science as well as the development of many new foam technologies. The emergence of foam systems appears to gradually replace water systems in many applications.

For the first time, foam systems break into the area of pharmaceutical wet granulation as a replacement for spraying systems. The first successful foam granulation industrial case study began in 2004 (Keary and Sheskey, 2004), and subsequently additional work has been published to fine-tune the technology (Cantor *et al.*, 2009; Sheskey *et al.*, 2007). This PhD thesis is the first thesis to report an independent research investigation on foam granulation.

1.1 Wet Granulation

Wet granulation is a particle size enlargement process whereby the primary particles are bound together by a fluid (also called a binder) through agitation to form granules of improved properties (Ennis and Litster, 1997). The process is typically carried out in a wet-agitated

granulator that imparts shear forces to promote active interaction between the particles and the liquid binder. The common types of wet-agitated granulators include drum granulators, pan granulators, fluidised-bed granulators and mixer-granulators, and this group of granulators can be commonly found in the fertiliser, agriculture, chemical and pharmaceutical industries (Snow *et al.*, 1997). Regardless of the type of granulator, the liquid binder can be added by pouring or spraying, or by melt granulation where solid binder is added and mixed with the powder while the granulator temperature is increased above the binder melting point (Ennis and Litster, 1997). A new liquid binder addition method has recently been invented, where the binder is added as an aqueous foam. This type of granulation is called foam granulation (Keary and Sheskey, 2004), and is the subject of interest in this thesis.

1.2 Foam

Foam is a colloidal dispersion system which is composed of a gaseous dispersion phase distributed in a continuous liquid phase. In general, foams are classified into wet or transient foam and dry or metastable foam. Wet foams are characterised by an assembly of spherical bubbles separated by thick liquid walls, whereas dry foams are characterised by a large number of polyhedral bubbles separated by liquid films of very small thicknesses (Malysa, 1992). Foams are thermodynamically unstable as the foam structure, subjected to gravity and other surface forces, changes irreversibly with time as a result of drainage, coarsening and coalescence (Saint-Jalmes and Langevin, 2002). Drainage generally refers to the effect of liquid flow within the foam, whereas coarsening and coalescence generally refer to the effects of gas diffusion and bubbles growth or rupture. These critical features and characteristics of foam depend largely on foam formation, stability and properties, and their mutual interdependences, which will be reviewed in this thesis (see *Chapter 2*).

1.3 The Understanding Gap in Foam Granulation

Significant progress has been made in understanding and controlling wet granulation processes, as well as foam as an individual discipline, but foam granulation still remains a developing area. Since its introduction in 2004, work on foam granulation processes have focussed on commercial formulations and processes, of direct relevance to the pharmaceutical companies applying the novel foam granulation process. Successful case studies demonstrated the high potential of foam granulation, but the trial experiments were conducted on complex

pharmaceutical formulations in commercial equipment which lack general applicability and systematic understanding (Cantor *et al.*, 2009; Keary and Sheskey, 2004; Sheskey *et al.*, 2007).

The existing wet granulation theories should be fundamentally applicable to foam granulation, but the potential differences in the critical variables controlling foam granulation remain unknown. There is a need to identify the key formulation properties and process parameters that control foam granulation to improve the application of foam granulation from a trial-and-error approach to a systematic control strategy. This forms the motivation for the research into foam granulation to fill the knowledge gap.

1.4 Research Aims

This PhD thesis studies the foam granulation, focussing on the foam induced wetting and nucleation process, by extending granulation and foam theories to include the mechanisms controlling foam nucleation and granulation. This has been approached by:

1. Identifying the effects of formulation properties.
2. Identifying the effects of process conditions.
3. Incorporating both formulation and process properties to produce a controlled-foam granulation process, with the goal of achieving proper control of the granule size distribution through improved understanding of the mechanism controlling binder dispersion and nucleation.

The areas of study will concentrate on the following aspects:

1. Single nucleus formation experiments – this work investigates the interactions between foam and powder particles on static powder beds, where single nucleus formation is observed by depositing a small amount of foam on loose powder beds.
2. Short-nucleation experiments – this work examines foam dispersion and nucleation on a moving lactose powder bed by delivering a small amount of liquid binder during a short granulating period in a high shear mixer-granulator.
3. Granulation experiments – this work investigates a series of foam granulation trials by delivering varying amounts of foamed binder at several different process conditions.
4. A case study of liquid distribution – this work examines the ability of foam granulation to create homogeneous granules with even liquid distribution as a function of granule

size. Comparison is also made with spray granulation at the same manufacturing conditions.

5. A case study of drug distribution – this work investigates the ability of foam granulation to create homogeneous granules with even distribution of drug component as a function of granule size. Comparison is also made with spray granulation at the same manufacturing conditions.

1.5 Thesis Outline

This thesis will present and discuss the key findings in the following chapters:

- **Chapter 2 LITERATURE REVIEW**

This chapter explores the vast applications of foam in other industries, including the general properties that make foam an effective medium, and reviews wet granulation processes, focussing on spray and foam binder delivery methods.

- **Chapter 3 SINGLE NUCLEUS FORMATION**

This chapter studies single nucleus formation by adding a single drop/foam of fluid onto a static powder bed. Foam and drop addition methods are compared, and the effects of material properties on liquid penetration and nucleus formation are evaluated.

- **Chapter 4 BINDER DISPERSION AND NUCLEATION**

This chapter examines the wetting and nucleation behaviour by delivering a small amount of fluid onto a moving powder bed to eliminate the effects of granule growth and breakage. Foam and spray binder deliveries are compared, and the effects of material and process properties on wetting and nucleation are evaluated.

- **Chapter 5 FOAM GRANULATION**

This chapter investigates foam granulation behaviour by delivering various amounts of foamed binder onto an agitated powder bed to include the effects of granule growth and breakage. The impact of process and material parameters are evaluated.

- **Chapter 6 A CASE STUDY OF LIQUID DISTRIBUTION**

This chapter evaluates foam granulation performance in delivering homogeneous granules with uniform moisture distribution. This is also compared to spray granulation at the same manufacturing conditions.

- **Chapter 7 A CASE STUDY OF DRUG DISTRIBUTION**

This chapter evaluates foam granulation performance in delivering homogeneous granules with uniform drug distribution. This is also compared to spray granulation at the same manufacturing conditions.

- **Chapter 8 CONCLUSIONS**

This chapter summarizes the findings and all the major conclusions of this work. Recommendations for future research are also suggested.

CHAPTER 2
LITERATURE REVIEW

2 LITERATURE REVIEW

This chapter reviews the general properties of foams and their applications in other technological processes, in addition to the current understanding and theories of wet granulation. The review of foam literature includes a description of foam structure and properties and the application of foam in other industries that involve foam-particle interactions. The wet granulation literature review includes the mechanisms of binder dispersion and nucleation, granule growth, and granule breakage. A summary of recent work on foam granulation is also presented.

2.1 Foam

Foams open different doors into science and technology, especially in a myriad of diverse useful applications. The complex science of foam and its varied uses have been a subject of research interest to academia, as well as an area of commercial importance in the chemical, cosmetic, food or other industries. A wealth of literature is available on the topic of colloidal dispersions, which are systems consisting of small particles, droplets or bubbles of one phase microscopically dispersed in another, including a range of colloid reference texts (Perkowitz, 2000; Prud'homme and Khan, 1996; Schramm, 1994b) and articles on the myriad of applied aspects (Arzhavitina and Steckel, 2010; Purdon *et al.*, 2003; Turner, 1981). It is not the aim of this thesis to fully explore the complex science of foam and its diverse uses, but the review will focus on some basic characteristics of foam and some of the particle-foam interactions which are specifically relevant to the incorporation of foam into a powder bed.

2.1.1 The structure of foam

Foam is created when a gas is dispersed into a liquid. It consists of polydisperse gas bubbles compressed on each other. The bubbles are separated by the thin liquid film called lamella. The connection of three lamellae is known as Plateau border (Pugh, 1996). Four Plateau borders join at a node (not shown) (Koehler *et al.*, 2000). Figure 2-1 illustrates the structure of foam.

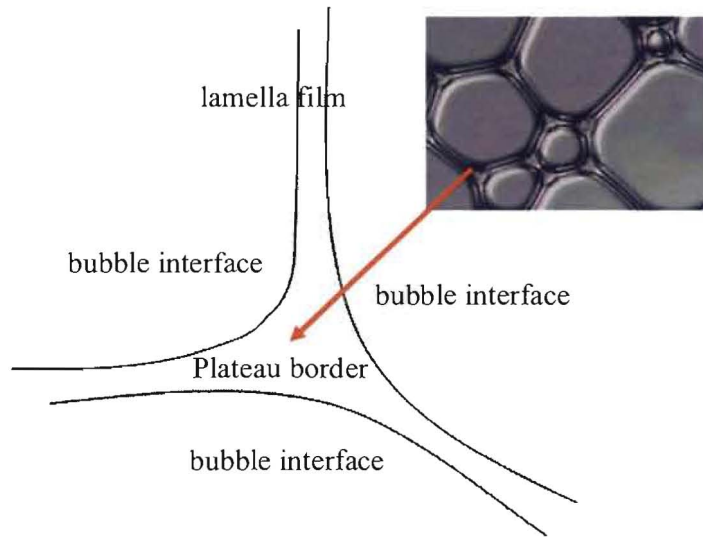


Figure 2-1 The structure of foam. The bubbles are separated by lamellae. Three lamellae connect to form a Plateau border.

The structure of foam changes continuously and irreversibly with time as a result of gravitational drainage, film rupture and coarsening (Saint-Jalmes and Langevin, 2002; Weaire and Phelan, 1996). These effects cause the bubbles to deform themselves into polyhedral cells. Due to the pressure differences between bubbles, small bubbles which have a higher internal pressure dissolve, leading to growth of the bigger bubbles (Bhakta and Ruckenstein, 1997; Gandolfo and Rosano, 1997). This effect is termed “disproportionation” or “Ostwald ripening” (Bergeron *et al.*, 2005; Pugh, 1996).

The pressure is lower in the Plateau borders due to the interfacial curvature, causing the liquid to drain from the lamellae to Plateau borders by a capillary suction effect (Pugh, 1996). However, this can also be opposed by the Gibbs/Marangoni effect, due to surface tension gradients along the air-liquid interface which acts to retain the film thickness (Pugh, 2005). As drainage proceeds, lamellae become thinner and the films which separate two adjacent bubbles eventually rupture. The consequence is coalescence of the neighbouring bubbles, leading to structural reorganisation of the foam and eventually its collapse (Bhakta and Ruckenstein, 1997).

2.1.2 Foam properties

The fundamental behaviour of foam drainage and coarsening depend on many parameters, related to the constituents (gas, liquid and surfactant) and the foam sample (bubble size, wetness and height). These physical and experimental factors affecting foam drainage and coarsening will be reviewed.

2.1.2.1 Foam drainage

Foam drainage is the flow of liquid through the film, Plateau border and node between the bubbles. The flow of liquid is driven by gravity and capillary forces and is resisted by viscous dissipation occurring within the fluid network (Saint-Jalmes, 2006). Gravity makes the liquid flow downward, and the Laplace pressure effect causes the liquid to flow from high liquid regions to low liquid regions. The presence of a gradient in the liquid fraction implies pressure gradients in the liquid (Koehler *et al.*, 2000). Since the pressure is lower in the Plateau border than in the film, this will naturally cause the liquid to flow from the films to the Plateau borders, where it drains through the channels to the bulk. A larger volume of liquid is therefore confined in the Plateau borders and only some liquid resides in the nodes and lamellae (Saint-Jalmes, 2006). A steady state flow of liquid is obtained when the gravity and capillary forces are balanced by the bulk and surface viscous dissipation (Carrier *et al.*, 2002; Saha *et al.*, 2009; Saint-Jalmes, 2006).

2.1.2.2 Foam coarsening

A foam also evolves by gas diffusion, which causes foam coarsening (Drenckhan *et al.*, 2005; Maurdev, 2006). This effect is due to “Ostwald ripening”, which is a thermodynamically-driven spontaneous process as a result of pressure difference in the bubbles (Louvet *et al.*, 2009; Malysa, 1992). As mentioned, the pressure of the gas is greater in small bubbles than in the larger bubbles, which constitutes a driving force for gas diffusion through the liquid films from small bubbles into larger ones. This leads to larger bubble growth at the expense of smaller bubbles (Gandolfo and Rosano, 1997). The bubbles initially formed are often small, roughly spherical bubbles separated by thick films. The films are disrupted as the bubbles deform one another. When bubble popping occurs, neighbouring bubbles are excited, causing more bubble deformation and dislocation. Due to bubble oscillations, the deformed bubbles move into the vacant space created by the burst bubbles. Films gradually thin and start to

oscillate, which precedes more bubbles bursting (Ding *et al.*, 2007). Eventually, the thin films between adjacent bubbles will rupture, leading to bubble coalescence and further drainage. On average, coarsening tends to increase the bubble mean size (Maurdev, 2006; Pugh, 2005).

2.1.2.3 Coupling between foam drainage and coarsening

During foam decay, drainage and coarsening effects are interrelated. Drainage and coarsening generally occur on a similar time-scale. During drainage, the bubble diameter increases significantly, and the drainage kinetics are accelerated by simultaneous coarsening. At the same time, the coarsening kinetics increases as foam drains, promoting bubble growth (Saint-Jalmes, 2006). These two mechanisms strongly interfere, and the end result from these coupled effects is the collapse of foam. The interplay between drainage and coarsening, which depends strongly on the physical and experimental parameters, determines the structure and properties of the foam (Saint-Jalmes, 2006; Saint-Jalmes and Langevin, 2002).

2.1.2.4 Relevant parameters controlling foam drainage and coarsening

The role of liquid properties in foam drainage and coarsening has been widely studied. Several critical physical and chemical parameters have been generally recognised, such as the density of foam, the bulk viscosity of foam, bubble size, foam wetness, the properties of the solution from which the foam is prepared, etc. (Hilgenfeldt *et al.*, 2001; Saint-Jalmes, 2006; Vera and Durian, 2002).

Changing the values of these parameters – the gas, bubble size, bulk viscosity, surface rheology and wetness of the foam, can induce drainage regime transitions from Poiseuille flow (where the flow in Plateau borders is immobile and rigid) to plug flow (the flow is more mobile) or vice versa. These effects can be compiled in terms of the bulk and surface dissipation using the interfacial mobility, M_l (Durand and Langevin, 2002; Koehler *et al.*, 2002; Koehler *et al.*, 2004; Ralph and Robert, 1965; Saint-Jalmes and Langevin, 2002):

$$M_l = \mu r / \mu_s \quad \text{Eq. [2-1]}$$

where μ is the bulk viscosity, μ_s is the surface shear viscosity and r is the radius of curvature of the Plateau border, which is proportional to the bubble diameter and liquid fraction.

Durand and Langevin (2002) also proposed another surface contribution for the balance between bulk and surface effects, which does not involve surface shear viscosity:

$$M_d = \mu D_s / Er \quad \text{Eq. [2-2]}$$

where D_s is a surface diffusion coefficient and E is the Gibbs elasticity of the interface.

The two models consider the contribution of different surface forces to the interfacial mobility, but they generally agree that plug flow occurs for $M_l > 1$ and $M_d > 1$, and Poiseuille flow occurs for $M_l < 1$ and $M_d < 1$ (Durand and Langevin, 2002; Koehler *et al.*, 2002; Koehler *et al.*, 2004; Ralph and Robert, 1965; Saint-Jalmes and Langevin, 2002):.

A draining foam might also be coarsening at the same time or vice versa. Saint-Jalmes (Durand and Langevin, 2002; Koehler *et al.*, 2002; Koehler *et al.*, 2004; Ralph and Robert, 1965; Saint-Jalmes and Langevin, 2002) indicated that the importance of coarsening during drainage can be determined by the ratio of drainage time to coarsening time, as represented by k :

$$k = \frac{4\mu H D_{eff} f(\varepsilon)}{K\rho g \varepsilon D^4} \quad \text{Eq. [2-3]}$$

where μ is the bulk viscosity, H is the foam height, D_{eff} is the diffusion coefficient, ε is the liquid volume fraction, ρ is the solution density, g is the gravity, D is the bubble diameter and $f(\varepsilon)$ describes the proportion of the bubble surface through which gas diffusion occurs as a function of liquid volume fraction.

For small values of k , there is no coarsening during drainage and the bubble diameter is constant during the process. When foam does not undergo coarsening during drainage, the drainage time depends very much on the liquid volume fraction (ε). For large values of k , drainage is enhanced by the simultaneous coarsening effects, which also accelerate bubble growth or vice versa. In this case, the drainage time is less dependent on the liquid volume fraction (ε). As foam height (H) increases, the coupling between drainage and coarsening effects are enhanced, and the dependence of the drainage time on liquid volume fraction (ε)

vanishes. As given by Eq. [2-3], the value of k depends on the bubble diameter, the foam height and the gas properties (Saint-Jalmes, 2006).

2.1.3 Foam characterization

From an optical, mechanical, thermal or electrical point of view, foam displays a tremendous range of characteristics – opaque or transparent, fluid-like or solid-like, conducting or insulating. To understand these properties of foam, several experimental techniques are available. A summary of these techniques to characterise foam is outlined in the following sections.

2.1.3.1 Foam column

The examination of a vertical draining foam is conceptually the simplest approach to characterise foam. In a standing foam, the foam collapses from the top to the bottom of the column, resulting in liquid accumulated at the bottom and gas bubbles moved to the top (Saint-Jalmes, 2006). Several different transitional structures may be observed at different heights as the foam decays, which is illustrated in Figure 2-2. Initially the foam consists of small, spherical bubbles and thick films near the base, while a polyhedral foam concentrated with high gas content and thin films is formed near the surface (Maurdev, 2006; Pugh, 2005).

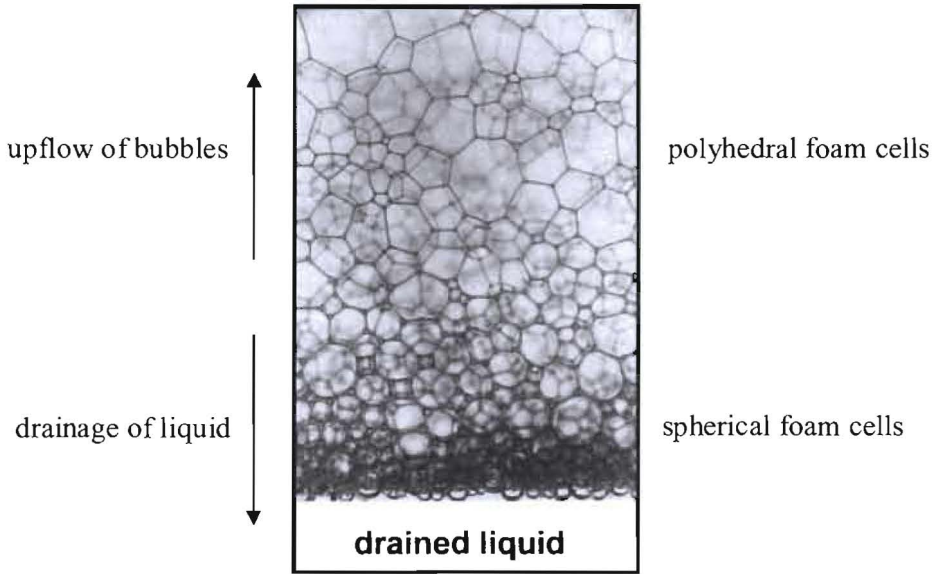


Figure 2-2 A vertical draining foam. Liquid drains to the bottom while bubbles upflow to the top, forming polyhedral bubbles near the top and spherical bubbles near the base (Pugh, 2005; Saint-Jalmes, 2006).

In general, volume (or height) of liquid drained with time, or the decrease of the local liquid fraction at a given position can be measured from the experiment. Some useful expressions are (Bergeron *et al.*, 2005):

$$V_f = V_l + V_g \quad \text{Eq. [2-4]}$$

$$\rho_f = (m_g + m_l)/V_f = (\rho_g V_g + \rho_l V_l)/V_f \quad \text{Eq. [2-5]}$$

where V_f , V_g and V_l are the volumes of foam, gas and liquid respectively, ρ_f , ρ_g and ρ_l are the densities of foam, gas and liquid respectively; and m_g and m_l are the mass of gas and liquid respectively.

As the density of gas is always much smaller than the density of liquid, the density of foam can be estimated using the following equation:

$$\rho_f \approx (\rho_l V_l)/V_f \quad \text{Eq. [2-6]}$$

By knowing the volume of foam and the respective densities of the gas and liquid, the average liquid and gas volume fractions in the foam can be obtained. One common expression used to characterise foam is given as “Foam Quality” (FQ), which quantifies the fraction of gas in the foam (Saint-Jalmes, 2006):

$$FQ = \frac{V_g}{V_g + V_l} \times 100\% \quad \text{Eq. [2-7]}$$

A foam quality of 88% means that the foam contains 88% air by volume. For a draining foam, the liquid volume fraction remaining in the foam at a given time is usually considered as a dynamic function:

$$\frac{V_l - V_l(t)}{V_f} \quad \text{Eq. [2-8]}$$

where $V_l(t)$ is the volume of liquid drained from the foam at a given time t .

2.1.3.1 Photographic methods

Video microscopy, which couples image capture boards with powerful computer tools, is one of the most useful methods to detect changes in foam structure (Calvert and Nezhati, 1987; Fains *et al.*, 1997). Images of the foam are captured at different times, from which the captured images can be transformed to determine the bubble size distribution and to monitor drainage as a function of time (Pugh, 2005). Typical data collected includes microscopy images of foam, bubble size graphs and bubble equivalent diameter at the 10th, 50th and 90th percentiles as a function of height (Pugh, 2005). A more advanced computer tool could also reveal the structural parameters, such as the relative thickness of the Plateau borders, junctions and films (Pugh, 2005). Some superior imaging devices include scanning (SEM) and transmission (TEM) electron microscopes. Preparation of a foam sample for observation in the SEM or TEM imaging generally requires freezing of the sample (Wilson, 1989).

2.1.3.2 Optical methods

A wet foam appears opaque, while a dry foam shows colours because rays of light are deflected or scattered by its bubbles and thin films (Boys, 1959; Vera *et al.*, 2001). Based on the scattering optics of foam, a variety of optical methods have been developed to study it, such as optical fibre-based methods, optical tomography, diffuse transmission spectroscopy and diffusing wave spectroscopy (Bergeron *et al.*, 2005; Pugh, 2005).

For optical fibre-based methods, a probe is used to detect the interfaces of bubbles based on the changes in light transmission. From this data, the chord lengths of foam cells can be obtained (Prud'homme and Khan, 1996). From optical tomography analysis, 3-D foam structure, including the volume, area and diameter of each bubble can be obtained (Pugh, 2005). Diffuse transmission spectroscopy is one of the most recent methods developed based on the measurement of the probability of an incident photon transmitted, from which analysis is made in terms of the structures responsible for scattering (Vera *et al.*, 2001). For diffusing wave spectroscopy, intensity fluctuations formed by multiple scattered light are measured rather than just the average (Vera *et al.*, 2001).

For laboratory-scale analytical instruments, Turbiscan is one of the optical analysers used for testing foam stability based on a multiple-light scattering approach. The analyser consists of a reading head which is equipped with a pulsed near infrared light source and transmission and backscattering detectors. The sample contained in a cylindrical glass measurement cell is scanned through by the reading head. The scanning acquires the transmission and backscattering data, from which the kinetic behaviour of the foam can be analysed (Mengual, 1999).

Optical methods are usually used in conjunction with an imaging device to allow direct visual observation. In general, image analysis and the correlations of the light reflectance changes with the dynamic properties of foam allow the study of drainage, coarsening, size distribution and motion of bubbles within the foam as a function of time.

2.1.3.3 Electrical resistance techniques

The electrical conductivity of foam is a useful property which can serve to characterise foam (Barigou and Davidson, 1994; Barigou *et al.*, 2001; Chang and Lemlich, 1980; Datye and

Lemlich, 1983; Maurdev, 2006). This method generally consists of a foam column fitted with electrodes along the column, which measure the foam conductance at different heights. Electrical conductivity measurements can also be used in conjunction with imaging devices, which provide information on the dynamic structure of foam as well as local foam conductance (and liquid fraction) as the foam evolves with time. A correlation of the conductivity data at various heights and liquid fraction can be obtained, where conductivity decreases at increasing height of the electrode due to the progressive decrease of the liquid content in the foam during foam decay (Pugh, 2005). Some models have also been proposed for the relation between foam conductivity and liquid fraction (Phelan *et al.*, 1996; Weaire *et al.*, 1995). Foam drainage profiles can also be measured to correlate foamability, foam stability and foam density with foam conductivity (Wilde, 1996).

2.1.3.4 Acoustical measurements

Acoustical measurements to study foam have also been reported (Ding *et al.*, 2007; Müller and Meglio, 1999; Vandewalle *et al.*, 2001). The method generally involves measuring sound radiation resulting from bubbles oscillations and bursts in foam using microphones, which are placed at different positions to measure the directional characteristic of the emitted sound. The corresponding spectra obtained from the recorded sound pressure and frequency signals can be analysed to determine the characteristics of an avalanching process of bubbles popping in a collapsing foam. This includes the destruction mechanisms of bubbles in foams, the bubble popping rate and the number distribution of bubble popping events. Micrographs showing size distributions of bubbles can also be obtained when image analysis is used in conjunction with acoustical measurements (Ding *et al.*, 2007; Vandewalle *et al.*, 2001).

2.1.4 Foam technology

Foam finds use in a wide range of industrial processes, such as detergents, cosmetics, food, fire-fighting agents, the petroleum industry and textile manufacturing (Prud'homme and Khan, 1996; Schramm, 2006). For many applications, foam possesses unique properties that make it superior to the traditional application of finite liquid droplets. Some examples and the major advantages of using foam as a replacement for water are outlined in the following sections.

2.1.4.1 Foam in the petroleum industry

In the petroleum industry, methods which employ steam or gas injection as the drilling fluid to drive oil out from a reservoir to a production well share a common difficulty stemming from the high mobility of the displacing agents which only sweep up the upper portion of the oil bearing zone, causing a reduced amount of oil recovered (Schramm and Novosad, 1990). To improve the sweep efficiency, foam acts as an effective displacing medium in the recovery of oil from the petroleum reservoir (Schramm and Novosad, 1992). The foam, which has an apparent viscosity higher than the displacing agent, reduces the gas mobility in the reservoir and diverts the displacing medium into the oil bearing zones that were previously unswept or underswept (Yan *et al.*, 2006).

2.1.4.2 Foam in the textile industry

The textile industry is another domain employing foams enormously, notably in the area of carpet dyeing, coating, dyeing and finishing operations (Turner, 1981). Spraying the finishing solution on the fabric has been traditionally used in textile processing, but the use of water as the vehicle for delivering chemicals to textiles has been hard hit due to the massive energy requirements for water-heating and water-evaporation operations (Wyles, 1978). The primary impetus for the development of foaming systems as a replacement for water systems was to achieve low wet pick-up and to conserve energy during processing (Bryant, 1979; Robert, 1982). Wet pick-up (WPU) indicates the weight of liquid taken up by a web of fabric and the energy required to dry the fabric. The lower the WPU, the lesser amount of water uptake by the fabric and the lower energy required to meet the drying requirements (Bryant, 1979; Ren, 2000). Foam with a relatively lower liquid volume fraction means that the water uptake by the fabric and the energy required to dry the fabric are reduced (Bryant, 1979; Turner, 1981). Product improvement was the parallel incentive for the development of the low wet pick-up concept (Robert, 1982). If as little as 10% water pick-up were applied, applying the chemicals (with the same 10% water) as foam increases the volume for the chemicals being applied which increases the chance for the chemicals to be distributed uniformly over the fabric (Robert, 1982; Turner, 1981). The air serves as a fluid extender to create a very large contact area between the chemicals and the fabric.

2.1.4.3 Foam in fire-fighting applications

As a fire-suppression agent in fire-fighting applications, foam has been widely used to extinguish fire, typically by smothering existing fires or when water is in short supply. Foaming agents used in fire-fighting, which contain surfactants that lower the surface tension of the foaming solution, enable foam to spread readily over the burning surface (Gardiner, 1998). In addition, the tendency of foam to adhere to surfaces of foam provides a blanketing and cooling effect for fire extinction (Perri and Conway, 1956). When water is in short supply, foam with a relatively low liquid volume fraction allows more efficient use of fire-fighting liquid (Magrabi, 2002). In addition, foam acts as a barrier to fume diffusion and thermal radiation, suppressing the spreading fumes and absorbing the heat emitted by the approaching fire (Magrabi *et al.*, 2000; Perkowitz, 2000).

2.1.4.4 Foam in the pharmaceutical and cosmetic industries

In the pharmaceutical sector, foam finds use in drug delivery applications as a carrier for active substances in topical formulations (Gottlieb *et al.*, 2003; Thomas *et al.*, 2000; Woodford and Barry, 1977). For effective topical administration, the applied agents must penetrate and permeate from one skin layer to another functionally and structurally different skin layer (Huang *et al.*, 2005). The use of foam as a vehicle for delivering therapeutic agents through the skin offers a number of dermatological advantages. Foam formulations provide emollient or drying functions to the skin (Tamarkin *et al.*, 2006b; Zhao *et al.*, 2010). They are less dense, and spread easily onto large areas of skin, with fewer residues remaining on the skin after application (Kealy *et al.*, 2008; Purdon *et al.*, 2003). More importantly, foam formulations have the ability to deliver a greater amount of drug with enhanced drug penetration and permeation through the skin layer, which also leads to an increase in efficacy (Huang *et al.*, 2005; Thomas *et al.*, 2000).

Foam has also become a prominent delivery system for cosmetically active substances (Arzhavitina and Steckel, 2010; Tamarkin *et al.*, 2006a). Foam characteristics such as large foam volume, good stability of foam, and slow foam drainage are critical for the functionality of foam cosmetic formulations. Some common products include shampoo, shaving foam, toothpaste and hair mousse. These products make use of foam to distribute the substances to enhance product application as required, for example, to keep the skin moistened by providing

enough rigidity to hold the fluid in place while using a relatively small amount of fluid (Arzhavitina and Steckel, 2010; Engels *et al.*, 1998).

2.1.4.5 Foam in cleaning

Foam also finds use in dust control (Cole and Taylo, 1991; Roe and Chen, 1997) and chemical cleaning processes (Brenner *et al.*, 1989; Simmons and Tulsa Okla, 1989). Foaming of cleaning and washing formulations provides immediate dust suppression by keeping the dust encapsulated within the foam (Mody and Jakhete, 1988). Foam is also particularly useful for cleaning and descaling industry equipment such as towers, large overhead lines and gas lines which cannot support the weight of liquids (Simmons and Tulsa Okla, 1989). Due to the need for complete contact of the inner surfaces of lines during the descaling operation, conventional methods usually consume excessive volumes of solvent. For foam cleaning, the ability to deliver the washing agent over a larger area and its strong adherence properties allow more efficient use of the washing agent and optimum contact with the entire inner surface of the tower or lines (Brenner *et al.*, 1989).

2.1.5 Foam-particle interactions

There are several applications involving foam-particle interactions which are specifically relevant to the incorporation of foam into a powder bed. This includes flotation of gold and paper inks (Churaev, 2005; Pugh, 2005; Ralston, 1983), suppression of dust on conveyor systems (Mody and Jakhete, 1988) and the use of particles to improve foam stability (Pugh, 1996). The presence of solid particles within the foam can promote foaming or defoaming, which can be desirable or undesirable depending on the specific demands of the application. These areas of foam-particle interactions are not the specific subject of this thesis, so they will not be discussed in detail here. Rather, the general effects of solid particles on foam properties will be discussed.

The presence of solid particles within the foam influences the foam properties in a complex way. Pugh (2005) demonstrated that the presence of particles with an intermediate critical degree of hydrophobicity and well-defined size will provide resistance to liquid drainage and contribute to foam stability. The particles stabilize foam by attaching themselves to the gas-liquid interface, modifying the radius of curvature of the gas-liquid film interface and causing

the decrease of pressure difference between the plateau borders and the three lamellae associated with it, leading to a more stable foam. The attached particles increase the tortuosity of the fluid drainage path and thus liquid passages become hindered in the film, causing retardation of drainage and film rupture (Pugh, 2005). Binks (2002) also claimed that foam stability can be enhanced by the presence of hydrophilic particles in the aqueous phase of the foam films due to the retarding effect on film drainage. In other cases, the use of hydrophobic particles was found to either increase the foam stability (Tang *et al.*, 1989) or decrease the foam stability (Garrett, 1979).

Foam stability is also dependent on particle size and concentration (Binks, 2002; Pugh, 1996; Tang *et al.*, 1989). Hudales and Stein (1990) found that larger particles of hydrophilic glass suspended in a CTAB solution (cetyltrimethylammonium bromide) enhanced foam stability, while smaller particles had no effect. Tang *et al.* (1989) found that the size and concentration of hydrophobic silica particles are the main control factors, where the stability of foaming SDSO₃ solution (sodium dodecyl sulfonate) increases with decreasing particle size and increasing concentration. For hydrophilic particles, Tang *et al.* (1989) found no apparent effect on the stability of foam.

Bindal *et al.* (2002) investigated the foaming ability without surface-active agents in a suspension of hydrophilic silica particles. The authors proposed that the colloidal particles stabilized the foam by arranging themselves into a layered structure between the gas bubbles, which provided resistance to bubbles coalescing (Bindal *et al.*, 2002). Kaptay (2003) studied the stabilizing criteria of foam by considering that the solid particles will form a certain structure by allocating themselves partly at the neighbouring gas-liquid interfaces and partly in the liquid gap between the interfaces when the gaseous bubbles interact with a number of solid particles. Kaptay (2003) claimed that foam stabilization requires a certain value of contact angle, which is a complex function of several parameters.

The existing studies of the effects of the wettability, size and concentration of solid particles on foam stability are conflicting. Perhaps foam stability is very dependent on the combined effects of the particle size and concentration and the surfactant type. From a colloid chemistry and physics point of view, parameters like surface tension, surface elasticity, surface viscosity, etc. have to be considered based on principles and theories concerning the interacting mechanisms

of stability, foam-particle interaction forces, and principles of attachment energies. These effects are described in detail in the references (Hunter, 2008; Pugh, 1996).

2.1.6 Foam flow in porous media

A porous medium or material is a solid matrix infused by interconnected pores (voids) which allows the transmission of the flow of fluid. Foam flow in porous media has been widely studied in many areas, especially in the petroleum industry. A wealth of literature describes the mechanisms of foam generation, destruction and transport in porous media and how the porous media controls foam texture and flow resistance (Gaughlitz *et al.*, 2002; Schramm, 1994b; Schramm, 2006). In powders, there is a distribution of pores acting as capillary tubes, drawing liquid into the interior of the powder bed. It appears that foam flow through the powder particles should be similar to foam flow in porous media.

In the context of foam flow in porous media, three fundamental pore-level in-situ foam generation mechanisms have been derived: “snap-off”, “lamella division” and “leave-behind” mechanisms (Dholkawala *et al.*, 2007; Gaughlitz *et al.*, 2002; Schramm, 1994b).

- Snap-off – a new gas bubble separated from the original gas by a liquid lamella is created when gas enters an initially liquid-filled pore

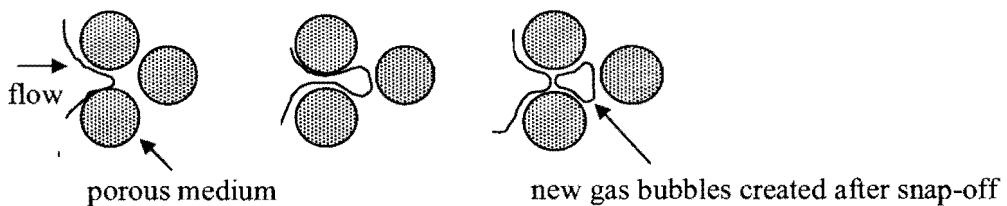


Figure 2-3 Schematic of the snap-off mechanism (reproduced from Schramm 1994).

- Lamellae division – a foam lamella is divided into two separate lamellae when the lamella meets a flow branch point

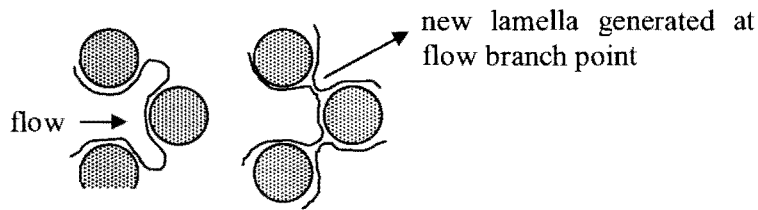


Figure 2-4 Schematic of the lamellae division mechanism (reproduced from Schramm 1994).

- Leave-behind – a foam lamella is created as two gas menisci pass through adjacent liquid-filled pore bodies

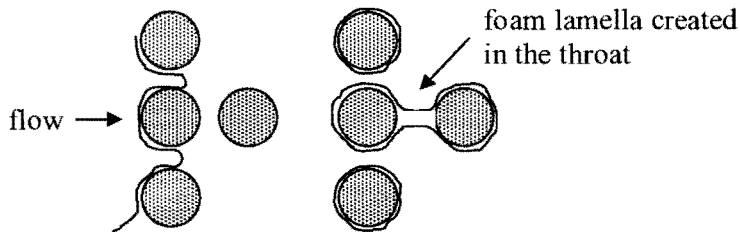


Figure 2-5 Schematic of the leave-behind mechanism (reproduced from Schramm, 1994).

The main mechanism responsible for foam destruction is capillary-suction coalescence – the merging of two films by a capillary pressure-induced phenomenon (Dholkawala *et al.*, 2007; Schramm, 1994a). As mentioned in *section 2.1.2.1*, higher capillary pressure in the film causes the liquid to flow from the films to the Plateau borders, eventually causing the film to thin and rupture. As a consequence of film instability, the liquid films move towards minimizing its surface energy by organizing itself into its minimal energy structures with the lowest interfacial area (Dholkawala *et al.*, 2007; Drenckhan *et al.*, 2005).

Keary and Shesky (2004) proposed that these mechanisms were also applicable to foam granulation (see *section 2.3*). It is not known how valid these mechanisms are in the foam granulation process, but the existing research expertise in these areas may indicate the relevant foam properties to be considered in foam granulation technology.

2.2 Wet Granulation

In wet granulation processes, powder particles are granulated into larger particles of improved physical and chemical properties through the use of a liquid phase and agitation forces. The process is generally considered to involve three sets of rate processes (Iveson *et al.*, 2001a):

- Wetting and nucleation
- Consolidation and growth
- Breakage and attrition

The first stage of wet granulation is wetting and nucleation, where the liquid binder first comes into contact with the powder bed, forming liquid bridges between the particles to hold them together into initial particle agglomerates (also called nuclei). Wetting commences by penetration (due to capillary action) or dispersion (due to mechanical mixing) of the liquid binder through the powder bed, causing nucleation of the particles into nuclei. The initial nuclei are often small and loose agglomerates (Iveson *et al.*, 2001a).

The consolidation and growth stage describes the growth of particles due to collisions with other particles or granules during granulation. This often results in the densification of granules, which also leads to the growth in granule size. For systems where insufficient liquid is added, consolidation and growth will not occur due to the low degree of liquid saturation of the granules, and the granule size is purely determined by the wetting and nucleation conditions (Iveson *et al.*, 2001a).

Breakage refers to the fracture of wet granules in the granulator while attrition refers to the fracture of dried granules in the granulator, drier or in subsequent product handling. Both processes will cause reduction in granule size due to impact or compaction in the granulator or during subsequent product handling (Iveson *et al.*, 2001a).

2.2.1 Wetting and nucleation

Wetting is defined as the first stage of liquid distribution, where the liquid first impacts on the powder surface. The initial wetting results in nucleation, where the particles are bound together by the liquid into loosely packed nuclei. Wetting and nucleation is generally considered to be the most critical stage for a variety of reasons:

- Poor wetting results in a mixture of over-wet and un-nucleated material, and leads to very poor nuclei size distributions (Litster *et al.*, 2001; Plank *et al.*, 2003)
- Poor initial nuclei size distributions often lead to poor final granule size distributions (Hapgood *et al.*, 2003)
- The phenomenon of wetting also influences the processes of fluids redispersion, component segregation and drying (Iveson *et al.*, 2001a)

In this section, we begin by describing the wetting and nucleation mechanisms, and discuss the phenomena of liquid penetration and dispersion during wetting and nucleation. We then look at the two important dimensionless groups – spray flux and penetration time, and present the nucleation regime map (Hapgood *et al.*, 2003). Note that these mechanisms have been developed for spray granulation, where the liquid binder is added as finely dispersed droplets.

2.2.1.1 Wetting and nucleation mechanisms

Iveson *et al.* (2001a) defined the wetting and nucleation process into four stages:

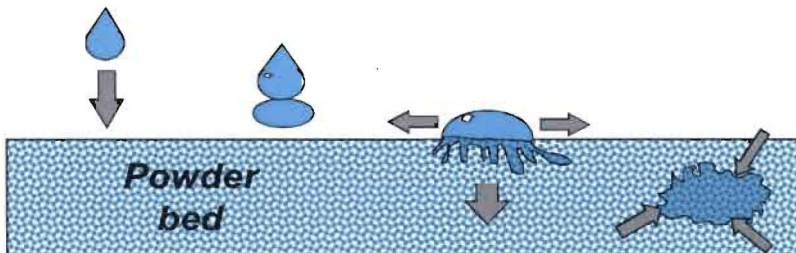


Figure 2-6 The four stages of wetting and nucleation (Iveson *et al.*, 2001a).

1. Liquid formation – liquid droplets are generated at some size distribution and frequency. The liquid can be distributed as different media, for example pouring, spraying, melt-granulation or foaming.
2. Liquid coalescence or overlap – liquid impacts on the powder surface, which may also coalesce at the powder bed surface or before impacting on the bed depending on the method of liquid formation.
3. Liquid spreading and penetration – liquid spreads across the bed surface and penetrates into the bed by wetting and capillary penetration, forming loosely packed nuclei.
4. Liquid dispersion – liquid is dispersed by mechanical mixing. Shear forces generated within the bed may break up clumps of wet materials to further distribute the liquid.

When the liquid wets the particles by capillary penetration or mechanical mixing, nucleation occurs to give a distribution of initial wetted aggregate – nuclei. Nuclei formation can be categorized into four main types of spreading phenomena in relation to the liquid and powder particle sizes and wetting characteristics (Hapgood *et al.*, 2007; Litster and Ennis, 2004):

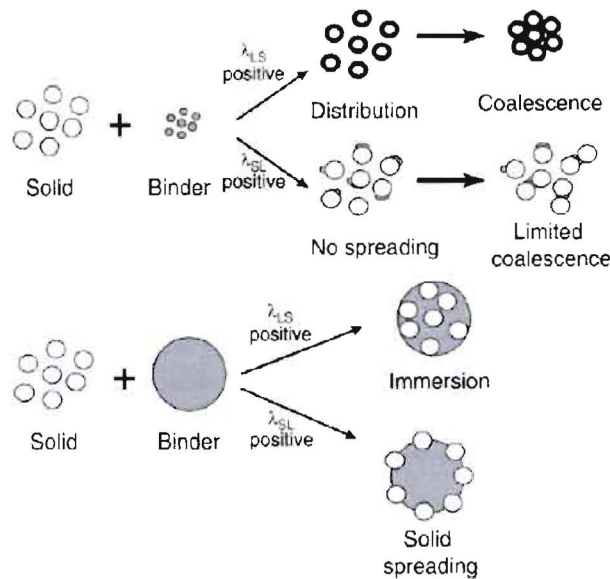


Figure 2-7 Different types of nucleation mechanisms (Hapgood *et al.*, 2007; Litster and Ennis, 2004).

For liquid droplets larger than the particles,

1. Immersion – the smaller solid particles are immersed by the liquid, producing nuclei with saturated pores.
2. Solid spreading – the wetting is thermodynamically favourable and the solid particles spread around the liquid. The nucleus formed is later defined as liquid marble (Hapgood and Khanmohammadi, 2009).

For liquid droplets smaller than the particles,

3. Distribution – the liquid distributes around the larger solid particles, producing wet particles that are not fully saturated and may have air trapped inside.
4. No spreading – the wetting is thermodynamically unfavourable and the solid particles do not spread around the liquid. There is limited coalescence when the wet particles collide with other dry particles.

The ability of the liquid binder to disperse and penetrate a powder mass is important in controlling the nucleation behaviour. The balance between liquid penetration and liquid dispersion via mechanical forces, which can be controlled by adjusting the process and/or formulation properties, will give rise to different nuclei formation behaviours, as described above. Formulation properties are described by the liquid penetration rate, which is set by wetting thermodynamics and kinetics (Hapgood *et al.*, 2002b; Hapgood *et al.*, 2003). Process variables are described by the dimensionless spray flux parameter (Litster *et al.*, 2001), which quantifies liquid distribution with volumetric flow rate, the average liquid drop size and the area of a powder bed exposed to incoming liquid. We will consider each of the phenomena of liquid penetration and liquid dispersion below.

2.2.1.2 Liquid penetration

Liquid penetration occurs spontaneously by capillary action when the liquid impacts the powder surface, wets and penetrates into the powder pores provided that the thermodynamics of the wetting are favourable and that the binder will always spread over the powder surface. The penetration of the drop then leads to the formation of a “nucleus”, and the nuclei properties depend strongly on the drop penetration time. The drop penetration time, t_p , is defined as the time taken for the drop to be fully drawn into the porous substrate with no liquid remaining on the surface (Hapgood *et al.*, 2002b).

As drop penetration is driven by capillary suction from the powder bed that contains a series of capillary pores, the average velocity at which liquid penetrates the pore can be described by the Washburn equation:

$$u = \frac{dh}{dt} = \sqrt{\frac{R\gamma_{LV} \cos\theta}{8\mu t}} \quad \text{Eq. [2-9]}$$

where h is the penetration height, t is the penetration time, R is the radius of the capillary, γ_{LV} is the surface tension, μ is the viscosity of the fluid and θ is the contact angle.

Consider that a drop of volume V_0 hitting the powder surface has a radius R_d equal to the radius of a spherical drop:

$$R_d = \left(\frac{3V_0}{4\pi} \right)^{1/3} \quad \text{Eq. [2-10]}$$

The volumetric flow rate is also given as:

$$-\frac{dV}{dt} = \pi R_d^2 \varepsilon u \quad \text{Eq. [2-11]}$$

where ε is the actual porosity of the bed.

Combining Eq. [2-9], Eq. [2-10] and Eq. [2-11], we have a differential equation for the volume of the drop at any time. The solution can be written in the form of:

$$V_l(t) = V_0 - \pi R_d^2 \varepsilon \left[\frac{R \gamma_{LV} \cos \theta}{2\mu} t \right]^{1/2} \quad \text{Eq. [2-12]}$$

By setting $V_l(t) = 0$ at complete drop penetration, the drop penetration time, t_p is given as:

$$t_p = 1.35 \frac{V_0^{2/3}}{\varepsilon^2 R} \frac{\mu}{\gamma_{LV} \cos \theta} \quad \text{Eq. [2-13]}$$

The drop penetration equation was derived separately by Middleman (1995) and Denesuk (1993), and was revised by Hapgood *et al.* (2002b) to estimate the drop penetration time for spray granulation applications. Hapgood *et al.* (2002b) introduced an effective porosity, ε_{eff} that takes account of the proportion of macrovoids that do not participate in fluid drainage.

The effective porosity, ε_{eff} is given as:

$$\varepsilon_{eff} = \varepsilon_{tap} (1 - \varepsilon + \varepsilon_{tap}) \quad \text{Eq. [2-14]}$$

where ε_{tap} is the tap porosity of the bed.

The effective pore radius is given as:

$$R_{eff} = \frac{\phi d_{32}}{3} \frac{\varepsilon_{eff}}{(1 - \varepsilon_{eff})} \quad \text{Eq. [2-15]}$$

where ϕ is the shape factor accounting for non-spherical shapes and d_{32} is the equivalent spherical diameter with the same surface to volume ratio as an irregular particle.

The drop penetration time can be calculated from the measurable properties of the powder and liquid. The drop penetration time is proportional to the viscosity of the liquid. Low viscosity liquid favours drop penetration, whereas high viscosity liquid corresponds to slow drop penetration times. For a given liquid viscosity, the drop penetration time is inversely proportional to the powder particle size. The coarser particle size is able to pack more closely, with the loose packing of the coarser particles closest to its tapped density compared to finer powder particle sizes, hence allowing a larger volume of liquid to penetrate through the powder structure. Clearly, drop penetration time is rapid when a small volume drop is involved (Hapgood *et al.*, 2002b).

The drop penetration time has been associated with the nuclei formation kinetics of a single drop. Several studies have found that the size of the nuclei granule is a direct function of the spray liquid droplet size (Ax *et al.*, 2008; Schaafsma *et al.*, 2000; Waldie, 1991; Waldie *et al.*, 1987). Ax *et al.* (2008) found that the drop size has a great influence on the granule size distribution. Using smaller nozzle sizes, which gave smaller drop sizes, produced smaller granules whereas using larger nozzle sizes or no nozzle (pouring) produced larger granules. Schaafsma *et al.* (2000) showed that the nucleation mechanisms and the resulting average granule size were significantly affected by the drop size and volume. A small nucleus was formed from one drop without drop coalescence. For many overlapping droplets, which consequently had a larger volume of liquid, large nuclei were formed.

2.2.1.3 Liquid dispersion

The nucleation behaviour depends strongly on the ability of the liquid binder to disperse as well as penetrate. The degree of liquid dispersion indicates the quality of the mixing between

the powder and the liquid, and is reflected directly in the nuclei and product size distributions. Attempts to describe the process of liquid dispersion across equipment scales have been made by characterising the relationship between liquid delivery rate and powder flux rate through the wetting zone. This is described by the dimensionless spray flux, ψ_a , which is defined as the ratio of the spray wetted area to the area flux of powder passing through the spray zone:

$$\psi_a = \frac{3\dot{V}}{2Ad_d} \quad \text{Eq. [2-16]}$$

where \dot{V} is the volumetric spray rate, A is the powder flux traversing the spray zone and d_d is the average drop diameter.

The dimensionless spray flux can be calculated from the measurable process properties. It is theoretically proportional to the volumetric spray rate of the liquid. Delivering the liquid at high volumetric flow rates corresponds to high spray flux conditions, which in turn results in larger agglomeration of the spray drops on the powder surface. For low spray flux conditions, the drops do not overlap onto each other and land individually on the powder surface. For a given liquid delivery rate, the dimensionless spray flux is inversely proportional to the powder flux and average drop diameter. Increasing the powder flux generally avoids significant overlap of drops hitting the powder bed (Hapgood *et al.*, 2004; Litster *et al.*, 2001). Although atomisation of liquid into finely dispersed droplets is intended to aid uniform drop distribution, it appears theoretically that over-atomisation can actually have an opposite effect (Plank *et al.*, 2003).

The dimensionless spray flux quantifies the density of drops landing on the powder surface, which is intended to capture the effects of drop overlap in the spray zone on the nucleation conditions and to provide a qualitative measure of the nucleation conditions and hence granulation. Experimental work was carried out investigating liquid distribution using the dimensionless spray flux, and it was found that changes in the dimensionless spray flux correlate with a measurable difference in powder surface coverage, which in turn influences the nuclei distribution (Hapgood *et al.*, 2004; Litster *et al.*, 2002; Litster *et al.*, 2001). The experimental studies showed that high spray flux conditions produced broad size distributions

due to drop overlapping effects. Operating granulation at low spray flux conditions reduces drop overlap and produces narrow size distributions (Hapgood *et al.*, 2004; Litster *et al.*, 2002; Litster *et al.*, 2001). This was proven further by performing Monte-Carlo simulations to model the fraction of the spray zone covered by droplets (Hapgood *et al.*, 2004). The scenario of drop distribution was simulated, and it was shown that a low dimensionless spray flux resulted in well-dispersed droplets that tend not to overlap while high dimensionless spray flux led to agglomeration of spray drops due to high spray density (Hapgood *et al.*, 2004).

The correlation between the dimensionless spray flux and the nuclei size distribution was also verified through a modelling study (Wildeboer *et al.*, 2005). The simulations extended the dimensionless spray flux by accounting for the effects of nuclei spreading and coalescence, as well as non-uniform spray patterns. Simulation results of nuclei coverage in the spray zone matched closely to the experimental data performed by Hapgood *et al.* (2004), showing that the dimensionless spray flux correlates well with the nuclei size distributions (Wildeboer *et al.*, 2005).

2.2.1.4 Nucleation regime map

We have seen how liquid penetration and liquid dispersion can affect nucleation conditions as separate processes through the penetration kinetics and the dimensionless spray flux. Combining the effect of the drop penetration time and the dimensionless spray flux, Hapgood *et al.* (2003) proposed a nucleation regime map, as shown in Figure 2-8, to describe the different nucleation conditions.

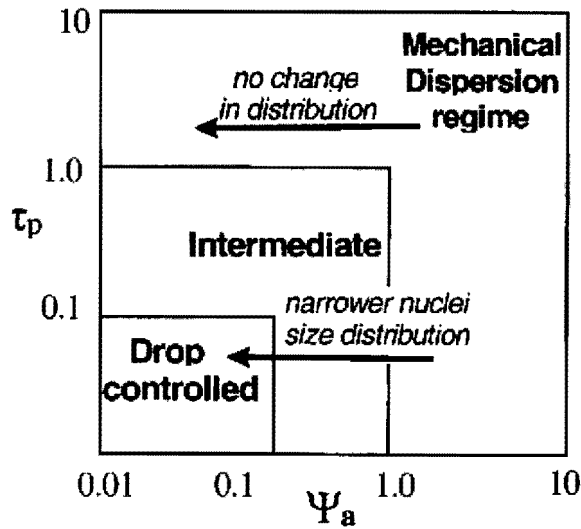


Figure 2-8 Nucleation regime map (Hapgood et al., 2003).

The nucleation regime map introduced a parameter, known as the dimensionless penetration time:

$$\tau_p = \frac{t_p}{t_c} \quad \text{Eq. [2-17]}$$

where t_p is the drop penetration time and t_c is the circulation time, which is the time taken for the powder to re-enter the spray zone.

The nucleation map shows three nucleation regimes: the drop-controlled, intermediate and mechanical dispersion regimes, which are defined by the relationship between the dimensionless spray flux (shown on the horizontal axis) and the dimensionless penetration time (shown on the vertical axis).

1. *Drop controlled*: each individual drop penetrates the powder bed to form one nucleus, which is characterised with low values of τ_p and ψ_a .
2. *Intermediate*: this regime is characterised with an intermediate τ_p and ψ_a between the drop controlled and mechanical dispersion regimes.

3. *Mechanical dispersion*: each drop is slow to penetrate the powder bed, and large nuclei or wet clumps are formed from many overlapping drops. Liquid distribution and breakage of these wet materials relies on the shear forces developed within the powder bed. This regime is characterised either with a high τ_p or a high ψ_a (or both).

In cases of good wetting and drop-controlled nucleation, liquid penetration is the predominant process (Hapgood *et al.*, 2002b; Hapgood *et al.*, 2003). The liquid must quickly wet into the powder to allow a single nucleus to be produced per drop (Hapgood *et al.*, 2002b; Hapgood *et al.*, 2003). The formation of a single nucleus from a single drop of liquid leads to a narrower nuclei size distribution. In general, small drops, low-viscosity fluids, porous powders, large powder pores, high surface tension and low contact angle favour good nucleation conditions (Hapgood *et al.*, 2002b).

Drop-controlled nucleation also requires low spray flux conditions (controlled by process properties as mentioned in *section 2.2.1.3*) as well as rapid penetration of liquid into the powder mass (controlled by formulation properties as mentioned in *section 2.2.1.2*). In general, low spray flux conditions are produced by atomising the liquid at a low liquid delivery rate and maintaining intensive mixing to improve liquid-powder interactions (Hapgood *et al.*, 2004).

In contrast, if the liquid does not wet the powder easily or if the penetration becomes too slow, large and highly saturated nuclei will be produced due to drop coalescence, which then leads to a broad nuclei size distribution. For slow penetrating systems (given by large drops, highly viscous liquid, low surface tension and high contact angle), or high spray flux (given by high liquid delivery rate and poor liquid-powder interactions), mechanical forces are important in controlling liquid distribution and nucleation conditions (Hapgood *et al.*, 2004).

2.2.2 Consolidation and growth

As nuclei are agitated during the granulation processes, they experience collisions with each other and with equipment surfaces. These collisions densify the granule, gradually saturating the granule pores. This process, which is referred to as consolidation, makes the granules stronger. When the granule pores are fully saturated, the granules begin to grow rapidly.

In this section, we begin by describing granule consolidation, followed by the different types of granule growth, and then present the growth regime map that defines the different growth regimes for granulation (Iveson and Litster, 1998b; Iveson *et al.*, 2001b).

2.2.2.1 Granule consolidation

Granules consolidate as they experience agitation and collisions with each other and with equipment surfaces. Sufficient granule consolidation will reduce their size and porosity, and may even squeeze the liquid to their surfaces. As a result, the granules become stronger, less deformable and even elastic in nature (Iveson and Litster, 1998a).

Granule consolidation affects the granule growth mechanisms. If the granules are slow to consolidate, the granules are slow to grow. As granules consolidate, the saturation of the granule pores increases and liquid will be gradually squeezed to the granules surface, enabling strong bonds to form between granules without the need for large amounts of deformation. This aids granule growth by coalescence, which can trigger rapid granule growth (Iveson and Litster, 1998a; Iveson *et al.*, 2001b). However, granule consolidation also increases granule yield stress generally, which in turn decreases the amount of deformation and the likelihood of coalescence (Iveson and Litster, 1998a). Overall, the net effect of consolidation depends strongly on the formulation properties.

Experimental work and modelling of granule consolidation have studied the effect of formulation properties, including particle size, liquid viscosity, liquid surface tension and liquid content (Ennis *et al.*, 1991; Iveson and Litster, 1998a; Iveson *et al.*, 1996). Decreasing particle size and/or increasing binder viscosity decreases the consolidation rate constant due to the increase in capillary, viscous and frictional forces (Iveson and Litster, 1998a; Iveson *et al.*, 1996). However, the effects of liquid viscosity and liquid content are highly interactive. Iveson and Litster (1998a) found that increasing the amount of a low viscosity liquid (water) may serve to lubricate the inter-particle contacts, increasing the extent of consolidation. Conversely, increasing the amount of a high viscosity liquid (glycerol) increases the viscous resistance to consolidation, which causes the granules to consolidate to less of an extent (Iveson and Litster, 1998a). Iveson and Litster (1998a) also found that lowering the liquid surface tension increased the granule consolidation rate, but the granules consolidate to less of an extent. There is a tendency for granules to dilate as well as consolidate during granule impacts, which

depends strongly on the complex interaction of capillary, viscous and inter-particle frictional forces.

2.2.2.2 Granule growth

Granule growth can be classified into a number of types of growth behaviour. The two broad classes of granule growth are steady growth and induction growth. Steady growth refers to the growth of granules at a steady rate, which means the rate of growth is approximately constant. Induction growth has been variously referred as the “nuclei” (Kapur, 1978), “no growth” (Smith and Nienow, 1983) or “compaction” (Hoornaert *et al.*, 1998) stages, where granules experience little growth or no growth for an induction period followed by a period of rapid growth. Other types of behaviour include “dry” free flowing behaviour, nucleation only, crumb behaviour and overwetting. For “dry” free flowing behaviour, particles remain dry and mostly un-nucleated. Nucleation only behaviour refers to the formation of nuclei granules from the liquid-addition phase without further granule growth (Butensky and Hyman, 1971). Crumb behaviour refers to the formation of a loose crumb material that is constantly breaking and reforming. Overwetting refers to the formation of oversaturated slush or slurry due to excessive liquid addition. These various types of granule growth are illustrated in the granule growth regime map (Iveson and Litster, 1998b; Iveson *et al.*, 2001b), which is presented in *section 2.2.2.5*).

For a particular system, the type of granule growth behaviour can be characterised as a function of two parameters: the maximum liquid pore saturation attained and the amount of granule deformation during impact (Iveson and Litster, 1998b; Iveson *et al.*, 2001b). We will introduce the two parameters below and describe how granules grow depending on the two parameters with the growth regime map (Iveson and Litster, 1998b; Iveson *et al.*, 2001b).

2.2.2.3 Maximum liquid pore saturation

When granule pores are saturated with liquid, granules begin to grow as they collide with each other. Therefore, the liquid saturation of the granule pores is an important parameter that influences the behaviour of granule growth. The maximum liquid pore saturation, S_{\max} is given as:

$$S_{\max} = \frac{w\rho_s(1-\varepsilon_{\min})}{\rho_l\varepsilon_{\min}} \quad \text{Eq. [2-18]}$$

where w is the mass ratio of liquid to solid, ρ_s is the solid density, ρ_l is the liquid density and ε_{\min} is the minimum porosity of the formulation attained.

Increasing the liquid content or decreasing the porosity increases the liquid pore saturation. At low liquid contents, the powder mass behaves as a dry powder. A slight increase in the liquid content promotes nuclei granule formation, but there is insufficient moisture for further growth. Weak granules that are highly deformable may also form, behaving like a loose crumb material that continually breaks and reforms. The powder may become a wet mass or display induction growth, steady growth or rapid growth when the maximum liquid pore saturation is reached, but it also depends on the amount of deformation during granule collisions (see *section 2.2.2.4*).

2.2.2.4 Stokes deformation number

As granules collide, they may coalesce or rebound, which decides whether granules will grow. This depends on the amount of granule deformation during collisions, which is characterised by a Stokes deformation number, St_{def} :

$$St_{def} = \frac{\rho_g U_c}{2Y_d} \quad \text{Eq. [2-19]}$$

where ρ_g is the granule density, Y_d is the dynamic yield stress and U_c is the representative collision velocity in the granulator. Both granule density and dynamic yield stress are measurable properties that correspond to the characteristic porosity reached by the granules in the granulator. The collision velocity in the granulator represents some sort of average velocity, which can be estimated for different types of process equipment (see Table 2-1).

Table 2-1 Estimates of U_c for different types of granulators (Litster and Ennis, 2004).

Type of granulator	Average U_c	Maximum U_c
Fluidized beds	$\frac{6U_b d_p}{d_b}$	$\frac{6U_b d_p}{d_b l_b^2}$
Tumbling granulators	ωd_p	ωD_{drum}
Mixer granulators	$\omega_i d_p, \omega_c d_p$	$\omega_i D_i, \omega_c D_c$

In Table 2-1, U_b is the bubble velocity, d_p is the particle diameter, d_b is the bubble size, l_b is the spacing between two bubbles, ω is the drum rotational speed, D_{drum} is the drum granulator diameter, ω_i and ω_c are the impeller and chopper speeds and D_i and D_c are the impeller and chopper diameters.

The Stokes deformation number is a measure of the ratio of the impact kinetic energy to the granule strength. For formulations which begin saturated, a weak system with granules that are highly deformable (high St_{def}), a slurry will form. For an intermediate strength system (intermediate St_{def}), steady growth will occur for granules that are sufficiently deformable. A low deformation system (low St_{def}) will display induction growth. The system may also behave as a dry powder mass, a crumb material or nucleation only, depending on the interaction between the Stokes deformation number and the liquid pore saturation. Section 2.2.2.5 describes the way that these two parameters influence the type of granule growth behaviour with the growth regime map, which also summarizes the effect of formulation and process properties on the granule growth behaviour (Iveson and Litster, 1998b; Iveson *et al.*, 2001b).

2.2.2.5 Granule growth regime map

Iveson *et al.* (1998b; 2001b) plots the relationship between the maximum pore saturation (shown on the horizontal axis) and the Stokes deformation number (shown on the vertical axis) on the granule growth regime map (see Figure 2-9). Figure 2-9 shows the different granule growth regimes and the effect of different variables on the position of a formulation on the growth regime map.

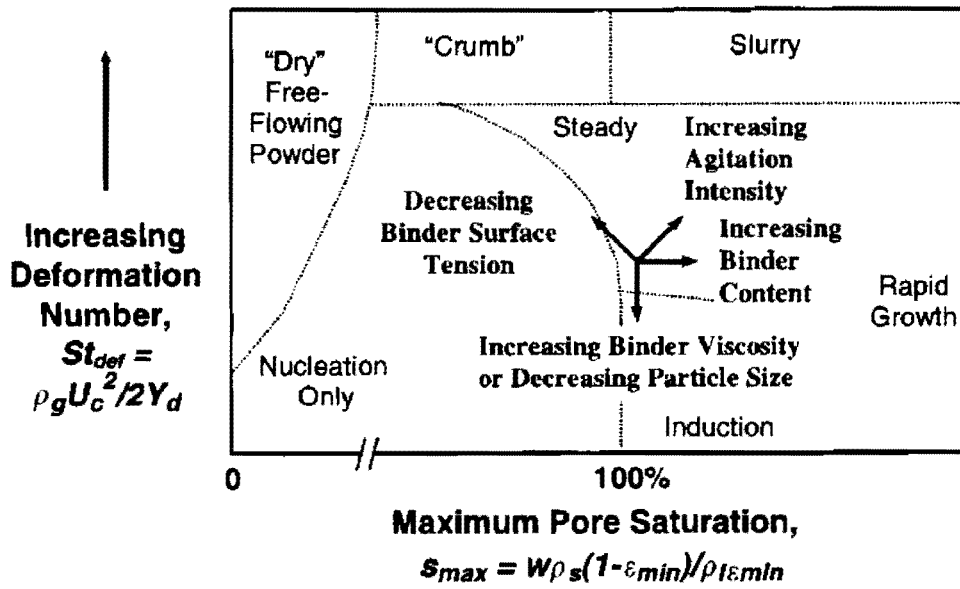


Figure 2-9 Granule growth regime map (Iveson and Litster, 1998b; Iveson *et al.*, 2001b).

The regime map illustrates the effects of major parameters such as liquid surface tension, particle size, liquid viscosity, agitation intensity and liquid content on the growth behaviour of granules. In summary:

- Decreasing liquid surface tension and/or increasing particle size decreases Y_g (hence increases St_{def}), which causes the system to be more likely to display steady growth, crumb or nucleation behaviour.
- Increasing liquid viscosity and/or decreasing particle size often results in induction granule growth behaviour.
- Increasing process agitation intensity increases U_c (hence increases St_{def}), which makes the system more likely to exhibit steady growth, rapid growth or causes the formation of an overwetted slurry (for $S_{max} > 100\%$) or a crumb material (for $S_{max} < 100\%$).
- Increasing the liquid content (increasing S_{max}) increases the granule growth rate, promoting granule growth from induction to steady growth or rapid growth (intermediate St_{def}) or the formation of an over-wetted slurry (for high St_{def}).

Granule growth behaviour is closely related to granule consolidation and deformation behaviour. As mentioned earlier, granules deform and consolidate when they collide, which is then followed by different types of granule growth behaviour. However, the growth of granules will occur when the adhesive forces between them are large enough to resist the separation

forces when they collide. Consolidation and coalescence are closely related, and granule growth must also consider whether the colliding granules will result in coalescence or rebound during their collision. Granule coalescence is considered in *section 2.2.2.6*.

2.2.2.6 Granule coalescence

If the granules are able to stick together when they collide, they will grow by coalescence. For successful granule coalescence, the kinetic energy of impact must be dissipated during collision so that the granules do not rebound, and the bond formed at the contact between the colliding granules must be strong enough to resist subsequent separation.

The success of coalescence can be measured by the viscous Stokes number, St_v . There are two models describing granule coalescence, proposed by Ennis *et al.* (1991) initially and later modified by Liu *et al.* (2000).

Ennis *et al.* (1991) modelled granule coalescence for non-deformable granules. The viscous Stokes number is given as:

$$St_v = \frac{4\rho_g U_c d_g}{9\mu} \quad \text{Eq. [2-20]}$$

where ρ_g is the granule density, U_c is the collision velocity, d_g is the granule diameter and μ is the liquid viscosity.

Ennis *et al.* (1991) considered that granule coalescence occurs when the viscous Stokes number is below the critical Stokes number, St_v^* which is defined as:

$$St_v^* = \left(1 + \frac{1}{e_r}\right) \text{Ln}\left(\frac{h_b}{h_a}\right) \quad \text{Eq. [2-21]}$$

where e_r is the coefficient of restitution, h_a is the height of surface asperities and h_b is the liquid layer thickness.

All colliding granules will result in granule coalescence growth for $St_v \ll St_v^*$.

Coalescence growth requires a low St_v and a high St_v^* , which can be promoted by increasing the liquid content and the liquid viscosity and decreasing the impact velocity. However, these changes also indirectly influence St_v^* . Increasing the liquid viscosity and decreasing the impact velocity will reduce the rate of consolidation (see *section 2.2.2.1*), which inhibits coalescence by decreasing St_v^* . This depends on the final ratio of St_v to St_v^* .

Liu *et al.* (2000) extended the model to include the effect of granule deformation. The modified viscous Stokes number is given as:

$$St_v = \frac{4\tilde{m}U_c}{3\pi\mu\tilde{D}^2} \quad \text{Eq. [2-22]}$$

where \tilde{D} is the harmonic mean granule diameter, \tilde{m} is the harmonic mean granule mass, U_c is the collision velocity and μ is the liquid viscosity.

Considering the effect of granule deformation during coalescence, the Stokes deformation number, St_{def} is given as (Liu *et al.*, 2000):

$$St_{def} = \frac{\tilde{m}U_c^2}{8\tilde{D}^3Y_d} \quad \text{Eq. [2-23]}$$

where \tilde{D} is the harmonic mean granule diameter, \tilde{m} is the harmonic mean granule mass, U_c is the collision velocity and Y_d is the plastic yield stress.

Liu *et al.* (2000) considered four different types of behaviour during collision as a function of the viscous Stokes number and the Stokes deformation number. Depending on the relative magnitudes of both parameters, the colliding granules may coalesce without surface contact, coalesce with elastic collisions, coalesce with plastic deformation, or they may rebound (Liu *et*

al., 2000). A detailed explanation of St_v versus St_{def} , showing regions of rebound and coalescence, is covered in the reference (Liu *et al.*, 2000).

2.2.3 Breakage and attrition

Granules break and attrite due to the forces of impact, wear or compaction in the granulator or by the handling of the granules. Basically, the process of breakage plays an important role in enhancing the material distribution and final strength of the granules, which helps to improve the properties of the granular products.

Breakage is the least understood of the three granulation rate processes, but the study of breakage has increasingly emerged over the recent years. In this section, we will consider the conditions for granule breakage and describe breakage from a process perspective, specifically the role of different variables on breakage in the granulator. More fundamental studies on breakage at the granule scale, specifically concerning the bonding forces and the strength of granules are given in other references (Hapgood *et al.*, 2007; Reynolds *et al.*, 2005; Salman *et al.*, 2007b).

2.2.3.1 Conditions for granule breakage

There are very few models available to predict conditions for granule breakage. For successful breakage, Tardos *et al.* (1997) considered that the applied kinetic energy during an impact must exceed the energy required for breakage. This analysis leads to the criteria to predict granule breakage, where the Stokes deformation number, St_{def} (see Eq. [2-19]) must exceed the critical value of the Stokes number, St_{def}^* , for breakage:

$$St_{def} \gg St_{def}^* \quad \text{Eq. [2-24]}$$

Granule breakage is promoted by a high Stokes deformation number. A low Stokes deformation number is associated with little breakage. However, there is very limited knowledge for testing the model at present and the fundamental basis for predicting breakage remains a developing area.

2.2.3.2 Effects of material and process variables on breakage at the process scale

There is very little quantitative theory available to predict the effect of material and process variables on granule breakage. Rather, this section considers the role of material and process variables on breakage behaviour indirectly, as inferred from the variations of some ensemble properties such as the granule average size, granule size distribution and the granule's susceptibility to breakage. The variables include liquid viscosity, liquid content, primary particle size, and impeller and chopper speed.

Eliassen *et al.* (1998) found that a low viscosity liquid results in weaker granules, which makes them more susceptible to breakage during the granulation process. More recently, van den Dries *et al.* (2003) found that increasing the viscosity increases the granule strength, which leads to a reduction of granule breakage. The effect of liquid viscosity on granule strength, which is affected by granule consolidation, is inter-related to liquid content (see *section 2.2.2.1*). A logical consequence is that increasing the liquid content (of low viscosity liquid) reduces the granule porosity. This generally results in an increase in granule strength, and hence a higher resistance to breakage.

The effect of viscosity on breakage may also be related to the primary particle size. Johansen and Schaefer (2001) reported that a larger primary particle size has to be granulated with a high viscosity liquid in order to obtain a granule strength that is sufficient to avoid breakage. Similarly, van den Dries *et al.* (2003) found that a decreasing particle size increases the granule strength, which leads to a decrease in granule breakage.

Changes in impeller or chopper speed often give rise to variations in granule average size and granule size distribution, from which granule breakage can be detected. Knight *et al.* (2000) and Eliassen (1999) reported that high impeller speeds increased granule breakage. Knight (1993) found that increasing the chopper speed reduces the width of the granule size distribution, but causes an increase in the average granule size. Schaefer *et al.* (1992) found that increasing the chopper speed causes a reduction in the average granule size and the width of the granule size distribution. An ambiguous influence of the impeller and chopper speeds on both the average granule size and the granule size distribution has been reported, but a decrease in the mean granule size or a reduction in the spread of granule size distribution in fact reveals

little about the breakage behaviour. It may be insufficient to solely rely on the changes in the granule size for granule breakage (Iveson *et al.*, 2001a).

2.3 Foam Granulation

Foam technology was introduced and patented by The Dow Chemical Company (Midland, MI) in 2003 for delivering aqueous binder systems in wet granulation applications. The inventors, Dr. Paul Sheskey and Dr. Colin Keary (who has previous expertise in the area of foams) came up with the concept of utilising foam for wet granulation processes. Foam granulation was first applied in the pharmaceutical industry for manufacturing tablets (Keary and Sheskey, 2004), and later it was tested using food model systems by the food industry (Miao *et al.*, 2009). Subsequently, additional work has been carried out to fine-tune the technology for the area of direct relevance to pharmaceutical applications (Sheskey *et al.*, 2006; Sheskey *et al.*, 2004a; Sheskey *et al.*, 2004b). Other potential application areas are continuous granulation (PharmTech.com, 2008) and the coating of tablets using foam (Sheskey *et al.*, 2009).

Foam granulation is gaining acceptance in the pharmaceutical industry (Dow, 2008), but it is currently more of an art than a science, and in practice it remains as a developing area. In this section, we will summarise the major research work done on foam granulation and address the need of further research for improving foam granulation technology from art to quantitative engineering.

2.3.1 Pioneering work on foam granulation

The pioneering work on foam granulation in 2004 reported a series of case studies which tested different commercial formulations, including one formulation that is highly sensitive to water addition and one formulation using binders with low surface activity (Keary and Sheskey, 2004). Later, direct scale-up of foam granulation from laboratory to pilot to manufacturing was demonstrated for both immediate-release and controlled-release model formulations (Sheskey *et al.*, 2007). The groundbreaking work has successfully created granules and tablets that were on-target at laboratory, pilot and manufacturing scales, and has demonstrated the operating potential and process flexibility inherent in foam granulation technology in the manufacture of pharmaceutical drugs.

To generate the foamed solution, a foam generator (Dow Wolff Cellulosics, USA) is set up with a pressure pot. The foam is made by passing air into liquid solution via the foam generator. Using the foam generator, the liquid solution and the compressed air can be mixed at a controlled ratio to produce the desired foamed binder. The foamed solution can be delivered at a controlled addition rate via a rigid plastic pipe connected with the foam generator onto the powder bed (not shown).

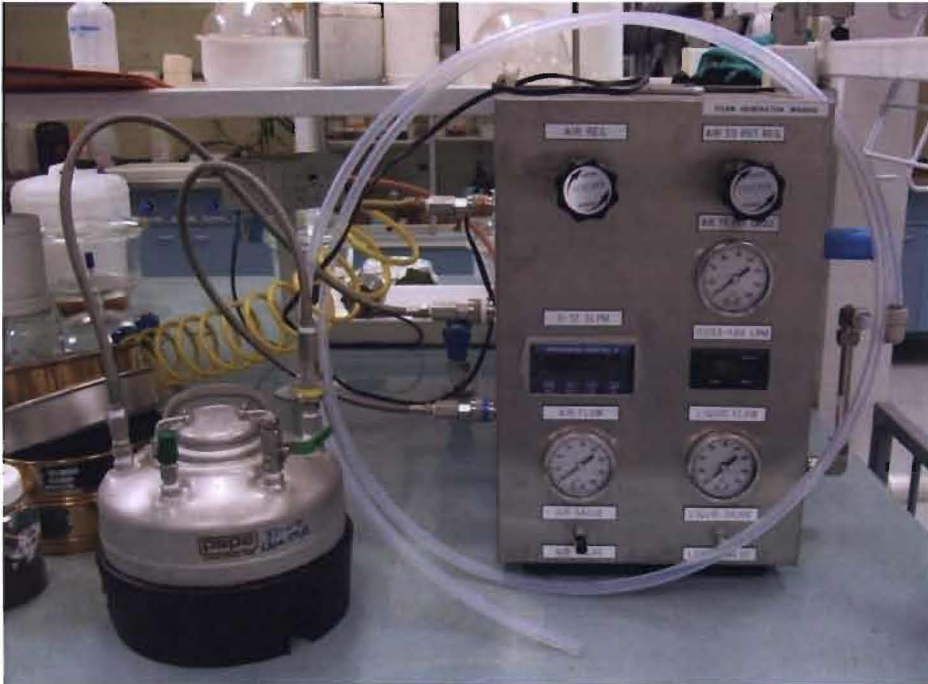


Figure 2-10 Equipment setup for foam generation – (right) foam generator and (left) pressure pot.

Figure 2-10 shows the foam generator and pressure pot. Pressurised air is supplied to the foam generator and the air is used to drive the liquid solution from the pressure pot into the foam generator. The air and liquid are mixed together at a junction, and the mixture is then passed through a packed meshed column to create a uniform foam. Valves are used to control the flowrates of the air and liquid.

By mixing the liquid solution with compressed air at a fixed delivery rate, the liquid solution can be made into an aqueous foam at a controlled foam quality. As given by Eq. [2-7], foam quality, FQ, is equivalent to the ratio of gas volume to total foam volume (Keary and Sheskey, 2004; Simmons and Tulsa Okla, 1989). The lower the gas content, the lower the foam quality.

In general, “wet foams” are defined as low quality foams, while “dry foams” are defined as high quality foams with lower liquid contents.

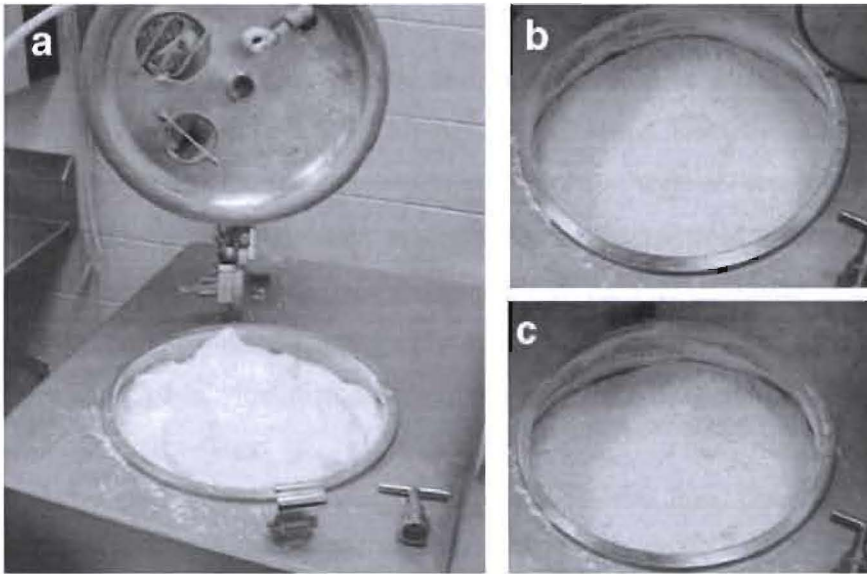


Figure 2-11 Foam granulation process showing (a) initial addition of foam (b) foam dispersion after one minute of mixing (c) after two minutes, all foam has been dispersed (Sheskey *et al.*, 2003).

Figure 2-11 shows photos of the batch foam addition process (Sheskey *et al.*, 2003), where the foam is added to the top of the dry powders contained in a 65-litre high shear granulator (a). After one minute of mixing (b), the majority of the foam is dispersed. After 2 minutes mixing time (c), no foam is visible.

Some key findings in the studies include (Keary and Sheskey, 2004; Sheskey *et al.*, 2007):

- Binder addition method: Foam is added to the granulator bowl at any location where it will not interfere with the powder flow or the blade, either as part of the granulator charging process or during operation, which simplifies the liquid addition process and eliminates spray nozzles entirely. Problems with selecting the correct nozzle, nozzle angle, drop size, nozzle location and arrangement are eliminated.
- Liquid binder amount required: Foam granulation was achieved with a lower liquid/binder usage compared to spray granulation, which was advantageous to granulating water-sensitive formulations and reducing drying and manufacturing times.

- Granulation process: Impeller torque profiles show faster processing and lower binder requirements for foam binder addition as compared to spray processes. Foam agglomeration commences instantly and achieves the endpoint torque in a shorter time than spray processes.
- Granule formation: Powders were uniformly granulated at a wider range of binder addition rates without any large lumps of overwetted and dry, non-agglomerated powders. Similar distribution and properties of granules were achieved.
- Scale-up: Scale-up was simplified as a result of reduced scaling issues such as nozzle placement, the number of nozzles and potentially the rate of binder addition. Liquid distribution was maintained adequately and process control was good on scale-up. Granule, tablet or in vitro dissolution properties of the drug products between scales were similar and on-target.
- Drug containment: Dusting was suppressed by the added foam layer and thereby drug losses due to dusting were minimized.
- Drug uniformity: Foamed binders distribute extremely low dose drugs with improved dose uniformity, which addresses one of the most challenging problems in the pharmaceutical industry (Sheskey *et al.*, 2004a; Sheskey *et al.*, 2004b).

Keary and Shesky (2004) also proposed a working hypothesis of a foam granulation mechanism to explain successful case studies of foam granulation. From the mechanisms described earlier for foam flow in porous media (see *section 2.1.6*), Keary and Shesky (2004) explained that the capability of foam to create new bridging lamellae between powder particles can act as a branch point for bubble regeneration when the lamellae are contacted by free gas or foam. The authors (2004) also mentioned the 'low wet pick-up' property of foam from the concept in the fabrics industry that could allow foam to penetrate dense materials. In addition, another crucial property of foam is that the bubbles in foam will keep flowing on the wet surface and will collapse and wet the surface only when it reaches a dry section (Turner, 1981).

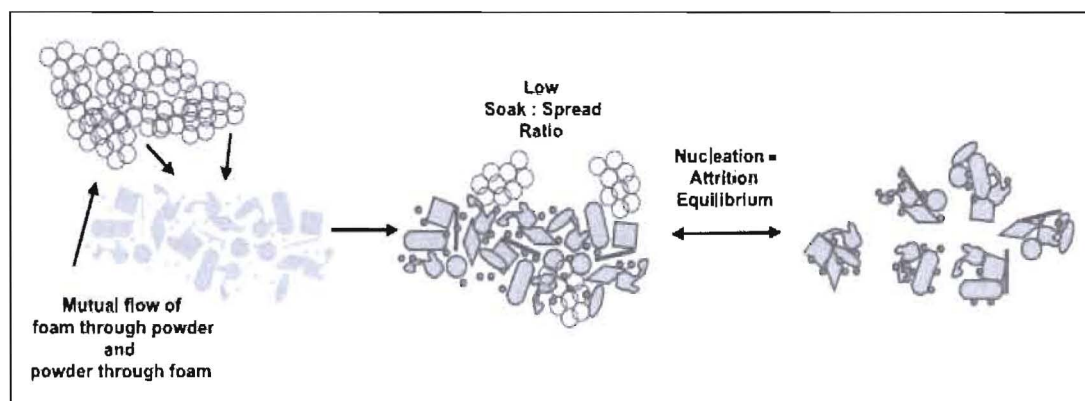


Figure 2-12 Nucleation process in foam granulation proposed by Keary and Sheskey (2004).

Combining these aspects, Keary and Shesky (2004) hypothesized that foam spreads through the powder bed more than it soaks into the bed (Figure 2-12). The low soak to spread ratio allows more binder solutions to be delivered over a large area, so particle surfaces are covered quickly. Additionally, excellent mutual flow between foam and powder phases enables rapid spreading and efficient particle coverage as compared to a drop of binder solution. However, interactions between foam and powder particles in this manner have not been reported in the literature and there are numerous details of this mechanism that remain to be studied.

Cantor *et al.* (2009) has evaluated the influences of foam and conventional binder deliveries (where the binder was added using a using a peristaltic pump) on the granulation physical and mechanical properties of high drug load formulations. The study was carried out using three representative model drug formulations – acetaminophen (APAP), metformin and aspirin, which are brittle, viscoelastic, and ductile respectively. Some key differences in the physico-mechanical properties of the drug manufactured by the two modes of binder delivery include:

- For APAP formulation, foam granulation improved the granule plasticity.
- For aspirin formulation, foam granulation produced a mixed deformation mechanism, showing plastic and brittle characteristics.
- For metformin formulation, conventional wet granulation improved the granule plasticity.
- No major differences in surface area and pore size between the different granulation batches.

The authors also claimed that the increase in plasticity for foam granulated formulations was possibly due to the improved surface coverage of the binder on the drug particles. While different mechanical properties were found for drug formulations exhibited different deformation characteristics, the authors concluded that the knowledge of the intrinsic mechanical properties of the drug can be useful as a guide to the selection of an appropriate granulation process to improve a drug product's manufacturability (Cantor *et al.*, 2009).

2.3.2 Some unique challenges with the use of foam granulation

The DOW Chemical Company has been leading the development of foam granulation technology. The early trial experiments successfully demonstrated some of the benefits and improvements compared to spray granulation on several formulations, as well as the simplicity of foam granulation scale-up from laboratory to pilot and manufacturing scale equipment (as outlined in *section 2.3.1*). However, there are numerous areas and unique challenges with the use of foam granulation that remain to be addressed:

- The experiments were conducted on complex pharmaceutical formulations, in commercial equipment, and lack general applicability.
- A mechanism of foam-powder interaction and nucleation is proposed, but the work is speculative. Until the foam nucleation mechanisms are better understood, foam granulation technology will have restricted application as a high-risk, trial-and-error granulation technique.
- The use of foam in pharmaceutical granulation processes is a new and unique approach, which is often challenging to gain global acceptance as the pharmaceutical industry is very conservative when it comes to new applications.

For foam granulation to be a generally accepted granulation approach, experiments on model systems are required to understand foam-powder interactions, to illuminate the variables controlling foam nucleation behaviour, and to determine the mechanisms controlling the foam granulation process. This thesis will address the current short-comings outlined above (also see *Chapter 1*).

2.4 Literature Summary

The subject of foam has attracted scientific interest for over one hundred years. A wealth of literature exists on the topic of foam formation, foam stability and foam properties. The widespread importance of foams has also powerfully established itself in a large variety of industrial branches. It is seen that the use of foam has increasingly emerged in many technological processes, with so many advantages to be gained by processing with foam systems that potentially foam technology may gradually replace water systems.

Over the years, the knowledge about wet granulation has significantly advanced from a black art to quantitative engineering. Continuous efforts have precipitated a large volume of work studying granulation of materials including minerals, foods and pharmaceuticals in equipment ranging from fluidised beds to high shear mixer-granulators. The understanding is now at the point where it can be directly used for rational particle design based on careful formulation and characterisation and manipulation (Litster, 2003).

Research into granulation as well as foams are an enormous, active and evolving research areas. Both disciplines are very well established, with a wealth of information published in the literature. However, the correlation between foam and granulation is still not well known. Foam granulation is obviously still in the early stages of development, and it remains a fertile area for research and development.

CHAPTER 3
SINGLE NUCLEUS FORMATION

Monash University

Declaration for Thesis Chapter 3

In the case of Chapter 3, contributions to the work involved the following:

Name	% contribution	Nature of contribution
Melvin X.L. Tan	80	Key ideas, Experimental development, Results interpretation & Writing up
Ling Shyong Wong	10	Experimental development & Results interpretation
Kwan Hoe Lum	10	Experimental development & Results interpretation
Dr. Karen Hapgood	Supervisor	Initiation, Key ideas, Editing and reviewing

Declaration by co-authors

The undersigned hereby certify that:

- (1) they meet the criteria for authorship in that they have participated in the conception, execution, or interpretation, of at least that part of the publication in their field of expertise;
- (2) they take public responsibility for their part of the publication, except for the responsible author who accepts overall responsibility for the publication;
- (3) there are no other authors of the publication according to these criteria;
- (4) potential conflicts of interest have been disclosed to (a) granting bodies, (b) the editor or publisher of journals or other publications, and (c) the head of the responsible academic unit; and
- (5) the original data are stored at the following location(s) and will be held for at least five years from the date indicated below:

Location(s)

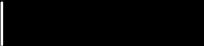
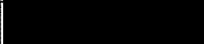
Department of Chemical Engineering, Monash University, Clayton Victoria 3800 Australia.

Signature 1

Signature 2

Signature 3

Signature 4

	Date
	
	
	
	

3 SINGLE NUCLEUS FORMATION

This chapter looks at single nucleus formation on static powder beds. The kinetics of single foam penetration into loosely packed powder beds were studied, and compared to the penetration of single drops. The impact of primary particle size and the binder concentration on the wetting and nucleation behaviour was investigated. A transformation map is presented to explain the quantitative results. Qualitative observations were made to examine foam penetration behaviour and the nuclei formed.

Publication: Tan, M.X.L., Wong, L.S., Lum, K.H., Hapgood, K.P., (2009). *Foam and drop penetration kinetics into loosely packed powder beds*. Chemical Engineering Science 64: 2826-2836.

Acknowledgements: The experiments with glass ballotini powders and initial data analysis were performed by Ling Shyong Wong and Kwan Hoe Lum as part of the CHE4118 Undergraduate Research Project, Department of Chemical Engineering, Monash University.

3.1 Introduction

The study of foam granulation begins with the examination of single nucleus formation on static powder beds, which involves placing small amounts of foam on loose powder beds representing the powder bed surface in a granulator. This technique is well established from studying nuclei formation with droplets, which is already seen as a useful test to understanding nucleation (Hapgood *et al.*, 2002b). The study can be extended to foams to determine the important properties controlling wetting and nucleation behaviour via foams, and to determine the similarities and differences from drop-induced wetting and nucleation. In this chapter, there are two important parameters to be considered: specific penetration time, t_{sp} , and nucleation ratio, K .

Penetration time is an important parameter controlling wetting and nucleation in the spray granulation process (see *section 2.2.1.2*). The penetration time is defined as the time required for the complete collapse of the foam or the complete disappearance of the drop from the powder surface. In this study, the mass of a liquid drop and the mass of the foam varied.

Therefore, the penetration time was normalized with respect to the fluid mass to obtain the specific penetration time, which is defined as the penetration time per unit mass of fluid added and is represented by:

$$t_{sp} = \frac{t_p}{m} \quad \text{Eq. [3-1]}$$

where t_p is the penetration time and m is the fluid mass.

The efficiency of fluid distribution within the powder bed to form nuclei can be reflected by the amount of powder nucleated per unit of fluid added, which is termed the “nucleation ratio”. A large nucleation ratio indicates more efficient wetting and nucleation by the liquid and hence less liquid is required to granulate a given mass of powder (Schaafsma *et al.*, 2000). In this study, the nucleation ratio is defined in terms of the nucleation mass ratio, K :

$$K = \frac{M_n}{M_f} \quad \text{Eq. [3-2]}$$

where M_n is the nuclei mass and M_f is the fluid mass.

In *Chapter 2*, we reviewed the interactions between foams and solid particles from several applications and how particles interact with foam in several research studies. However, none of the mentioned processes utilize foam the same way as in foam granulation, and the existing research has mainly focused on the foam without much concern for the particle phase. The subject of foam flow in porous media is well known, but what about when the porous media is a static powder bed? The key question to be answered in this chapter is: what happens when a small amount of foam is placed on a powder surface?

3.2 Experimental

3.2.1 Materials

Three grades of glass ballotini powders (AC, AE and AH, Potter Industries, Australia) and two different size distributions of lactose monohydrate (100 mesh and 200 mesh, Wyndale, New Zealand) were used in the experiments.

Particle size distribution and particle density data were based on vendor specifications. The bulk density and tapped density were determined in a 25ml measuring cylinder. By sifting a known weight of powder into the measuring cylinder, the bulk density was determined as the mass of the powder divided by the total volume that the powder occupies. By manually tapping the cylinder until the volume of the powder remained constant, the tapped density was determined as the mass of the powder divided by the volume of the powder occupies after tapping.

A loosely packed powder bed was prepared by sieving the particular powder into a petri dish, and the bed surface was scraped smooth using a metal spatula. The dimensions of the petri dish and the powder weight added to each dish were measured to calculate the bed porosity using Eq. [3-3]:

$$\varepsilon = 1 - \frac{V_{particle}}{V_{bed}} \quad \text{Eq. [3-3]}$$

where ε is the porosity of the powder bed, $V_{particle}$ is the volume of the particles (calculated by the division of the mass over the true density of the powder) and V_{bed} is the volume of the powder bed.

Table 3-1 summarises the properties of the powders used in the experiments.

Table 3-1 Powder properties.

Powder	Grade	Particle size distribution (μm)	Particle density (g/cm^3)	Bulk density (g/mL)	Tapped density (g/mL)	Loose packed porosity (-)
Glass ballotini	AC	125-250	2.47	1.4	1.4	0.41-0.44
	AE	90-150	2.47	N/A	N/A	0.37-0.44
	AH	45-90	2.47	1.4	1.5	0.43-0.47
Lactose monohydrate	100 mesh	75-250	1.54	0.65	0.88	0.54-0.58
	200 mesh	75-180	1.54	0.46	0.68	0.67-0.82

Several concentrations of hydroxylpropyl cellulose, HPC (100,000Mw, Sigma Aldrich, Australia), and hydroxylpropyl methylcellulose, HPMC (Methocel E3PLV, Dow Wolff Cellulosics, USA), were used to vary the fluid viscosity in the foam and drop penetration experiments. Liquid binders were prepared by dispersing HPC/HPMC powders in distilled water according to the required binder concentration (3% and 6% HPC; 4%, 6%, 8% and 10% HPMC). A small amount of food dye (Queens Fine Food Ltd., Australia) was added to the solutions to assist the visibility of fluid penetration.

The foam quality produced by the Airspray foam dispenser was estimated by dispensing the foam into a measuring cylinder and allowing it to drain under gravity with time. The initial volume of foam was measured and the liquid content of the foam was determined by measuring the volume of liquid obtained after the foam had collapsed into liquid in the measuring cylinder. Foam quality was estimated according to Eq. [2-7]. Table 3-2 summarizes the properties of the liquid binders used in the experiments.

Table 3-2 Liquid binder properties.

Liquid binder	wt% of binder in water (%)	Viscosity (mPa.s)	Density (g/mL)	Foam quality (%)
HPC	3%	5	0.943	87
	6%	80	0.954	51
HPMC	4%	7.9	0.961	92
	6%	18.7	0.986	90
	8%	40.6	1.015	83
	10%	82.5	1.026	76

3.2.2 Methods

Drop and foam penetration experiments were performed with a 6mL syringe and a handheld Airspray 150mL foam dispenser respectively. The Airspray foam dispenser is a plastic container with a special dispenser cap that can incorporate a certain amount of air into the solutions to enable the foaming of fluids. A picture of the foam dispenser is illustrated in Figure 3-1. The foam dispenser/syringe was clamped at 2cm above the bed surface for the binder fluid to detach and fall onto the powder bed to minimize the impact of the height of fall. The powder bed was placed on the balance so that the amount of fluid added could be measured, as illustrated in Figure 3-1.

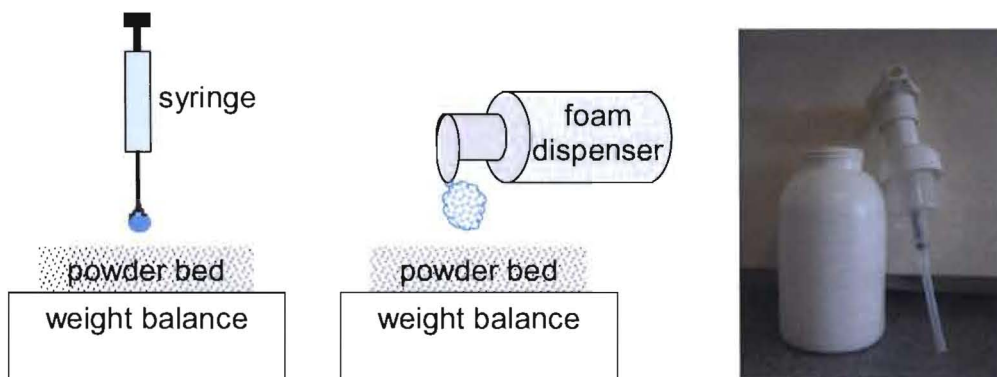


Figure 3-1 (left) Drop penetration experiment (middle) Foam penetration experiment (right) Foam dispenser.

The penetration time was measured using a stopwatch, which in conjunction with the fluid mass measurement (by the balance) enabled the calculation of the specific penetration time according to Eq. [3-1].

Nuclei collection was performed by placing the sieve on top of the dish and inverting them, which allowed the nuclei to be sieved out from the powder bed. The nuclei were extracted with care to minimize the loss of nuclei mass. Each excavated nucleus was weighed. The nucleation ratio was obtained by plotting the mass of dried nuclei versus the mass of fluid added according to Eq. [3-2].

For selected experiments, the process of foam penetration into powder beds was recorded using a Motic SMZ168 optical microscope to observe foam penetration behaviour. From the captured images, the propagated front of the drainage and spreading when foam impacts on the powder surface was estimated using ImageJ software.

3.3 Results

3.3.1 Foam and drop specific penetration times

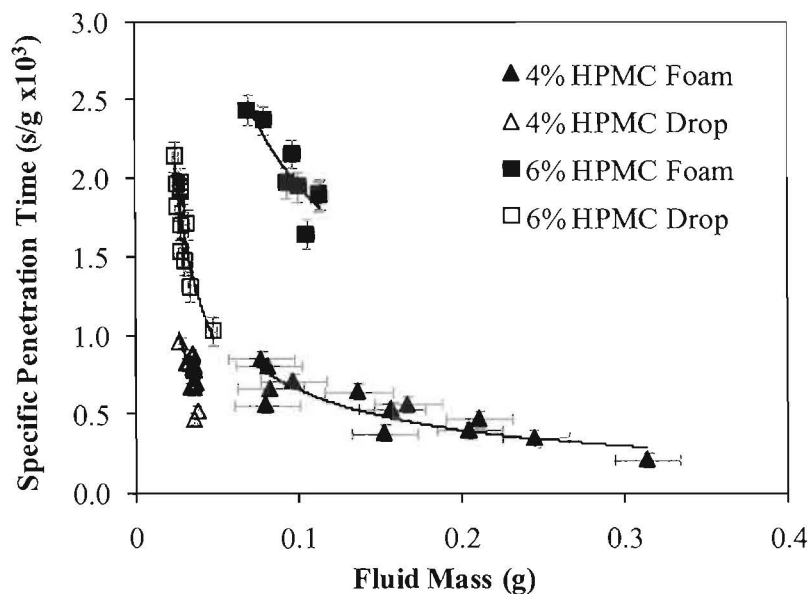


Figure 3-2 Comparison of specific penetration times between HPMC foam and drop penetrations on 200 mesh lactose.

Figure 3-2 compares the foam and drop specific penetration times for HPMC binder fluid on 200 mesh lactose powder. The trends for both foam and drop addition methods are similar when specific penetration time are plotted against fluid mass. Despite the small ranges of fluid mass for some fluid–powder systems, it can be seen that specific penetration time increases with decreasing fluid mass for both foams and drops. This may be attributed to the fact that liquid drained out from foam films will also be absorbed into the powder mass, which is similar to the drop penetration process.

The results indicate that at a given specific penetration time, a much greater mass of binder fluid can be absorbed for foam delivery compared to drop delivery. This is clearly an advantage for foam granulation. As both liquid binder and foam properties are interactively affecting the penetration time, we cannot reach any general conclusions at this stage until the roles of both liquid binder and foam properties on the overall penetration times are clearly determined.

There were many changing variables, such as the powder structure and the binder fluid mass, which need to be taken into consideration when comparing the penetration time between foam and drop penetrations. Nonetheless, the similar trend of specific penetration time between foam and drop penetrations suggests that liquid drainage, one of the characteristic of foam, plays a vital part in the mechanism of foam imbibition into powder pores. This will be further examined in *Chapter 4*.

3.3.2 Effect of particle size on foam specific penetration time

Fluid penetration into the bed depends on the size distribution of pores in the powder bed, and changing the powder particle size may assist or restrict the fluid flow. This is investigated by using glass ballotini powders and lactose powders with various particle sizes to alter particle packing and porosity of the bed.

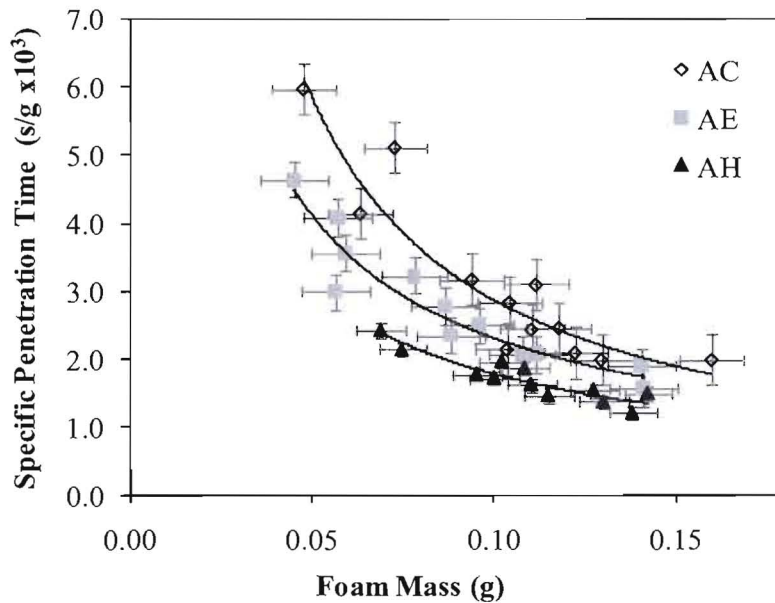


Figure 3-3 Effect of glass ballotini powder particle size on specific penetration times for 10% HPMC foamed binders.

Figure 3-3 shows the results of foam penetration into glass ballotini. It is seen that the penetration of 10% HPMC foam into AC grade (coarse) glass ballotini powder requires the longest specific penetration time, followed by the penetration on AE grade (medium) and AH grade (fine) glass ballotini powders.

For 4% HPMC foam penetration, Figure 3-4 indicates that the penetration shows little difference between the three grades of glass ballotini. It is probable that 4% HPMC penetration into the different grades of glass ballotini was relatively quick, and the small differences between the resultant penetration times are swamped by the data variation. Note that the fitted trendline shows the largest specific penetration time occurred with the coarsest powder beds (AC grade).

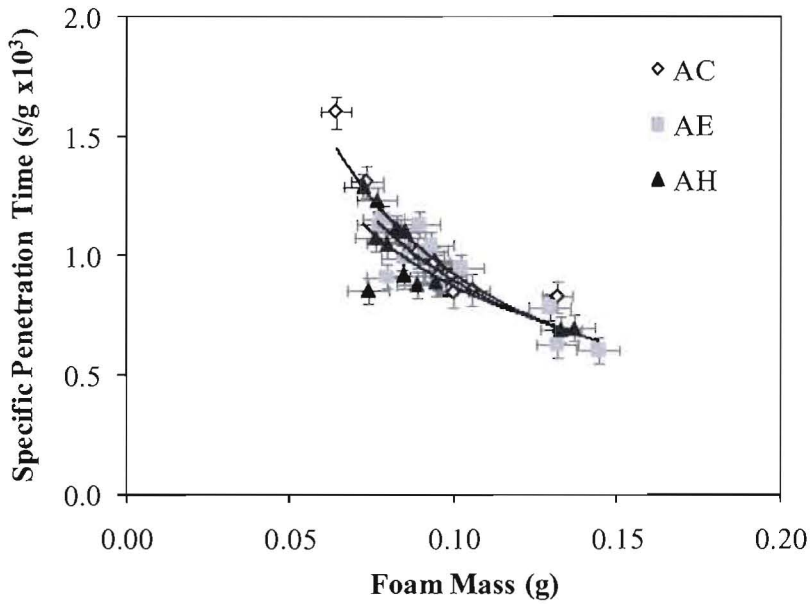


Figure 3-4 Effect of glass ballotini powder particle size on specific penetration times for 4% HPMC foamed binders.

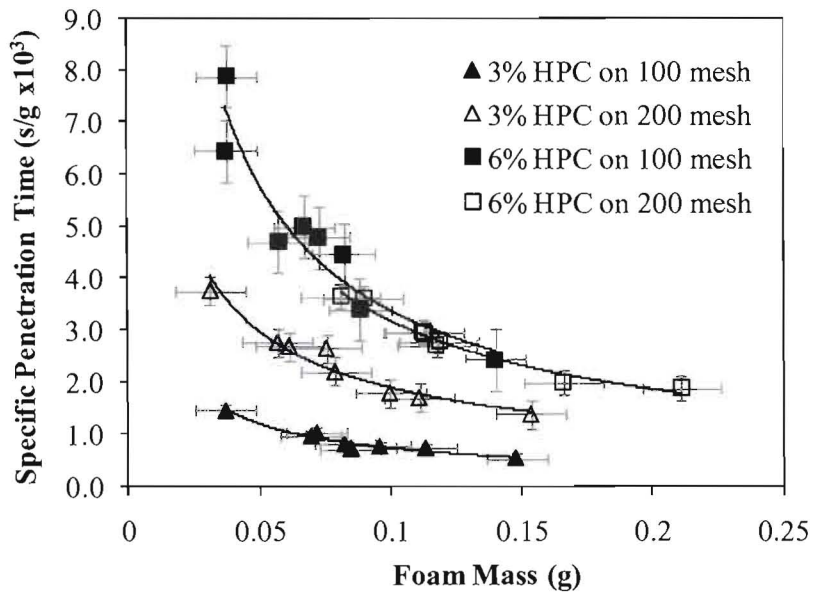


Figure 3-5 Effect of lactose powder particle size on specific penetration times for HPC foamed binders.

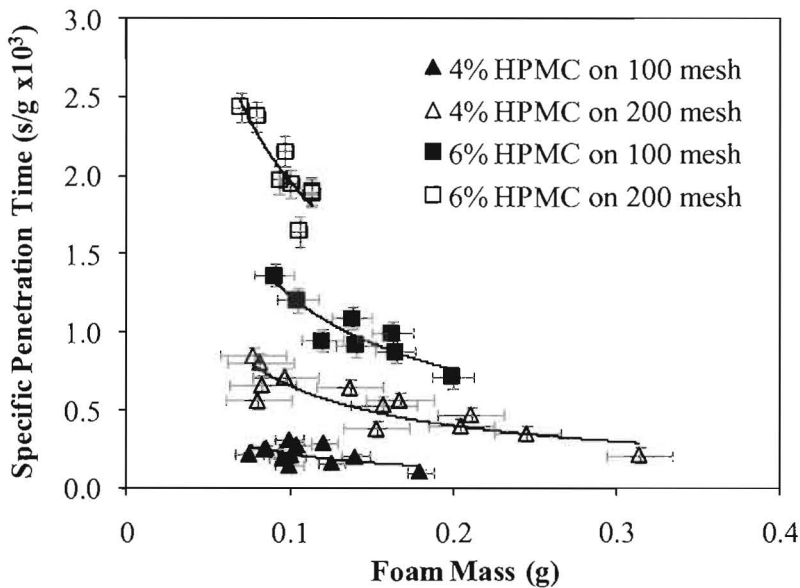


Figure 3-6 Effect of lactose powder particle size on specific penetration times for HPMC foamed binders.

Figure 3-5 and Figure 3-6 show the effect of lactose powder particle size on specific penetration times for HPC and HPMC foamed binders, respectively. The results show clear differences between the specific penetration times on 100 mesh (coarse) and 200 mesh (fine) lactose powders. For both foamed HPC and HPMC binders, powder beds prepared with 100 mesh lactose powder permits faster foam penetration compared to the 200 mesh lactose powder. For 6% foamed HPC, the comparatively close specific penetration times between the dispersions on 100 mesh and 200 mesh lactose are most likely due to the viscosity effect which appears to have been the dominant variable, masking any powder size impact. Nonetheless, the results shown in Figure 3-5 and Figure 3-6 indicate that powder beds prepared with coarse lactose particles generally allow faster penetration into the powder pores compared to fine lactose particles.

According to the drop penetration time equation (Eq. [2-13]), penetration time is inversely proportional to the pore size. Large pore sizes accommodate larger volumes of fluid and permit faster fluid drainage. Powder beds prepared with coarser particles should contain larger pores within the powder bed, which allow for shorter penetration times, as it was seen previously. Additionally, the coarse lactose is more free flowing and less porous than the fine fraction,

which is indicated by both the tapped density and the loose packed porosity data in Table 3-1. The coarse lactose bed structure was fairly homogenous, and relatively few macrovoids were present in the powder bed as the loose packing of the coarse lactose was closest to its tapped density. It was observed during the preparation of the powder beds that the surface packing of 200 mesh lactose was quite non-uniform even after scraping it level, reflecting the higher Hausner ratio (defined as the ratio of the actual porosity to the tapped porosity) for this powder (Hapgood *et al.*, 2002b). In practice, the liquid front will tend to halt when a macrovoid is present which is usually the case for irregularly packing powder beds (Hapgood *et al.*, 2002b). The presence of macrovoids appears to have contributed to the slow penetration times observed for 200 mesh lactose powder.

The effect of particle size on foam specific penetration time can be quite dramatic, but the results are contradictory between glass ballotini and lactose powder. Generally, the bed structure of glass ballotini always remains homogenous with low Hausner ratio (Hapgood *et al.*, 2002b). In this case, the larger number of pores contained within the smaller size fractions have a higher capillary driving force that induces faster liquid penetration, as seen for the penetrations into AH grade glass ballotini.

It is hard to vary porosity without changing powder pore size and vice versa as they are closely related in practice. As the true powder pore size is not accurately known, precise prediction of the effect of particle size on penetration time is difficult.

3.3.3 Effect of binder concentration on foam specific penetration time

The effect of binder properties on foam specific penetration time can be predicted using the existing drop penetration theory. It is clearly seen from Figure 3-5 and Figure 3-6 that specific penetration time increases in proportion to the binder concentration, as the increasing fluid viscosity slows the velocity of liquid penetration. This is consistent with the drop penetration time equation, where penetration time is proportional to viscosity (Eq. [2-13]).

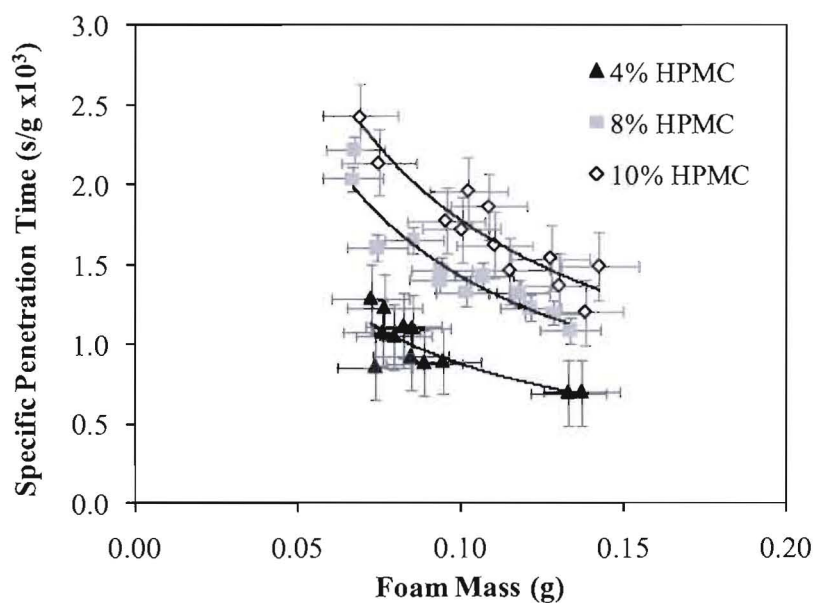


Figure 3-7 Effect of binder concentration on specific penetration times for HPMC foam penetrations on AH grade glass ballotini powders.

For glass ballotini powders, the same trends were obtained. As seen from Figure 3-7, the penetration of 10% HPMC foam into AH grade glass ballotini powder results in the largest specific penetration time, followed by 8% HPMC and 4% HPMC foams. For other grades of glass ballotini powder, the results are consistent (see Figure 3-8 and Figure 3-9).

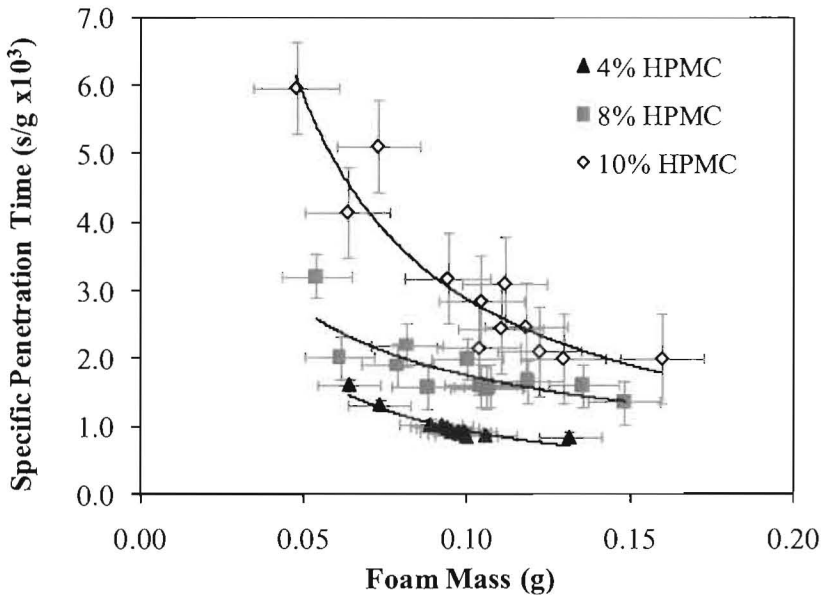


Figure 3-8 Effect of binder concentration on specific penetration times for HPMC foam penetrations on AC grade glass ballotini powders.

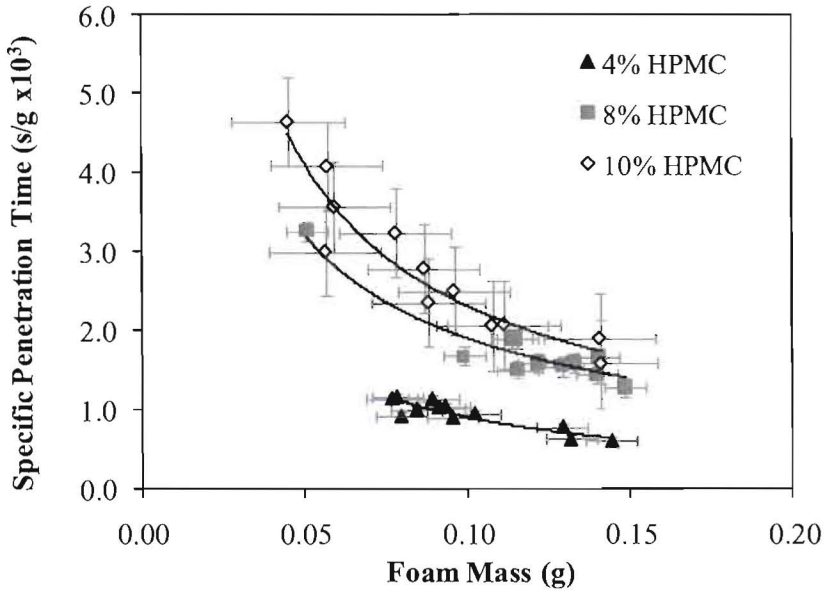


Figure 3-9 Effect of binder concentration on specific penetration times for HPMC foam penetrations on AE grade glass ballotini powders.

At this stage, it is unclear whether foam viscosity and/or foam quality are responsible for the change in penetration time, as both variables are affected by changes in the binder concentration. The viscosity of foams is dependent upon both the foam quality and the liquid-phase viscosity, which are critical in determining foam penetration time. Foam quality is expected to play a key role in foam induced wetting and nucleation, as it defines the percentage of gas contained within the foam and is related to the flowability of the fluid and thus the penetration time. This will be examined in *Chapter 4*.

Results in this study have assumed that the gas drawn in and contained within the foam, by the foam dispenser, is approximately equal, although in practise the amount of air probably decreases as the fluid viscosity increases. For a fixed amount of air incorporated, viscous solutions will produce highly elastic foams (Keary and Sheskey, 2004) and will have a lower tendency to foam compared to less viscous solutions. Low viscosity solutions are easy to foam and often can result in stable foams of high quality and high density. Therefore, 6% HPC foam is expected to have a lower foam quality than 3% HPC foam. This is also indicated by the estimated foam quality data in Table 3-2. As a general rule, increasing viscosity of the liquid from which the foam is prepared decreases the drainage rate of foams and stabilizes the foams (Pugh, 1996). In this case, foam specific penetration time was affected by both binder concentration and foam quality.

3.3.4 Foam and drop nucleation ratios

When binder fluid is brought into contact with powder, the particles are nucleated by the fluid to form granules. The efficiency of foam nucleation in terms of the mass of nuclei formed per mass of fluid added is examined by considering the nucleation ratio.

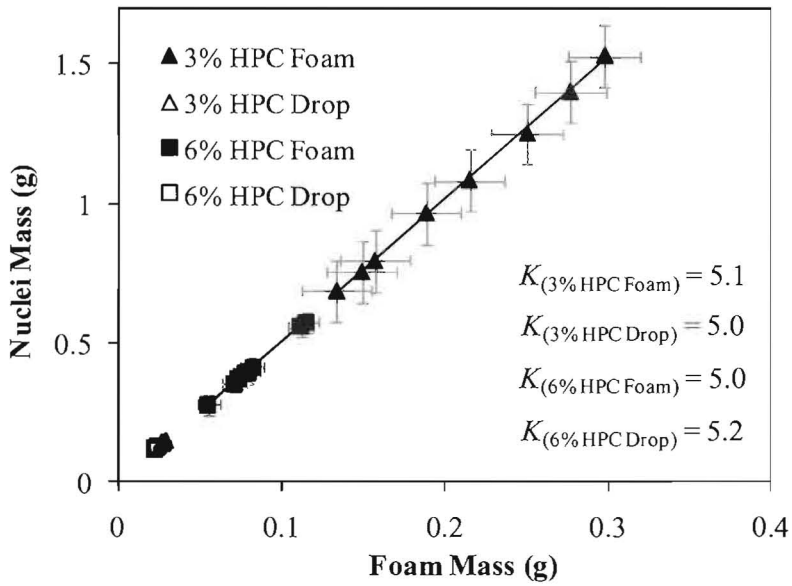


Figure 3-10 Comparison of HPC foam and drop nucleation ratios on AC grade glass ballotini. Gradient of graph indicates nucleation ratio, K .

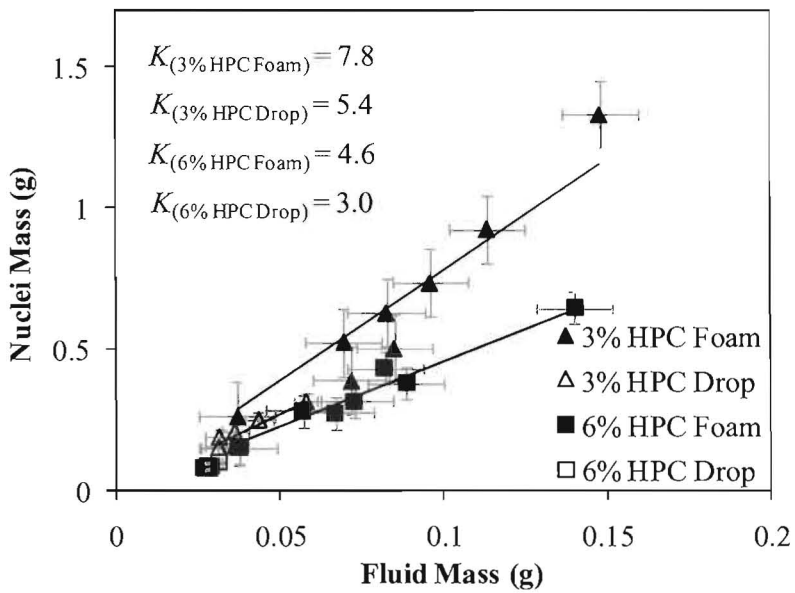


Figure 3-11 Comparison of HPC foam and drop nucleation ratios on 100 mesh lactose. Gradient of graph indicates nucleation ratio, K .

It can be seen from Figure 3-10 and Figure 3-11 that increasing binder fluid mass increases nuclei mass. The gradient of the plots in Figure 3-11, Figure 3-12, Figure 3-14 and Figure 3-15 represents the nucleation ratio, K (with subscript to indicate the particular fluid-powder system). Foam and drop nucleation ratios for glass ballotini powders (Figure 3-10) are similar irrespective of whether the binder is added as an aqueous foam or a liquid droplet. This implies that the amount of powder nucleated per gram of binder fluid added appears to be approximately constant regardless of the binder addition method. In other words, for the same number of grams of glass ballotini powder to be nucleated, the minimum amount of binder fluid required is unchanged. This similar nucleation ratio is likely due to the uniform particle packing of glass ballotini that always allow even liquid distribution within the powder bed. Liquid distribution throughout the glass ballotini powder pores to effect nucleation will be similar between foam and drop nucleation methods.

However, this is not the case in nucleating lactose powder. For lactose powders, foams have larger nucleation ratios. For example, $K = 7.8$ g powder/g liquid for 3% HPC foam versus $K = 5.4$ g powder/g liquid for 3% HPC drop on 100 mesh lactose (Figure 3-11). For the same number of grams of fluid, foam induced nucleation nucleates more powder than drop induced nucleation; which supports a key finding of Keary and Sheskey (2004), who found that foam granulation used lower amount of fluids to achieve similar average granule sizes. The larger nucleation ratio obtained using the foam addition method also implies that foam addition provides better liquid distribution within non-uniform powder beds, as the liquid is in contact with a much larger mass of powder.

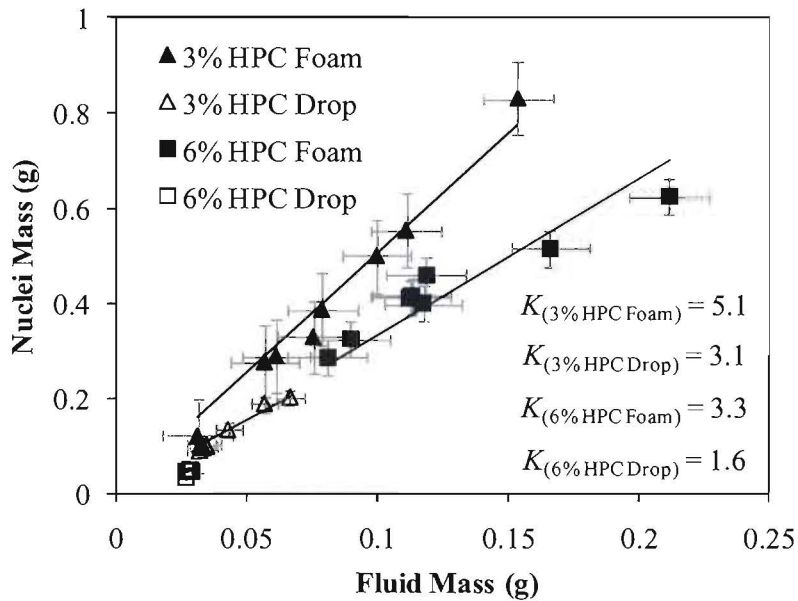


Figure 3-12 Comparison of HPC foam and drop nucleation ratios on 200 mesh lactose. Gradient of graph indicates nucleation ratio, K .

As seen in Figure 3-12, the same trend was obtained for 200 mesh lactose powders where foam induced nucleation has led to a larger nucleation ratio compared to drop induced nucleation. Drop penetration into lactose powders with irregular packing structures is often restricted due to the presence of macrovoids (Hapgood et al., 2002), while the foam addition method offers a better efficiency of liquid distribution into the powder bed.

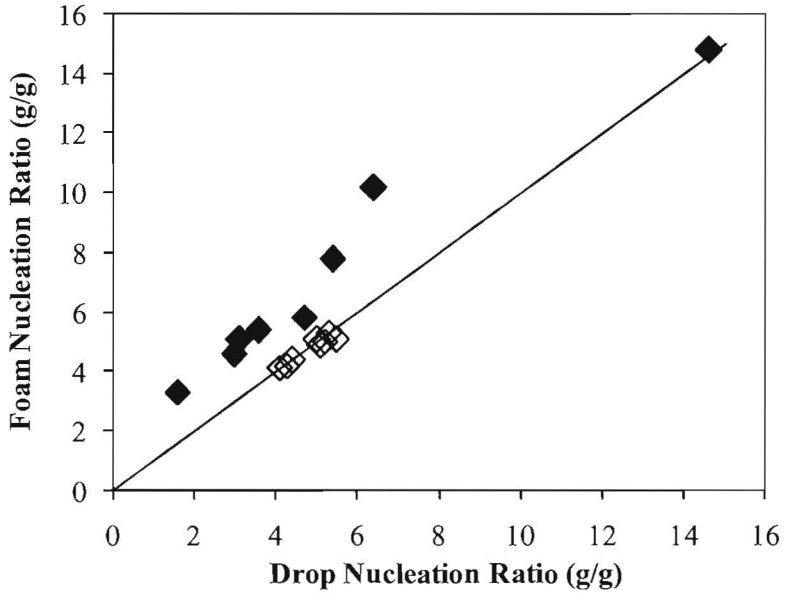


Figure 3-13 Comparison of nucleation via foams and drops. Filled dots indicate nucleation on lactose powder – improved nucleation efficiency with foam induced nucleation method. Unfilled dots indicate nucleation on glass ballotini – similar nucleation efficiency.

Figure 3-13 shows the nucleation ratio data from nucleation on lactose and glass ballotini powders using HPMC and HPC binder fluids. Foam and drop induced nucleation on glass ballotini produced a similar nucleation ratio, and hence most data are scattered around or on the equality line. However, nucleation on lactose powder via foams improves nucleation efficiency, and hence the data is scattered above the equality line. For complete foam and drop nucleation ratio data, see Table 3-3 and Table 3-4, respectively

Table 3-3 Estimated foam nucleation ratios.

Foamed binder / Powder	3%	6%	4%	6%	8%	10%
	HPC	HPC	HPMC	HPMC	HPMC	HPMC
Glass ballotini						
AC	5.1	4.9	5.3	N/A	5.1	4.9
AE	N/A	N/A	4.8	N/A	4.7	4.7
AH	4.1	4.1	4.7	N/A	4.4	4.2
Lactose monohydrate						
100 mesh	7.8	4.6	14.8	10.2	N/A	N/A
200 mesh	5.1	3.4	5.8	5.4	N/A	N/A

Table 3-4 Estimated drop nucleation ratios.

Liquid binder / Powder	3%	6%	4%	6%	8%	10%
	HPC	HPC	HPMC	HPMC	HPMC	HPMC
Glass ballotini						
AC	5.0	5.2	5.3	N/A	5.5	5.1
AE	N/A	N/A	4.9	N/A	4.9	4.4
AH	4.3	4.1	4.3	N/A	4.4	4.3
Lactose monohydrate						
100 mesh	5.4	3.0	14.6	6.4	N/A	N/A
200 mesh	3.1	1.6	4.7	3.6	N/A	N/A

The nucleation ratio can be considered to represent the minimum amount of fluid required to granulate each powder. Spray granulations generally use considerably more liquid than the minimum, due to short processing time and inefficient dispersion, including the presence of wet patches. Litster (2003) indicated that most industrial granulators do not operate in the drop-controlled regime, owing to formulation properties and/or spray flux limitations. Most

processes are operating at a much higher spray flux than would be ideal, resulting in poor binder distribution through the powder and thus forming coarse and wet granules that are hardly broken up. These wet patches due to non-uniform binder distribution represent wasted binder fluid that could have been used to granulate more powder if it had been distributed effectively. Extra liquid is needed than the minimum to compensate for the inefficient dispersion, which in turn leads to a correspondingly longer delivery time. In contrast, it seems that the distribution of foam within the powder pores is more effective, considering each gram of foam nucleates more powder, as shown in the previous section, and thus it is easier to achieve granulation using a smaller amount of liquid.

3.3.5 Effect of particle size on foam nucleation ratio

The size of nuclei formed from a given amount of liquid depends on the powder properties (size and porosity) as well as the binder properties (binder concentration and viscosity). In this section, the effect of the particle size on nuclei formation is considered quantitatively.

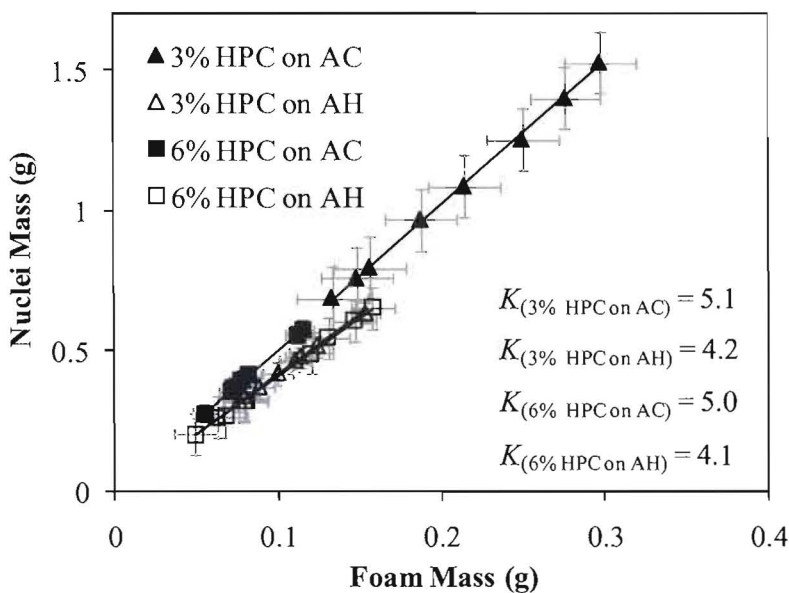


Figure 3-14 Effect of glass ballotini particle size on nucleation ratio, K , for HPC foamed binders.

Figure 3-14 shows a clear correlation between nuclei mass and binder fluid mass for 3% and 6% HPC foams used to nucleate two grades of glass ballotini powder. Foam induced

nucleation of a coarser powder tends to form larger nuclei. The graphs show that the nucleation ratios for AC (coarse) powder beds are slightly larger than that of AH (fine) powder beds.

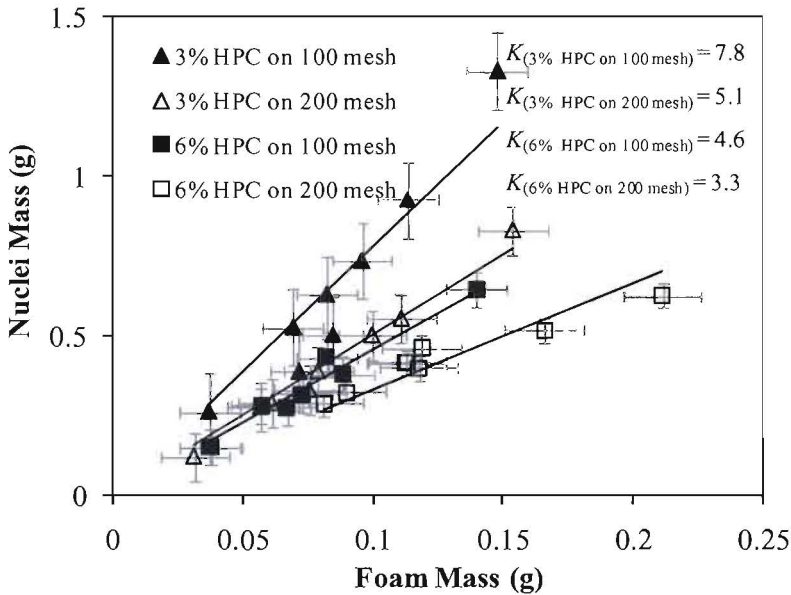


Figure 3-15 Effect of lactose particle size on nucleation ratio, K , for HPC foamed binders.

Figure 3-15 shows the effect of lactose particle size on nucleation ratio generated using HPC foamed binders with particular binder concentrations. Again, for a given amount of foam mass, coarser (100 mesh) lactose powders create larger nuclei. In other words, increasing the particle size increases the nucleation ratio. It was observed that the fine fraction (200 mesh) of lactose did not pack as well as the coarse fraction, and it likely contains more macrovoids which will restrict the liquid penetration and hence the extent of nucleation.

3.3.6 Effect of binder concentration on foam nucleation ratio

From Figure 3-14, it is seen that nucleation of both AC and AH glass ballotini powders using 3% or 6% HPC foam exhibit no significant difference in the nucleation ratio. Larger differences in binder concentration of the foamed binder may be required to show an effect on glass ballotini powders.

The effect of the binder concentration on the nucleation ratio is much more pronounced for lactose powders, as can be seen from Figure 3-15. The nucleation ratio increases with

decreasing HPC concentration in the foamed binder, i.e. for each gram of binder fluid added, a larger number of grams of powder are nucleated by using a lower binder concentration. Decreasing binder viscosity or binder concentration will improve wetting uniformity, allowing a deeper extent of fluid flow and penetration into the powder pores, which is thus likely to create larger nuclei with a good distribution of binding fluid. Similarly with drop penetration (Schaafsma, 1998), foam induced nucleation using a less viscous binder generally undergoes faster nucleus growth and results in a larger final nucleus size.

3.3.7 Nuclei morphology

Qualitative observations of the morphology of the nuclei formed showed interesting features.

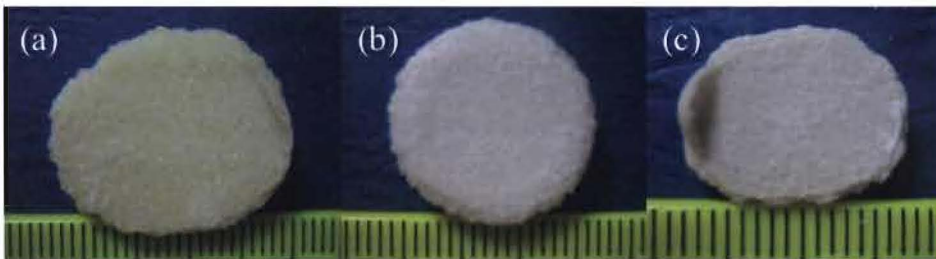


Figure 3-16 Foam created nuclei – (a) 3% HPC on AC grade glass ballotini. (b) 6% HPC on AC grade glass ballotini. (c) 6% HPC on AH grade glass ballotini. Scale is in millimetres.

Figure 3-16 shows the nuclei produced from glass ballotini using HPC foamed binder. Glass ballotini powder always formed nuclei with flat and smooth surfaces. Lactose powder produced mushroom-shaped nuclei (Hapgood *et al.*, 2004), as shown in Figure 3-17. The nuclei are strong and highly saturated in the centre core, and weak and less saturated in the outer shell. The fragile outer shell of the nuclei often breaks during excavation, leaving only the stronger “stalk”.



Figure 3-17 Foam created nuclei – (a) 4% HPMC on 200 mesh lactose. (b) 6% HPMC on 200 mesh lactose. (c) 3% HPC on 100 mesh lactose. Scale is in millimetres.

One important difference between the nuclei created from foam and drops can be seen in Figure 3-17(a) to (c). The nuclei created from foamed binder contain large pores at the powder surface. In foam dispersion, nucleation occurred by the drainage of liquid from foam into the powder. Simultaneously, the air from the interior of the powder must rise up through the powder to the surface to escape. It is believed that the air rising and venting through the powder surface created the large, visible pores. These pores are not observed in similar nuclei formed by drops (Hapgood *et al.*, 2004).

3.4 Discussion

3.4.1 Foam penetration behaviour

Microscopy observations of the penetration of a mass of foam into the powder bed, as shown in Figure 3-18, Figure 3-19 and Figure 3-20 were made to view foam penetration behaviours.

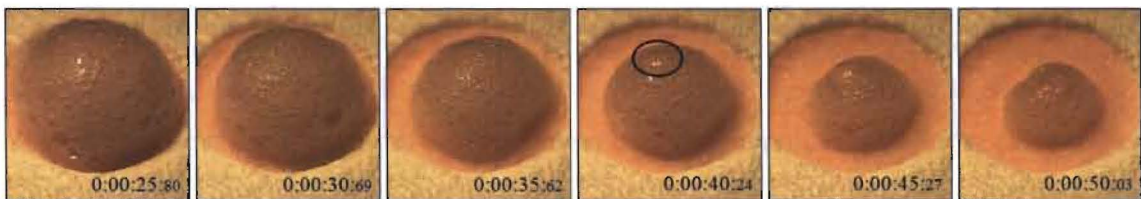


Figure 3-18 4% HPMC foam penetration on a 100 mesh lactose powder bed.

Figure 3-18 shows the penetration of 4% HPMC foam into a 100 mesh lactose powder bed. When foams impact on the powder surface, bubbles coalesce and liquid drainage takes place, as well as fluid penetration into the powder pores. As drainage proceeded, bubbles in the foam were observed to move around and to squeeze one another within the foam. Some bubbles were observed to grow as the films between the bubbles thinned. When bubbles grew, the

liquid within them drained downwards, and the bubbles nearby were forced to migrate. A bubble ruptures when its surface becomes too thin due to liquid drainage. It can be seen from the microscopy image that at 40 seconds one large bubble at top was about to burst. The popped bubble causes further liquid drainage and bubble rupture. Following the bursting of each bubble, the bubbles nearby instantaneously shift into the empty space created by the popped bubble, leading to fluid redistribution within the foam. At the same time, the powder pores absorb the liquid drained out from the films, shrinking the foam blob in the pattern of decreasing drawing area (Denesuk, 1993). This behaviour can be also seen for 8% HPMC foam penetration, as shown in Figure 3-19.

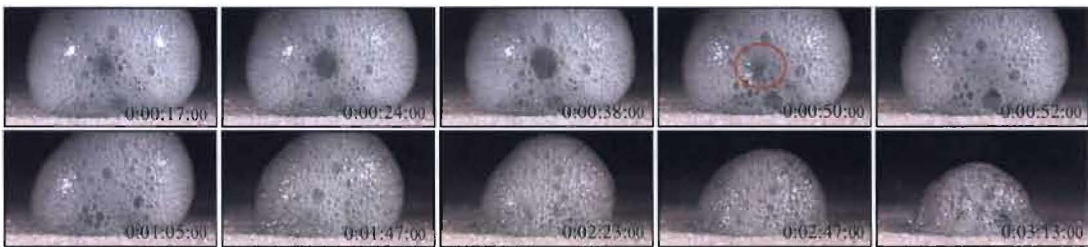


Figure 3-19 8% HPMC foam penetration on an AC grade glass ballotini powder bed.

From Figure 3-19, it is seen that one particular bubble, shown in a circle, was growing gradually until bursting at about 50 seconds, which caused the nearby bubbles to move into the empty space created, followed by fluid redistribution and foam shrinkage. This interaction between the bubbles and liquid continues until all the foam has completely sunk into the powder bed. For 4% HPMC foam, bubble movement within the foam was seen to be relatively rapid. 8% HPMC foam is thicker and the bubbles are denser within the foam blob. For low viscosity foams, liquid flow is less restricted and able to flow easily within the thin films and small bubbles. High viscosity foams slow down liquid draining through the film and suppress the growth of the bubbles. As seen in Figure 3-19, the 8% HPMC bubbles are smaller, and bubble motion within the foam is more sluggish, which has resulted in a longer penetration process.

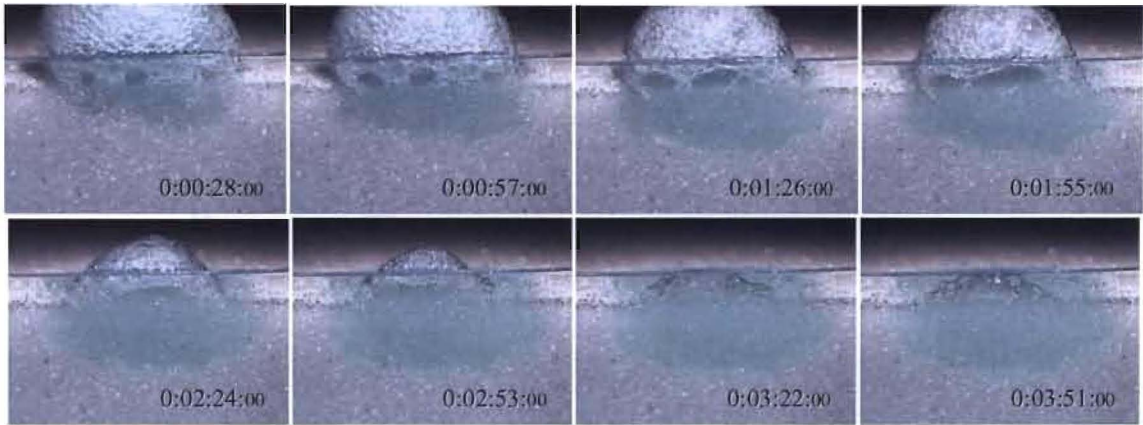


Figure 3-20 8% HPMC foam penetration on an AC grade glass ballotini powder bed.

Figure 3-20 shows the images of 8% HPMC foam deposited on the side of an AC grade glass ballotini powder bed. It can be seen that large bubbles were formed at the base of the foam. Smaller bubbles merged, creating larger bubbles which continued to grow in size with time until the bubbles ruptured. As bubbles rupture, the liquid drains and spreads across the powder bed, causing the liquid wetting front to propagate vertically and spread horizontally. It seems that the foam penetration has incurred a larger footprint from the spreading front than the draining front, which supports that foam spreads through a powder bed more than it soaks into the bed (Keary and Sheskey, 2004). The extent of fluid penetration and spreading within the powder bed is very crucial to the nucleation process.

From Figure 3-20, the change in the propagated wetting front for vertical drainage and horizontal spreading were estimated in terms of the fraction of propagated depth and width relative to the final propagated depth and width.

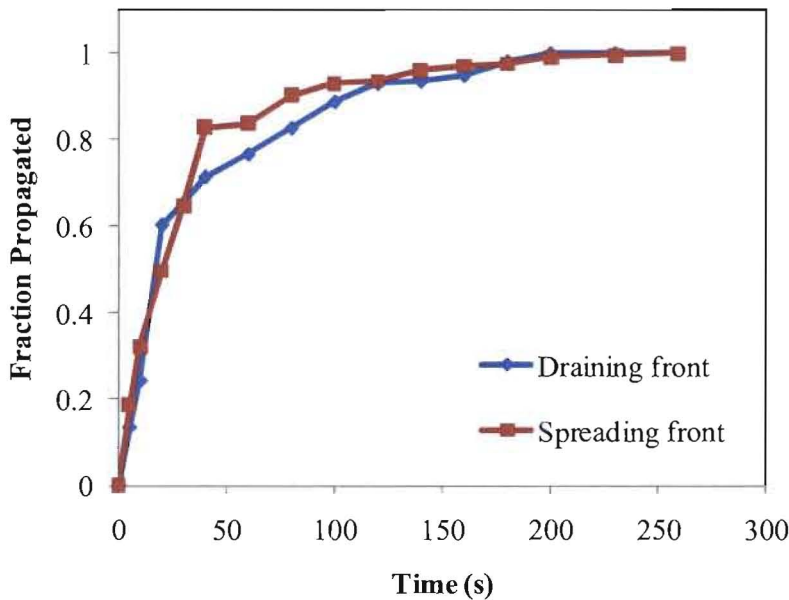


Figure 3-21 Propagation of wetting front caused by 8% HPMC foam penetration on an AC grade glass ballotini powder bed.

Figure 3-21 plots the propagated fraction of the wetting fronts against time. As represented by the initial slopes of the curves, the results show that the draining and spreading fronts both increase at a similar rate. Both the wetting fronts advance at a faster rate initially, and they then decrease exponentially until the foam is completely absorbed into the bed. A small difference can be seen after 50s, where the spreading front seems to have stopped advancing before the foam has fully penetrated into the powder bed. After 150s, almost all of the liquid initially in the foam has penetrated into the powder bed and the small amount remaining forms a dry foam, which does not cause any significant propagation of the wetting front when the foam collapses. Since in reality the fluid drains and spreads in 3-dimensions, observation of the wetting front due to foam drainage and spreading in 2-dimensions is imprecise to determine and mostly qualitative.

Clearly, the rate of liquid penetration and the propagated wetting front induced by foam/drop penetration are affected by both the foamed liquid binder and the powder properties. Without detailed characterisation of the foamed liquid binder and the powder properties, the penetration time study has not completely revealed the rate at which foam/drop penetrates into the powder pores and its relationship with the propagation of wetting front. However, we postulate that

there are two potential rate limiting steps during drop or foam penetrations, as illustrated in Figure 3-22.

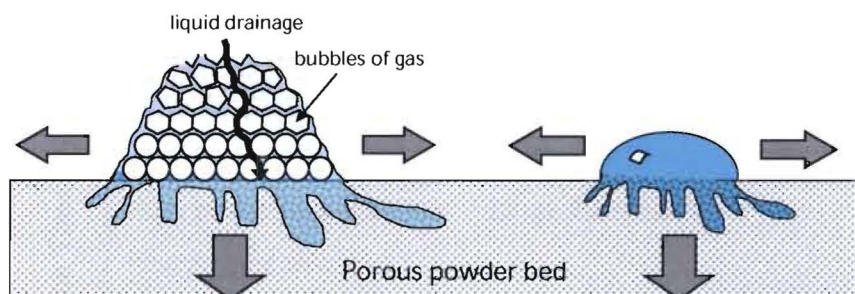


Figure 3-22 Rate limiting step of liquid penetration – (a) foam penetration: liquid in foam undergoes a tortuous path before penetrating into powder pores and (b) liquid droplet penetration: liquid as a whole, is absorbed into powder pores.

For a liquid droplet sitting on a porous surface, the liquid is pulled into the powder pores due to the capillary effect. This capillary action applies to both foam and drops sitting on the powder surface. However, the difference between these two cases is that liquid in the droplet is a continuous phase. In contrast, the liquid in the foam will have to undergo a tortuous flow path before reaching the powder surface and penetrating into the powder pores. Rather than being absorbed as a continuous liquid drop, the liquid in the foam which contacts the powder particles is distributed as thin layers at the bubble surfaces, and the remainder of the liquid has to drain through the lamellae between the bubbles. The tortuous path through the bubble lamellae includes the processes of foam penetration as mentioned previously. Liquid drainage through the foam depends critically on the interstitial viscosity, foam quality and presumably also on the bubble size. Therefore, liquid drainage may be the rate limiting step in foam penetration, which potentially affects the propagated wetting front and thus the nucleation process. To investigate this phenomena further, the studies of foam drainage will be covered in *Chapter 4*.

3.4.2 Effect of feed properties on foam wetting and nucleation

Good wetting and nucleation are generally required to ensure a controlled granulation, but establishing the ideal wetting and nucleation conditions with the required feed formulations is often challenging, as there are many different feed formulations with widely varying properties.

Extensive and expensive granulation experiments are required to develop each new formulation. Thus, developing a method to predict the granulation behaviour of a formulation is highly desirable. Although the conditions in an agitated powder bed are expected to be different, the study of single nucleus formation on a static powder bed can be a useful approach to understand wetting and nucleation.

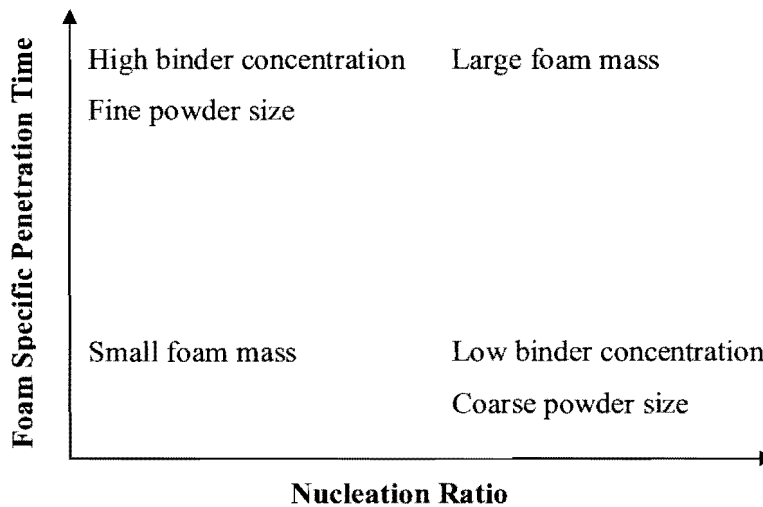


Figure 3-23 Effects of feed properties on foam specific penetration time and nucleation ratio.

Figure 3-23 summarizes the effects of formulation properties on foam penetration time and nucleation ratio (which is also proportional to nuclei size), and may be useful as a brief guide to the formulation for foam induced nucleation. For instance, using a small foam mass is expected to create small nuclei and vice versa. If the objective is to obtain relatively large nuclei granules, it is suggested that either a low binder concentration or a coarse powder can be used, which offers an alternative between the binder and the powder for the selection of feed materials. Note that if the foam is fast to penetrate the powder bed (which is assisted by low binder concentration and/or coarse powder), it will lead to the formation of large nuclei with a potential broad nuclei size distribution. It is postulated that a slow penetrating system with a high binder concentration and/or a fine powder will cause a decrease in the nuclei size and potentially reduces the spread of the nuclei size distribution. In this case, the process and granule attributes would be expected to be controlled by mechanical dispersion since the foam penetration kinetics are slow. This relationship between the penetration kinetics and the nuclei

size distribution appears to contradict the existing nucleation regime map for sprays (Hapgood *et al.*, 2003).

This proposition of a material selection guide to nuclei size distribution changes for foam granulation cannot be confirmed until the direct relationship between foam drainage, penetration time and nuclei size distribution is determined. Further experiment of nucleating/granulating the powder using different feed formulations to determine the foam induced wetting and nucleation conditions in a real moving powder bed is considered in *Chapter 4*. Once the effects of formulation properties on foam induced nucleation/granulation are known, this will help in the selection of materials in the subsequent stage of study – foam granulation, and can mainly focus on the process changes.

3.5 Conclusions

This study is the first to present an overview of wetting and nucleation kinetics via both foams and drops in wet granulation processes. The effects of binder and powder properties on the penetration time and nucleation ratio were examined. Results showed that:

Specific penetration time increases with:

- Increasing foam mass
- Increasing foam concentration
- Decreasing powder size

Nucleation ratio increases with:

- Increasing foam mass
- Decreasing foam concentration
- Increasing powder size

The study of the effects of binder and powder properties on the penetration time and nucleation ratio can provide a guideline to the materials selection for future work on foam nucleation/granulation. Comparisons between foam and drop nucleation ratios have indicated that nucleation of powder via foams provides better liquid usage and improved liquid

distribution efficiency compared to the nucleation via drops on lactose powder, although nucleation ratios on glass ballotini were equivalent.

Visual observations of foam displaced on the powder bed have suggested that the bubble movement and liquid drainage are critical to the foam penetration process. It is postulated that liquid drainage may be the rate limiting step in foam penetration, which can affect the wetting and nucleation process. To investigate this phenomena further, the study of foam induced wetting and nucleation in a real moving powder bed is considered in *Chapter 4*.

CHAPTER 4
BINDER DISPERSION AND NUCLEATION

Monash University

Declaration for Thesis Chapter 4

In the case of Chapter 4, contributions to the work involved the following:

Name	% contribution	Nature of contribution
Melvin X.L. Tan	100	Initiation, Key ideas, Experimental development, Results interpretation & Writing up
Dr. Karen Hapgood	Supervisor	Initiation, Key ideas, Editing and reviewing

Declaration by co-authors

The undersigned hereby certify that:

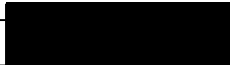
- (1) they meet the criteria for authorship in that they have participated in the conception, execution, or interpretation, of at least that part of the publication in their field of expertise;
- (2) they take public responsibility for their part of the publication, except for the responsible author who accepts overall responsibility for the publication;
- (3) there are no other authors of the publication according to these criteria;
- (4) potential conflicts of interest have been disclosed to (a) granting bodies, (b) the editor or publisher of journals or other publications, and (c) the head of the responsible academic unit; and
- (5) the original data are stored at the following location(s) and will be held for at least five years from the date indicated below:

Location(s)

Department of Chemical Engineering, Monash University, Clayton Victoria 3800 Australia.

Signature 1

Signature 2

	Date
	
	

4 BINDER DISPERSION AND NUCLEATION

This chapter looks at binder distribution in wet granulation and focuses on the nucleation stage, where nuclei are formed during the initial binder distribution. Nucleation experiments were carried out to study the formation of nuclei by the foam and spray delivery methods in a high shear mixer-granulator. Two wetting and nucleation mechanisms for foam granulation are postulated to explain the quantitative results, which are also supported by qualitative observations of the distribution of foams on a dynamic powder bed as they penetrate into the bed under different powder flow conditions in a high shear mixer-granulator.

Publication: Tan, M.X.L., Hapgood, K.P., *Foam granulation: Binder dispersion and nucleation in mixer granulators*. Chemical Engineering Research and Design. In Press, Accepted Manuscript ([doi:10.1016/j.cherd.2010.07.001](https://doi.org/10.1016/j.cherd.2010.07.001)).

4.1 Introduction

In the previous chapter, the wetting interaction between foam and powder particles and the subsequent formation of single nuclei were examined on static powder beds. The attention on the foam-particle interaction now widens to real moving powder beds. The interaction between the liquid masses and the powder particles during the initial liquid distribution is of great importance to the success of wet granulation.

In spray granulation, the powder is agitated while binder is delivered onto the moving powder from above. The binder is dispersed throughout the powder bed by its own spreading and capillary penetration as well as by the dynamic bulk shearing and impacting motion of the powder bed, and subsequently forms the initial granules, or nuclei. The interactions between these processes influence the wetting and nucleation, and subsequent granule formation (Iveson et al., 2001). Capillary penetration is controlled by the formulation properties, while the powder bulk motion is controlled by the impeller speed and the powder properties. The ability of the binder to wet and penetrate the powder mass determines whether highly-saturated and over-sized agglomerates or uniformly-saturated and narrow size range granules are produced. Therefore, a uniform wetting and nucleation process, which generally leads to a controlled granulation process, requires appropriate processing with adequate choice of binder and powder at proper process conditions.

For high shear wet granulation, the interactions of binder and powder particles are complex in nature as the dynamic environment leads to a variety of shear and impacts that may affect the binder dispersion and nucleation, and subsequent granule formation (Saleh *et al.*, 2005). Understanding binder dispersion and nucleation is a key topic in high-shear wet granulation that has been studied extensively in the literature (Hapgood *et al.*, 2003; Knight *et al.*, 1998; Knight *et al.*, 2000; Litster *et al.*, 2002; Litster *et al.*, 2001; Plank *et al.*, 2003).

Hapgood *et al.* (2003) demonstrated the critical importance of binder dispersion and nucleation in determining the size and the spread of the granule size distribution. They defined two regimes of nucleation applicable to spray granulation – the drop controlled regime and the mechanical dispersion regime. The relevant nucleation regime is defined by the drop penetration time and by the dimensionless spray flux (Litster *et al.*, 2001). Also see *Chapter 2 – section 2.2.1*.

The dimensionless spray flux (Litster *et al.*, 2002; Litster *et al.*, 2001) quantifies the degree of binder dispersion as a function of binder delivery rate, powder velocity and spray nozzle parameters (spray width and drop size) on the nuclei size distribution. A large dimensionless spray flux implies a high binder addition rate and slow powder motion, which generally produces a broad granule size distribution (Hapgood *et al.*, 2003; Litster *et al.*, 2001). The binder droplet size and the binder addition rate are controlled by the atomisation process, while the powder bulk motion is controlled by either the impeller speed (for a mixer granulator) or by the fluidising air velocity (for a fluid-bed).

The drop controlled regime occurs at low drop penetration time and low spray flux; otherwise, the nucleation process is dominated by mechanical dispersion (Hapgood *et al.*, 2003), where the effective agitation of the powder is required to disperse the fluid efficiently. Wildeboer *et al.* (2007) designed a novel nucleation apparatus to produce narrow sized nuclei, which operates only in the drop controlled regime and therefore avoids several binder dispersion problems. Knight *et al.* (1998; 2000) also showed that granule growth and breakage strongly depend on the initial binder distribution method – pouring, spraying, or instantaneous addition. They also showed that the initial nuclei size distribution was always bimodal, and that it was directly reflected in the final product size distribution, despite many minutes of mixing in a “high shear” mixer. These studies were all conducted by different research groups using

different formulations, granulation equipment and process conditions, and they all found that the way that the binder is initially distributed in the powder bed has a strong effect on the entire granulation process.

One of the primary parameters in the dimensionless spray flux is the surface velocity of the powder as it moves beneath the spray. In a high shear mixer-granulator, powder velocity is controlled by the impeller speed. The flow patterns in the mixer-granulator can affect product transformations as the raw materials are converted into granular product. The impeller motion creates shear and impact within the granulator, and these forces are significantly related to the powder flow patterns in the granulator (Iveson *et al.*, 2001a). Two powder flow patterns have been identified in the mixer-granulators: bumping and roping. At low impeller speed, bumping flow occurs, where the powder bed rotates slowly and the powder surface remains horizontal with little vertical turnover. At high impeller speed, roping flow occurs, where the powder follows a toroidal flow path and the upper powder surface tumbles towards the centre of the rotating hub (Litster *et al.*, 2002; Ramaker *et al.*, 1998).

Roping flow is recommended for effective binder distribution (Litster *et al.*, 2002), particularly in the mechanical dispersion regime. However, there is still potential for uneven binder distribution in many high shear mixer-granulators, especially at the production scale (Plank *et al.*, 2003). Tardos *et al.* (2004) found that the shear forces in a high shear mixer-granulator were much lower than expected, especially during the dry mixing stage. As granulation proceeds, the powder bed becomes wetter and more cohesive, causing the shear to increase (Tardos *et al.*, 2004) and the powder flow to transition into roping flow (Plank *et al.*, 2003). However, it is not uncommon for the entire process to operate in bumping flow for most of the time, especially in mixers with simple low and high speed settings. Using larger mixers to process a larger amount of material requires a proportional increase in the mixing forces required, but the applied impeller forces are generally lower due to the common use of the tip-speed scaling rule. This is why roping, toroidal motion of the powder bed is usually seen in lab-scale mixers rather than in production scale mixers (Plank *et al.*, 2003). Plank *et al.* (2003) concluded that uneven binder distribution is likely to be especially problematic at the production scale, which supports that the mixer-granulator has a large tendency to operate in bumping flow. In addition, the lack of vigorous agitation in production scale mixer-granulators often makes maintaining a low dimensionless spray flux essentially impractical, which can

result in ineffective binder dispersion and the formation of large, highly saturated nuclei which grow into extremely large granules, causing downstream production problems.

In summary, although binder distribution in spray granulation can be controlled by using a low spray flux to stay within the drop controlled nucleation regime, this is currently difficult to achieve outside of a laboratory, partly due to equipment design limitations and partly due to traditional views of acceptable processing conditions. Case studies of foam granulation (Cantor *et al.*, 2009; Keary and Sheskey, 2004) indicate that foam granulation uses less fluid to produce a granulated product with equivalent performance to a spray process, which implies that foam improves the distribution of the binder through the powder. Although the main binder dispersion mechanisms are now relatively well understood when the binder is added as a spray, there are no mechanistic studies of how the binder fluid is distributed using the foam addition method.

This chapter looks at binder distribution in wet granulation and focuses on the nucleation stage by performing short foam nucleation experiments, where a small amount of foam is added to the granulator and the amount and size of the resulting nuclei are analysed. Nuclei size distributions are measured as a function of foam properties and impeller speed in a high shear mixer-granulator. This data is also compared to the nuclei formed by spray delivery at the same conditions. The foam drainage behaviour of the foam and the surface of the powder as it experiences different powder flow conditions in the granulator were also examined.

4.2 Experimental

4.2.1 Materials

The powder used was lactose monohydrate (100 mesh, Wyndale, New Zealand). An aqueous solution of 4% HPMC (Methocel E5PLV, Dow Wolff Cellulosics, USA) was used as the binder fluid. A small quantity of red food dye (Queens Fine Food Ltd., Australia) was dissolved in the binder solution to assist with visual observations of the nuclei granules. Table 4-1 indicates the powder and liquid binder properties, which were obtained from vendor specifications.

Table 4-1 Powder and liquid binder properties.

Powder/Liquid binder	Grade	Viscosity (mPa.s)	Particle size distribution (μm)
Lactose monohydrate	100 mesh	-	75-250
4% HPMC	E5PLV	19.1	-

4.2.2 Methods

4.2.2.1 Nucleation experiments

To study the nucleation process, impeller speed and foam quality were varied and the changes in the nuclei size distribution were observed. The experiments focussed on short granulation time studies in order to study the initial wetting and nucleation stage, and minimise the effects of granule coalescence, attrition and breakage. This method has been used previously to study nucleation using a spray (Litster *et al.*, 2002; Litster *et al.*, 2001).

Nucleation experiments were conducted in a high shear mixer-granulator (KG-5, Key International Inc., New Jersey, USA). The granulator has a three-bladed impeller with a variable speed setting. The granulator bowl is 203mm in diameter and has a volume of 5 litres, with a standard nozzle port mounted on top of the perspex lid for binder addition. The bowl contains only the impeller blade. The chopper was not used during the experiments (see Figure 4-1).

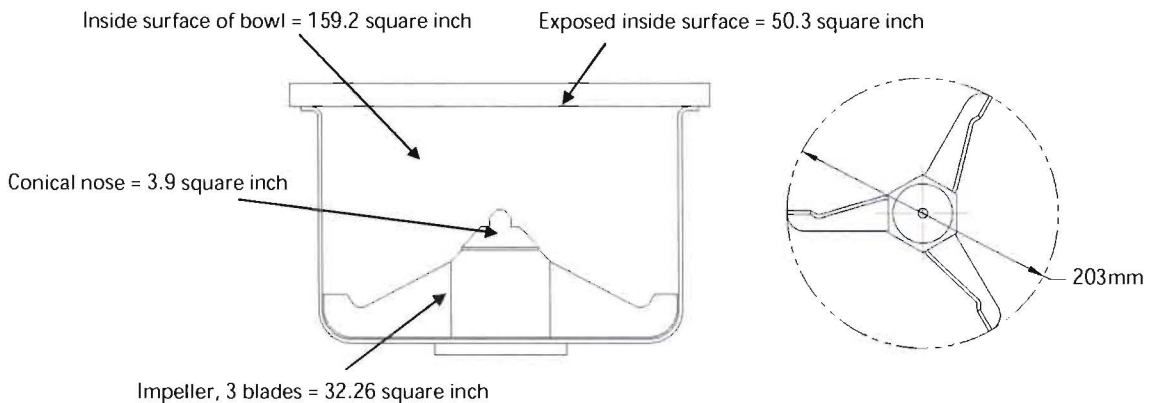


Figure 4-1 (left) Product contact area of KG-5 bowl that are exposed and come in contact with the product (right) Dimensions of three bladed impeller (Key International Inc.).

For spray delivery, a single flat nozzle (TP650017) connected to a 5-litre spray pot (Spraying Systems, Wheaton, USA) was positioned through the nozzle port to allow the spraying of binder at 0.1l/min. For foam delivery, a plastic pipe was connected to a foam generator (Keary and Sheskey, 2004) where the binder is mixed with air to produce different qualities of foamed binder. The foam entered the granulator via a delivery pipe positioned in the nozzle port. In this study, we deliberately varied the foam quality more widely to test the process over a broad range of conditions. Foam qualities of 67%, 83% and 97%, representing nominal “Low”, “Medium” and “High” foam qualities respectively, were used in the experiments. For full details of the foam generator, see *Chapter 2 – section 2.3.1*.

For both foam and spray granulation, a small amount of liquid binder (50mL) was added to 1500g of powder at a binder addition rate of 0.1L/min. Two impeller speeds – 125rpm and 455rpm, designated as “Low” and “High” respectively, were used in the experiments. The corresponding tip speeds were 1.3m/s and 4.8m/s respectively. At a 125rpm impeller speed, the dry powder was in the bumping regime, whilst the 455rpm impeller speed produced roping flow. The impeller was stopped immediately after the 30 second binder addition step. At the end of each 30 second experiment, no foam was visible at the top of the powder surface. The dispersion of the foam was also filmed using a video camera (30 frames per second, 8MP resolution).

4.2.2.2 Sieving experiments

After the nucleation experiments, the wet granules were gently placed in a thin layer on large flat trays and dried overnight in a convection oven set at 50°C. The dried granules were then sieved through a 250µm screen to separate the nuclei from the un-nucleated powder. This sieve size was chosen as the cut-off boundary size between nucleated and non-nucleated material as the lactose powder used has a particle size distribution range between 75µm-250µm. It is possible to form nuclei below 250µm via breakage of larger granules. However, the mass percentage is very small compared to the mass of the nuclei formed. The nuclei created from the red binder solution can also be distinguished based on the colour of the collected materials. Visual inspection of the powder less than 250µm found no signs of pink or broken granules.

To size the nuclei, the nuclei samples were sieved using a mechanical dry sieve shaker (Retsch A200, Australia) with the following sieve size fractions: pan, 45µm, 63µm, 90µm, 125µm,

180 μm , 250 μm , 425 μm , 630 μm , 850 μm , 1mm and 2mm. The mass retained on each sieve was measured using a balance with 0.01g accuracy. In each experiment, 10-35% of the dry powder formed nuclei >250 μm , which means that approximately 150-500g of nuclei were formed, depending on the experimental conditions. This is a much larger quantity of nuclei than used in the studies by Litster *et al.* (2002; 2001) and hence the main source of error would be due to normal sampling and weighing variations.

From the sieve analysis, the weight mean diameter, d_m can be determined:

$$d_m = \frac{\sum_i M_i d_i}{\sum_i M_i} \quad \text{Eq. [4-1]}$$

where M_i is the particle mass fraction of sieve size interval i and d_i is the mean diameter of sieve size interval i in micrometers.

4.2.2.3 Foam drainage characterisation

To characterise the foam, the drainage properties of the foams were evaluated at the three foam qualities (67%, 83% and 97%) used in the experiments. The drainage properties of different foams were examined by obtaining the light transmission profile (Mengual, 1999) from a Turbiscan (Formulation, France). All experiments were conducted at room temperature conditions (23°C-25°C).

To measure the drainage properties of the foam samples, a small amount of foam is pumped directly from the foam generator into a glass test tube which is then inserted into the Turbiscan. The height of the foam in the tube was kept as constant as possible and ranged between 60mm-70mm. The liquid level in the bottom of the tube gradually rises due to progressive breakdown of the foam, until the foam has completely collapsed into liquid. The liquid level in the tube increases with time and stabilizes after a finite time when the foam has completely collapsed (see Figure 4-2).

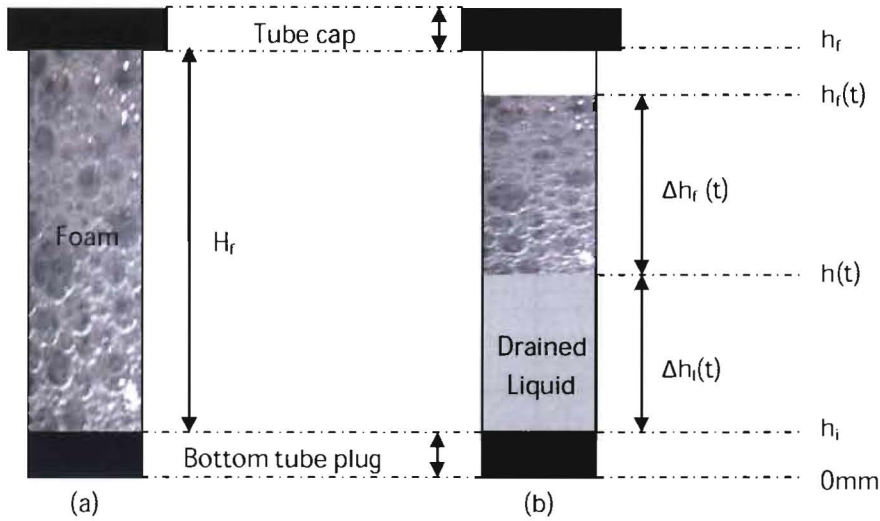


Figure 4-2 Change of foam and liquid fraction in a cylindrical glass measurement tube (a) at initial time $t = 0$ (b) after time t .

The light transmission profile (Figure 4-3) measures the dynamic heights of the foam-air interface, and the foam-liquid interface, as the foam slowly collapses over time. The light is transmitted easily through the liquid phase, but the presence of the opaque foam diffracts and blocks the light, leading to reduced light transmission. The Turbiscan data tracks the positions of the foam-liquid and foam-air interfaces as a function of time, and then uses this data to calculate the foam quality and drainage rate of the foam sample.

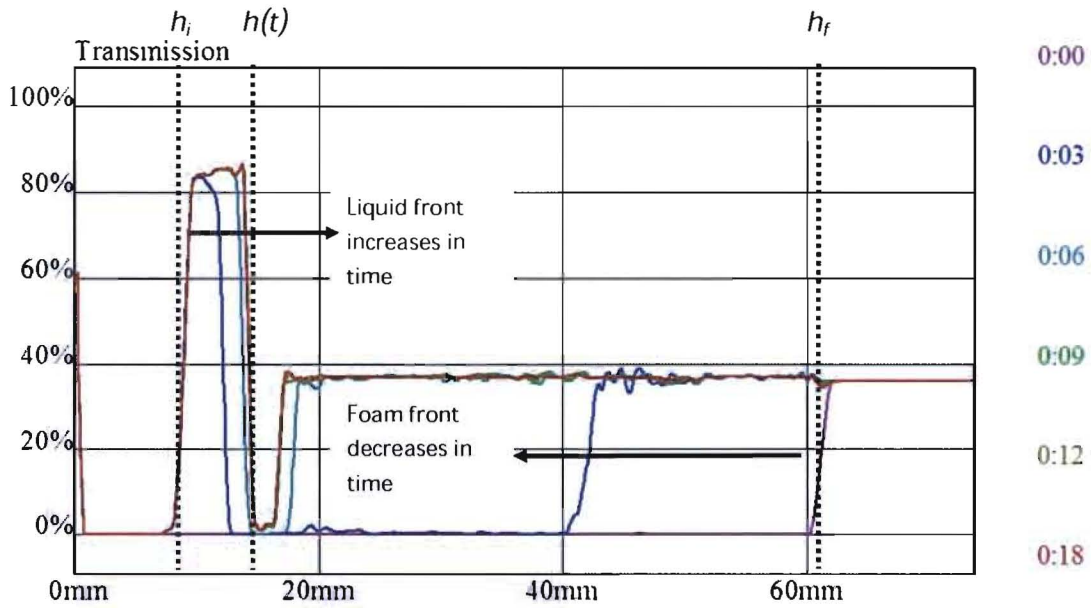


Figure 4-3 Light transmission profile of HPMC foamed binder. The right hand side legend indicates the colour key for the six profiles from $t = 0$ minutes (0:00) to $t = 18$ minutes (0:18).

Figure 4-3 shows the light transmission profile (%T) as a function of the height for a sample of HPMC foam in the scanning tube from time $t = 0$ minute to $t = 18$ minutes. The tube plug is located between 0mm to 7mm, which always has 0% transmission at any time. At $t = 0$, the opaque structure of the foam always results in 0%T in the foam zone. In this case, the foam has an amount equivalent to 60mm height in the tube. As time increases, the foam drains from the top to the bottom while liquid drains and accumulates from the bottom. This evolution of foam in time give rises to 80%T corresponding to the liquid and 38%T corresponding to the empty section of the tube. 38%T corresponds to the scanning across the transparent tube when foam has collapsed.

From the transmission profile, several parameters can be defined to describe the transitional change of foam and liquid in the cylindrical glass tube (as illustrated in Figure 4-2). Section h_i to h_l represents the liquid front and section h_l to h_f represents the foam front. The section from 0mm to h_i is the bottom tube plug.

At $t = 0$, the foam height (H_f) corresponding to the amount of foam introduced into the tube can be obtained as:

$$H_f = h_f - h_i \quad \text{Eq. [4-2]}$$

The liquid content in the foam (H_l) can be obtained at complete foam breakdown as:

$$H_l = h_l - h_i \quad \text{Eq. [4-3]}$$

Based on the ratio of foam and liquid heights in the tube, the foam quality (FQ) as defined in Eq. [2-7] can be calculated for the sample using:

$$\left(1 - \frac{H_l}{H_f}\right) \times 100\% \quad \text{Eq. [4-4]}$$

The drained liquid height as a function of time (Δh_l) can be obtained as:

$$\Delta h_l(t) = h(t) - h_i \quad \text{Eq. [4-5]}$$

where $h(t)$ is the liquid height at time t .

This rate of increase of the liquid fraction at the bottom of the tube is proportional to the drainage rate of the foam. The fraction of the foam which has collapsed, $f_{collapsed}(t)$ can be indicated as a dimensionless change of liquid fraction in the foam at any given time:

$$f_{collapsed}(t) = \frac{\Delta h_l(t)}{H_l} \quad \text{Eq. [4-6]}$$

Note that the “height” mentioned in this context is equivalent to volume of the tube that has a constant cross section area.

The addition of the foam into the tube causes some minor collapse, and the foam qualities calculated after addition to the scanning tube were 2%-3% lower than the initial foam quality exiting the foam generator. This difference in foam quality is minor and is not expected to have significantly affected the results.

4.3 Results

4.3.1 Foam drainage

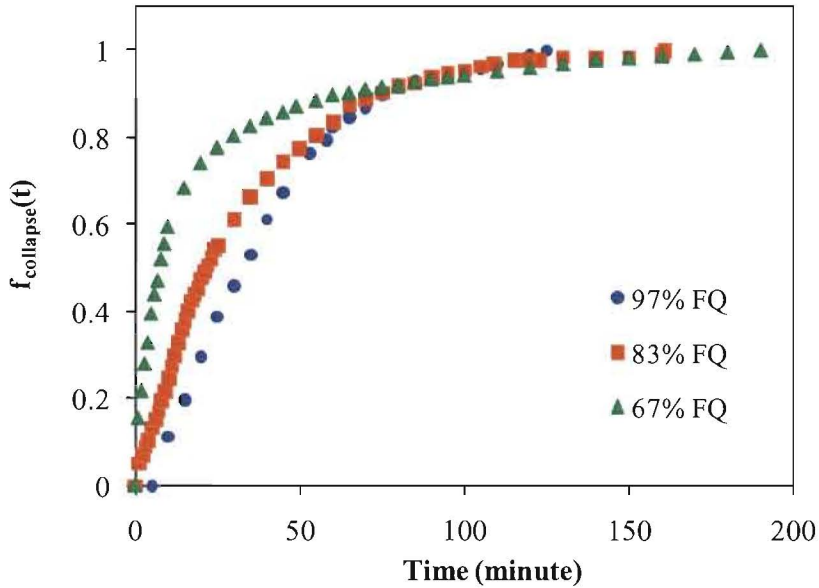


Figure 4-4 Drainage profiles of HPMC foams at foam quality (FQ) – 97% FQ, 83% FQ and 67% FQ.

Figure 4-4 shows the drainage profile for three different foam qualities of HPMC foam obtained from the Turbiscan. The lowest foam quality of 67% had the fastest drainage rate, followed by 83% and 97%, as indicated by the slope of the drainage profile. A steeper slope indicates a larger drainage rate, where the foam breaks down in a shorter decay time. A high quality foam has a closely packed bubble structure, resulting in a stable foam that tends to resist bubble coalescence and liquid drainage. In contrast, low quality foam has larger and fewer bubbles and forms an unstable foam. An unstable foam entrained with a larger amount of liquid also results in a larger pressure head and in turn a greater tendency for gravitational drainage (Magrabi, 2002; Saint-Jalmes, 2006). The physical chemistry factors affecting foam drainage stability are a complex issue beyond the scope of this study (Pugh, 1996; Saint-Jalmes, 2006).

For a constant cross-sectional area of the tube, the volume of liquid is equivalent to the liquid level in the tube. Hence, the drainage profiles in Figure 4-4 can be described by:

$$V_l(t) = V_o(1 - e^{-\lambda t}) \quad \text{Eq. [4-7]}$$

where λ is the drainage constant for certain type of foam and $V_l(t)$ is the volume of liquid drained at time t . As t becomes large, $V_l(t)$ approaches a volume V_o of the original fluid used to produce the foam. The drainage constant was obtained by fitting Eq. [4-7] to the data, as shown in Table 4-2. This empirical model only considers liquid drainage that contributes to foam stability, and does not attempt to incorporate the fundamental microscopic mechanisms of bubble coalescence and lamellae thinning during the foam decay process.

Table 4-2 Foam drainage properties.

Binders	Foam quality (%)	Drainage constant λ (min^{-1})
	97	0.026
HPMC	83	0.031
	67	0.057

From Table 4-2, it is seen that the drainage constant increases with decreasing foam quality, indicating that a low quality foam drains at a faster rate compared to a high quality foam. This information on the foam drainage properties provides an understanding of the wetting behaviour as a function of foam quality, which is useful to interpret the nucleation conditions later in the experiments.

4.3.2 Foam dispersion behaviour

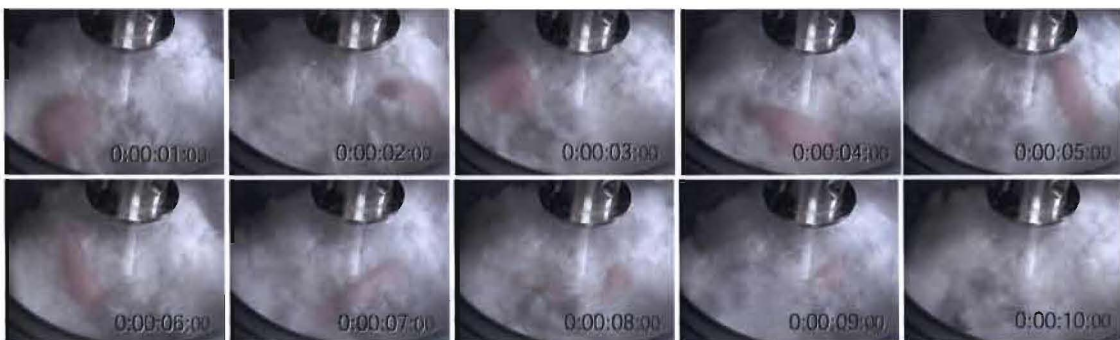


Figure 4-5 Foam dispersion (shown in pink) during powder bumping flow.

Figure 4-5 and Figure 4-6 show the behaviour of foam during the initial contact with a dynamic powder bed under bumping and roping conditions in the mixer granulator. At different powder flow conditions, the foam was observed to undergo different motion due to the changes in shear flow created by the impeller speed. The wetting and nucleation processes occurring during foam dispersion were also influenced by the powder flow conditions.

At bumping flow, the foam was initially stable and remained in its original shape as it moved with the powder bed. After a period of powder rotation, the foam began to elongate and deform. This can be seen from 4 seconds onwards (Figure 4-5) as the foam was pulled apart by the powder rotation. This motion of foam can be explained as follows. The foam was initially static and little drainage occurred. Foam elongation begins as the powder rotation stretches the foam due to the relative motion of the particles and the highly deformable nature of the foam. We believe that this behaviour is critical for the efficient spreading of foam, as elongation of the foam further distributes the binder over a larger particle surface area and helps ensure efficient binder delivery and particle coverage.

During the elongation process, we believe that the foam also drains into the powder, establishing liquid bridges with the powder particles to form nuclei. In addition, the top layer of powder particles is slowly immersed into the foam to form nuclei due to the bumping motion. In bumping flow, wetting and nucleation occur by localised drainage and random collisions of particles into the foam at the powder surface. These two effects combined eventually lead to complete dispersion of the foam, which forms a thin, flat and highly saturated layer on the powder surface, similar to the shapes observed in *Chapter 3*. The volume of powder wetted is proportional to the area of contact between the foam and powder. In this case, the foam was dispersed after around 10 seconds under bumping flow conditions.



Figure 4-6 Foam dispersion (shown in pink) during powder roping flow.

In contrast, under roping flow, the foam is quickly dispersed in a much shorter time (Figure 4-6). Under this intense agitation flow, the foam disappeared from view (and was assumed to be dispersed) within 1 second. The foam quickly moved towards the centre of the bowl as soon as the powder motion commenced. This implies that under roping flow, the majority of wetting and nucleation occurs beneath the powder surface by mechanical mixing. The roping flow distributes the fluid within the foam into a much larger volume of powder, and produces nuclei with a much lower saturation. Mechanical mixing is presumably able to provide fast and efficient dispersion of the foam within the powder bed, and therefore efficient wetting and nucleation may be expected under roping flow conditions.

4.3.3 Nuclei formation

Figure 4-7 shows examples of the nuclei granules obtained after dispersion of the small quantity of foam. All nuclei obtained from pre-sieving (see *section 4.2.2.2*) were larger than 250 μm . Visual inspection of the material collected in the pan for signs of the dye colour confirmed that the pan comprised only of unwetted primary feed powder – no nuclei agglomerates were seen to pass through the 250 μm sieve.

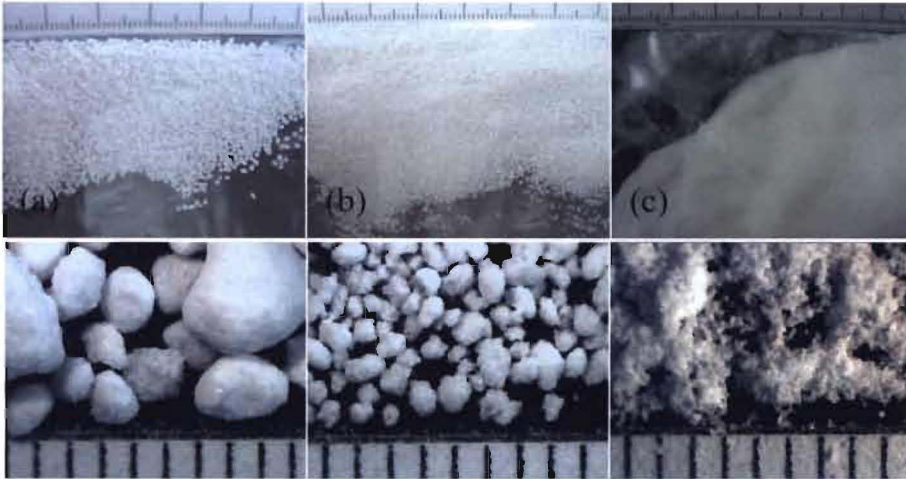


Figure 4-7 Images of nuclei samples (a) $>1\text{mm}$ (b) $850\mu\text{m}-425\mu\text{m}$ (c) non-granular materials $<250\mu\text{m}$. Scale is in millimetres.

Figure 4-7 shows that the granular and non-granular materials can be clearly differentiated from the appearance of the products. The coarse nuclei $>250\mu\text{m}$ were irregular in shape with rough surfaces and were quite different from the fine $<250\mu\text{m}$ powders.

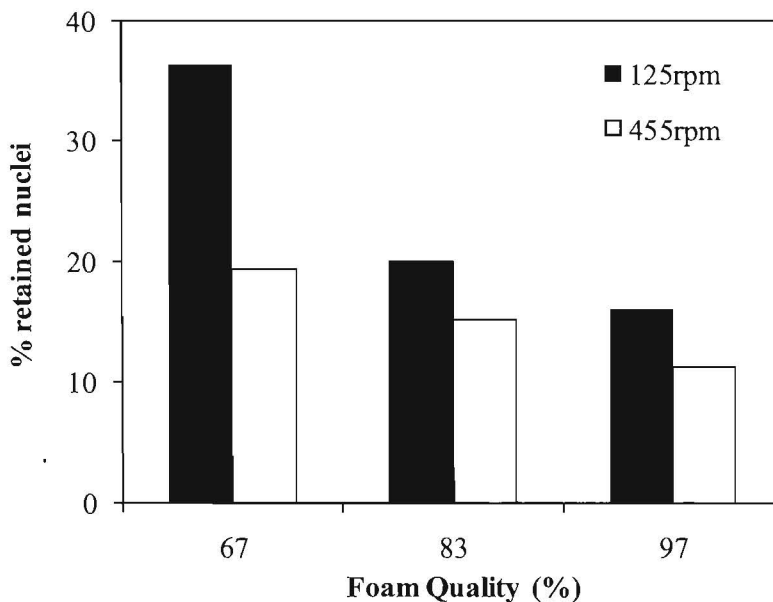


Figure 4-8 Nuclei formation as a function of impeller speed and foam quality. The “% retained nuclei” is defined as the mass fraction of nuclei larger than $250\mu\text{m}$.

Figure 4-8 shows the mass fraction of nuclei greater than 250 μm retained from each nucleation experiment (shown as “% retained nuclei” on the vertical axis). The same amount of foam is added in each experiment. The degree of nucleation, as reflected by the mass fraction of nuclei formed, is significantly affected by changing foam quality and/or impeller speed. This trend is significant when the materials are granulated under less intense mixing conditions, i.e. comparing 125rpm and 455rpm impeller speeds. At 125rpm impeller speed (bumping flow regime), a large fraction of nuclei (~37%) is obtained using low quality foam (67% FQ). This mass fraction decreases steadily as the foam quality increases up to 97% FQ. Under roping flow conditions at 455rpm, the fraction of nuclei formed is much more consistent, although there is still a decrease in the fraction of nuclei as the foam quality increases. We speculate that the effect of foam quality could be completely eliminated if an even higher impeller speed was used. Nonetheless, the influence of foam quality on the fraction of nuclei formed is significantly minimized when the powder is undergoing roping flow.

We postulate that the differences in the fraction of nuclei formed are the result of differences in the wetting and dispersion behaviour of the foams. Low quality foam produces a larger extent of wetting and nucleation, giving the largest fraction of nuclei compared to high quality foam. As high quality foam is also less saturated per unit volume of binder, it in theory is unable to form highly saturated, strong nuclei due to a lower liquid amount and fewer liquid bridges. These weak nuclei are therefore easily broken into fines smaller than 250 μm , which were not counted as nuclei in this study.

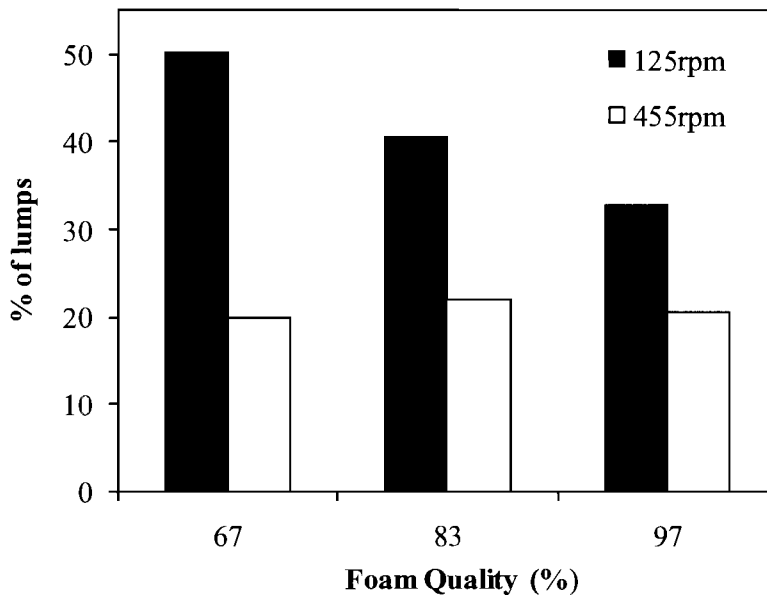


Figure 4-9 Mass fraction of lumps (nuclei >2mm) as a function of impeller speed and foam quality.

Figure 4-9 compares the fraction of “lumps”, defined as nuclei larger than 2mm, formed during the short granulation experiments. These coarse nuclei can be easily formed via nucleation (not granule growth), especially in the absence of sufficient mechanical mixing during the initial binder addition phase. Figure 4-9 shows that the proportion of “lumps” is much higher under bumping flow (125rpm) as a result of poor binder dispersion. A low fraction of lumps is desired, as a result of 50% lumps means that 50% of the granules formed (see Figure 4-8) were larger than 2mm. Decreasing the foam quality in bumping flow (125rpm) led to a large increase in the formation of lumps from 30% to 50%, suggesting that low quality foam is undesirable in the absence of vigorous agitation conditions. Low quality foam tends to create more lumps, which is compounded when there is insufficient mechanical force to assist binder dispersion.

The formation of lumps is significantly reduced when the impeller speed is increased to 455rpm. The coarse nuclei >2mm obtained at a high impeller speed remain constant at approximately 20% regardless of the foam quality. Again, this implies that the formation of foam nuclei can be controlled by mechanical dispersion using roping flow. Increasing the impeller speed in a mixer-granulator aids binder dispersion by increasing both the shear forces

and the powder collision in the granulator. Clearly, the good powder mixing achieved at a high impeller speed allows more uniform distribution of the powder and the binder, which then minimises the formation of lumps. Alternatively, the mechanical action may also break the large agglomerates into fine nuclei.

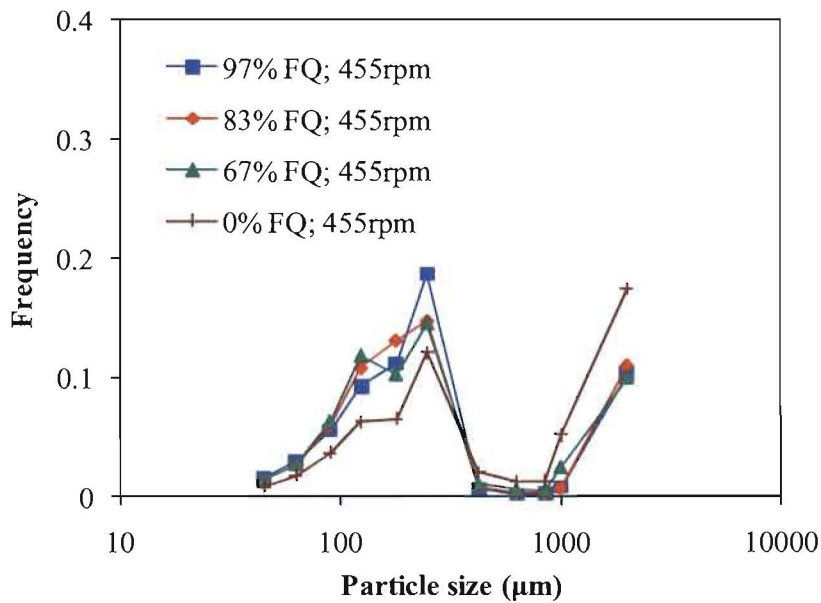


Figure 4-10 Nuclei size distributions at 455rpm impeller speed as a function of foam quality. Note that 0% FQ indicates spray delivery.

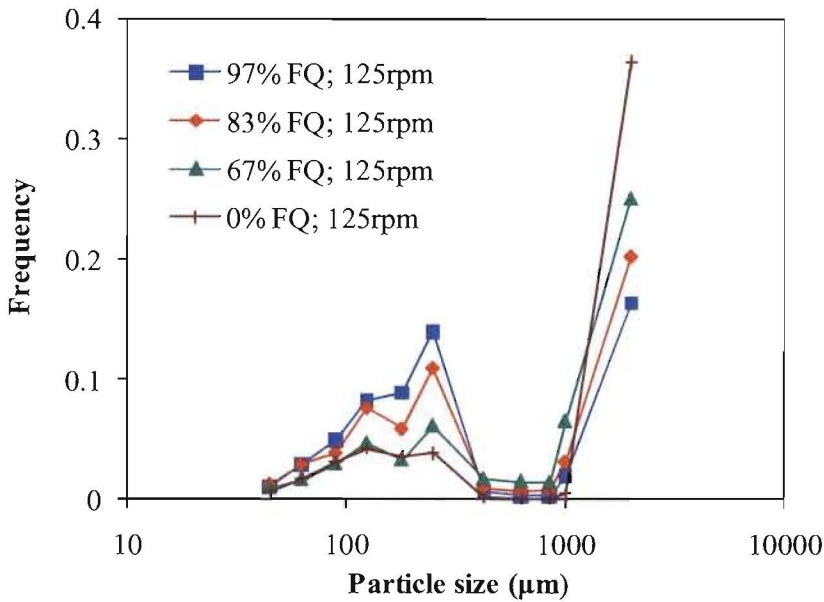


Figure 4-11 Nuclei size distributions at 125rpm impeller speed as a function of foam quality. Note that 0% FQ indicates spray delivery.

Figure 4-10 and Figure 4-11 show the nuclei size distribution as a function of foam quality, including 0% FQ (which represents a spray) at 455rpm and 125rpm impeller speed respectively. The nuclei size distribution changes in response to both the impeller speed and the foam quality. Delivering the liquid binder as a foam at 97% FQ caused a reduction in the spread of the nuclei size distribution and the fewest lumps when the powder was experiencing bumping flow at 125rpm (Figure 4-11). In contrast, under roping flow at 455rpm, changes in foam quality show no significant effect as the nuclei size distributions are all very similar regardless of the foam quality.

The nuclei size distributions at a low impeller speed (125rpm, bumping flow) shown in Figure 4-11 are broader and contain more large “lumps” compared to roping flow conditions (see Figure 4-10). This trend becomes worse when low quality foam is used. Figure 4-11 shows that decreasing the foam quality has resulted in an increase in the spread of the nuclei size distribution, with an increasing fraction of large agglomerates. In this case, the nuclei size distribution is significantly affected by the foam quality when the mixing conditions are less intense.

Figure 4-10 and Figure 4-11 also compare nucleation by foam delivery and spray delivery (0% FQ). For spray delivery, the nuclei size distributions produced at 125rpm and 455rpm impeller speeds are broader compared to foam delivery. This is supported by the weight mean diameter (see Table 4-3), where spray delivery (0% FQ) has produced coarser nuclei at both impeller speeds, compared to foam delivery at all foam qualities. Increasing the impeller speed to 455 rpm produced sufficiently strong powder agitation to reduce the number of large agglomerates, and produced a nuclei size distribution similar to that of foam delivery, although not quite as good.

Table 4-3 Weight mean diameter of nuclei at varied impeller speed and foam quality. Note that 0% indicates spray delivery.

Foam quality (%)	125rpm impeller speed	455rpm impeller speed
	Weight mean diameter d_m (μm)	
0	2252	1358
67	1805	849
83	1444	860
97	1192	827

The effect of changing foam quality at varied impeller speeds on the nuclei size can also be indicated by the weight mean diameter. Table 4-3 shows that at a 125rpm impeller speed, decreasing foam quality shows an increase in the weight mean diameter from 1192 μm to 1805 μm . The nuclei obtained via foam granulation at a 455rpm impeller speed are very similar in size, regardless of the foam quality used. In both cases, the use of a spray (0% FQ) results in a much larger mean granule size.

4.4 Discussion

4.4.1 Comparing nucleation by foam delivery and spray delivery

Changes in the particle size distribution in response to changes in the binder delivery method have been described extensively in the literature (Bardin *et al.*, 2004; Butensky and Hyman, 1971; Knight *et al.*, 1998; Scott *et al.*, 2000; Wauters *et al.*, 2002). Of the different types of binder addition methods available in wet granulation processes, the foam addition method is

the newest approach for distributing the liquid and achieving a controlled granule size distribution.

Nucleation experiments in this chapter evaluated the binder dispersion and the nuclei size distributions after spray and foam binder addition. The process of wetting and nucleating the powders appear to be different for foams vs. sprayed droplets. This, in turn, can result in varying degrees of binder dispersion, which is generally reflected in the nuclei size distribution. In this study, atomisation of the binder at the same processing conditions (binder amount, flow rate, impeller speed and mixing time) has led to a broader spread of the nuclei size distributions, indicating that the quality of mixing between the powder particles and the binder is strongly affected by the binder addition method. As instantaneous uniform binder dispersion is impossible during initial binder addition (Knight *et al.*, 2000), an initially bimodal nuclei size distribution is still inevitable with both foam and spray delivery (see Figure 4-10 and Figure 4-11). However, nucleation experiments performed using the foam addition method achieved narrower nuclei size distributions with far fewer coarse “lumps”, demonstrating the potential of foam granulation to achieve improved binder distribution, compared to traditional spray delivery. Further experiments over a wider range of conditions are considered in *Chapters 5, 6 and 7*.

Although the penetration of the foam into the powder bed was quite long under the low-agitation intensity of bumping flow, the fraction of “lumps” formed during nucleation was far less compared to the equivalent spray conditions. Spray drops are unable to spread laterally across the powder bed and they penetrate mostly vertically into the powder bed wherever they land. Drop penetration is the predominant mechanism in spray granulation, combined with drop coalescence due to high spray flux and/or long drop penetration times, which form coarse nuclei (Hapgood *et al.*, 2003; Litster *et al.*, 2002; Litster *et al.*, 2001). In these short granulation experiments, there is not much time drop for significant mechanical dispersion, and the nuclei formed by penetration of the binder droplets are presumably more saturated, forming coarse nuclei.

In contrast, the foamed binder can deform and elongate over the powder bed, particularly during roping flow. The elongated foam covers a larger area of particles as it becomes distributed and interacts with the powder particles. The increase in foam contact area means

that a larger area of dry powder which was not initially at the top layer of the bed comes into direct contact with the wet foam, distributing the liquid more effectively. This is somewhat analogous to reducing the spray flux by increasing the area of the spray zone in spray granulation. In addition, the foamed binder contains many small bubbles of gas within the liquid binder, so the granules are likely to be less saturated. The lower liquid amount means fewer liquid bridges, and the foam nuclei may also be weaker and more easily dispersed via mechanical dispersion forces.

The tremendous increase in the liquid-air surface area when the binder fluid is converted into a foam presumably also increases the coverage of the particles with liquid i.e. a larger surface area of the particles will have liquid present, as the liquid is spread very thinly through the foam. This implies that the wetting zone area is larger during foam binder addition, compared to spray binder addition. Based on the concept of dimensionless spray flux (Ψ_a), this should also theoretically imply a lower Ψ_a through an increased “spray zone” for foam binder delivery, considering that the liquid addition rate and the velocity of powder traversing the wetting zone under the same impeller speed are the same (Litster *et al.*, 2001). A lower effective spray flux is in agreement with the reduction in the spread of the nuclei size distributions, and particularly with the reduction in the proportion of coarse granules (Hapgood *et al.*, 2003). However, it is not immediately apparent how dimensionless spray flux will quantitatively describe foam granulation at this stage. Detailed characterisations of foam and droplet motion during granulation are recommended in the future to understand the microscopic interactions between the foam/droplet and the particles, which will help in characterising the particle coverage processes.

Large scale industrial granulation processes typically operate well outside of the drop controlled regime, and generally operate in the mechanical dispersion regime (Litster, 2003). In addition, most large scale mixer granulators operate in bumping flow (Plank *et al.*, 2003) where the mechanical agitation is insufficient to disperse the liquid rapidly. Assuming that mechanical dispersion is the governing mechanism in most industrial processes, foam granulation may be a more robust process which forms fewer lumps, indicating better liquid dispersion. Since foam granulation is simpler to scale-up compared to matching flow rate, drop size and spray area of a spray nozzle (Keary and Sheskey, 2004; Sheskey *et al.*, 2007), the improvement in the nuclei formation shown in this work indicates that foam granulation offers

controlled nucleation conditions over a wide range of powder mixing conditions, which should result in improved control of the overall granulation process.

4.4.2 Proposed foam wetting and nucleation mechanisms

From the results, the quality of the nuclei created varies depending on the interactions between the impeller speed and the foam quality. Nucleation with low quality foam and poor powder agitation (i.e. bumping powder flow) produced the widest nuclei size distribution, including a large proportion of lumps. Using high quality foam created a narrower nuclei size distribution with fewer lumps. When roping flow was developed in the mixer-granulator, the tightest nuclei size distributions were produced. During powder roping flow, the influence of foam quality on the nuclei size was minimised.

Therefore, foam-induced nucleation is sensitive to changes in both impeller speed and foam quality. Depending on the particular foam qualities and impeller speeds, different wetting and nucleation mechanisms may dominate. Two mechanisms of wetting and nucleation for foam granulation are proposed: the “foam drainage” controlled regime and the “mechanical dispersion” controlled regime.

In the “foam drainage” wetting and nucleation mechanism, binder dispersion and nucleation are driven by liquid penetration due to foam drainage. Nuclei formation by foam penetration at the powder surface can occur when there is insufficient mechanical force to assist binder dispersion. There is potential for uneven distribution of binder, where localised over-wetting can occur provided that foam drainage occurs before the mixing of powder comes into force. This, in turn, can result in the formation of coarse nuclei. The nuclei size distribution thus broadens as a result of poor binder dispersion. This mechanism was observed for bumping flow, particularly for the low quality foam, as foam drainage rate is inversely proportional to foam quality (see Figure 4-4). Nucleation experiments performed at a 125rpm impeller speed support the existence of a foam drainage nucleation mechanism in foam granulation, which is similar to “drop controlled” nucleation for spray granulation (except the nuclei size distribution with drop controlled is generally narrow).

In the “mechanical dispersion” regime, powder mixing dominates the wetting and nucleation mechanism, and foam drainage has a minimal effect. Uniform binder dispersion will be created

by rapid breakup of the foam due to the shear and agitation induced by mechanical mixing to form homogenous nuclei. This was observed for roping flow, where the foam was quickly dispersed into the powder in less than a second (see Figure 4-6) and the proportion of lumps was low and independent of the foam quality used. Nuclei formed by mechanical dispersion of the foam were generally smaller, as the mechanical impacts developed in powder roping flow conditions are more effective in breaking any large agglomerates into fine nuclei during the nucleation phase. A narrower size distribution is thus obtained as a result of excellent mechanical binder dispersion and nucleation. Foam quality is not a critical variable in this case, as mechanical mixing dominates over the foam drainage mechanism in the formation of nuclei, although foam drainage may still have a minor influence. Nucleation experiments performed at a 455rpm impeller speed support the existence of a mechanical dispersion nucleation mechanism in foam granulation.

In both cases of low and high foam quality, it should be noted that mechanical dispersion is essential for good binder dispersion and nucleation processes. If the mixing is poor, high quality foam hardly incurs any wetting and nucleation due to its low drainage rate. In this case, mechanical mixing is required to create binder dispersion and nucleation. On the other hand, low quality foam is able to induce a high degree of wetting, thus forming coarse nuclei due to its high drainage tendency. In general, good foam nucleation will therefore require mechanical mixing to break over-sized agglomerates into fine nuclei.

Note that although there are some similarities between drop controlled nucleation of sprays and foam drainage controlled nucleation, foam granulation cannot currently be “fitted” into the nucleation regime map for sprays. The nucleation mechanisms for foam versus spray are quite different and sometimes appear to contradict the existing nucleation regime map for sprays (Hapgood *et al.*, 2003). During spray granulation, the drops land on the powder and either penetrate quickly into the powder (drop controlled) or are slowly dispersed mechanically by the powder agitation.

In both of the new foam nucleation regimes we have proposed, the time scale for drainage and penetration of the foam into the powder is far too long to control nucleation, although it appears to influence it. In the end, the foam binder is always dispersed by powder agitation and mechanical dispersion. The key variable is the agitation intensity, and specifically whether the

granulator is operating in bumping or roping flow. However, in roping flow, the foam is dispersed much more quickly. Taking the example shown in Figure 4-6, there is less than one second of contact time between the foam and the upper powder surface before the liquid is dispersed into the powder bed. The time available for foam drainage is minimal and a thin, elongated layer of wet powder is formed at the contact line between the base of the foam and the upper surface of the powder. The vigorous roping flow rapidly pulls the entire lump of foam towards the centre of the mixer and down towards the blades, where it is presumably dispersed in a region of very high shear over a much larger volume of powder.

In contrast, for bumping flow, the foam in Figure 4-5 remains on the powder surface for ~11 seconds. During this time, the foam may drain into the powder pores, and the rate that this occurs depends on the foam quality and the binder viscosity (which was not varied in this study). A fast draining foam will have enough time to form a saturated powder base directly beneath the foam, the same size as the foam footprint. This large, highly saturated mass of wet powder will need to be dispersed by mechanical agitation forces, which are low due to the bumping flow. The saturated powder mass is unlikely to completely disperse, but probably fragments into several smaller pieces, which we measure as “lumps” >2mm. Fewer lumps will form if a high quality foam is used, as the slower drainage rate will form a much smaller saturated base. At the end of the 11 seconds shown in Figure 4-5, a large quantity of the liquid will still be in the foam. The foam is weak and easily dispersed, even under bumping flow conditions, and the final nuclei distribution will contain fewer lumps than the fast draining foam case, but more than if roping flow was used in the experiment.

It is difficult to make direct comparisons with the existing nucleation regime map for spray granulation, since the foam drainage controlled regime can be considered similar to the drop controlled regime of sprays (as both involve the penetration of binder fluid into the powder bed) but can also be considered to be similar to high spray flux conditions, due to the highly saturated and coarse nuclei that are formed. Further work is considered in *Chapter 5, 6 and 7*.

4.5 Conclusions

This chapter studied the binder dispersion and nucleation processes by foam delivery, and compared it to that of using spray delivery. Comparing foam and spray delivery at the same

processing conditions, nucleation experiments in this study showed that narrower nuclei size distribution can be obtained by adding the liquid binder as a foam. This demonstrates the potential of achieving superior binder distribution inherent in the foam granulation technology for wet granulation processes.

Nucleation by a foam addition method was found to be influenced by foam quality and the powder flow conditions, which can be controlled by the impeller speed. Nucleation experiments performed at varied foam quality and impeller speeds showed that low quality foam has achieved the worst binder dispersion and nucleation, producing the broadest nuclei size distribution at a low impeller speed. Increasing the impeller speed, which improves the powder mixing, compensates for the effect of foam quality and achieves a similar quality of binder dispersion and nucleation, resulting in similar nuclei size distributions regardless of the foam quality.

Two wetting and nucleation mechanisms for foam granulation have been proposed: “foam drainage” and “mechanical dispersion”. The two proposed mechanisms describe the binder dispersion and nucleation by foam based on the interactions of foam drainage and powder flow conditions. Mechanical dispersion ultimately disperses the fluid throughout the powder for both regimes. The difference between the two regimes is that in foam drainage controlled nucleation, the foam forms a thin, highly saturated layer beneath the foam before it is dispersed. The fluid in this highly saturated clump may eventually be dispersed by break up, depending on the powder agitation conditions. This understanding of foam induced wetting and nucleation mechanisms are the foundation for future work considered in *Chapters 5, 6 and 7*.

CHAPTER 5
FOAM GRANULATION

Monash University

Declaration for Thesis Chapter 5

In the case of Chapter 5, contributions to the work involved the following:

Name	% contribution	Nature of contribution
Melvin X.L. Tan	100	Initiation, Key ideas, Experimental development, Results interpretation & Writing up
Dr. Karen Hapgood	Supervisor	Initiation, Key ideas, Editing and reviewing

Declaration by co-authors

The undersigned hereby certify that:

- (1) they meet the criteria for authorship in that they have participated in the conception, execution, or interpretation, of at least that part of the publication in their field of expertise;
- (2) they take public responsibility for their part of the publication, except for the responsible author who accepts overall responsibility for the publication;
- (3) there are no other authors of the publication according to these criteria;
- (4) potential conflicts of interest have been disclosed to (a) granting bodies, (b) the editor or publisher of journals or other publications, and (c) the head of the responsible academic unit; and
- (5) the original data are stored at the following location(s) and will be held for at least five years from the date indicated below:

Location(s)

Department of Chemical Engineering, Monash University, Clayton Victoria 3800 Australia.

Signature 1

Signature 2

	Date
	
	

5 FOAM GRANULATION

This chapter considers a series of foam granulation studies at a range of material and process conditions. The impact of material and process variables on foam granulation behaviour in a high shear mixer-granulator is studied. The two wetting and nucleation mechanisms for foam granulation (proposed in the previous chapter) are evaluated by linking the granulation study with previous studies on single nucleus formation and nuclei formation by the nucleation-only mechanism. Transformation maps are presented to explain the changes in granule size distribution in response to changes of material and process parameters on the basis of the wetting and nucleation mechanisms.

5.1 Introduction

So far in the exploration of foam granulation, we have considered foam induced wetting and nucleation on the basis of single nucleus formation on static powders and nuclei formation with a small amount of foamed binder solution, where granulation is limited to a nucleation-only mechanism. We have analysed the factors that affect foam induced wetting and nuclei formation, and defined two wetting and nucleation mechanisms – “foam drainage” and “mechanical dispersion” from the small scale of examining single nucleus formation (see *Chapter 3*) and binder dispersion and nucleation (see *Chapter 4*).

To further evaluate and validate the proposed mechanisms, the study now expands to the granulation process. The granulation study considers a series of foam granulation experiments at a range of material and process conditions to identify the variables that influence the foam granulation process. A series of experimental studies which link single foam penetration experiments, nucleation-only experiments and granulation experiments at both short times and when granulating through to the final solution level is also presented.

5.2 Experimental

5.2.1 Materials

The powders used were lactose monohydrate (100 mesh and 200 mesh, Wyndale, New Zealand) and microcrystalline cellulose (Avicel PH101, Sigma Aldrich, Australia). The liquid binders used were 4% HPMC and 8% HPMC (Methocel E5PLV, Dow Wolff Cellulosics,

USA). A small quantity of food dye (Queens Fine Food Ltd., Australia) was dissolved in the binder solution for visual observations during the experiments. Table 5-1 indicates the powder and liquid binder properties, which were obtained from vendor specifications.

Table 5-1 Powder and liquid binder properties.

Powder/Liquid binder	Grade	Viscosity (mPa.s)	Average particle size (μm)
Microcrystalline cellulose	PH 101	-	50
Lactose monohydrate	100 mesh	-	150
	200 mesh	-	75
4% HPMC	E5PLV	19.1	-
8% HPMC	E5PLV	164	-

5.2.2 Methods

5.2.2.1 Single foam penetration

A 4% HPMC binder was made into aqueous foam with a controlled foam quality using the foam generator (see *section 2.3.1*). A measured amount of foam was then carefully placed onto a static powder bed. The powder beds were prepared by sieving a known amount of 100 mesh lactose powder into a petri dish through a 500 μm sieve. The calculated porosity of the powder bed ranged between 0.61-0.63. The penetration time of the foam was measured as a function of foam quality. For details of the procedure, see *Chapter 3 – section 3.2.2*.

5.2.2.2 Nucleation study

Nucleation experiments were performed in a moving powder bed inside a high shear mixer-granulator. The impeller speed was varied to study the initial foam dispersion and nucleation. A predetermined small amount of foamed binder was added which was sufficient to induce nucleation while avoiding growth and breakage by keeping the saturation low (Iveson and Litster, 1998b). Also refer to *Chapter 4 – section 4.2.2* for details of the procedures.

A 4% HPMC foamed binder prepared at a controlled foam quality using the foam generator was delivered at a rate of 0.1L/min for 10 seconds to 1500g of 100 mesh lactose powder, while the impeller was running at either 105rpm, 205rpm, 295rpm or 515rpm respectively. The

impeller was allowed to run for a further 60 seconds after the binder addition device was removed.

After the experiments, the bed was gently removed and placed in a thin layer on large flat trays so that any wet or fragile nuclei or clumps that might have formed were minimally disturbed. Each tray of powder was dried overnight in a fan-forced oven at 50°C.

The primary particles have particle size distributions ranging from 75µm-250µm. A 250µm sieve size was selected as the cut-off boundary size to separate the nucleated materials from the un-nucleated materials. Any nuclei or clumps larger than 250µm were retained by the sieve, and the un-nucleated particles smaller than 250µm were collected in the collecting pan. Nuclei below 250µm may possibly be formed, but it is practically negligible. This procedure has been used before in spray granulation (Litster *et al.*, 2002; Litster *et al.*, 2001).

To measure the nuclei size distribution, the screened nuclei samples were sieved using a mechanical dry sieve shaker (Retsch A200, Australia) with the following sieve size fractions: pan, 250µm, 425µm, 630µm, 850µm, 1mm, 2mm and 4mm.

5.2.2.3 Granulation experiments

Granulation experiments were carried out with the equipment setup as shown in Figure 5-1. A foam generator was set up with a liquid binder storage tank to introduce the binder as an aqueous foam into a high shear mixer-granulator. The foamed binder was made by combining air with the liquid binder via the foam generator to prepare the desired foam. The foamed binder can be delivered onto the powder bed at a controlled addition rate via a rigid plastic pipe connected to the foam generator. The overhead granulator chopper was not used during the experiments. For full details of the foam generator and the granulator, see *Chapter 2 – section 2.3.1* and *Chapter 4 – section 4.2.2*.



Figure 5-1 Foam granulation experimental setup – (left) high shear mixer-granulator, (middle) liquid binder storage pot and (right) foam generator.

Three powder formulations were used – a pure 100 mesh lactose powder, a 1:1 mass ratio of microcrystalline cellulose and 100 mesh lactose powder mixture, and a 1:1 mass ratio of microcrystalline cellulose and 200 mesh lactose powder mixture. The formulations were initially mixed in the granulator for at least 1 minute before the addition of foamed binder. The required quantity of foamed binder was delivered at the specified flowrate, generally at 0.1L/min. The air flowrate was adjusted to achieve the required foam quality. For some experiments, the granulation was continued after liquid binder addition was stopped to study the effect of wet massing (defined as continued impeller motion after liquid binder addition has ceased). Table 5-2 summarises the operating conditions for the granulation experiments.

Table 5-2 Operating conditions for granulation experiments.

Powder formulation	Liquid binder	Air addition rate (l/min)	Liquid addition rate (l/min)	FQ (%)	Impeller speed (rpm)
100 mesh lactose	4% HPMC	0.5	0.1	83	295
		1.0	0.1	91	295
		3.0	0.1	97	295
		1.0	0.2	83	295
		1.0	0.1	91	515
		3.0	0.1	97	515
100 mesh lactose and microcrystalline cellulose (1:1 mass ratio)	4% HPMC	0.5	0.1	83	295
		0.5	0.1	83	515
		1.0	0.1	91	295
		1.0	0.1	91	515
200 mesh lactose and microcrystalline cellulose (1:1 mass ratio)	4% HPMC 8% HPMC	0.5	0.1	83	295
		1.0	0.1	91	295
		0.5	0.1	83	295
		1.0	0.1	91	295

After each experiment, the granule samples were tray-dried at 50°C overnight in a fan-forced oven. The moisture content of the granules was checked from the mass of the wet granules obtained after sampling and the loss in weight after heating overnight at 50°C. To measure the granule size distributions, sieving analysis was performed using a mechanical dry sieve shaker (Retsch A200, Australia) in an ordered set of sieves: 25µm, 32µm, 45µm, 63µm, 90µm, 125µm, 180µm, 250µm, 425µm, 630µm, 850µm, 1mm, 2mm and 4mm.

The mass distribution of granules allowed the estimation of the evolution of three fractions – fine particles with sizes less than 180µm, intermediate granules having sizes between 180µm and 1000µm and the coarse agglomerates with sizes larger than 1000µm. These size classifications correspond to the typical size ranges in many granulation processes, and are greatly relevant to the applications in pharmaceutical production.

5.3 Results

The results presented are divided into two main sections:

- The granulation study comprises of a series of foam granulation experiments, which investigate the impact of operating and material properties on foam granulation behaviour in a high shear mixer-granulator. The variables studied include liquid to solid ratio, foam quality, impeller speed, wet massing time, feed particle size, binder concentration and foam delivery rate.
- A summary study of single foam penetration, nucleation and granulation experiments is presented at the end.

5.3.1 Foam granulation profiles

Figure 5-2, Figure 5-3 and Figure 5-4 show the evolution of fines, intermediate and coarse mass percentages versus liquid to solid ratio (L:S) during foam addition on coarse lactose (Figure 5-2), on a 1:1 ratio of microcrystalline cellulose and coarse lactose mixture (Figure 5-3), and on a 1:1 ratio of microcrystalline cellulose and fine lactose mixture (Figure 5-4). The evolution of these fractions with time shows evidence for the transition of granulation rate processes in the foam granulation process.

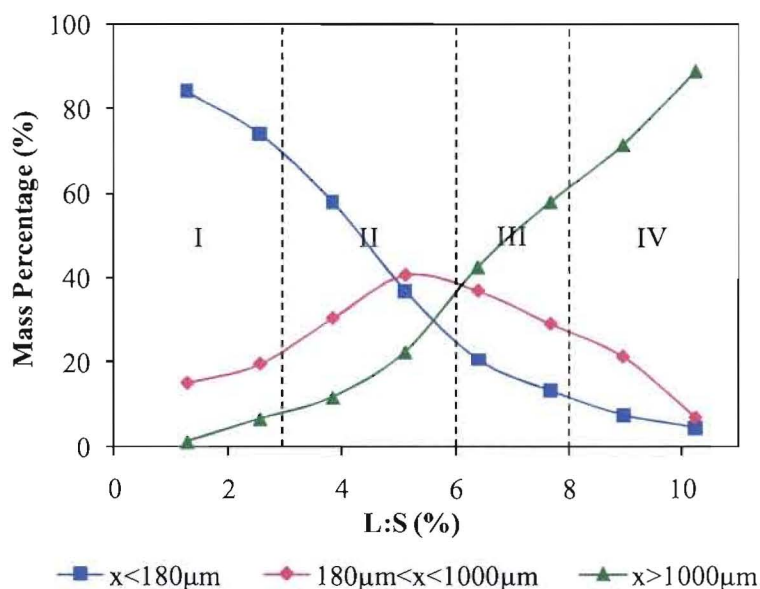


Figure 5-2 Foam granulation profile of 97% FQ foam addition on 100 mesh lactose powder: evolution of particle diameter x – fines ($0\mu\text{m} < x < 180\mu\text{m}$), intermediate ($180\mu\text{m} < x < 1000\mu\text{m}$) and coarse ($x > 1000\mu\text{m}$) mass percentage.

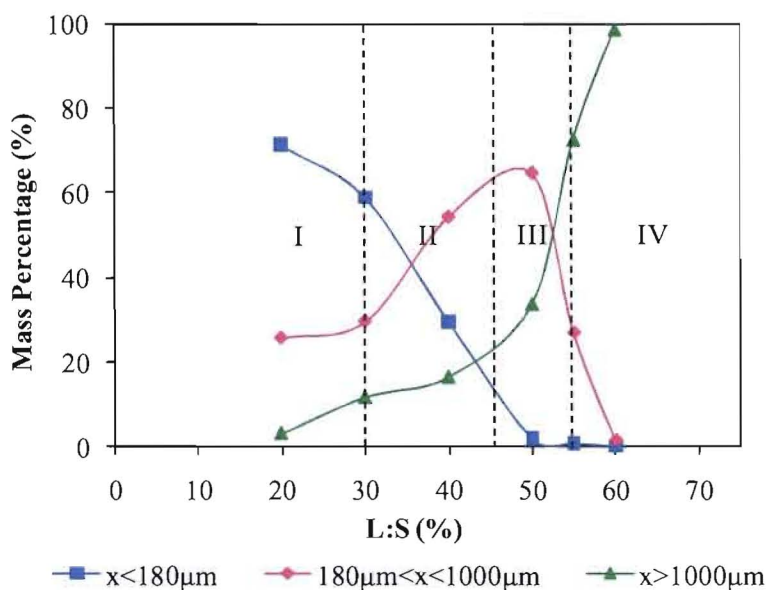


Figure 5-3 Foam granulation profile of 91% FQ foam addition on 100 mesh lactose and microcrystalline cellulose mixture: evolution of particle diameter x – fines ($0\mu\text{m} < x < 180\mu\text{m}$), intermediate ($180\mu\text{m} < x < 1000\mu\text{m}$) and coarse ($x > 1000\mu\text{m}$) mass percentage.

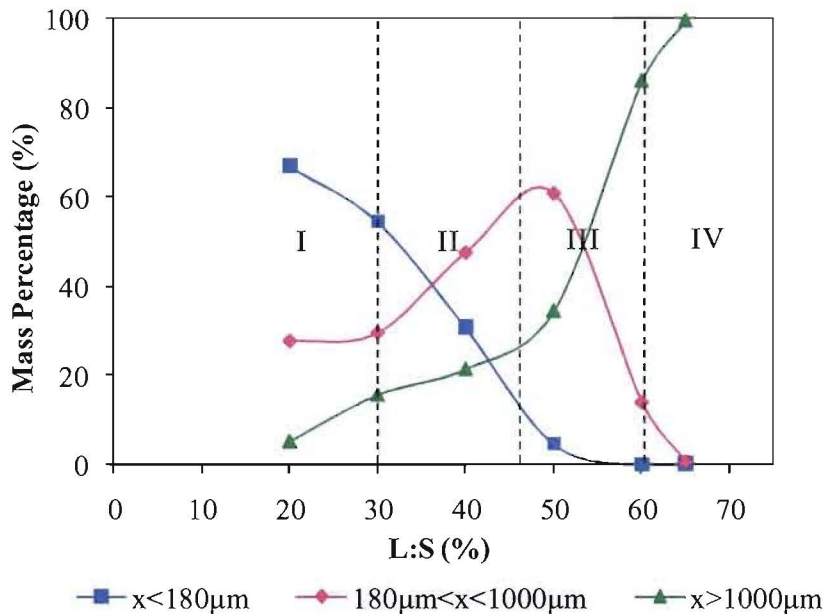


Figure 5-4 Foam granulation profile of 83% FQ foam addition on 200 mesh lactose and microcrystalline cellulose mixture: evolution of particle diameter x – fines ($0\mu\text{m} < x < 180\mu\text{m}$), intermediate ($180\mu\text{m} < x < 1000\mu\text{m}$) and coarse ($x > 1000\mu\text{m}$) mass percentages.

Regardless of the formulation or operating conditions, all experiments experience transition through four phases of the granulation process: I) wetting and nucleation II) growth III) overwetting and IV) caking:

- I. Wetting and nucleation: This regime corresponds to the initial binder addition and nucleation phase, where initial nuclei begin to form (Figure 5-5(a)).
- II. Growth: This regime corresponds to the growth of granules, where spherical granules are produced from collisions between fine/intermediate granules and intermediate granules, rather than coalescence of larger granules (Figure 5-5(b)). The onset of growth of the coarse class tends to lag behind that of the intermediate class, implying a consolidation-layering mechanism for which the fine particles are layered onto the larger granules (decrease of fines). This is indicated by the bell-shaped curve of the intermediate granule mass percentage and a rapid decrease of the percentage of fine

particles. As growth proceeds, the intermediate granules reach a maximum mass percentage, while the coarse granule mass percentage shows a constant ascent.

- III. **Overwetting:** The granulated mixture becomes too wet at higher liquid to solid ratios. This phase shows a regular decrease of the fine and intermediate granules, accompanied by a sudden increase in the fraction of the coarse granules. This implies that following layering growth, coalescence between the “layered granules” occurs, which leads to the rapid increase in the fraction of the coarse granules. The intermediate particles remain visible on the outer layer of the coarse granules (Figure 5-5(c)).
- IV. **Caking:** Coarse granules further coalesce and consolidate to produce huge and highly saturated agglomerates (Figure 5-5(d)).



Figure 5-5 Microscopy images of (a) wetted particles and initial nuclei (b) spherical granules (c) overwetted granules and (d) cake.

5.3.2 Effect of foam quality

Figure 5-6 and Figure 5-7 show the granule size distributions as a function of foam quality for granulation of a 200 mesh lactose and microcrystalline cellulose mixture and a 100 mesh lactose and microcrystalline cellulose mixture, respectively. The granule size distributions are shifted to different extents by changing the foam quality.

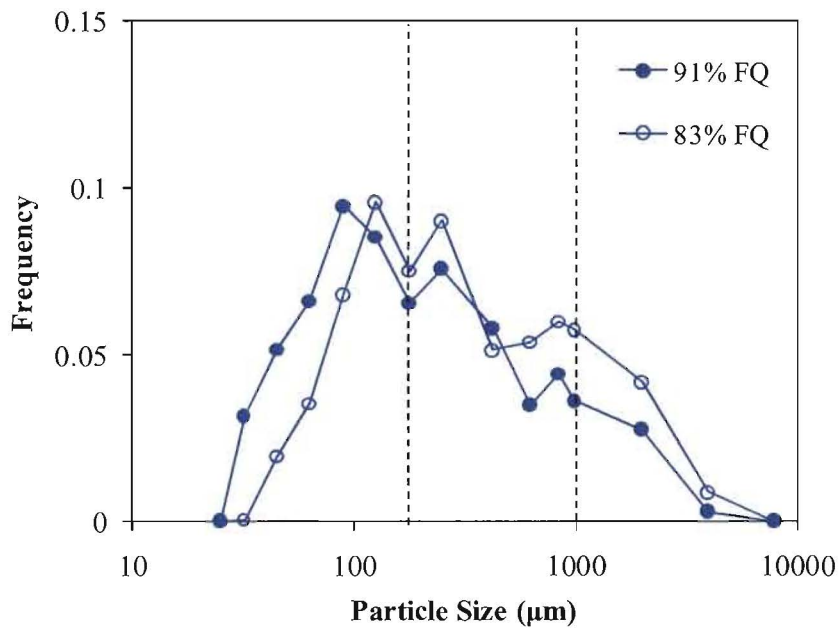


Figure 5-6 Granule size distribution as a function of foam quality – 4% HPMC, 200 mesh lactose and microcrystalline cellulose mixture, 40% L:S, 295rpm. The dotted lines divide the granule size (x) into fine ($x < 180 \mu\text{m}$), intermediate ($180 \mu\text{m} < x < 1000 \mu\text{m}$) and coarse ($x > 1000 \mu\text{m}$) fractions.

Figure 5-6 shows that granulating the powder at 83% FQ has led to more of the fine fraction being granulated, producing a larger fraction of coarse granules. The granule size distribution is coarser compared to granulation at 91% FQ.

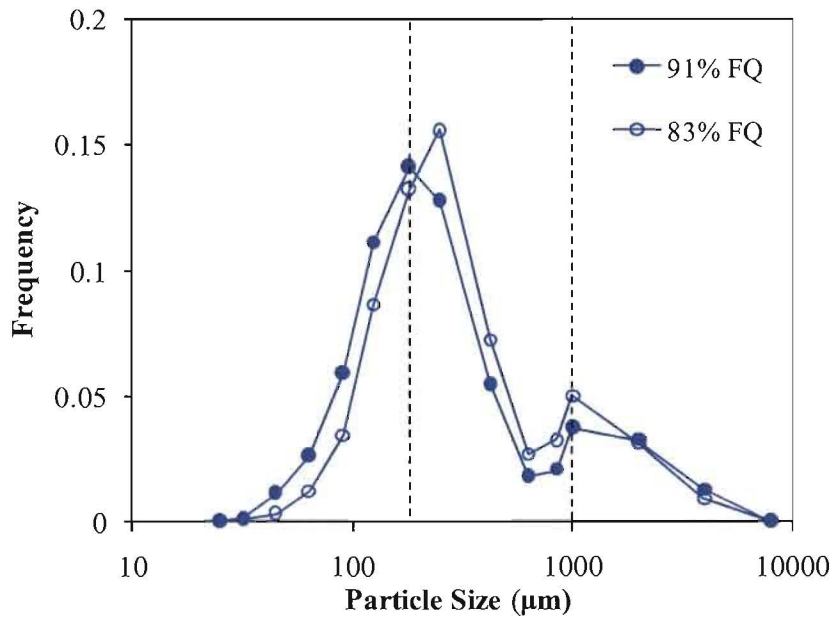


Figure 5-7 Granule size distribution as a function of foam quality – 4% HPMC, 100 mesh lactose and microcrystalline cellulose mixture, 40% L:S, 295rpm. The dotted lines divide the granule size (x) into fine ($x < 180\mu\text{m}$), intermediate ($180\mu\text{m} < x < 1000\mu\text{m}$) and coarse ($x > 1000\mu\text{m}$) fractions.

Figure 5-7 shows a similar trend for a 100 mesh lactose and microcrystalline cellulose mixture, although the differences appear to be relatively small compared to the previous case with a 200 mesh lactose and microcrystalline cellulose mixture (see Figure 5-6). It is seen that for 83% FQ, the granule size distribution is slightly skewed towards larger sizes compared to 91% FQ. It is probable that 100 mesh lactose is readily wettable, which may have minimised the effects of wetting from different foam qualities.

5.3.3 Effect of impeller speed

Figure 5-8 and Figure 5-9 show the evolution of fine, intermediate and coarse fractions as a function of impeller speed. Operating the impeller at 295rpm or 515rpm produce different changes to the granule size fractions at each granulation phase (see *section 5.3.1*).

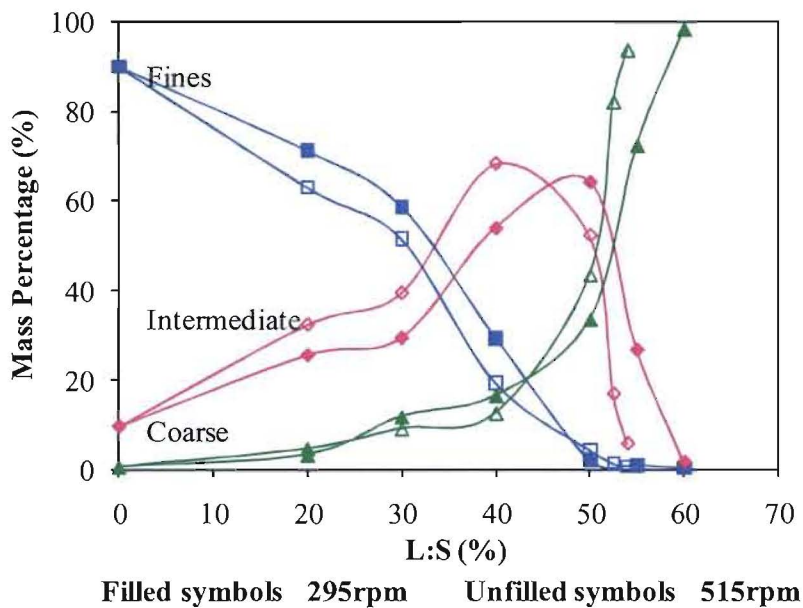


Figure 5-8 Effect of impeller speed on the evolution of fine, intermediate and coarse fractions – 4% HPMC, 100 mesh lactose and microcrystalline cellulose mixture, 91% FQ.

During the initial phase of wetting and nucleation, increasing the impeller speed produces a lower percentage of fine granules, indicating that the nucleation rate process is enhanced at a high impeller speed. At the expense of fine particles, the intermediate fraction increases to a larger proportion at a high impeller speed. Both trends show that the nucleation and/or coalescence of fine and intermediate fractions, and possibly the growth of granules are promoted, when a high impeller speed is used. As granule growth begins, the formation of coarse particles tends to be restricted at high impeller speed. The proportion of coarse particles is lower at a high impeller speed, indicating that the breakage rate process is intensified by the impeller.

As granulation proceeds further, the fine and the intermediate fractions become largely agglomerated. The agglomeration extent increases at a high impeller speed, which leads to a lower proportion of the fine and intermediate fractions. This trend indicates that the coalescence rate process is being enhanced. As the fine and intermediate fractions coalesce, the coarse fraction increases significantly. This phenomenon becomes worse when a high impeller speed is used, as reflected by a larger proportion of coarse granules.

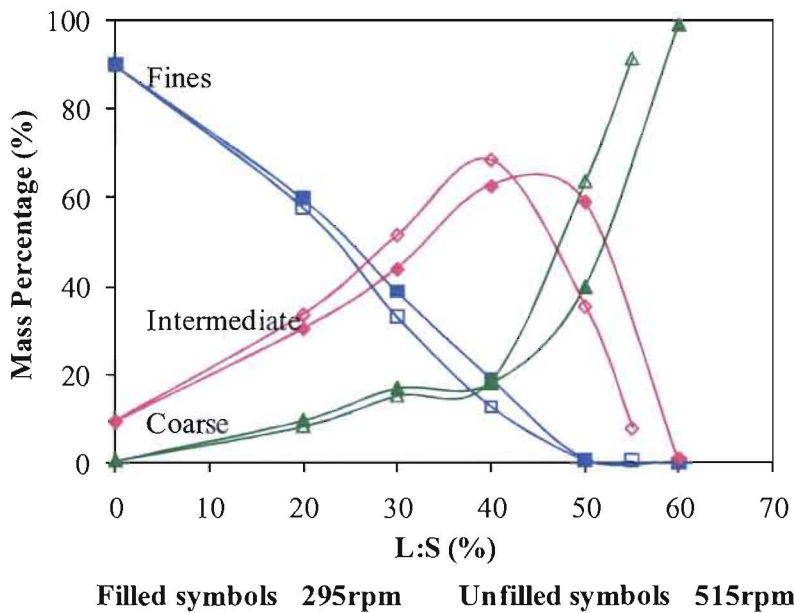


Figure 5-9 Effect of impeller speed on the evolution of fine, intermediate and coarse fractions – 4% HPMC, 100 mesh lactose and microcrystalline cellulose mixture, 83% FQ.

Figure 5-9 shows the same trend for the effect of the impeller speed on foam granulation behaviour for 83% FQ as for 91% FQ. Similarly, a high impeller speed enhances the nucleation rate process, leading to more of the fine particles being granulated into intermediate and coarse fractions. Granule growth causes fine particles to grow further into intermediate granules, but the formation of coarse agglomerates is limited at a high impeller speed. However, the coarse fraction increases more rapidly as granulation proceeds further, indicating undesired granule growth and densification at a high impeller speed.

Overall, the above results show that increasing the impeller speed reduces the foamed binder amount required to promote the transition between the granulation phases. Clearly, a high impeller speed creates an intense mixing between the foamed binder and the particles, which improves binder dispersion and increases the collision frequency between wetted particles. The implication is that the progress rate of granulation will be enhanced, thus reducing the amount of foamed binder required to achieve a similar granulation extent. However, beyond the overwetting regime, the rate of coarse particle formation is also enhanced by a high impeller speed, where the coarse particles rapidly turn into undesired agglomerate lumps. It is also shown in Figure 5-10 that a high impeller speed promotes the formation of large agglomerates

compared to a low impeller speed. Note that both batches are over-granulated, as the experiments were specifically ‘pushed’ to their limits in these cases.

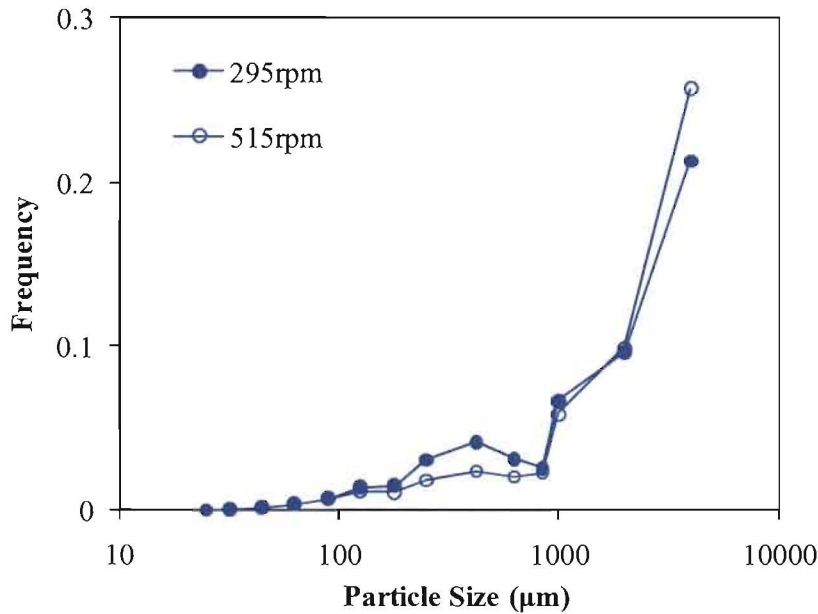


Figure 5-10 Granule size distribution as a function of impeller speed – 4% HPMC, 100 mesh lactose, 91% FQ, 9% L:S.

It should be noted that if the impeller speed becomes too high, fine particles can be generated from granule breakage due to mechanical stress. This can result in a bimodal granule size distribution, with a coarse agglomerated fraction concentrated on the higher end and a fine powder fraction concentrated on the lower end. This was not a problem in the current study, but may be a problem for other formulations.

5.3.4 Effect of wet massing

Figure 5-11 and Figure 5-12 show the changes in granule size distributions after 8% foam addition and wet massing for between 0.5 minute to 2 minutes for granulation with 91% FQ and 83% FQ, respectively. The data immediately after the end of foam binder delivery is shown (top), followed by the data at 30 second wet massing intervals.

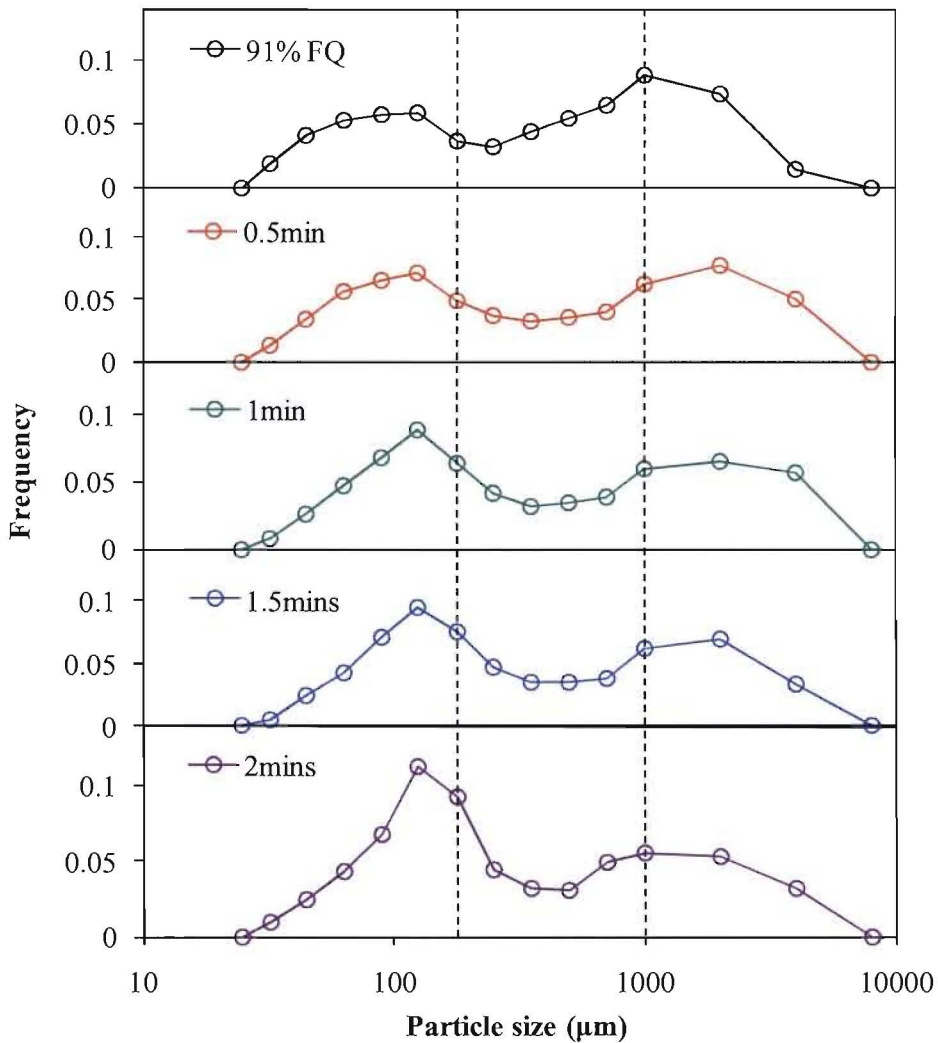


Figure 5-11 Granule size distribution at 91% FQ as a function of wet massing time – 4% HPMC, 200 mesh lactose, 8% L:S, 295rpm. The dotted lines divide the granule size (x) into fine ($x < 180\mu\text{m}$), intermediate ($180\mu\text{m} < x < 1000\mu\text{m}$) and coarse ($x > 1000\mu\text{m}$) fractions.

For 91% FQ, it is seen that longer wet massing times lead to an increase in the proportion of fine and intermediate fractions with a decrease in the coarse granules, indicating granule breakage. During wet massing, smaller granules in the size range $100\mu\text{m}$ - $500\mu\text{m}$ appear to be formed by breakage of the granules larger than $1000\mu\text{m}$.

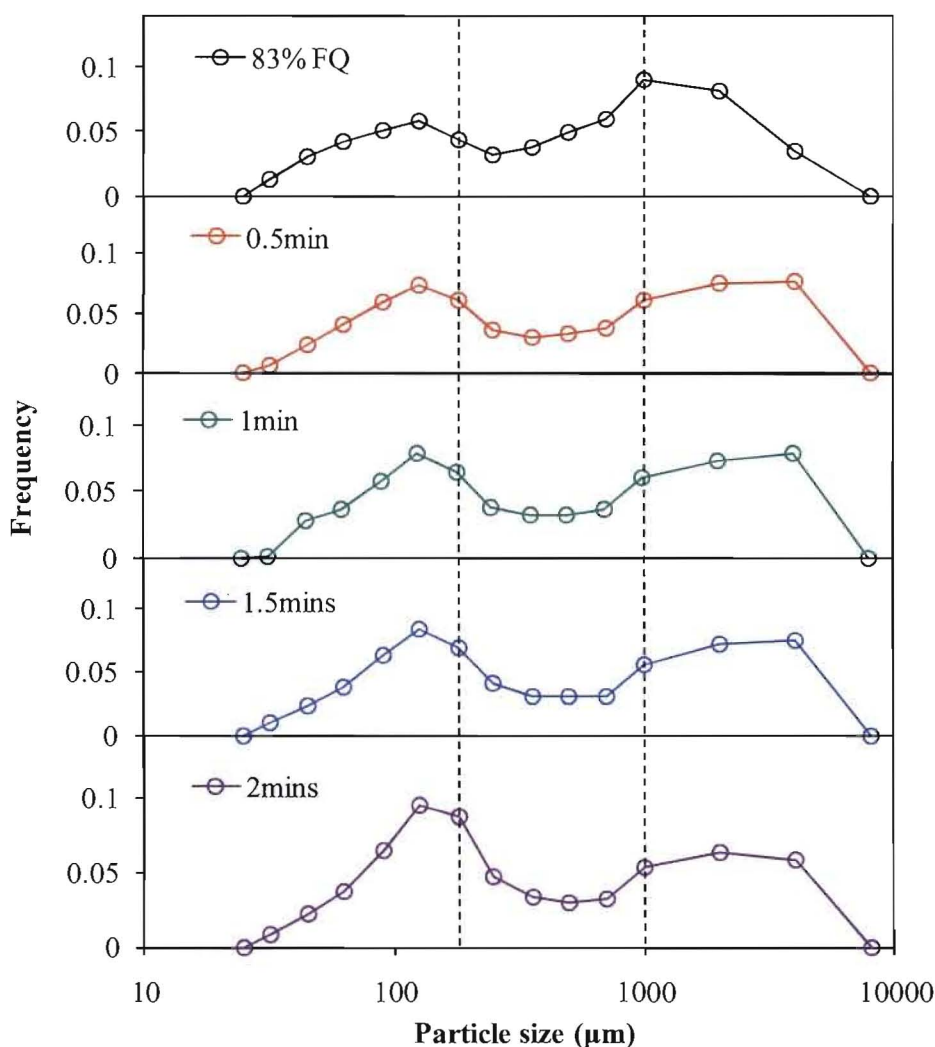


Figure 5-12 Granule size distribution at 83% FQ as a function of wet massing time – 4% HPMC, 200 mesh lactose, 8% L:S, 295rpm. The dotted lines divide the granule size (x) into fine ($x < 180\mu\text{m}$), intermediate ($180\mu\text{m} < x < 1000\mu\text{m}$) and coarse ($x > 1000\mu\text{m}$) fractions.

Figure 5-12 shows the same trend when 83% FQ is used. Similarly, wet massing causes a decrease in the granule size distributions with an increase in fines produced by the breakage of coarse granules. The size distributions in Figure 5-11 and Figure 5-12 look similar but close inspection shows that the 83% FQ batch starts off with more coarse granules and still has a higher proportion of coarse granules at the end of the wet massing period. This is shown more clearly in Figure 5-13, which plots the change in average granule size (d_{50}) with wet massing time for both foam qualities.

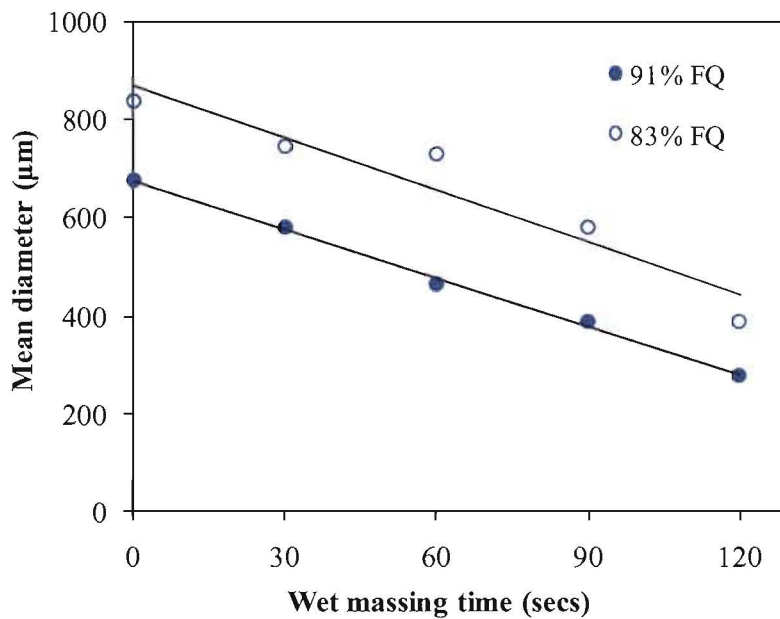


Figure 5-13 Granule mean diameter (d_{50}) as a function of wet massing time.

The granule mean diameter decreases with increasing wet massing time in both cases (91% FQ and 83% FQ), which supports the trend of breakage. Foam delivery at 91% FQ generates a smaller initial average granule size, which also eventually leads to a smaller final average granule size from the batch at the end of wet massing. In comparison, the 83% FQ batch has a larger final average granule size at the start and the end of wet massing, despite breakage causing a decrease in the average granule size. This difference in the initial average granule size remains throughout the wet massing period, which indicates that the granulation retained a “memory” of the original size distribution.

As shown by the parallel fitted trendlines for the two different batches, the breakage rate is constant in each case regardless of the foam quality used to add the liquid binder. For the 83% FQ batch, more coarse granules are formed at the start of the batch, and these granules break down at a constant rate during wet massing, but the size distribution is always larger than the 91% FQ batch. This implies that the breakage rate is controlled by the granule saturation and is independent of the binder foam quality.

In both cases (91% FQ and 83% FQ), the granule size distributions at the end of foamed binder addition show a large fraction of coarse granules (>1mm). Note that these large agglomerates

formed at 8% liquid level are mostly “overwetted” granules (see *section 5.3.1*). As shown in Figure 5-11, Figure 5-12 and Figure 5-13, the decrease in the granule size (distributions) with prolonged mixing show how wet massing is able to easily disperse the large agglomerates within 2 minutes. This also suggests that the granules were weak and easily dispersed via mechanical dispersion forces presumably due to fewer liquid bridges. The foamed binder contains many small bubbles of gas within the liquid binder, so the granules are likely to be less saturated. Measurements of the liquid content of granules will be considered in *Chapter 6*.

However, prolonged or high intensity mixing does not always create granule breakage. It can also lead to excessive granule densification and uncontrollable growth if too much liquid has been added, which makes mixing a difficult variable to manipulate (Iveson *et al.*, 2001a; Knight *et al.*, 2000). Moreover, it is not easy to determine the optimum liquid binder level beforehand, and the required liquid binder amount usually varies from batch to batch. This is shown in Figure 5-14, Figure 5-15 and Figure 5-16, where three granulation batches with 97% FQ, 91% FQ and 83% FQ, respectively, undergo wet massing after 10% foam addition. The very coarse granule size distributions show no trend of granule breakage after wet massing for a period of 4 minutes.

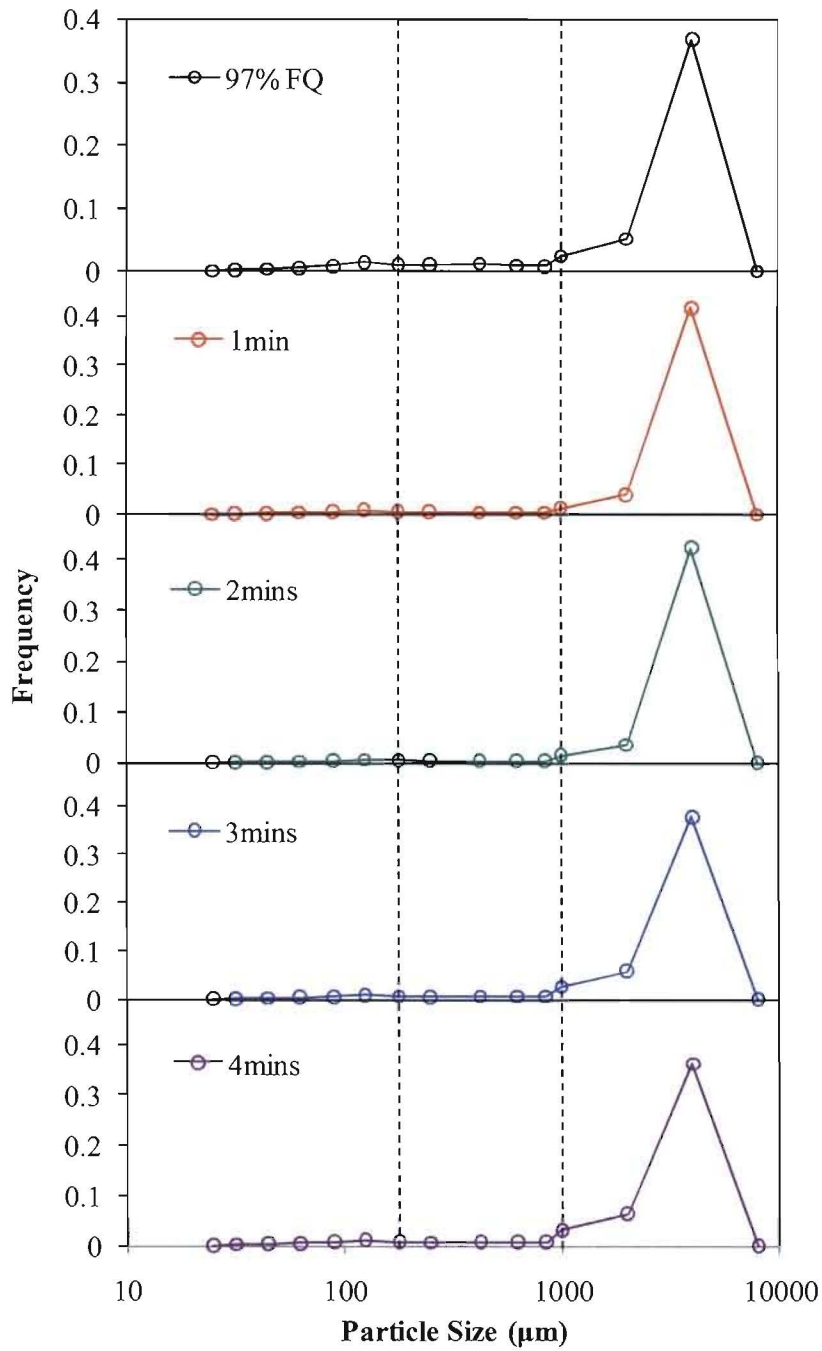


Figure 5-14 Granule size distribution at 97% FQ as a function of wet massing time – 4% HPMC, 100 mesh lactose, 10% L:S, 295rpm. The dotted lines divide the granule size (x) into fine ($x < 180 \mu\text{m}$), intermediate ($180 \mu\text{m} < x < 1000 \mu\text{m}$) and coarse ($x > 1000 \mu\text{m}$) fractions.

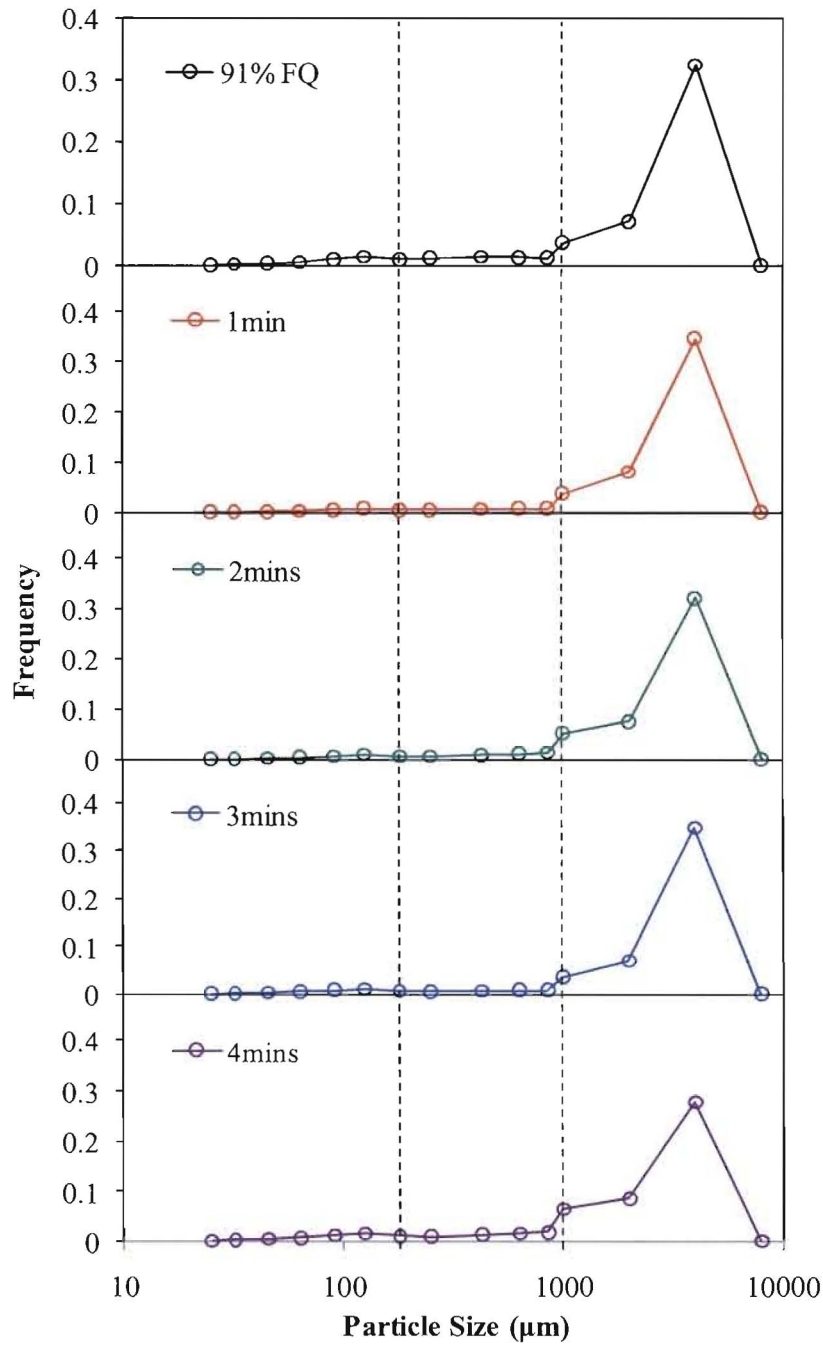


Figure 5-15 Granule size distribution at 91% FQ as a function of wet massing time – 4% HPMC, 100 mesh lactose, 10% L:S, 295rpm. The dotted lines divide the granule size (x) into fine ($x < 180 \mu\text{m}$), intermediate ($180 \mu\text{m} < x < 1000 \mu\text{m}$) and coarse ($x > 1000 \mu\text{m}$) fractions.

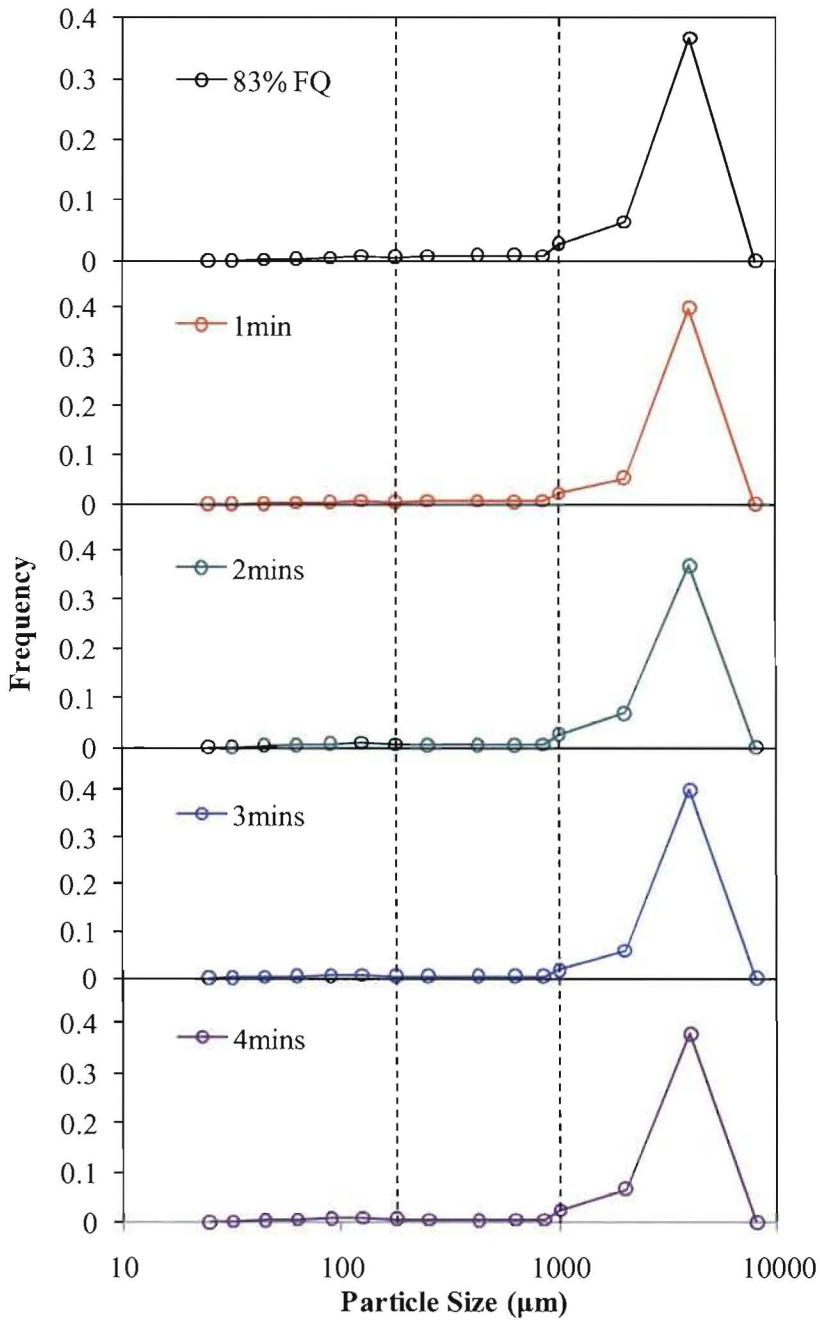


Figure 5-16 Granule size distribution at 83% FQ as a function of wet massing time – 4% HPMC, 100 mesh lactose, 10% L:S, 295rpm. The dotted lines divide the granule size (x) into fine ($x < 180\mu\text{m}$), intermediate ($180\mu\text{m} < x < 1000\mu\text{m}$) and coarse ($x > 1000\mu\text{m}$) fractions.

5.3.5 Effect of primary particle size

Figure 5-17 and Figure 5-18 show the granule size distributions as a function of primary lactose particle size for granulation with 91% FQ and 83% FQ respectively. As indicated in both figures, the “fine” represents the 1:1 mass ratio of 200 mesh lactose and microcrystalline cellulose powder mixture and the “coarse” represents the 1:1 mass ratio of 100 mesh lactose and microcrystalline cellulose powder mixture.

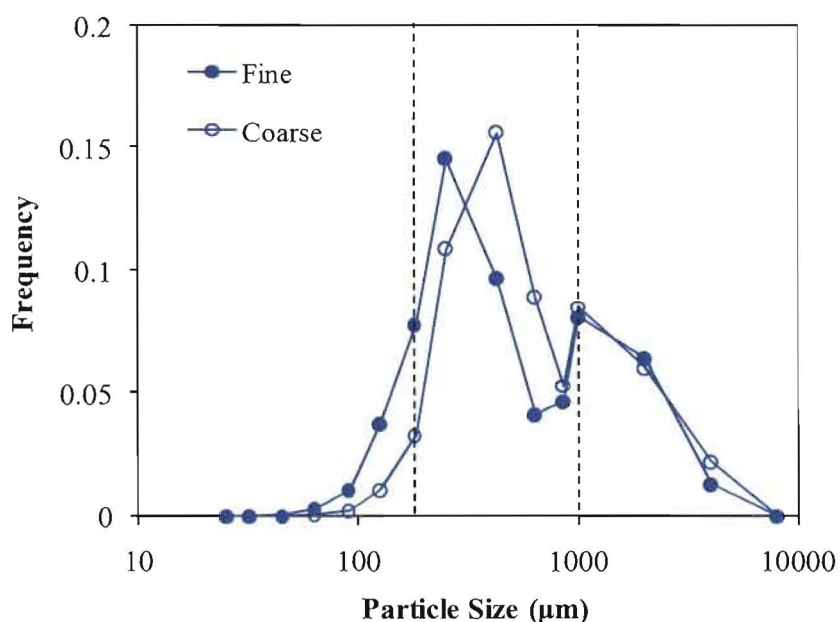


Figure 5-17 Granule size distribution at 91% FQ as a function of primary lactose particle size – 4% HPMC, lactose and microcrystalline cellulose mixture, 50% L:S, 295rpm. The dotted lines divide the granule size (x) into fine ($x < 180\mu\text{m}$), intermediate ($180\mu\text{m} < x < 1000\mu\text{m}$) and coarse ($x > 1000\mu\text{m}$) fractions.

For 91% FQ, the primary lactose particle size has a proportional effect to the granule size distribution, with the use of coarse lactose in the mixture leading to a coarser granule size distribution. There is a large fraction of granules concentrated around the $425\mu\text{m}$ size fraction for the coarse mixture, whereas the granule size is spread around the $250\mu\text{m}$ size fraction for the fine mixture. At the same liquid binder level, the coarser mixture produced a larger granule size distribution. As shown in Figure 5-18, the same results were obtained for the granulation batches with 83% FQ.

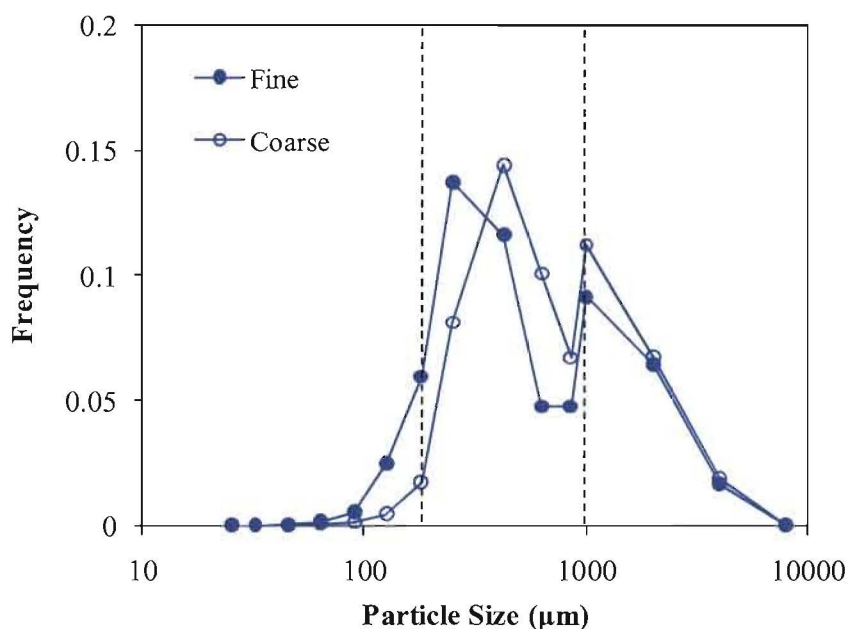


Figure 5-18 Granule size distribution at 83% FQ as a function of primary lactose particle size – 4% HPMC, lactose and microcrystalline cellulose mixture, 50% L:S, 295rpm. The dotted lines divide the granule size (x) into fine ($x < 180\mu\text{m}$), intermediate ($180\mu\text{m} < x < 1000\mu\text{m}$) and coarse ($x > 1000\mu\text{m}$) fractions.

As reported in many studies (Belohlav *et al.*, 2007; Iveson and Litster, 1998a; Johansen and Schaefer, 2001; Keningley *et al.*, 1997; Knight *et al.*, 1998; Kristensen and Schaefer, 1987), more binder fluid is required to form a liquid bridge between the particles when the primary particle size is smaller. The granule attributes are influenced by the surface area of the primary particles. The large contact surface of fine particles leads to high cohesive forces within the powders itself, increasing particle-particle interactions and thereby inhibiting granulation through which fluid must be squeezed between particles to grow. In addition, the packing of the powder bed also influences on the amount of binder fluid required to form the liquid bridges. Fine powders consolidate more slowly and tend to form more porous granules which will require a greater volume of binder fluid to reach saturation (Iveson *et al.*, 2001a). In comparison, the granules formed from coarse powders consolidate and densify quickly into larger, less porous granules (Mackaplow *et al.*, 2000).

The results are in agreement with the material transformation map proposed from the study of single nucleus formation (see *Chapter 3*). The transformation map suggests that a fine powder

system will act as a slow penetrating system and will result in a smaller nucleation ratio. This implies that the fine powder system requires a larger amount of foamed binder in order to create a similar nuclei size compared to a coarse powder system. This difference of the binder amount requirement is affected by the packing of the particles in the granulator. As the packing of a fine powder bed is generally irregular and contains macrovoids (Hapgood *et al.*, 2002b), foam induced wetting and nucleation tends to be restricted such that small nuclei are created. The fine powder bed has a higher volume density of inter-particle contacts, implying that a larger number of liquid bridges can be formed between the fine particles. A greater amount of binder fluid is thus required to wet through the more porous powder bed exposed with a large surface area of the particles for granulation to occur. At the same liquid binder level, the coarse particles therefore are granulated into larger granules compared to the fine particles.

5.3.6 Effect of binder concentration

The effect of binder concentration was studied using 4% HPMC and 8% HPMC foamed binders. Since the binder concentration has a proportional relationship to viscosity, 4% HPMC represents the low viscosity binder whereas 8% HPMC represents the high viscosity binder.

Figure 5-19 and Figure 5-20 show the granule size distributions as a function of binder concentration for the granulation batches with 91% FQ and 83% FQ, respectively. Both systems show the same trend, where the high viscosity foamed binder produced a larger granule size distribution compared to the low viscosity foamed binder at the same foam quality.

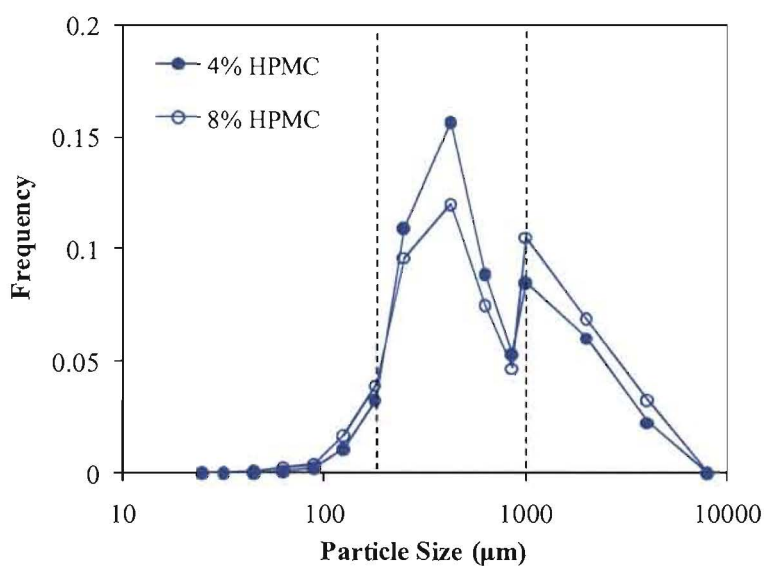


Figure 5-19 Granule size distribution for 4% HPMC and 8% HPMC at 91% FQ – 100 mesh lactose and microcrystalline cellulose mixture, 50% L:S, 295rpm. The dotted lines divide the granule size (x) into fine ($x < 180\mu\text{m}$), intermediate ($180\mu\text{m} < x < 1000\mu\text{m}$) and coarse ($x > 1000\mu\text{m}$) fractions.

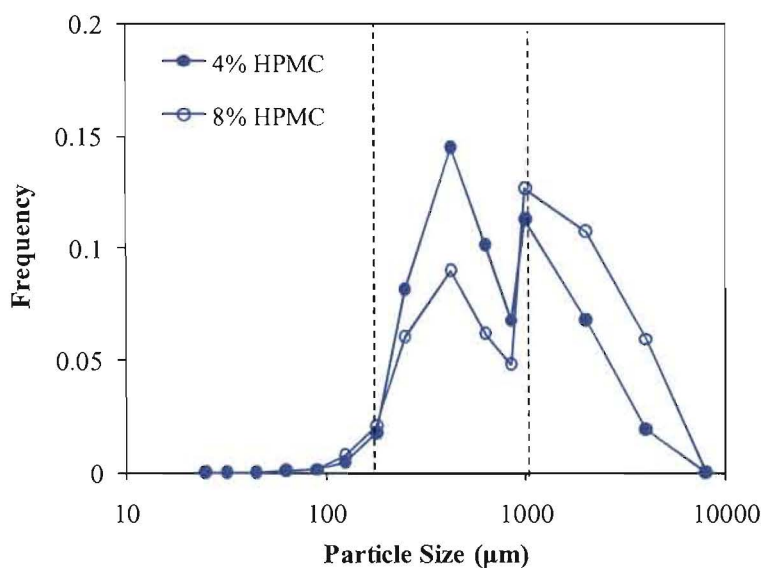


Figure 5-20 Granule size distribution for 4% HPMC and 8% HPMC at 83% FQ – 100 mesh lactose and microcrystalline cellulose mixture, 50% L:S, 295rpm. The dotted lines divide the granule size (x) into fine ($x < 180\mu\text{m}$), intermediate ($180\mu\text{m} < x < 1000\mu\text{m}$) and coarse ($x > 1000\mu\text{m}$) fractions.

The viscosity effects are complex, and may be different above and below some critical liquid content as at different granulation stages (Ennis, 1996; Ennis *et al.*, 1991; Hoornaert *et al.*, 1998; Iveson and Litster, 1998b; Keningley *et al.*, 1997; Mills *et al.*, 2000; Schaefer and Mathiesen, 1996). When the binder fluid is added as a spray, a high viscosity binder retards the wetting kinetics (which leads to a high density of drop coalescence and the formation of large nuclei), improves granule growth due to an increase in dynamic bridge strength and energy dissipation according to the Stokes criteria, increases the strength of the granules and makes them less susceptible to breakage (Iveson *et al.*, 2001a). All of these effects incur an increase in the spread of the granule size distribution at a high binder viscosity. It could be an unknown combination of all these effects, but the end result is similar when a high viscosity binder is introduced as an aqueous foam.

Initially, this appears to be in disagreement with the postulation from the transformation map (see Figure 3-23), where a high binder concentration will act as a slow penetrating system, and will cause a decrease in the nuclei size and the reduction in the spread of the size distribution. However, the transformation map only considers the size of a single nucleus formed with respect to the penetration kinetics of a single blob of foam on static powder beds. For foam granulation on a dynamic powder bed, nucleation, granule growth and breakage occur simultaneously. The granulation process involves multiple nuclei formation, which may coalesce or break due to collisions with other nuclei granules or forces of impact from the impeller or granulator wall. In addition, the study of single nucleus formation varied the binder concentration, which changed the foam viscosity and also indirectly changed the foam quality. The effect of reduced foam quality was not taken into account quantitatively as the Airspray foam dispenser was not able to control the foam quality. Foam quality was shown to play an important role during foam induced wetting and nucleation in *Chapter 4*.

Comparing high and low binder concentrations, the former is less foaming and tends to form an unstable foam of low foam quality, which in fact has a higher drainage rate than a stable foam of high foam quality despite that liquid penetration into the powder pores may be retarded due to high viscosity effect. In this case, foam quality dominates the effect of binder viscosity, indicating that high concentration binders of low foam quality tend to result in the formation of coarse nuclei and broad nuclei granule size distributions due to localised wetting and nucleation during the granulation process. This reasoning explains the results shown in

Figure 5-19 and Figure 5-20, where the high binder concentration results in coarser granule size distributions compared to the low binder concentration.

5.3.7 Effect of foam delivery rate

The effect of foam delivery rate was investigated by granulating the powder at 0.1L/min and 0.2L/min, which represents a low foam delivery rate and a high foam delivery rate, respectively.

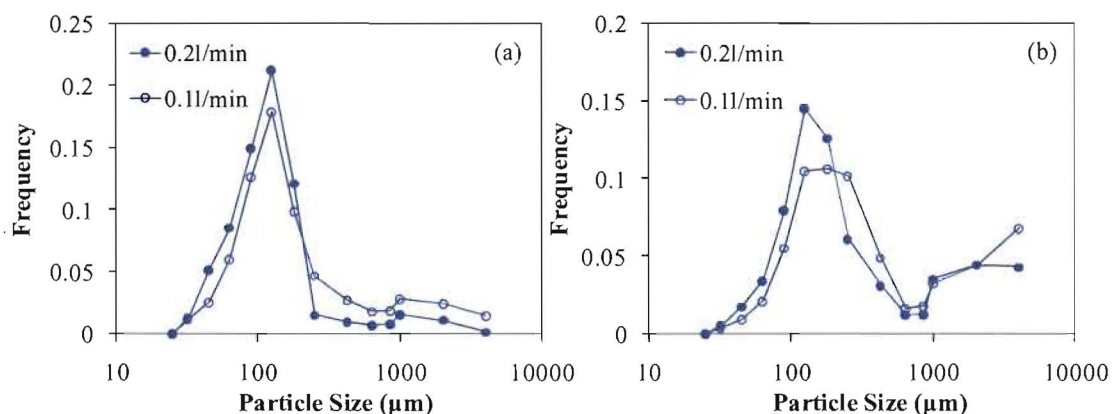


Figure 5-21 (a) Initial granule size distribution at 3% liquid to solid ratio (b) Final granule size distribution at a 5% liquid to solid ratio – 4% HPMC, 100 mesh lactose powder, 83% FQ, 515rpm.

Figure 5-21 shows the granule size distributions as a function of foam delivery rate at 3% and 5% liquid to solid ratios, which correspond to the stages of nucleation and growth, respectively (see Figure 5-2). The differences in the granule size distributions are relatively small because the lactose formulation is readily wettable and requires only a small amount of liquid binder. Nonetheless, it is seen that a low foam delivery rate increases the spread of the granule size distributions. Figure 5-21(a) indicates that a low foam delivery rate produces a larger initial granule size distribution after 3% liquid binder addition. Figure 5-21(b) shows that the granulation retained the “memory” of the nucleation stage, where a larger final granule size distribution was also produced at 5% liquid binder level.

It appears that a high foam delivery rate is relatively advantageous in reducing the spread of the granule size distribution. At a high foam delivery rate, it is probable that the foam has not

been able to wet into the powder bed quickly, as the foam may coalesce with the subsequent incoming foam before penetrating into the powder pores. The coalesced foam probably takes longer to penetrate and wet through the powder, and may be mechanically dispersed instead. At a low foam delivery rate, localised wetting and nucleation may occur before the next added foam comes into the granulator. In this case, a high foam delivery rate appears to be desirable to avoid the formation of coarse nuclei granule (due to liquid drainage). This reasoning contradicts the concept of dimensionless spray flux (see *Chapter 2 – section 2.2.1.3*), which requires further investigation with a wider range of foam addition rates.

However, it would not usually be possible to add the total volume of foam required for a granulator bowl that has an insufficient volume to accommodate the powder and the foam. This can be an issue for foam binder addition due to the substantial increase in the binder volume. A possible scenario is that the granulator may be overfilled with a large amount of foam (and powder) if the foam delivery rate is higher than the powder turnover rate, hindering the mixing initially. The options are either to increase the mechanical energy of mixing, mix for a longer period of time, use a less stable foam, or add the foamed binder intermittently. In addition to the equipment limitation issue, direct comparison of foam delivery rate is difficult, as a change to the foam addition rate would modify the amount of foam delivery time required for a given amount of granulating fluid, and thus the mixing time. These changes could potentially lead to variations in granule growth and densification, which have not been investigated further in this thesis.

5.3.8 A summary of single foam penetration, nucleation and granulation studies

A series of experiments which links single foam penetration, nucleation and granulation studies is presented as a summary below. In this summary study, 4% HPMC is used as the granulating fluid with 100 mesh lactose as the powder.

5.3.8.1 Single foam penetration

In an attempt to relate nuclei formation to foam penetration kinetics, a summary study of single foam penetration on a static powder bed is presented.

Figure 5-22 shows the plot of specific penetration time versus the foam quality, with error bars showing the standard error of the mean for 5 measurements. It is seen that the penetration of the foam is highly influenced by the foam stability, which is characterised by foam quality. A higher foam quality produces a more stable foam, which takes longer to drain and penetrate into the powder bed. Therefore, increasing the foam quality has a proportional effect on the foam penetration time, which has a strong correlation to the wetting and nucleation kinetics. Complete foam penetration may be longer than anticipated by the traditional wet granulation process, but it is expected that wetting and nucleation can occur as soon as liquid drainage begins.

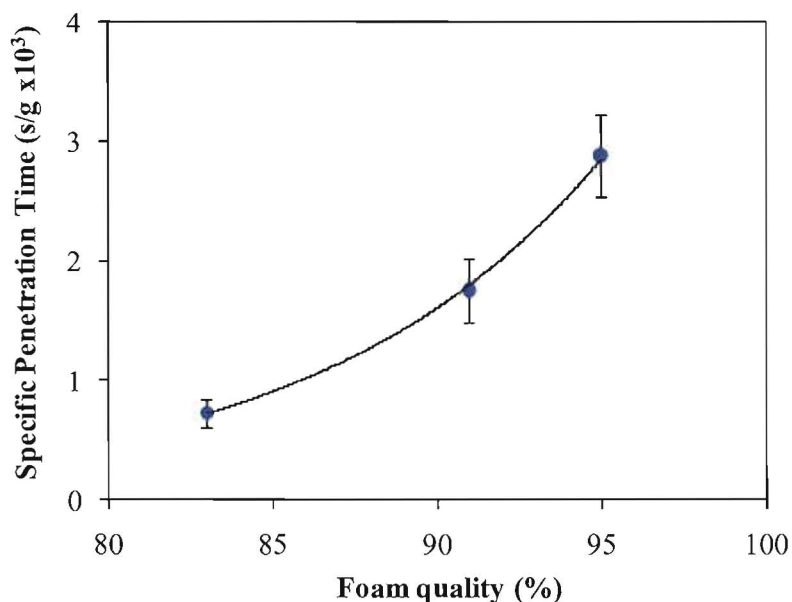


Figure 5-22 Effect of foam quality on 4% HPMC foam penetration into a 100 mesh lactose powder bed.

5.3.8.2 Nuclei formation by nucleation-only

A summary study of nuclei formation in a moving powder bed is presented, where the granulation is limited to nucleation with minimal granule growth and breakage effects.

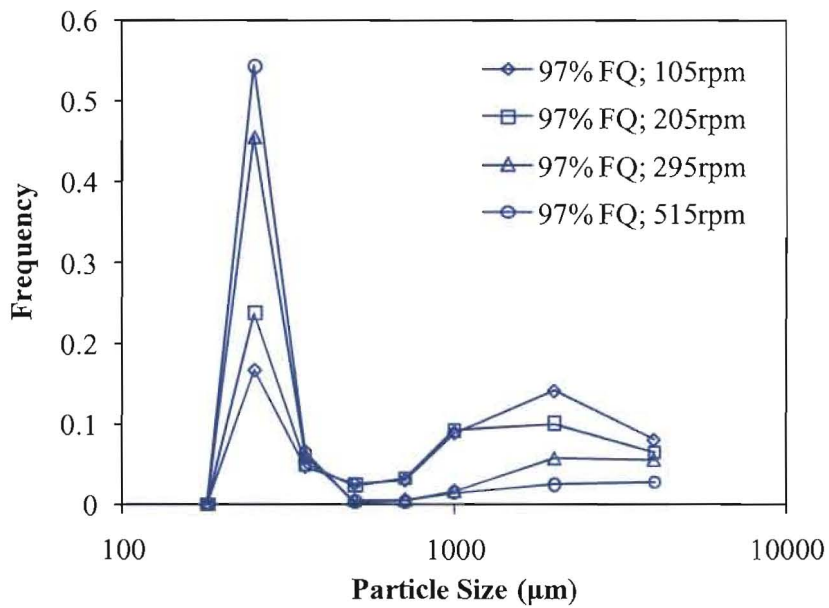


Figure 5-23 Nuclei size distribution as a function of impeller speed at 97% FQ – 4% HPMC, 100 mesh lactose powder, 1% L:S.

Figure 5-23 shows the nuclei size distributions as a function of impeller speed for 97% FQ. It is seen that the proportion of coarse nuclei (greater than 1mm) decreases and the proportion of fine nuclei (smaller than 500 μ m) increases when the impeller speed is increased from 105rpm to 515rpm. Figure 5-24 shows the same trend when 83% FQ is used.

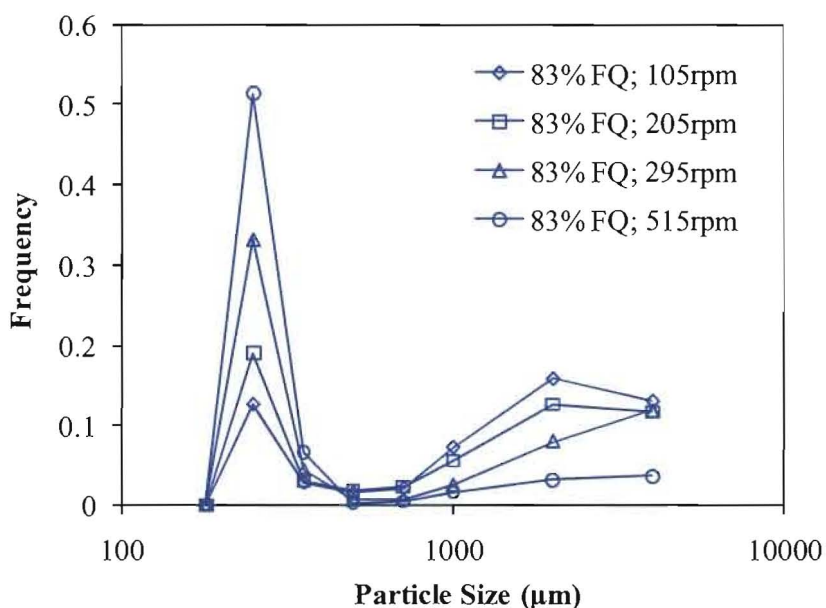


Figure 5-24 Nuclei size distribution as a function of impeller speed at 83% FQ – 4% HPMC, 100 mesh lactose powder, 1% L:S.

Increasing the impeller speed from 105rpm to 515rpm causes the powder to experience a more intense roping motion due to the increased mechanical energy of mixing. Mechanical dispersion is enhanced due to higher shear and powder flow impact, which improves the homogeneity in liquid distribution. As a consequence, this limits the formation of coarse nuclei and causes a reduction in the spread of the nuclei size distribution.

During the experiments, it was observed that the quality of foam dispersion was also affected by the foam quality. Initially, the 97% FQ foam was observed to be poorly incorporated within the powder as the foam was moving on top of the powder surface. At the same impeller speed, it was observed that the drainage effect was more significant for 83% FQ, which helps to disperse the foam rapidly. This is also supported by Figure 5-22, where the foam penetration at 97% FQ is relatively slower than the foam penetration at 83% FQ, indicating that nuclei formation due to liquid drainage is less significant at a high foam quality. This difference in the foam penetration kinetics is likely to cause variations in the degree of nucleation. Overall, there were more fine nuclei and fewer coarse nuclei with the 97% FQ foam. These results are in agreement with a previous study using different formulations and process conditions (see

Chapter 4), which confirms that foam dispersion and nucleation depend on the interactions of foam quality and impeller speed.

5.3.8.3 Granulation as a function of liquid to solid ratio

Figure 5-25 shows the granule size distributions as a function of foam quality at different liquid binder levels, which correspond to the stages of wetting and nucleation (3%), growth (4-5%), overwetting (6-8%) and caking (10%) (see Figure 5-2). As the granulation proceeds from stage to stage with an increase in the liquid binder level, the granule size distributions show a strong trend with the curves progressively shifting towards the upper sieve fraction. A logical consequence of increasing the liquid binder level is that the granulation extent increases, with a decrease in the fine size fraction and an increase in the coarse size fraction.

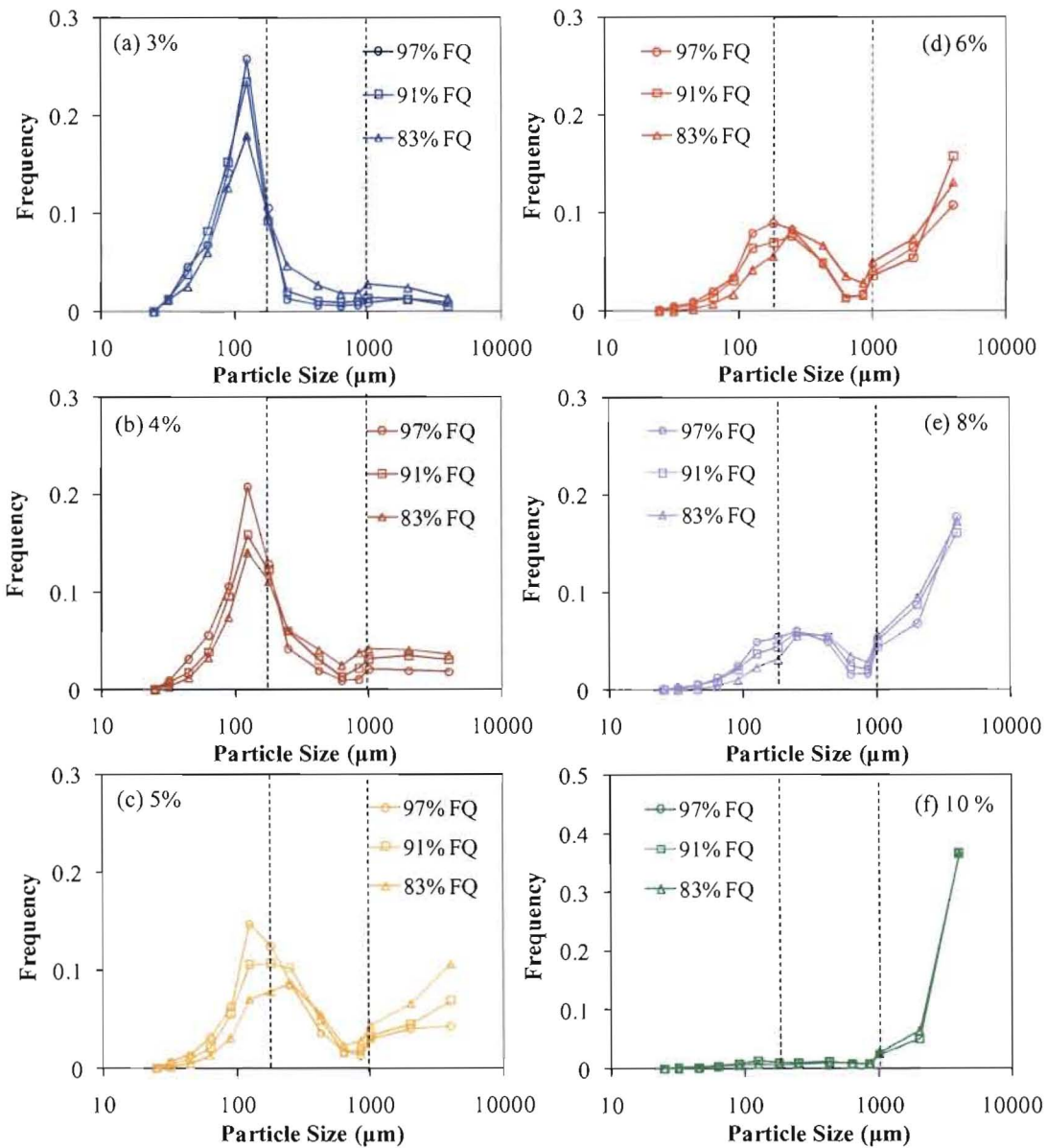


Figure 5-25 Granule size distribution as a function of foam quality at a liquid to solid ratio of (a) 3% L:S (b) 4% L:S (c) 5% L:S (d) 6% L:S (e) 8% L:S (f) 10% L:S – 4% HPMC, 100 mesh lactose powder, 295rpm. The dotted lines divide the granule size (x) into fine ($x < 180 \mu\text{m}$), intermediate ($180 \mu\text{m} < x < 1000 \mu\text{m}$) and coarse ($x > 1000 \mu\text{m}$) fractions.

It is seen that the granule size distributions are shifted to different extents by the different foam qualities. For granulation with 83% FQ, the granule size distributions are shifted towards the upper end of the coarse fraction. There is a gradual shift from the fine sieve size to the coarse sieve size as the foam quality decreases. Decreasing the foam quality increases the spread of

the initial granule size distributions (at the wetting and nucleation stage), which also leads to wider granule size distributions at the subsequent granulation stage. This trend diminishes at the stages where the powders become over-granulated at liquid binder levels larger than 8%. These over-granulated batches consist of predominantly “overwetted” and highly saturated coarse agglomerates, in which the granule size distributions are practically identical regardless of the foam quality.

Selected granulation batches using 91% FQ and 97% FQ are considered at a much higher impeller speed (515rpm) in Figure 5-26.

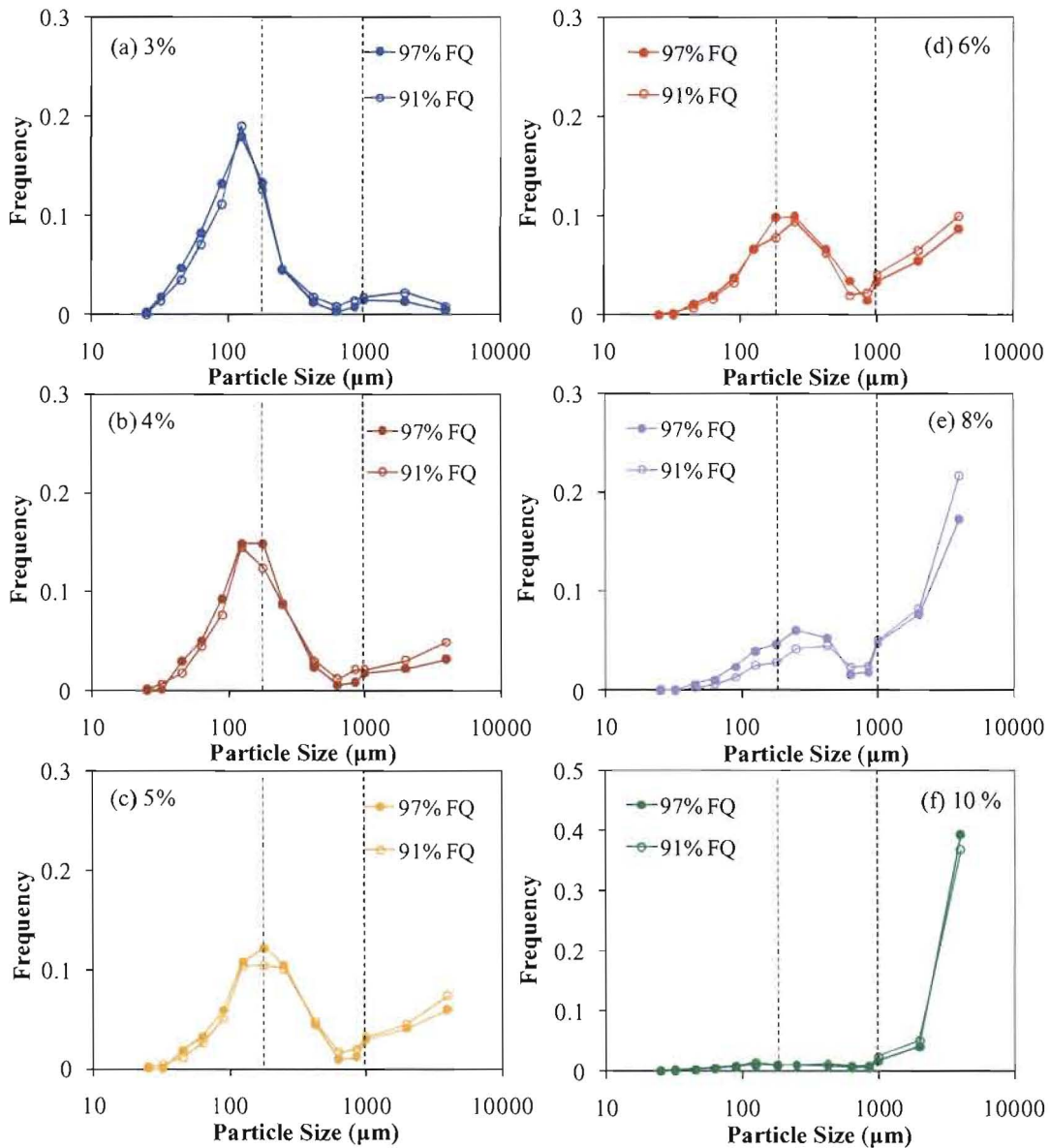


Figure 5-26 Granule size distribution as a function of foam quality at a liquid to solid ratio of (a) 3% L:S (b) 4% L:S (c) 5% L:S (d) 6% L:S (e) 8% L:S (f) 10% L:S – 4% HPMC, 100 mesh lactose powder, 515rpm. The dotted lines divide the granule size (x) into fine ($x < 180 \mu\text{m}$), intermediate ($180 \mu\text{m} < x < 1000 \mu\text{m}$) and coarse ($x > 1000 \mu\text{m}$) fractions.

Figure 5-26 shows the granule size distributions as a function of the foam quality at different liquid binder levels. Similarly, the granulation extent increases with an increase in the liquid binder level, which also broadens the granule size distributions. At a 515rpm impeller speed, the powder experienced roping flow, where the mixing between the powder and the foam was more intense. Under roping flow conditions, the granule size distributions were similar regardless of the foam quality, even though increasing the liquid binder level increases the spread of the granule size distribution. In this case, the impeller speed offsets the change in foam quality, producing practically identical granule size distributions. Note that the granule size distributions may still show a small difference, with the lower foam quality leading to larger and wider granule size distributions.

Although the liquid binder level may have exceeded the optimum level, producing rather wide granule size distributions, it is seen that the granule size distributions show consistent trends when foam quality and/or impeller speed is changed.

5.4 Discussion

Granulation design relies on the knowledge of a complicated collection of transformations, which describe the many ways in which the raw materials are converted into granular products (Mort *et al.*, 2007; Mort and Tardos, 1999). The sets of operating parameters and material properties that are typically critical to the transformations in granulation processes include liquid to solid ratio, foam quality, impeller speed, wet massing time, feed particle size, binder concentration and liquid delivery rate. This chapter describes the impact of these parameters on foam granulation behaviour in a high shear mixer-granulator, focussing on the transformations of dispersion and wetting coverage. On the basis of transformations, we first categorise each of the process and material parameters, and then describe the interaction between the parameters and the granule size distribution.

5.4.1 Wetting and nucleation mechanisms

In *Chapter 4*, two wetting and nucleation mechanisms have been proposed for foam granulation – “foam drainage” and “mechanical dispersion”. As shown in this chapter, changing the process parameters and material properties shifted the granule size (distribution) accordingly due to the changes in the wetting and nucleation mechanism from “foam drainage”

controlled to “mechanical dispersion” controlled or vice versa. Based on this relationship between transformations, process parameters, material properties and granule attributes, we can categorise each of the process and material parameters as a function of dispersion and wetting coverage using a transformation map. The transformation map, illustrated in Figure 5-27, shows two groups of process/material parameters as either “foam drainage” controlled systems or “mechanical dispersion” controlled systems. The group of parameters shown in the upper end of the vertical axis of the transformation map represents the fast penetration system, where the wetting and nucleation is “foam drainage” controlled. The group of parameters shown in the upper end of the horizontal axis represents the slow penetrating system, where the wetting and nucleation is “mechanical dispersion” controlled.

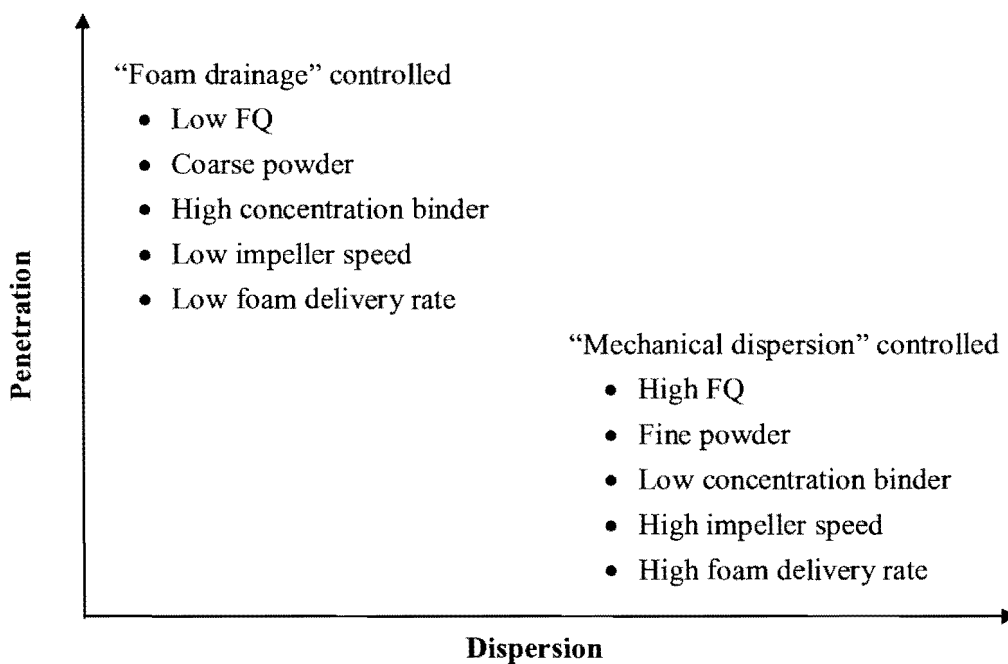


Figure 5-27 Dispersion and wetting coverage transformation map for foam granulation

For fast penetrating systems, the wetting and nucleation is “foam drainage” controlled, as the liquid drains quickly and wets into the powder mass to form nuclei. For example, the use of coarse powder beds will induce easier and faster liquid drainage, as it is more free flowing and fairly homogeneous with less macrovoids present in the powder bed (Hapgood *et al.*, 2002b). This is also shown in *Chapter 3*, where the liquid wetting front will tend to halt when a macrovoid is present which is often the case for fine powder beds. Low quality foams are fast

to drain compared to high quality foams (see *Chapter 4*). Systems with high concentration binders, low impeller speeds and low foam delivery rates have the same characteristic, where the wetting and nucleation depends on the “foam drainage” effect.

For slow penetration systems, the wetting and nucleation is “mechanical dispersion” controlled, which means that the dispersion of foam relies on mechanical mixing since foam drainage kinetics are slow. Systems with high foam quality, fine powder beds, low concentration binders, high impeller speeds and high foam delivery rates are characterised as equivalent to “mechanical dispersion”. In this case, the wetting and nucleation is determined by the powder flow conditions in the granulator.

5.4.2 Relative interaction of process/material parameters

Here, we consider each of the process and material parameters on the basis of transformations to describe their impacts on one of the most fundamental granule properties, size (distribution). Figure 5-28 shows the transformation maps summarising the interaction of process/material parameters with respect to impeller speed and the net effect on granule size distribution (GSD).

Note that a high impeller speed is generally the desired setting for high shear granulation. However, the setting does not always give the ideal powder flow condition for optimum granulation. Most large scale mixer granulators operate in poor powder flow conditions, even with a high speed setting, where the mechanical agitation is often insufficient to disperse the liquid binder effectively (Plank *et al.*, 2003). In general, powder flow can be controlled by the impeller speed, but they are not proportionally related.

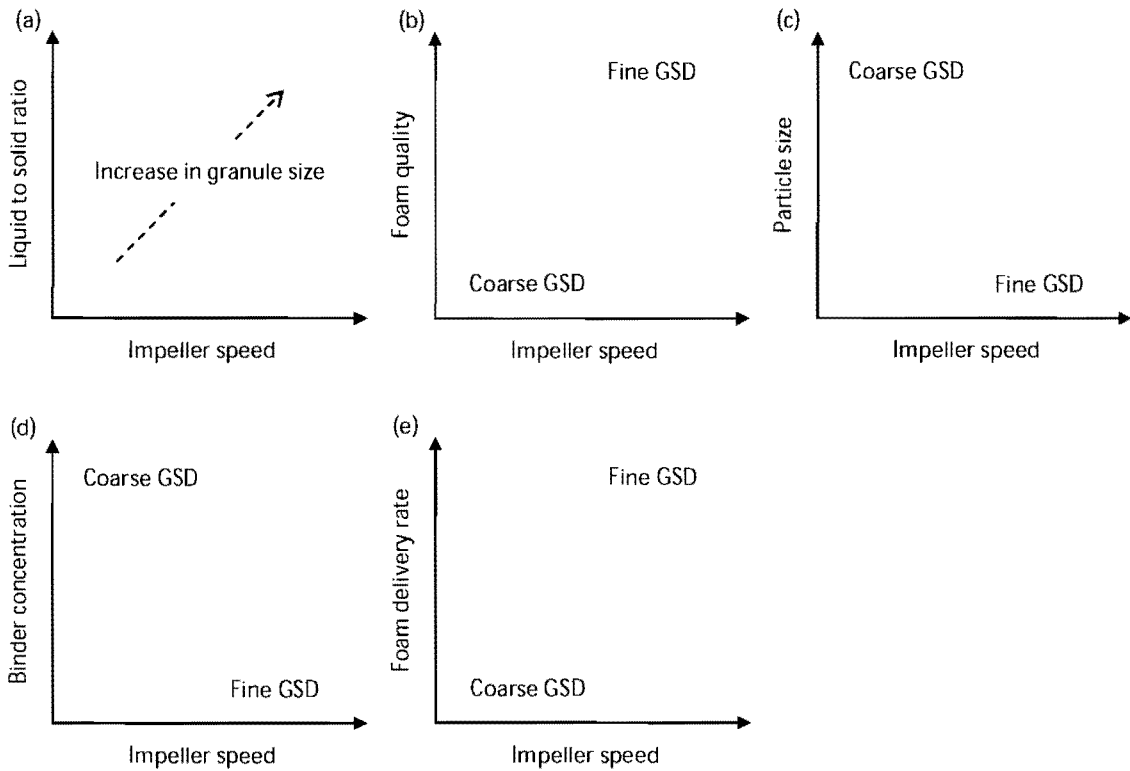


Figure 5-28 Process parameters and material properties transformation maps for foam granulation. “GSD” indicates “Granule Size Distribution”.

Figure 5-28(a) indicates that increasing the liquid to solid ratio with increasing impeller speed will lead to an increase in the granule size. Increasing the liquid to solid ratio is expected to increase the granule size. With increasing impeller speed, this effect can be enhanced as the existing granules undergo densification whereby the granules become harder and their surfaces become more adhesive. Further densification will provoke uncontrollable growth, increasing the granule size significantly. This is indicated by the foam granulation experiments shown in *section 5.3.1*. Note that the increase in the granule size may be due to induction growth, steady growth or rapid growth. The different types of growth are not considered in this case.

Figure 5-28(b) indicates that decreasing the foam quality will give rise to a coarse GSD at low impeller speeds as this system is driven by “foam drainage” controlled wetting and nucleation. The opposite of this system, given by high foam quality, is “mechanical dispersion” controlled, which will produce a fine GSD. This is supported by the foam granulation experiments shown in *section 5.3.2*.

Figure 5-28(c) shows that increasing the particle size will result in a coarse GSD, as a coarse powder bed is more likely to incur localised wetting and nucleation by the “foam drainage” controlled mechanism since the mechanical dispersion is poor. The drainage effect is less significant for a fine powder bed, where the wetting and nucleation is governed by “mechanical dispersion”, which is associated with a fine GSD. This is supported by the granulation experiments shown in *section 5.3.5*.

Figure 5-28(d) indicates that increasing the binder concentration will create a coarse GSD. The drainage effect is significant since increasing the binder concentration is equivalent to lowering the foam quality. In contrast, a fine GSD will be formed for low binder concentrations. This is indicated by the foam granulation experiments shown in *section 5.3.6*.

Figure 5-28(e) shows that a coarse GSD will be produced with a low foam delivery rate, considering that the drainage effect is more significant. In contrast, a high foam delivery rate is relatively advantageous in creating a fine GSD, provided the impeller speed is sufficiently high to disperse the foam. This is supported by the foam granulation experiments shown in *section 5.3.7*.

The summary study linking single nucleus formation, nucleation and granulation studies demonstrated the importance of the two wetting and nucleation mechanisms in foam granulation processes. Large granule size distributions consistently occurred with fast penetrating systems and vice versa, supporting the existence of “foam drainage” controlled and “mechanical dispersion” controlled wetting and nucleation mechanisms for foam granulation. On the basis of the two wetting and nucleation mechanisms, the transformation maps summarize the effects of process and material parameters on the granule size distributions. The transformation maps should prove to be useful in identifying the dominant mechanisms controlling wetting and nucleation processes and in rationalizing the trends of granule size distribution in response to the changes of the process/material parameters.

5.5 Conclusions

This chapter studied the impact of process and material parameters on foam granulation processes and demonstrated the critical importance of wetting and nucleation in determining the granule size distributions for foam granulation. It was shown that:

- Decreasing the foam quality resulted in the formation of coarser nuclei granules and led to a larger granule size distribution.
- The foam quality effect can be minimized by increasing the impeller speed. Increasing the impeller speed to achieve roping flow limits coarse nuclei granule formation and/or breaks the coarse nuclei granules rapidly, creating similar granule size distributions. However, the mechanical forces are not always sufficient to counteract the foam quality effect.
- Foam induced “overwetted” granules can be relatively easy to disperse through wet massing. In this case, increasing the wet massing time caused a reduction in the average granule size and reduced the spread of the granule size distribution due to breakage. However, prolonged mixing may also lead to granule coalescence and rapid granule growth, which makes mixing a difficult variable to manipulate.
- Decreasing the feed particle size caused a decrease in the average granule size and a reduction in the spread of the granule size distribution. The same trends were obtained by increasing the binder concentration.
- A high foam delivery rate appeared to be relatively advantageous in creating a narrow granule size distribution, provided sufficient mechanical forces are supplied.
- “Foam drainage” controlled and “mechanical dispersion” controlled wetting and nucleation mechanisms pose strong effects on the initial nuclei size distribution, and the effects are retained through to the final granule size distribution.

Nucleation in foam granulation involves “foam drainage” and “mechanical dispersion”, and the granule size distribution depends on the interactive effects of the two mechanisms. The proposed transformation maps should prove to be useful in identifying the dominant mechanisms controlling wetting and nucleation processes and in rationalizing the granule size distribution as a function of the relative interaction of process/material parameters.

CHAPTER 6
A CASE STUDY OF LIQUID DISTRIBUTION

Monash University

Declaration for Thesis Chapter 6

In the case of Chapter 6, contributions to the work involved the following:

Name	% contribution	Nature of contribution
Melvin X.L. Tan	100	Initiation, Key ideas, Experimental development, Results interpretation & Writing up
Dr. Karen Hapgood	Supervisor	Initiation, Key ideas, Editing and reviewing

Declaration by co-authors

The undersigned hereby certify that:

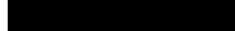
- (1) they meet the criteria for authorship in that they have participated in the conception, execution, or interpretation, of at least that part of the publication in their field of expertise;
- (2) they take public responsibility for their part of the publication, except for the responsible author who accepts overall responsibility for the publication;
- (3) there are no other authors of the publication according to these criteria;
- (4) potential conflicts of interest have been disclosed to (a) granting bodies, (b) the editor or publisher of journals or other publications, and (c) the head of the responsible academic unit; and
- (5) the original data are stored at the following location(s) and will be held for at least five years from the date indicated below:

Location(s)

Department of Chemical Engineering, Monash University, Clayton Victoria 3800 Australia.

Signature 1

Signature 2

	Date
	
	

6 A CASE STUDY OF LIQUID DISTRIBUTION

This chapter compares foam and spray granulation by evaluating the granulation behaviour in a high shear mixer-granulator. A case study evaluating the performance of foam and spray granulation in achieving uniform liquid distribution is presented. The wet and dry granule size distributions and the moisture distribution in granules for both systems are compared. A regime map is presented to describe the observed granulation behaviour for the systems.

6.1 Introduction

A key aspect in wet granulation is the uniformity of liquid distribution. Ensuring uniform liquid distribution generally gives rise to controlled granule growth and breakage, which eventually leads to the formation of homogeneous granules. For poor liquid distribution, the granules will be immersed with uneven liquid binder content, with the large granules associated with more liquid binder than the smaller granules. Continued granulation will lead to uneven granule growth, as large granules continue to grow steadily due to higher saturation while small, low saturation granules remain in the nucleation stage or display crumb behaviour. The small granules may display little or no granule growth, but this induction stage will end, and rapid coalesce growth will occur as soon as the granules become sufficiently surface wetted. For systems that become over-wetted, the granules will turn into a slurry (Iveson *et al.*, 2001a).

The success of forming granules of uniform properties (size, content etc.) often depends on the distribution of fluid binder within the powder as the fluid first comes into contact with the surface of a powder bed. As represented by a large number of efforts attempted to improve the distribution of liquid binder throughout a moving powder bed (Litster *et al.*, 2002; Litster *et al.*, 2001; Wildeboer *et al.*, 2007), ensuring uniform liquid binder distribution during wet granulation is a recognized need in the pharmaceutical industry to achieve uniform granule size distributions. A monomodal, narrow granule size distribution has often been reported to be a consequence of uniform liquid binder distribution (Ax *et al.*, 2008; Knight *et al.*, 1998; Litster *et al.*, 2002; Reynolds *et al.*, 2004; Smirani-Khayati *et al.*, 2009).

The key formulation properties and process parameters that control the granulation rate processes have been well established, and in some cases, regime maps are becoming available for granulation process design and control. Since a decade ago, work has been directed to produce regime maps that describe and enable prediction of nuclei granule formation (Hapgood *et al.*, 2003; Iveson and Litster, 1998b; Iveson *et al.*, 2001b; Rough *et al.*, 2005a; Rough *et al.*, 2005b). These maps illustrate the behaviour of nuclei granule formation based on the system parameters (formulation properties and process parameters) that dictate the operating regime in any particular system.

Using a similar approach, this chapter attempts to develop a regime map to describe and map out the key processes in foam and spray granulation. A case study is also presented to evaluate the performance of foam and spray granulation in producing homogenous granules with uniform moisture content.

6.2 Experimental

6.2.1 Materials

The powders used were lactose (100 mesh, Wyndale, New Zealand) and microcrystalline cellulose (Avicel PH101, Sigma Aldrich, Australia). Both powders are commonly used as excipients in the pharmaceutical industry. The liquid binder used was 4% HPMC (Methocel E5PLV, Dow Wolff Cellulosics, USA). A small quantity of food dye (Queens Fine Food Ltd., Australia) was dissolved in the binder solution for visual observation during the experiments. Table 6-1 indicates the powder and liquid binder properties, which were obtained from vendor specifications.

Table 6-1 Powder and liquid binder properties.

Powder/Liquid binder	Grade	Viscosity (mPa.s)	Average particle size (μm)
Microcrystalline cellulose	PH 101	-	50
Lactose monohydrate	100 mesh	-	150
4% HPMC	E5PLV	19.1	-

6.2.2 Methods

Granulation experiments were carried out in a high shear mixer-granulator. The overhead chopper was not used during the experiments. The granulator was equipped with a digital readout of impeller power consumption during granulation. The experimental setup was shown previously in *Chapter 5* (see Figure 5-1).

The powder bed comprised of a 1:1 ratio of a lactose and microcrystalline cellulose powder mixture. The powder mixture was dry-mixed for at least 1 minute before liquid binder addition. For foam granulation, the liquid binder was delivered at a flowrate of 0.1L/min and mixed with air supplied at a flowrate of 0.5L/min or 1.0L/min, which generated aqueous foams of foam quality (FQ) – 83% FQ and 91% FQ, respectively. For spray granulation, a single flat nozzle (TP650017) connected to a 5-litre spray pot (Spraying Systems, Wheaton, USA) was positioned through the nozzle port to allow the spraying of binder at the same conditions. Liquid binder addition was carried out for a designated period until the liquid binder reached the desired amount. The impeller was set to a constant speed for a given formulation. Table 6-2 summarises the operating conditions for the granulation experiments.

Power consumption values during granulation of two different formulations, a microcrystalline cellulose and 100 mesh lactose powder mixture, and a 100 mesh lactose powder were recorded. The power consumption profiles were used to monitor the progress of granulation, where appropriate, by linking with the granule size distributions to compare foam and spray granulation.

Table 6-2 Operating conditions for granulation experiments.

Liquid binder	Powder formulation	FQ (%)	Impeller speed (rpm)
4% HPMC	100 mesh lactose and microcrystalline cellulose	0	295
		83	295
		91	295
4% HPMC	100 mesh lactose and microcrystalline cellulose	0	515
		83	515
		91	515
4% HPMC	100 mesh lactose	0	295
		83	295
		91	295

Sampling was carried out at designated time intervals. For wet granule sieving, the wet granule samples were frozen using liquid nitrogen immediately after they were removed from the granulator. The frozen granules were sieved, and their moisture content was determined by weighing the wet granule sieve fractions after the liquid nitrogen had evaporated and again after drying overnight in an oven (Mackaplow *et al.*, 2000; Wauters *et al.*, 2002). Each sample was sieved into 180 μ m, 250 μ m, 355 μ m, 500 μ m, 710 μ m, 1mm and 2mm size fractions. Dry granule sieving was performed after drying in a fan-forced oven at 50°C overnight. This produces moisture content of the granules as a function of size in the following fractions: <250 μ m, >250 μ m, >500 μ m, >1mm and >2mm.

The average moisture content of the granules was also checked from the mass of the wet granules obtained after sampling and the loss in weight after drying. To measure the granule size distribution, sieving analysis was carried out using a mechanical dry sieve shaker (Retsch A200, Australia) in an ordered set of sieves: pan, 25 μ m, 32 μ m, 45 μ m, 63 μ m, 90 μ m, 125 μ m, 180 μ m, 250 μ m, 425 μ m, 630 μ m, 850 μ m, 1mm, 2mm and 4mm. The weight mean diameter can also be determined by using Eq. [4-1].

6.3 Results

6.3.1 Granule size distribution

Figure 6-1 shows the granule size distributions for foam granulation (91% FQ and 83% FQ) and spray granulation (0% FQ) at a 295rpm impeller speed. Figure 6-2 shows similar data at a higher impeller speed (515rpm). In all cases, increasing the liquid binder level increases the average granule size and the spread of granule size distribution, in which the peak of the granule size distribution shows a steady monotonic increase from around 125 μ m to 4000 μ m.

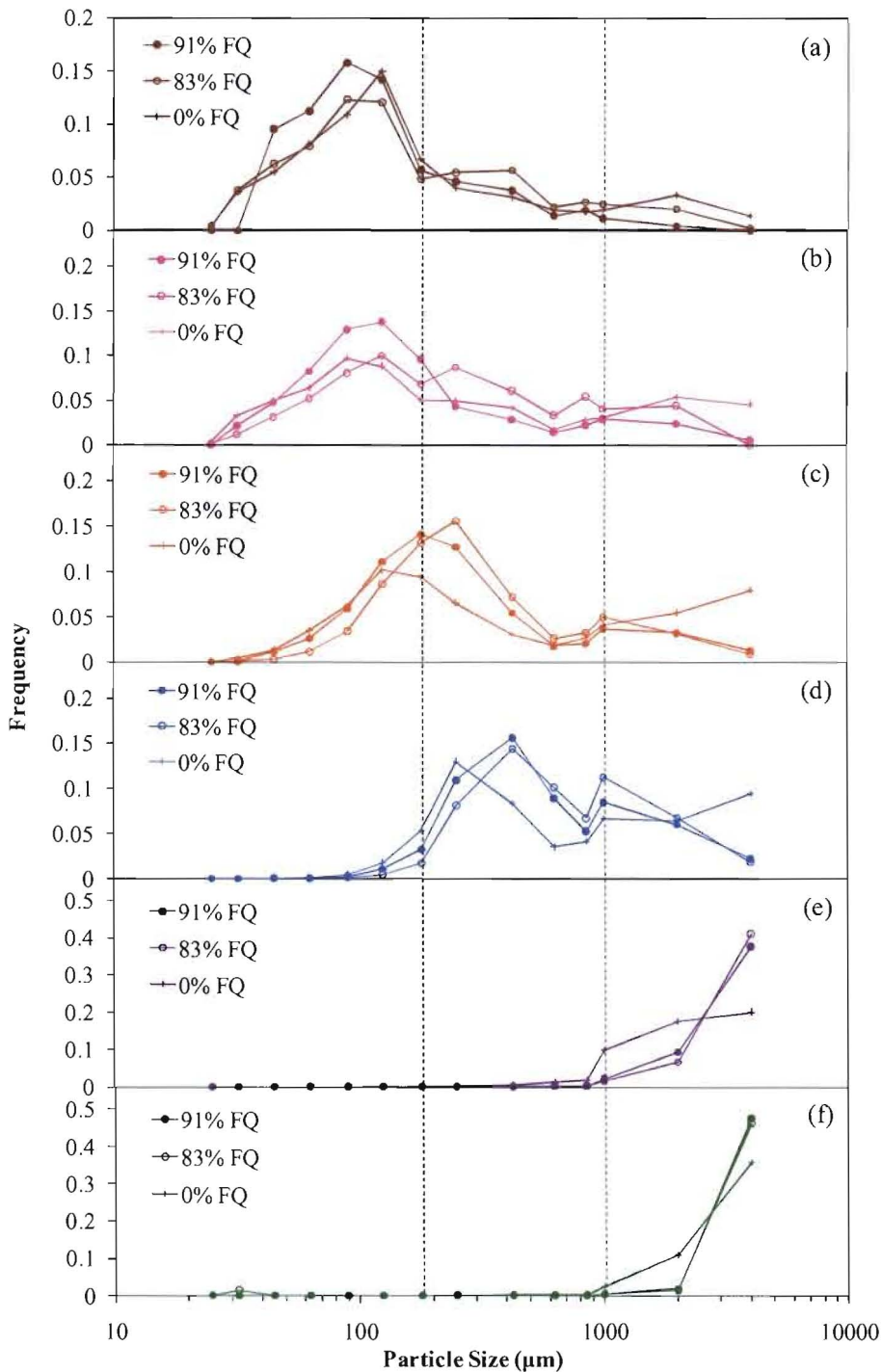


Figure 6-1 Granule size distribution as a function of foam quality at 295rpm after (a) 20% (b) 30% (c) 40% (d) 50% (e) 60% foam addition and (f) after 1min wet massing – 4% HPMC, 100 mesh lactose and microcrystalline cellulose mixture. The dotted lines divide the granule size (x) into fine ($x < 180\mu\text{m}$), intermediate ($180\mu\text{m} < x < 1000\mu\text{m}$) and coarse ($x > 1000\mu\text{m}$) fractions.

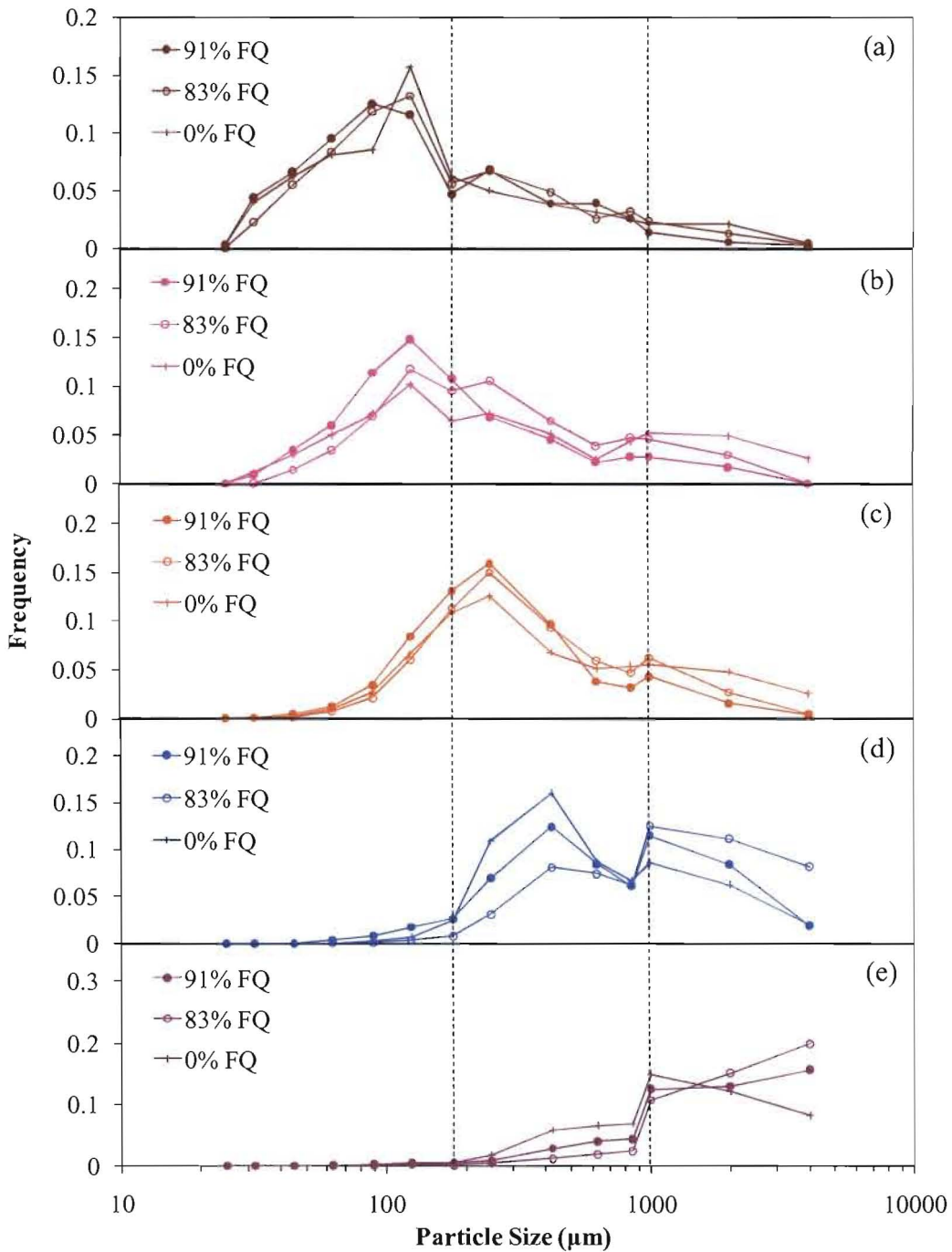


Figure 6-2 Granule size distribution as a function of foam quality at 515rpm after (a) 20% (b) 30% (c) 40% (d) 50% (e) 55% foam addition – 4% HPMC, 100 mesh lactose and microcrystalline cellulose mixture. The dotted lines divide the granule size (x) into fine ($x < 180 \mu\text{m}$), intermediate ($180 \mu\text{m} < x < 1000 \mu\text{m}$) and coarse ($x > 1000 \mu\text{m}$) fractions.

As mentioned in *Chapter 5*, granulation can be defined into the stages of (I) wetting and nucleation, (II) growth, (III) overwetting and (IV) caking. Here, we compare the evolution of granule size distribution as a function of foam quality in response to the changes of granulation from one stage to another.

6.3.1.1 *Wetting*

At a 20% liquid to solid ratio (Figure 6-1(a) and Figure 6-2(a)), the initial granule size distributions are almost identical for both foam granulation (91% FQ and 83% FQ) and spray granulation (0% FQ). The granule size distributions are monomodal, and contain mainly ungranulated particles. The added liquid only gives rise to a slightly increased cohesion of the mass due to the excellent water-absorption property of microcrystalline cellulose (Chang and Chang, 2007). This stage is classified as wetting.

6.3.1.2 *Nucleation*

At a 30% liquid to solid ratio (Figure 6-1(b) and Figure 6-2(b)), nuclei begin to form. The granule size distributions show a peak at around the 125 μ m size fraction, with a small increase in the intermediate and coarse fractions. This is most likely due to nucleation. With spray, the granule size distribution shows the largest fraction of coarse nuclei compared to foam. The nucleation effect is more pronounced for spray granulation, followed by foam granulation at 83% FQ and 91% FQ.

6.3.1.3 *Growth*

At a 40% liquid to solid ratio (Figure 6-1(c) and Figure 6-2(c)), the granule size distributions show an increase in the peak from the 125 μ m to the 250 μ m size fraction. With spray, the coarse nuclei continue to grow into coarser granules, producing the broadest granule size distribution. Foam granulation at 83% FQ also creates a broader granule size distribution than 91% FQ.

6.3.1.4 *Overwetting*

At a 50% liquid to solid ratio (Figure 6-1(d) and Figure 6-2(d)), the granule size distributions are bimodal and show a large increase in the fraction of coarse granules. In all cases, the bimodal granule size distributions show two peaks around the 425 μ m and 1000 μ m size

fractions, suggesting that the granulation becomes unstable as a result of uneven granule growth.

In both cases of 295rpm and 515rpm impeller speeds, foam granulation with 83% FQ resulted in a broader granule size distribution than 91% FQ. For spray granulation at 295rpm, the granule size distribution is generally less uniform, with the granules distributed on the lower end of the fine size ($\sim 125\mu\text{m}$) and the upper end of the coarse size ($\sim 4\text{mm}$). The distribution of granules were improved by increasing the impeller speed to 515rpm, where the granules were evenly distributed with fewer coarse granules. It is noted that for foam granulation at a 515rpm impeller speed, the granule size distributions are actually skewed towards larger sizes compared to at a 295rpm impeller speed (see Figure 6-1(d) and Figure 6-2(d)). The effect of impeller speed was discussed in more details in *Chapter 5 – section 5.3.3*.

6.3.1.5 Caking

For liquid binder levels greater than 55%, most fine and intermediate fractions disappeared, and there was a tremendous increase in the fraction of coarse granules. The coarse granules were further densified into larger agglomerates after the batches were wet massed. In all cases, the granule size distributions were concentrated around the 4mm size fraction after 1 minute of wet massing.

6.3.2 Weight mean diameter

Figure 6-3 shows the evolution of the granule weight mean diameter (see Eq. [4-1]) and the mass percentage of fines (previously defined as granules smaller than $180\mu\text{m}$). For both foam (91% FQ and 83% FQ) and spray (0% FQ) granulation, it is clear that increasing the liquid binder level (liquid to solid ratio) increases the granulation extent, which also increases the average granule size. The same trends were observed for both low impeller (295rpm) and high impeller (515rpm) settings. The results at 295rpm are shown in Figure 6-3, while those at 515rpm are shown in Figure 6-4.

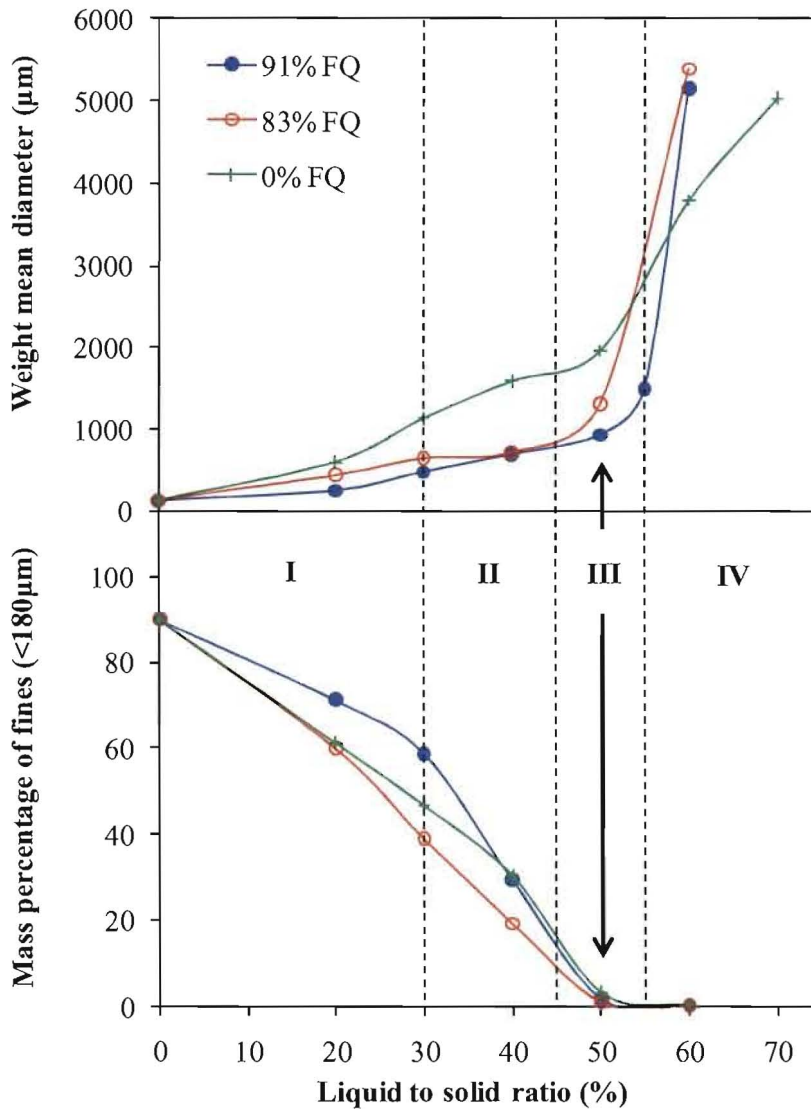


Figure 6-3 Weight mean diameter as a function of liquid binder level at a 295rpm impeller speed for foam (91% FQ and 83% FQ) and spray (0% FQ) granulation – 4% HPMC, 100 mesh lactose and microcrystalline cellulose. The dotted lines divide the granulation into (I) wetting and nucleation, (II) growth, (III) overwetting and (IV) caking.

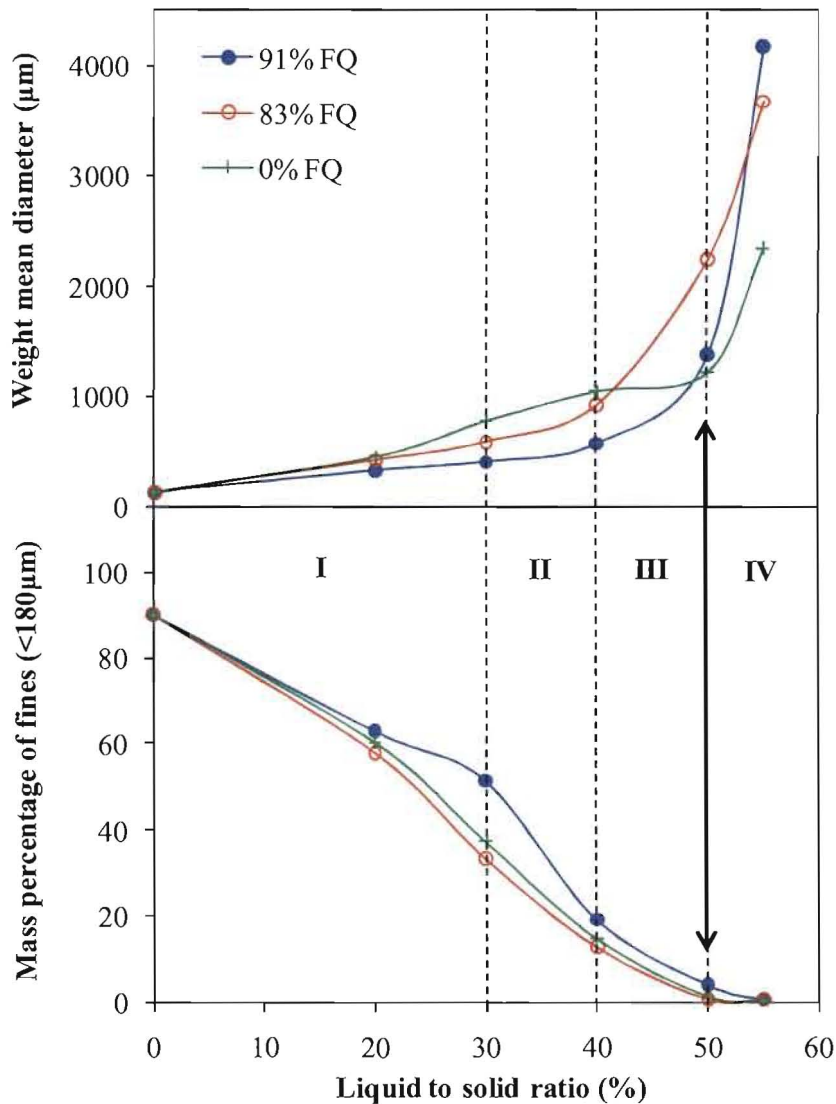


Figure 6-4 Weight mean diameter as a function of liquid binder level at a 515rpm impeller speed for foam (91% FQ and 83% FQ) and spray (0% FQ) granulation – 4% HPMC, 100 mesh lactose and microcrystalline cellulose. The dotted lines divide the granulation into (I) wetting and nucleation, (II) growth, (III) overwetting and (IV) caking.

In both Figure 6-3 and Figure 6-4, the changes of granule weight mean diameter correspond well to the evolution of granulation state (as defined previously in *Chapter 5 – section 5.3.1*). As granulation proceeds from wetting and nucleation to growth, and then to overwetting and caking, the weight mean diameter shows a corresponding increase. Note that the liquid binder level (liquid to solid ratio) required to cause the increase in granule weight mean diameter (also

to promote the transition between the granulation phases) decreases with increasing the impeller speed. The effect of impeller speed was discussed in more detail in *Chapter 5 – section 5.3.3*.

Both Figure 6-3 and Figure 6-4 indicate that foam granulation and spray granulation display different granule growth behaviour. Spray granulation tends to produce steady granule growth, where the granules show a steady increase in the weight mean diameter as granulation proceeds. For foam granulation, induction growth behaviour was observed. The granule weight mean diameter shows a small increase initially, which is then followed by a substantial increase. Note that the increase in granule weight mean diameter decreases with increasing foam quality, which indicates that increasing the foam quality facilitates induction growth behaviour.

From Figure 6-3 and Figure 6-4, it is seen that the fraction of fine granules in all of the foam and spray granulation batches has a profound effect on the granule growth behaviour. As indicated by the marked arrow, the disappearance of the fine granules coincides with the end of the granule induction growth stage (or the onset of rapid granule growth). It seems that the presence of the fine particles in the granulation batches controls the granule induction growth period. When the fine granules have disappeared, granule induction growth behaviour ceases. This behaviour was also shown by Wauters *et al.* (2002), in the granulation of copper concentrate (chalcopyrite) in a rotating drum granulator. The finding implies that the induction period can be shortened by removing the fines, which is similar to the effect of increasing the liquid binder level (Iveson *et al.*, 2001a).

6.3.3 Moisture distribution

A separate set of granulation experiments was carried out in a case study to evaluate the performance of foam and spray granulation in achieving uniform liquid distribution. The wet and dry granule size distributions and the moisture distribution as a function of granule size for foam and spray granulation were compared.

6.3.3.1 Wet and dry granule size distributions

Figure 6-5 shows the wet and dry granule size distributions after liquid binder addition and 2 minutes of wet massing for foam granulation (91% FQ and 83% FQ) and spray granulation (0% FQ). All of the granule size distributions at the end of liquid binder addition were relatively wide. Both wet and dry granule size distributions show a large fraction of granules greater than 1 mm.

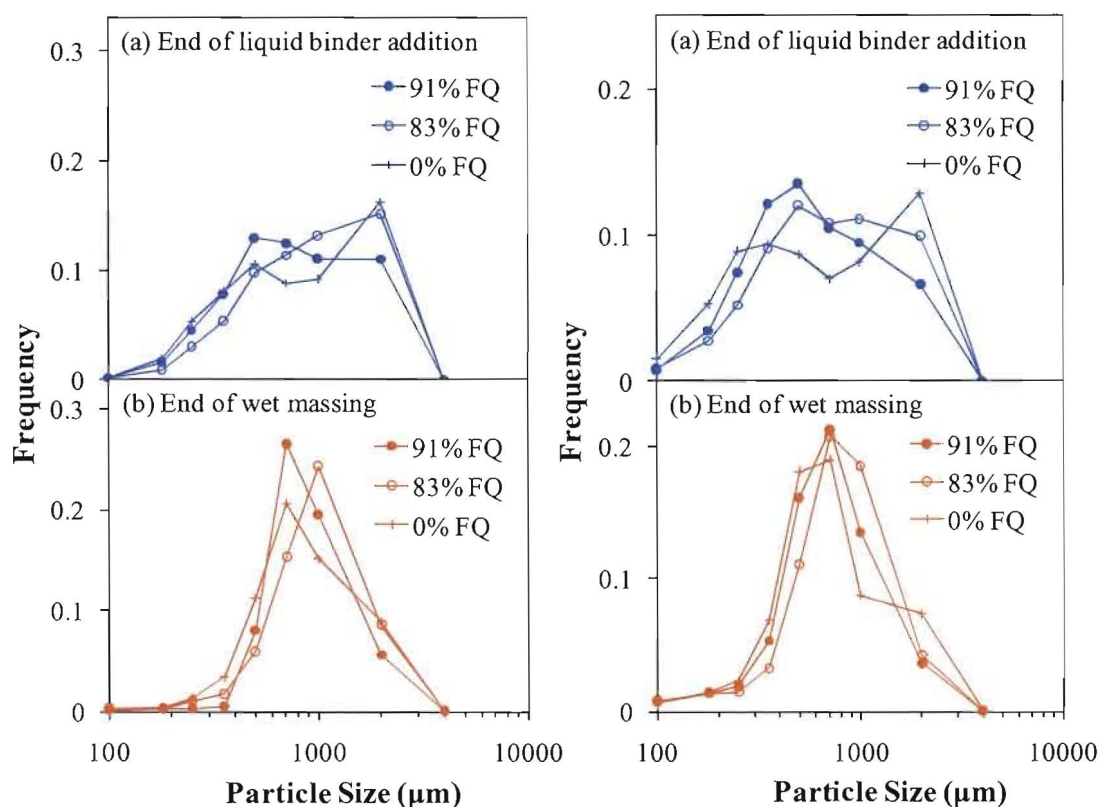


Figure 6-5 Wet (left) and dry (right) granule size distributions after (a) liquid binder addition (b) 2 minutes of wet massing for foam (91% FQ and 83% FQ) and spray (0% FQ) granulation – 4% HPMC, 100 mesh lactose and microcrystalline cellulose mixture, 50% L:S, 515rpm.

More specifically, spray granulation has generated the largest fraction of granules greater than 2mm at the end of binder addition. The granule size distribution immediately after spray delivery of liquid binder is the widest, followed by foam binder addition with 83% FQ and then 91% FQ. This trend is indicated by both the wet and dry granule size distributions, despite

that the granule size distributions are slightly different. The minor differences in the wet and dry granule size distributions after sieving are probably due to the difference in the strength of wet and dry granules as a result of the nitrogen freezing and drying processes, and/or sampling variations.

After 2 minutes of wet massing, the granule size distributions became monomodal. The granule size is concentrated around the 500 μ m-1000 μ m size fraction. This shows that wet massing has led to the breakage of the coarse granules into smaller fractions for both foam and spray granulation. The overall granule size distributions are practically similar, although the size distribution of granules for foam granulation is slightly skewed towards larger sizes compared to spray granulation.

6.3.3.2 Moisture content in granules

Figure 6-6 shows the distribution of moisture content after 50% liquid binder addition as a function of granule size class for foam granulation (91% FQ and 83% FQ) and spray granulation (0% FQ). In all cases, it was found that the moisture was concentrated mainly in the large granules. The finer fractions were associated with relatively less moisture.

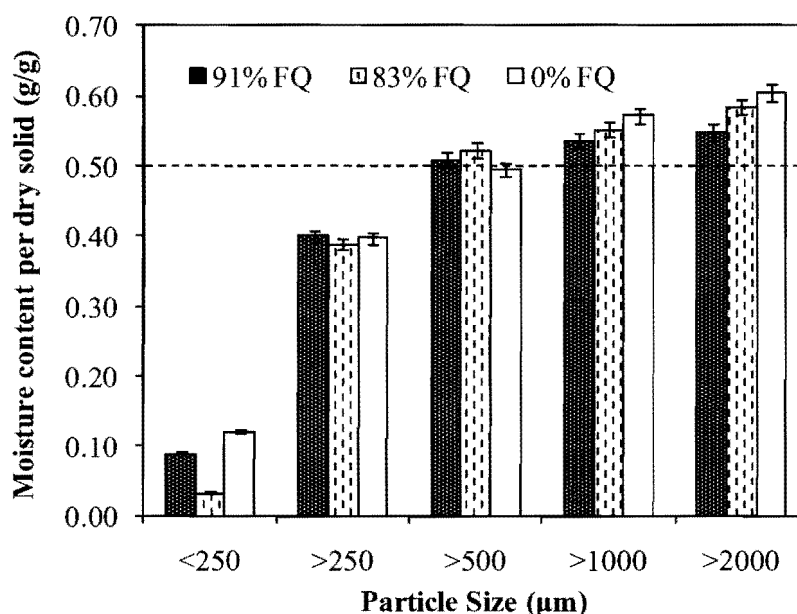


Figure 6-6 Moisture content after 50% liquid binder addition as a function of granule size class for foam (91% FQ and 83% FQ) and spray (0% FQ) granulation – 4% HPMC, 100 mesh lactose and microcrystalline cellulose mixture, 515rpm.

The moisture content in the foam bounded granules was slightly more homogeneously distributed compared to spray bounded granules. For fractions greater than 1000 μm , the moisture content in the spray bounded granules has the largest deviation (around 10%) from the theoretical moisture content (as shown by the dashed line). It is also seen that the moisture distribution is generally more uniform in the granules formed at 91% FQ compared to 83% FQ.

Figure 6-7 shows the distribution of moisture content after 2 minutes of wet massing as a function of granule size class for foam granulation (91% FQ and 83% FQ) and spray granulation (0% FQ).

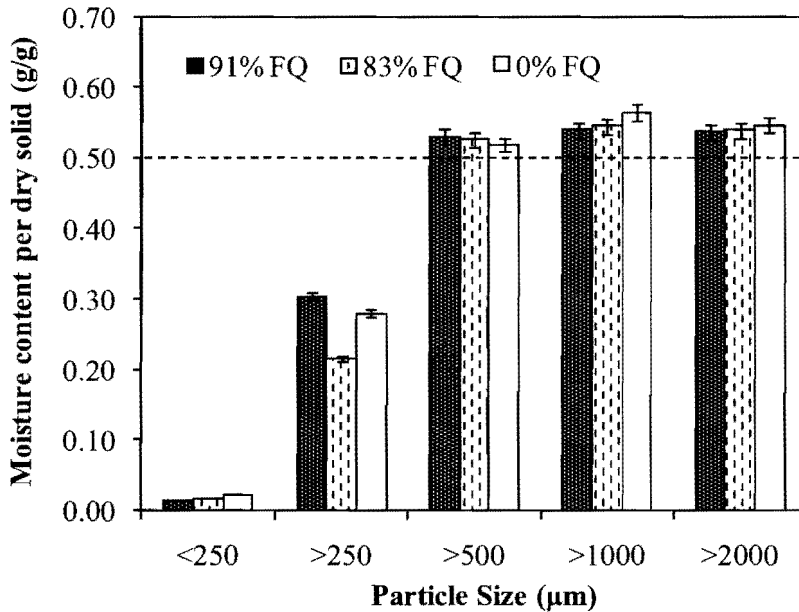


Figure 6-7 Moisture content after 2 minutes of wet massing as a function of granule size class for foam (91% FQ and 83% FQ) and spray (0% FQ) granulation – 4% HPMC, 100 mesh lactose and microcrystalline cellulose mixture, 515rpm.

At the end of wet massing, it is seen that the moisture distribution in the granules was improved, with now around 5% deviations from the theoretical moisture content (as shown by the dashed line). For both foam and spray bounded granules, the moisture content in the granules was distributed among the 500µm-1000µm granule size fraction. The fine fractions (smaller than 500µm) were associated with less moisture than the larger granules. It is expected that the smaller granules are less saturated, solely in terms of satisfying the mass balance. The <250µm fraction has low moisture content as the fraction is mostly the ungranulated powder which does not contain internal pores (because they are not granules).

6.3.4 Power consumption profile

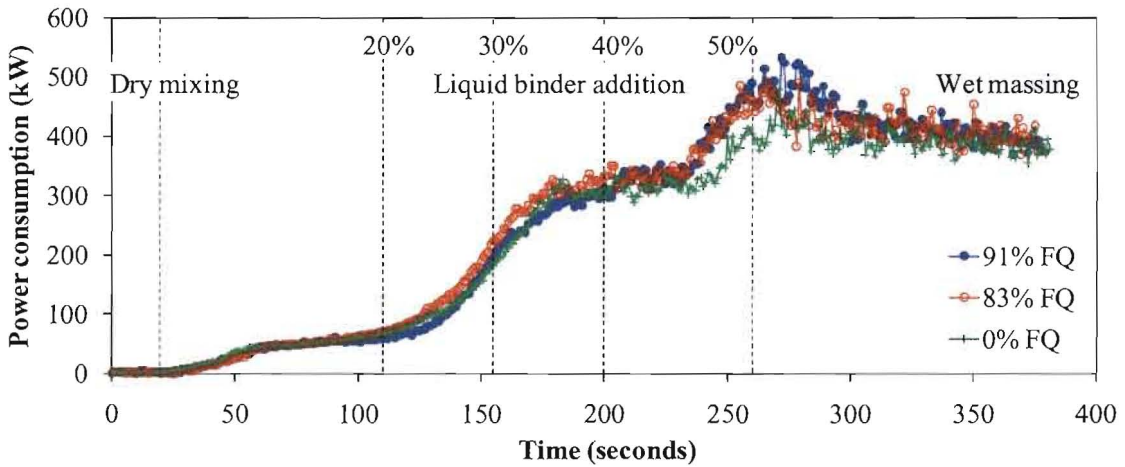


Figure 6-8 Power consumption profiles during foam (91% FQ and 83% FQ) and spray (0% FQ) granulation of 100 mesh lactose and microcrystalline cellulose mixture – 4% HPMC, 515rpm. The processes started with dry mixing, followed by liquid binder addition and ended with wet massing.

Figure 6-8 shows the power consumption during foam granulation (91% FQ and 83% FQ) and spray granulation (0% FQ) relative to the power consumption during the dry mix for a 1:1 mass ratio of lactose and microcrystalline cellulose mixture. The power consumption profiles obtained are very similar to the classical power consumption curves shown in Figure 6-9 (Bier *et al.*, 1979; Leuenberger *et al.*, 2009). Note that our granulation was ceased before phase V, i.e. before a slurry was formed.

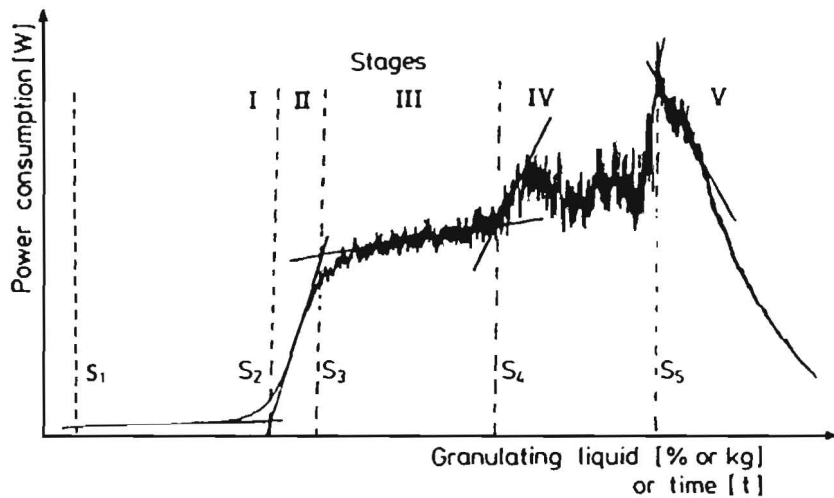


Figure 6-9 Division of a power consumption curve according to Leuenberger (1982; 2009).

The impeller power consumption curves are divided into dry mixing, liquid binder addition and wet massing stages. Note that the power pauses for granule sampling at specific liquid levels were not shown on the curves. For both foam and spray granulation, the power consumption profiles show similar trends - starting with a constant value during the dry mixing stage, rising steeply with liquid binder addition, and levelling off into a plateau where power consumption becomes stable. No significant difference was observed between the three batches, except spray granulation showed a lower rise in the power consumption value at around 240 seconds.

During the dry mixing stage, the power consumption was constant. As liquid binder addition began, the added fluid gave rise to a slightly increased cohesion of the mass, which also caused a small increase in the power consumption value. A decrease in the slope is then observed, which is interpreted as the result of lubrication of the powder mass, which reduces the strength of the bulk and consequently the stress on the impeller.

As liquid binder addition continued, an abrupt increase in the power consumption occurred at around 130 seconds. The increase in the power consumption at a liquid binder level greater than 30% signals the start of the formation of liquid bridges between the primary particles, where nuclei begin to form. When the liquid binder level was raised to about 35%-40%, the power consumption curves began to level off. It has been reported that the optimal amount of granulating liquid is located at this plateau phase of liquid binder addition (Bier *et al.*, 1979;

Leuenberger, 2001; Leuenberger *et al.*, 2009; Levin, 2006; Liu *et al.*, 2009). As shown in *section 6.3.1*, the corresponding granule size distribution is shown to be more or less well defined at this granulation stage.

A further addition of liquid binder produced a second rapid rise in the power consumption as a result of the combined effects of the increased granule size and moist cohesion (due to increased liquid content). Liquid binder addition was ceased at 260 seconds, which was then followed by wet massing. The power consumption showed a slight increase at the start of wet massing, suggesting that there was continuous dispersion of the additional fluid. The slight drop in the power consumption and the following levelling off indicates that there was no free fluid left to be mixed during the final minute of wet massing. This pattern of power consumption profile indicates that the granulation with a liquid binder level $\geq 50\%$ corresponds to the “irreversible overwetting” phase (phase IV shown in **Error! Reference source not found.**), where the granules have reached the transition from funicular to capillary state (Bier *et al.*, 1979; Goldszal and Bousquet, 2001; Leuenberger *et al.*, 2009; Newitt and Conway-Jones, 1958). As shown in *section 6.3.1*, the corresponding granule size distributions support this trend.

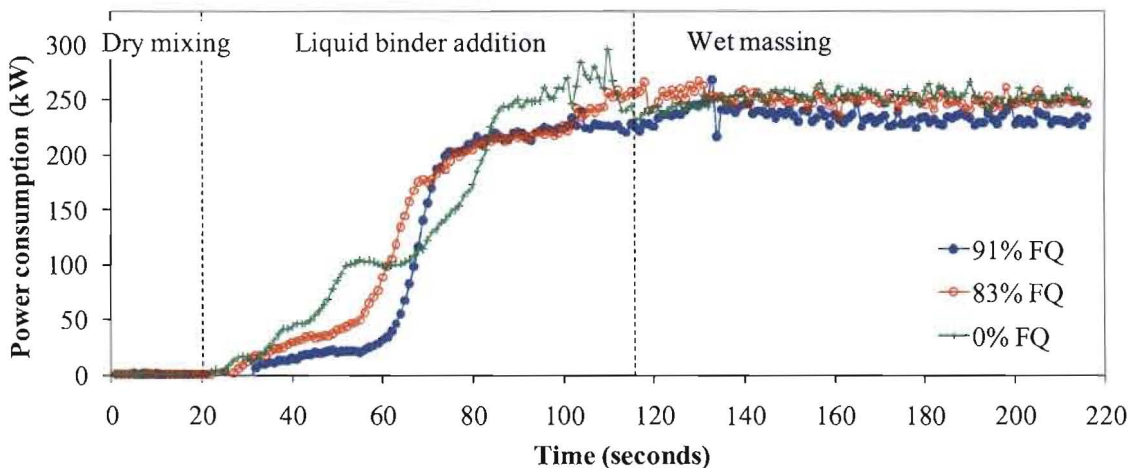


Figure 6-10 Power consumption profiles during foam (91% FQ and 83% FQ) and spray (0% FQ) granulation of 100 mesh lactose – 4% HPMC, 295rpm. The processes started with dry mixing, followed by liquid binder addition and ended with wet massing.

Figure 6-10 shows the power consumption during foam granulation (91% FQ and 83% FQ) and spray granulation (0% FQ) of pure 100 mesh lactose powder. The power consumption profiles show similar transition stages to the previous formulation shown in Figure 6-8. The initial dry mixing period gives rise to a constant power consumption, followed by a steady increase in power consumption due to liquid binder addition. It is seen that foam granulation with 91% FQ and 83% FQ and spray granulation (0% FQ) produced different rates of power consumption value rise. Spray granulation incurs the fastest rate of power rise followed by foam granulation at 83% FQ and then 91% FQ. Foamed binder addition involves some lag time between binder addition and ramp-up to final power consumption as agglomeration builds over time, and this lag time increases as foam quality increases; whereas spray binder addition causes a shorter lag time and faster agglomeration behaviour. It is noted that the power consumption pass through a local maxima when the liquid binder is added as a spray, suggesting non-uniform liquid binder distribution and uncontrolled granule growth.

At a critical liquid binder level, the power consumption shows a sudden rapid increase. It is noted that for spray granulation, the power consumption did not increase during spray binder addition between 50 seconds and 65 seconds, which is likely due to the lubrication effect of the powder mass. However, this pattern is not recognised in either case of foam granulation for the pure lactose power formulation.

For foam granulation at 83% FQ and 91% FQ, the power consumption enters the plateau phase at about 90 seconds. At this stage, foamed binder addition did not cause a significant increase in the power consumption, suggesting that the added foam was well incorporated into the powder mix. The power consumption stayed relatively stable until the end of wet massing. In contrast, a continued increase of the power is observed for spray binder addition. The plateau phase begins at about 120 seconds during the wet massing phase. This difference in the power consumption profile between foam and spray granulation possibly suggests that foamed binder is easier to disperse than spray binder. Considering the optimal amount of liquid binder lies in the plateau phase of liquid binder addition (Leuenberger *et al.*, 2009), the result also implies that foam granulation requires a lower amount of liquid binder compared to spray granulation for a 100 mesh lactose powder formulation.

For the 100 mesh lactose and microcrystalline cellulose mixture, foam and spray granulation show relatively small differences in the power consumption profiles, probably due to the water-absorption property of microcrystalline cellulose. The powder is able to absorb the liquid binder into its porous configuration before becoming saturated, thus delaying its capacity to form liquid bridges, and holding up the changes of power consumption in response to liquid binder addition. For 100 mesh lactose powder that is readily wettable, apparent differences in the power consumption are observed between foam and spray granulation. The differences in the power consumption suggest that foam and spray granulation exhibit different granulation behaviour, which will be discussed in the following section.

6.4 Discussion

Both foam and spray granulation promote granule formation through the use of a liquid binder. Spraying produces small droplets of liquid binder, whereas foaming generates small bubbles of gas contained within the liquid binder. Both processes differ in the nature of liquid binder addition, but they are generally carried out in an effort to enhance the distribution of binding fluid. Poor distribution of binding fluid usually results in uncontrolled granule nucleation and growth, which can lead to the formation of inhomogeneous granules with broad size distributions. It is therefore important to understand the mechanisms controlling foam granulation, and to establish the interrelationships between liquid distribution, granule nucleation and growth, and granule size distribution.

6.4.1 Foam versus spray granulation mechanisms

6.4.1.1 Wetting and nucleation

It is well known that uneven initial distributions of liquid during granulation will cause some powders to receive more liquid binder than others, thus leading to the formation of large, wet nuclei, and relatively small, dry nuclei. The large, wet nuclei continue to become surface wet and grow further into larger granules as granulation proceeds. The end result is a broad final granule size distribution (Iveson *et al.*, 2001a). This granulation behaviour is indicated by the granule size distributions presented in Figure 6-1 and Figure 6-2. Granulation starting with a broad initial granule size distribution eventually also leads to a broad final granule size distribution.

During the wetting and nucleation stage, it is commonly recognised that the spray droplets of binder penetrate the powder mass to create nuclei if the penetration time is small (Hapgood *et al.*, 2003). As the penetration often falls outside of the drop-controlled regime (Hapgood *et al.*, 2003; Litster, 2003; Plank *et al.*, 2003), the resultant nuclei size distribution is often bimodal due to initial uneven nucleation, where some particles are nucleated into larger nuclei while others remain unnucleated. Drop penetration controlled is essentially the ideal nucleation mechanism for spray granulation, while this can be undesirable for foam granulation (see *Chapter 5*). For foam granulation, liquid penetration is relatively insignificant, but the drainage effect becomes more pronounced as foam quality decreases. Liquid penetration controlled nucleation in foam granulation in fact produces an equivalent effect with spray induced nucleation operating outside of the drop-controlled regime, which can lead to the formation of broad granule size distributions. The mechanisms controlling foam nucleation granulation were discussed in detail in *Chapter 5*.

In this chapter, further evidence to support the proposed mechanisms controlling foam granulation is given by the power consumption profiles shown in *section 6.3.4*. From the pure lactose granulation, we have seen that the corresponding power consumption profile for spray binder delivery showed the fastest rate of power consumption rise, followed by foam binder delivery at 81% FQ and then 91% FQ during the initial granulation stage. As granulation proceeded, the power consumption for spray binder delivery continued to increase non-monotonically, while the power consumption for foam binder delivery stayed relatively stable but reached the plateau phase earlier. Note that this behaviour of power consumption change was not observed in the granulation of the lactose and microcrystalline cellulose powder mixture due to the water absorption property of microcrystalline cellulose.

It is clear that the power consumption increases with increasing liquid binder content, which also signifies the increase in the saturation of the powder mass or the formation of nuclei granules (Holm *et al.*, 1985a; b; Leuenberger *et al.*, 2009). The earlier onset of power consumption rise during initial spray binder delivery is likely to indicate an increase in the powder saturation and the amount of nuclei formed. The spray droplets penetrate as a continuous phase, which likely create a more saturated powder mass (and form more initial granules). This means that spray granulation tends to involve early liquid penetration wetting and nucleation. However, with foam granulation, the delay in the power consumption rise

suggests that nucleation by liquid penetration wetting is relatively insignificant in this case. Note that the power consumption value rise also delays with increasing the foam quality for foam granulation, indicating that early liquid penetration and nucleation effects are insignificant for higher foam qualities. This was seen in the case of pure the lactose formulation (see Figure 6-10).

In addition, it is probable that the foam induced nuclei were so weak initially that any nuclei formed were mechanically dispersed into fines. Spray induced nuclei are presumably more saturated and stronger due to localised drop penetration. It should be noted that nucleation by the drop penetration mechanism in this case mostly falls out of the drop-controlled regime (Hapgood *et al.*, 2003), where the penetration in fact involves coalescence of multiple drops. This is supported by the granule size distributions presented in Figure 6-1 and Figure 6-2, which show broad initial granule size distributions with unnucleated fines and larger nuclei (>1mm). At the wetting and nucleation stage, the relatively large nuclei are mostly attributed to slow-to-disperse big clumps being formed by uneven drop penetration. The granule size distributions are generally less uniform compared to foam binder addition.

Drop-controlled nucleation is the ideal regime to obtain narrow nuclei size distributions for spray granulation (Hapgood *et al.*, 2003), but operating in this regime is often difficult. Particularly at the production scale, there is a large potential for high shear spray granulation to operate outside of the drop-controlled regime (Litster, 2003; Plank *et al.*, 2003), which means that the granulation process generally relies on mechanical mixing. In *Chapter 4*, we have seen how foam can be efficiently dispersed by mechanical mixing, and a narrower nuclei size distribution with fewer lumps can be obtained. In this case, foam granulation appears as a superior alternative by showing strong performance in creating rapid dispersion and efficient particle coverage. Given that most full scale spray granulation processes operate in the mechanical dispersion regime, switching to foam granulation would improve liquid distribution and reduce the formation of large granules whilst maintaining the same solution flowrate and overall granulation time.

6.4.1.2 Growth behaviour

After wetting and nucleation, the nuclei compact and grow during the subsequent granulation, where the nuclei enter the induction growth stage. It is clear that large granules are associated

with more moisture than the small granules, which is also shown by the results presented in *section 6.3.3.2*. As mentioned earlier, the large, wet granules continue to become surface-wet during the compaction. Relatively small, dry nuclei will layer onto those surface-wet nuclei, creating large granules with the relatively small nuclei granules remaining visible on the outer layer of the large granules (as shown in Figure 5-5). Only until all small, dry nuclei have disappeared will further granulation then cause the large nuclei granules to coalesce with each other, entering the rapid growth stage. This behaviour is indicated by Figure 6-3 and Figure 6-4, which show that the disappearance of fine granules coincides with the end of the induction stage. In other words, rapid granule growth begins as soon as all of the fine granules have been picked up by the larger granules. This behaviour was shown by Wauters *et al.* (2002), in drum granulation.

When the granules enter the growth stage, foam granulation appears to cause extensive growth, forming more large granules compared to spray granulation. This is indicated by the final granule size distributions presented in Figure 6-1 and Figure 6-2. This trend of granule size distribution changes suggests that foamed binder may initially inhibit nucleation or growth, but once the liquid is there, the foamed binder will promote rapid granule growth. In other words, foam granulation tends to exhibit induction growth behaviour initially, and rapid growth behaviour later. This behaviour of foam granulation is also supported by the weight mean diameter data shown in Figure 6-3 and Figure 6-4, which show a small increase initially followed by a rapid increase of the average granule size later on. Note that the increase of the weight mean diameter increases with decreasing foam quality and increasing impeller speed, indicating that the induction growth effect tends to diminish at these conditions. In comparison, our results also show that spray granulation tends to display steady growth in this case.

6.4.2 Moisture distribution

The case study comparing the performance of foam and spray granulation in delivering homogeneous granules shows that the moisture distribution in the large granules deviates the most at the end of spray binder addition, followed by foam binder addition at 83% FQ and then 91% FQ (see Figure 6-5). There are two possible reasons for this result, which can be attributed to the different wetting and nucleation mechanisms involved in foam granulation (at different foam qualities) and spray granulation:

1. *Spray granulation was operated outside of the drop-controlled regime* (Hapgood *et al.*, 2003). The nuclei granules were created from an uneven drop distribution. Due to localised (multiple) drop penetration, coarse, highly saturated nuclei granules were created. This is supported by the wet and dry granule size distributions at the end of spray binder addition, which show a large fraction of coarse granules. The coarse granules are more saturated, while the fine granules are associated with a lower moisture content (see Figure 6-5 and Figure 6-6). The fine nuclei were possibly the ungranulated particles or fragments broken from the coarse granules due to attrition.
2. *Foam granulation was operated in the mechanical dispersion regime*. Localised liquid penetration is relatively less significant, which is likely to have created fine, less saturated nuclei granules due to mechanical dispersion. However, foam binder addition at a low foam quality can still cause nucleation by the foam drainage mechanism, forming coarse, saturated nuclei granules. This is supported by the wet and dry granule size distributions and the moisture distribution in granules at the end of foam binder addition, where foam binder addition at 83% FQ has created a larger fraction of coarse granules associated with more moisture compared to 91% FQ (see Figure 6-5 and Figure 6-6).

For both foam and spray granulation, the moisture distributions in granules were improved at the end of wet massing, despite the slight deviations from the theoretical moisture content. This improvement in moisture distribution is clearly due to the effect of further mixing. The wet and dry granule size distributions show that the coarse granules are redispersed into finer granules at the end of wet massing, resulting in uni-modal granule size distributions. It is likely that the moisture was also mechanically redistributed (see Figure 6-5 and Figure 6-7).

The performances of foam and spray granulation in delivering homogeneous granules were shown to successfully create granules of reasonably well-distributed moisture at the end of the granulation process. This case study demonstrates the successful use of mechanical mixing in redispersing the granules and improving the moisture distribution, although the granulation may initially operate outside of the ideal operating regime.

6.4.3 A regime map

Iveson's growth regime map (see Figure 2-9) shows the different classes of granule growth behaviour based on two parameters: the typical amount of granule deformation during impact and the liquid saturation of the granules. The map was shown to be useful in predicting the granule growth behaviour, but measuring the Stokes deformation number, St_{def} (the vertical axis in Iveson's growth regime map) and the maximum liquid pore saturation, S_{max} (the abscissa in Iveson's growth regime map) is often difficult in practise (Iveson and Litster, 1998b; Iveson *et al.*, 2001b). The two dimensionless group require information on the fundamental properties such as granule deformability, dynamic yield stress, characteristic porosity which are time-dependent characteristics (Iveson and Litster, 1998b; Iveson *et al.*, 2001b).

Here, we propose a regime map based on Iveson's growth regime map (Iveson and Litster, 1998b; Iveson *et al.*, 2001b) to describe the granulation behaviour for the foam and spray systems as mentioned above. The map, as shown in Figure 6-11, summarises the granulation behaviour for the systems as a function of impeller speed, foam quality and liquid to solid ratio. The regime map is relatively more practical as it is plotted in terms of the granulating condition – impeller speed, liquid to solid ratio and foam quality which can be easily determined.

The map shows the regimes of operation for the key processes in granulation: (I) wetting and nucleation, (II) growth – induction, steady and rapid growth, (III) overwetting, and (IV) caking.

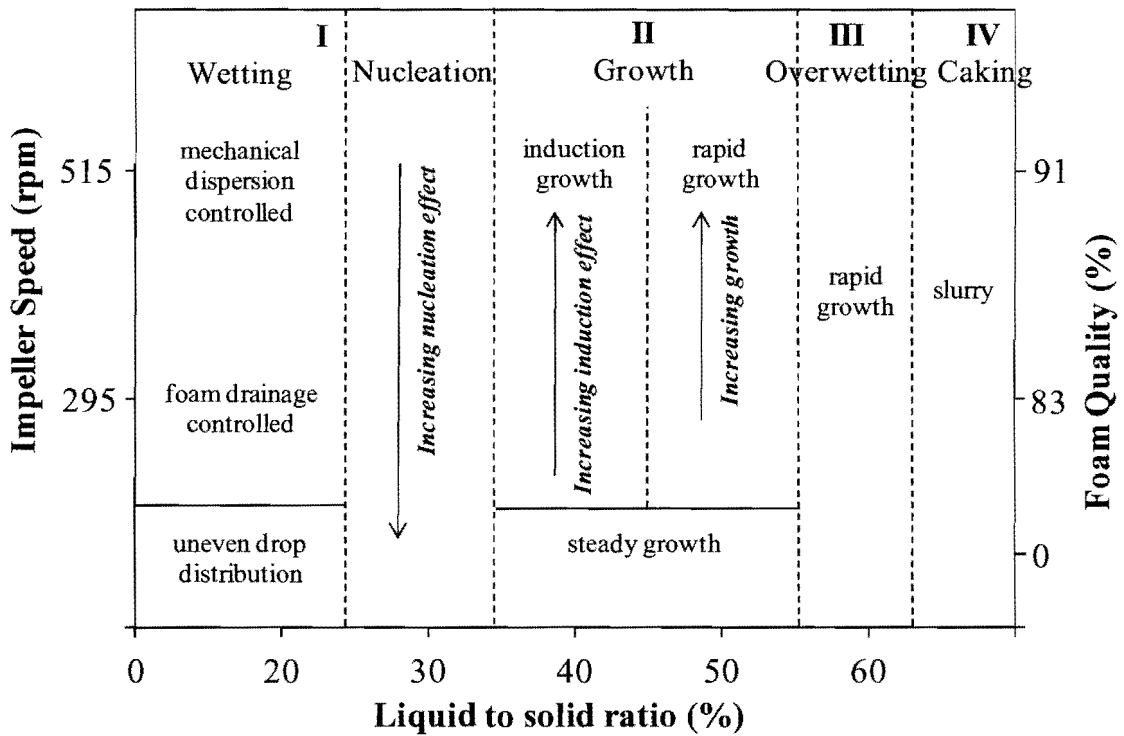


Figure 6-11 Regime map for the granulation systems – foam versus spray. The dotted lines divide the granulation into (I) wetting and nucleation, (II) growth, (III) overwetting and (IV) caking.

At low liquid binder levels, the mass behaves as an essentially dry powder. The added liquid binder causes wetting-only behaviour as the liquid binder is mainly absorbed into the microcrystalline cellulose powder. At slightly higher liquid binder levels, nucleation occurs. For foam granulation, decreasing the foam quality from 91% FQ to 83% FQ enhances the nucleation effect due to drainage-controlled nucleation, where particles are nucleated into nuclei non-uniformly. Increasing the foam quality to 91% FQ shifts the wetting and nucleation to mechanical-dispersion controlled, where the nucleation effect due to localised liquid penetration is low. The two wetting and nucleation mechanisms for foam granulation were verified previously, and the controlling parameters for the two wetting and nucleation mechanisms were given in a list of transformation map (see *Chapter 5*). For spray granulation (0% FQ), liquid penetration is the predominant mechanism (van den Dries and Vromans, 2004; 2009). This has led to a more pronounced nucleation effect for spray induced wetting and nucleation operated outside of the drop-controlled nucleation regime, where the liquid penetration involved uneven drop distribution.

Increasing the liquid binder level shifts the granulation from nucleation to granule growth. Spray granulation tends to exhibit steady granule growth, while foam granulation shows induction granule growth followed by rapid granule growth. In the induction regime for foam granulation, decreasing the impeller speed and/or increasing the foam quality will increase the induction effect. In the rapid growth regime for foam granulation, increasing the impeller speed and/or decreasing the foam quality aids granule consolidation or coalescence due to large liquid amounts and more liquid bridges, which reduce the induction effect and promote a more rapid growth (provided breakage does not occur).

At very high liquid binder levels, both foam and spray granulation enter the rapid granule growth regime. The fine and intermediate granules disappear as they layer onto the larger granules, forming “overwetted” granules (see Figure 5-5). It was shown previously that wet massing is able to break and disperse these “overwetted” granules into finer granules (see *Chapter 5 – section 5.3.4*). When excess liquid binder is added, the systems eventually form a slurry regardless of the impeller speed and foam quality.

6.4.3.1 Implications of the regime map

The regime map for the granulation systems provides an understanding of the interacting effects between impeller speed, foam quality and liquid binder level on the granulation transition phases involved in foam and spray granulation. The control strategy for a granulation system should depend on the regime in which that system lies.

If a granulation system lies in the wetting/nucleation regime, it will never grow rapidly provided its induction time is never exceeded. The granule size distribution shall be controlled by the wetting and nucleation conditions – “foam drainage” or “mechanical dispersion” controlled (see *Chapter 5*). Decreasing the foam quality will promote nucleation, but too low of a foam quality is generally undesired if highly saturated and coarse nuclei are created by “foam drainage” controlled wetting and nucleation. “Mechanical dispersion” controlled wetting and nucleation would be the ideal operating regime provided the system lies below a critical liquid content that any mechanical impact will not aid in granule coalescence and the formation oversized agglomerates.

In the granule growth regime, decreasing the foam quality reduces the induction growth effect. This is often undesirable, as it may shift from the induction region to the rapid growth region. The effect is similar with increasing the liquid binder level, where rapid growth occurs when excessive liquid binder is added. Although mechanical dispersion is the ideal operating mode for foam granulation, care must be taken that impeller speed does not increase extensively, as increasing the impeller speed in the granule growth regime will promote rapid growth and a slurry can be formed.

The regime map defines the transition of granulation stages as a function of material and process properties. The regime map should prove to be useful in tailoring the key material and process parameters for a targeted granulation state. Changing the material and/or process variables also changes the granule size distribution. This was also illustrated in the transformation maps given in *Chapter 5* on the basis of the wetting and nucleation mechanisms. The regime map and the transformation maps shown in *Chapter 5* should provide a basis to customise formulations and compare the different granulation behaviour and the granule size distributions for foam granulation processes.

6.5 Conclusions

In this chapter, foam granulation was compared to spray granulation in a high shear mixer-granulator. Granule size distributions and power consumption during granulation were studied as a function of impeller speed, foam quality and liquid to solid ratio. The moisture distribution in foam-bound granules and spray-bound granules after liquid binder addition and wet massing were also compared.

The moisture distribution in the granules showed a deviation from the theoretical moisture content at the end of the liquid binder addition. Spray binder addition shows the largest deviation, followed foam granulation at 83% FQ and then 91% FQ. For both foam and spray granulation, wet massing successfully redispersed the coarse granules and improved the moisture distribution in the granules. The case study demonstrated the successful use of mechanical mixing in creating homogeneous granules.

A regime map is presented by plotting impeller speed, foam quality and liquid to solid ratio to illustrate the granulation behaviour for the systems investigated. Spray granulation tends to involve drop penetration nucleation outside of the drop-controlled regime (Hapgood *et al.*, 2003), whereas foam granulation operates favourably in the mechanical dispersion regime. For spray induced nucleation, the initial granule size distributions showed a larger fraction of coarse nuclei as a result of uneven drop penetration and nucleation effects. For foam granulation, mechanical dispersion produced more uniform granule size distributions for liquid binder levels below the overwetting limit. The opposite was observed when the granulation entered the rapid growth regime. In the growth regime, spray bounded granules showed steady granule growth, whereas foam bounded granules tended to exhibit induction granule growth, followed by rapid granule growth behaviour. For foam granulation, decreasing the foam quality reduces the induction growth effect and promotes rapid granule growth.

This regime map, along with the transformation maps illustrating the impact of material and process parameters given in *Chapter 5* have great potential to help design and control foam granulation systems.

CHAPTER 7
A CASE STUDY OF DRUG DISTRIBUTION

Monash University

Declaration for Thesis Chapter 7

In the case of Chapter 7, contributions to the work involved the following:

Name	% contribution	Nature of contribution
Melvin X.L. Tan	90	Initiation, Key ideas, Experimental development, Results interpretation & Writing up
Thanh H. Nguyen	10	Experimental development, Editing and reviewing
Dr. Karen Hapgood	Supervisor	Initiation, Key ideas, Editing and reviewing

Declaration by co-authors

The undersigned hereby certify that:

- (1) they meet the criteria for authorship in that they have participated in the conception, execution, or interpretation, of at least that part of the publication in their field of expertise;
- (2) they take public responsibility for their part of the publication, except for the responsible author who accepts overall responsibility for the publication;
- (3) there are no other authors of the publication according to these criteria;
- (4) potential conflicts of interest have been disclosed to (a) granting bodies, (b) the editor or publisher of journals or other publications, and (c) the head of the responsible academic unit; and
- (5) the original data are stored at the following location(s) and will be held for at least five years from the date indicated below:

Location(s)

Department of Chemical Engineering, Monash University, Clayton Victoria 3800 Australia.

Signature 1

Signature 2

Signature 3

	Date
	
	25/11/2010
	

7 A CASE STUDY OF DRUG DISTRIBUTION

This chapter compares foam and spray granulation by evaluating the performance of foam and spray granulation in achieving uniform drug distribution. Single nucleus formation via foam/drop penetration, power consumption during granulation, granule size distribution and the drug distribution in granules for foam and spray granulation were compared. The mechanisms controlling foam and spray wetting and nucleation was analysed and the possible major contribution to the variation in drug distribution in the granules was identified.

Acknowledgements: Sincere gratitude is given to Thanh H. Nguyen for the collaboration and her assistance in conducting the sieve fraction assay measurements.

7.1 Introduction

The previous chapter has evaluated the performance of foam and spray granulation in achieving uniform liquid distribution within the granules. This chapter continues to look at the contribution of uniform liquid distribution in delivering granules with homogeneous drug content.

Although granulation is intended to yield a homogenous product, the process is often complicated by the presence of heterogenous materials during the granulation process. The uniformity of drug distribution in the granular materials can be highly influenced by the presence of these heterogeneous materials due to the mismatch in the chemical and physical properties. A few important factors contributing to the heterogeneity problem include:

1. Wetting characteristics of formulation

Granule heterogeneity problems arise especially in the pharmaceutical industry when the formulation contains hydrophilic and hydrophobic components. The formulation components exhibit different affinity to the granulating agent (Vemavarapu *et al.*, 2009; Zhang *et al.*, 2002), in which the hydrophilic materials will be preferentially granulated by the hydrophilic granulating agent, leaving the hydrophobic materials ungranulated. Although surfactant may be used in the formulation to overcome the poor wettability of hydrophobic material, this is not always possible due to economic feasibility or chemical compatibility among the formulations (Hapgood and Khanmohammadi, 2009).

2. *Dissolution properties of formulation*

Drug particles and excipient exhibit different extents of dissolution to the granulating agent. On addition of liquid binders, dissolution of drug and/or excipient may take place unevenly. The dissolved quantities also depend on the ratio in which the formulation are mixed in the solid state. Either a loss or gain of the drug content from the wetted region or other areas of the mass can be expected (Ojile *et al.*, 1982).

3. *Relative particle size between the drug component and excipient*

Strong heterogeneities arise by selective growth of granules are attributed to the effect of particle size differences between the raw materials (Johansen and Schaefer, 2001; Scott *et al.*, 2000). According to the Stokes theory (Ennis *et al.*, 1991), a smaller particle radius has a low Stokes number (St). Provided St is smaller than the threshold Stokes number, coalescence due to successful collisions between small feed particles is more likely to occur rather than collisions between large feed particles (Iveson *et al.*, 2001a). This is common in pharmaceutical manufacturing cases where the drug active substance particle size is generally smaller than the excipient particle size. The coarse fractions therefore exhibited the highest drug concentration, while the fine fractions mainly consisted of ungranulated excipients (Hapgood *et al.*, 2002a; van den Dries and Vromans, 2002; van den Dries and Vromans, 2003). In cases when the drug active substance particle size is larger than the excipient particle size, the fine fractions are enriched with the drug active substance (Vromans *et al.*, 1999). Although milling may help limiting preferential granulation to improve drug distribution, the reduction of particle size is compromised by the increasing tendency for particles to aggregate which may not always result in homogeneity of granules (Zhang and Johnson, 1997).

4. *Granulation process conditions*

A few studies have also related the inhomogeneity phenomena to the granulating conditions. Vroman *et al.* (1999) investigated the effect of impeller speed on the homogeneity of the granules for cases when the drug and the excipients have a small primary particle size difference. A more homogeneous distribution of drug was achieved at low impeller speed as the liquid bridge attraction forces between the particles and the destructive forces of the impeller exerted on the powder mass were balanced to give appropriate granule growth. Bouwman *et al.* (2006) studied the fragmentation, growth and densification rates as a function powder and liquid properties. It was proposed that homogeneous granular mixture could be

achieved by changing either the liquid binder amount or the liquid binder viscosity to promote an equilibrium growth and breakage for material exchange by disintegration, deformation and distribution mechanisms between the granules during granulation. Van den Dries *et al.* (2003) also indicated that granules are susceptible to a poor distribution of the ingredients when the material exchange by breakage during growth is poor.

5. *Uniformity of binder distribution*

Binder distribution in wet granulation, as a mean to promote material exchange between the particles through a liquid binding agent, is critical for good distribution of ingredients within the granules. Differences in binder distribution have been observed, where small particles tend to take up more binder than coarse particles, resulting in high binder concentration found in larger granules composed of predominantly fine particles (Kobubo and Sunada, 1996; Scott *et al.*, 2000). Although granule heterogeneity may be attributed to several effects as reviewed above, the primary cause that leads to the formation of inhomogeneous granules during wet granulation is the uniformity of binder distribution. A poor binder distribution generally produces poor uniformity of granule content.

In this chapter, a case study is presented to evaluate the performance of foam and spray granulation in achieving uniform drug distribution by carrying out the granulation using salicylic acid as the drug model and lactose as the excipient of varying concentrations in the mixture formulation. Single foam/drop penetration experiments were also carried out on static powder beds comprised of varying concentrations of hydrophobic/hydrophilic glass ballotini mixture and salicylic acid/ lactose mixture. Previous study on single nucleus formation from liquid penetration on a static powder bed has been shown to be useful in understanding how powder particles interact with liquid masses for wet granulation purposes. The attention in this chapter now widens to the interaction of liquid masses with mixtures of hydrophilic and hydrophobic particles.

7.2 Experimental

7.2.1 Materials

The powders used were glass ballotini (AC, Potter Industries, Australia), lactose (100 mesh and 200 mesh, Wyndale, New Zealand) and salicylic acid (Merck, Australia). Half of the glass

ballotini was coated with silanised sigmacote (Sigma Aldrich, Australia) to change the particle surface to hydrophobic (Hapgood and Khanmohammadi, 2009). The liquid binders used were 4% HPMC and 6% HPMC (Methocel E5PLV, Dow Wolff Cellulosics, USA). Table 7-1 indicates the powder and liquid binder properties, which were obtained from vendor specifications.

Table 7-1 Powder and liquid binder properties.

Powder	Grade	Viscosity (mPa.s)	Average particle size (μm)
Salicylic acid	-	-	50
Lactose monohydrate	100 mesh	-	150
	200 mesh	-	75
4% HPMC	E5PLV	19.1	-
6% HPMC	E5PLV	60.1	-

7.2.2 Methods

7.2.2.1 Single foam/drop penetration

Droplets and aqueous foams of 4% HPMC and 6% HPMC binders were produced using a 6mL syringe and a handheld Airspray 150ml foam dispenser respectively. A measured amount of fluid was then carefully placed onto a static powder bed. The powder beds were prepared by sieving a known amount of powder into a petri dish through a 500 μm sieve. The powder beds used comprised of a range of concentrations of hydrophobic/hydrophilic glass ballotini mixture and salicylic acid/200 mesh lactose mixture. Table 7-2 summarises the powder compositions used in the experiments, including the porosity of the powder bed for each mixture.

Table 7-2 Powder compositions and loosed packed porosity.

wt% in mixture		Loosed packed porosity (-)
Hydrophobic glass ballotini	Hydrophilic glass ballotini	
5	95	0.47
10	90	0.47
15	85	0.48
20	80	0.48
25	75	0.45
50	50	0.49
75	25	0.49

wt% in mixture		Loosed packed porosity (-)
Salicylic acid	200 mesh lactose	
0	100	0.67
20	80	0.69
40	60	0.73
60	40	0.74
80	20	0.76
100	0	0.78

For glass ballotini powder mixtures, the porosities of the powder beds are uniform across all degrees of powder formulation hydrophobicity, which range between 0.45 and 0.49. For salicylic acid and 200 mesh lactose powder mixtures, the porosities of the powder beds increase steadily from 0.67 to 0.78 as salicylic acid component increases in the powder beds.

The time for the fluid to penetrate into the powder bed was recorded. Specific penetration time, which is defined as the penetration time per unit mass of fluid added was determined (see Eq. [3-1]). The measurement of fluid added and the nuclei mass obtained enabled the calculation of nucleation ratio, which is defined as mass of nuclei per unit mass of fluid added (see Eq. [3-2]). For full details of the procedures, see *Chapter 3 – section 3.2.2*.

7.2.2.2 Granulation experiments

Granulation experiments were carried out in a high shear mixer-granulator. Overhead chopper was not used during the experiments. The granulator was also equipped with a digital readout of impeller power consumption during granulation. For details of the procedures, see *Chapter 5 – section 5.2.2*.

The granulation experiments involved conducting a series of granulation processes on powder mixtures comprised of a range of concentrations of salicylic acid and (100 mesh/200 mesh) lactose powders. The granulation process started with dry mixing for at least 1 minute, followed by liquid binder addition for 90 seconds and ended with wet massing for 2 minutes after the liquid binder addition step was completed. For foam granulation experiments, 4% HPMC foamed binder was delivered at a flowrate of 90mL/min with 1000mL/min of air to produce a foam binder of 92% foam quality. For spray granulation experiments, the liquid binder was also delivered at a flowrate of 90mL/min using a nozzle and pressure pot system containing the liquid binder. The impeller speed was set at 285rpm, in which the dry powders are mixing in roping regime.

After the granulation process, the granular materials were tray-dried in a fan-forced oven at 50°C overnight. Once dried, representative samples were prepared by using a manual powder chute splitter for granule size distribution measurement and sieve assay analysis.

7.2.3 Analysis

The recorded power consumption values during granulation were analysed using the “peak estimation” method (Betz *et al.*, 2003; 2004; Laicher *et al.*, 1997; Leuenberger *et al.*, 2009). The power consumption curve can be fitted using a polynomial approximation:

$$y = ax^4 + bx^3 + cx^2 + dx + e \quad \text{Eq. [7-1]}$$

where y is the power value, x is the time and a , b , c , d and e are constants. The ‘peak’ (turning point) of the derivative of the profile ‘in process’, $\frac{dy}{dx}$ can then be calculated as:

$$\frac{dy}{dx} = 4ax^3 + 3bx^2 + 2cx + d$$

Eq. [7-2]

The granules were sieved using a mechanical dry sieve shaker (Retsch A200, Australia) in an ordered set of sieves: pan, 125 μm , 180 μm , 250 μm , 355 μm , 500 μm , 710 μm and 1000 μm . For sieve assay analysis, the granules were combined into size fractions of >180 μm , >250 μm , >500 μm , >710 μm and >1000 μm . For each size fraction, sieve fraction assay was performed by dissolving a 5 gram sample in 100mL of methanol to dissolve the salicylic acid (leaving the lactose powder undissolved). Vacuum filtration process was performed by filtering out the lactose powder from the solution containing methanol, lactose powder and dissolved salicylic acid through a filter paper (Whatman filter grade number 2, 8 μm pore size). The lactose filtrate weight obtained allows the calculation of the average granule composition in each size fraction.

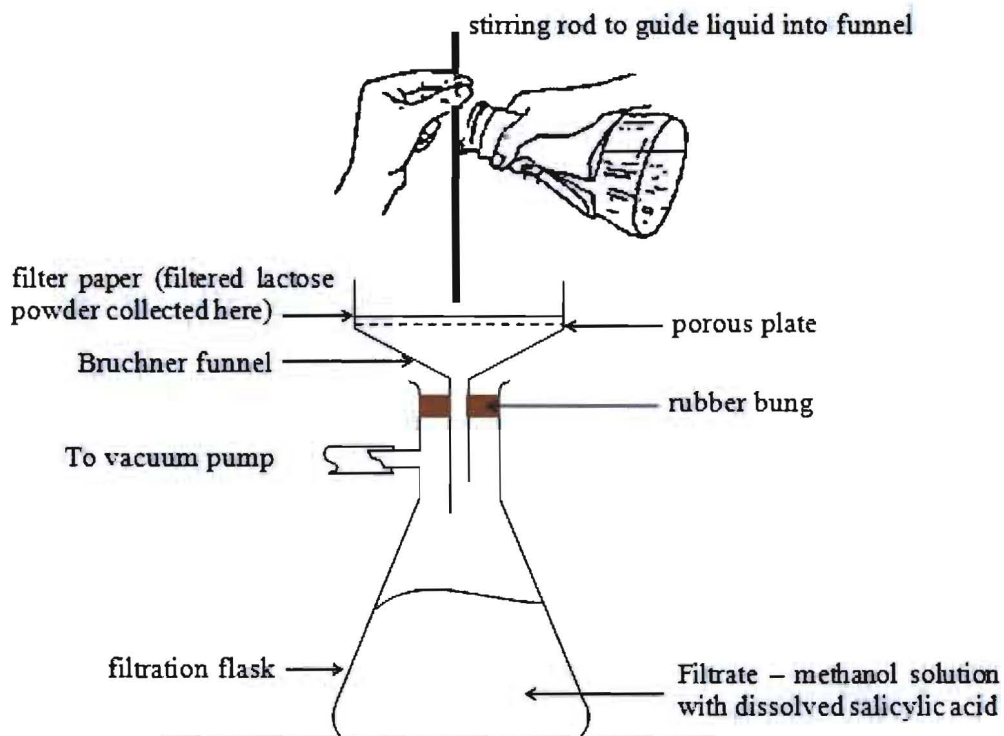


Figure 7-1 Schematic diagram of vacuum filtration of salicylic acid/lactose/methanol solution for filtration of lactose powder.

Figure 7-1 shows the schematic diagram of the setup for vacuum filtration of salicylic acid/lactose/methanol solution. The methanol solution containing dissolved salicylic acid and undissolved lactose powder was poured carefully through the filter paper held in place by

Bruchner funnel, into a vacuum filtration flask connected with a vacuum pump. Calibration of the vacuum filtration method found that the amount of lactose retained from the vacuum filtration was accurate within $\pm 5\%$ of the theoretical powder composition (Nguyen *et al.*, 2010).

7.3 Results

7.3.1 Foam and drop specific penetration times

Figure 7-2 shows the specific penetration time for HPMC foam and a HPMC droplet penetrating into glass ballotini powder beds of varying degree of hydrophobicity. For both foam and drop penetration, the specific penetration times increases in proportion to the hydrophobicity of the powder bed. Increasing the proportion of hydrophobic glass ballotini in the powder mixture has a more significant effect on drop specific penetration time whereas the effect is comparatively small on foam specific penetration time. It is noted that no result was recorded at 100wt% hydrophobic conditions as the powder-liquid contact angle was greater than 90 degrees, resulting in an infinite penetration time.

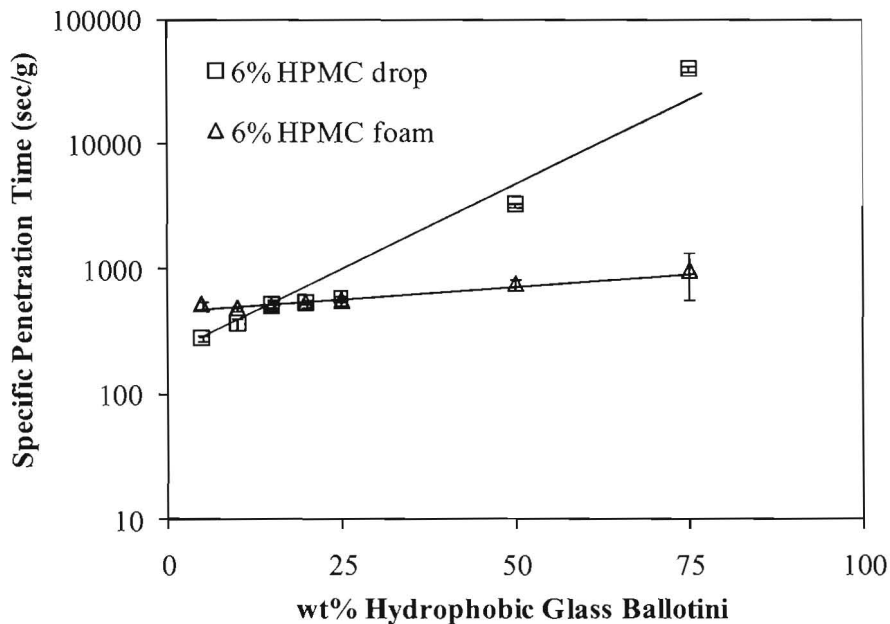


Figure 7-2 Foam and drop specific penetration times as a function of wt% hydrophobic glass ballotini.

For salicylic acid and 200 mesh lactose powder mixtures, Figure 7-3 shows that increasing the proportion of salicylic acid in the powder mixture decreases the specific penetration time. Similarly, drop specific penetration time is more significantly affected by increasing the proportion of salicylic acid in the powder mixture whereas the effect is relatively minor on foam specific penetration time.

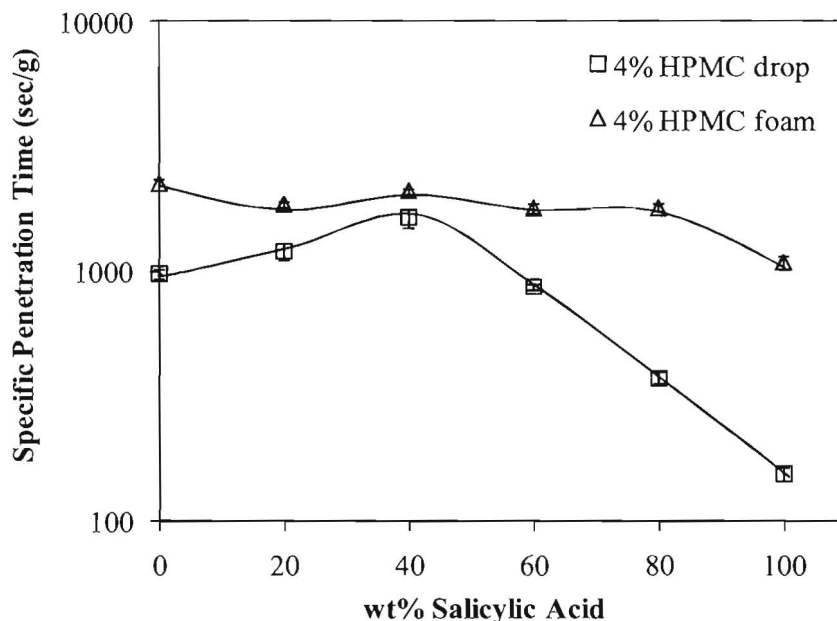


Figure 7-3 Foam and drop specific penetration times as a function of wt% salicylic acid.

The decreasing specific penetration time at increasing proportion of salicylic acid indicates that the presence of salicylic acid promotes liquid penetration of the HPMC binder solution. The penetration is favoured in the powder bed packed with larger number of salicylic acid particles due to a larger number of pores contained within the smaller fractions (salicylic acid). Powder beds enriched with salicylic acid particles will thus induce faster liquid penetration due to a higher capillary driving force. This is indicated by the porosity data shown in Table 7-2, where the porosity of the powder bed increases steadily from 0.66 to 0.78 as salicylic acid component increases in the powder bed.

In both cases (glass ballotini/salicylic acid blends), the foam specific penetration time is relatively insensitive to the formulation hydrophobicity for all proportions of the hydrophobic component in the powder mixture, compared to the drop specific penetration time. The

presence of salicylic acid favours liquid penetration for drops of HPMC solution, which implies that the drops of HPMC solution exhibit a lower contact angle with the salicylic acid than with the lactose powder, although the changes in the packing structure of the powder bed may also play a role. This penetration behaviour indicates that HPMC binder is able to wet the salicylic acid, which is the opposite behaviour of what was expected. Foam specific penetration time remains constant regardless of the formulation hydrophobicity, showing that foam penetration is insensitive to the properties (physical and/or interfacial) of the powder bed. This suggests that the hydrophobicity of the formulation is not a controlling factor in foam induced nucleation. It may be that the rate limiting step controlling foam penetration into the powder is the rate of liquid drainage through the foam. This was discussed in more details in *Chapter 3, 4, 5 and 6*.

7.3.2 Foam and drop nucleation ratios

Figure 7-4 plots the nucleation ratio as a function of the proportion of hydrophobic glass ballotini in the powder mixture for foam and drop addition methods. Increasing proportion of hydrophobic component in the powder mixture decreases the drop nucleation ratio. In contrast, the hydrophobicity of the powder mixture does not significantly affect the foam nucleation ratio.

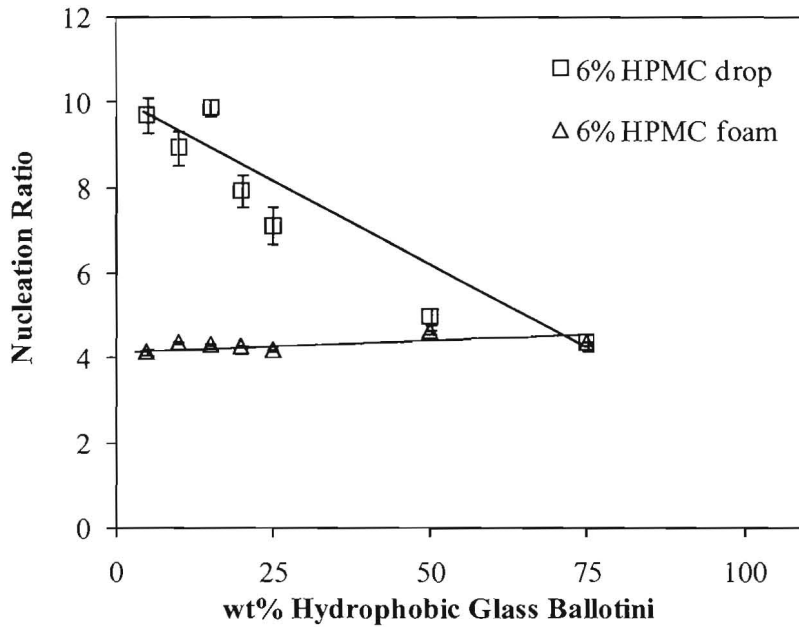


Figure 7-4 Foam and drop nucleation ratios as a function of wt% hydrophobic glass ballotini.

It can also be seen from the nuclei morphology, as shown in Figure 7-5 and Figure 7-6, that foam and drop produce different nuclei structure and size for powder beds comprised of different proportions of hydrophobic and hydrophilic components.

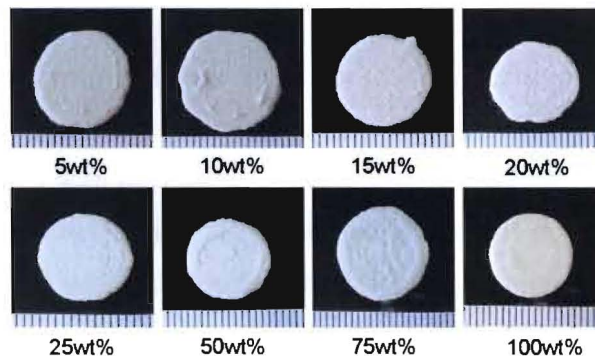


Figure 7-5 Nuclei produced from 6wt% HPMC foam on glass ballotini powder mixtures. Scale indicates millimetres.

From Figure 7-5, it can be seen that the nuclei structure and size is fairly uniform for all degrees of powder hydrophobicity in foam induced nucleation. Glass ballotini particles were strongly binded, forming hemispherical saturated nucleus.

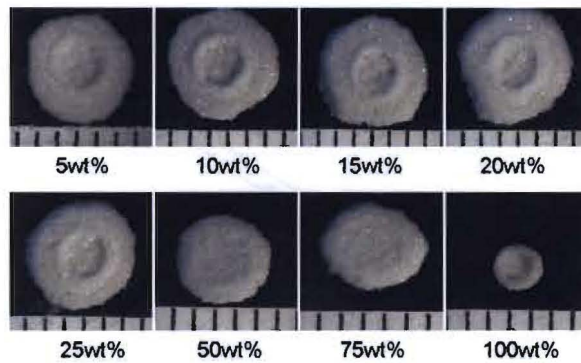


Figure 7-6 Nuclei produced from 6wt% HPMC drops on glass ballotini powder mixtures. Scale indicates millimetres.

For drop induced nucleation, the nuclei structure is altered as the powder hydrophobicity of the powder mixture increases (Figure 7-6). At predominantly hydrophilic powder beds, a hemispherical saturated nucleus is produced. As the powder hydrophobicity increases, the outer powder layer surrounding the centre nucleus thins out until at 100wt% hydrophobic conditions a collapsed hollow nucleus of concave shape is formed. This nuclei morphology was observed previously (Nguyen *et al.*, 2009; Nguyen *et al.*, 2010).

Figure 7-7 plots the nucleation ratio as a function of the proportion of salicylic acid in the powder mixture for foam and drop addition methods. The plot shows a similar trend that drop nucleation ratio decreases with increasing hydrophobicity of the powder mixture. In this case, foam nucleation ratio also declines as the proportion of salicylic acid increases in the powder mixture. This is due to the weak adherence of the salicylic acid onto the nuclei which increases the likelihood of attrition and breakage to form small, weak nuclei.

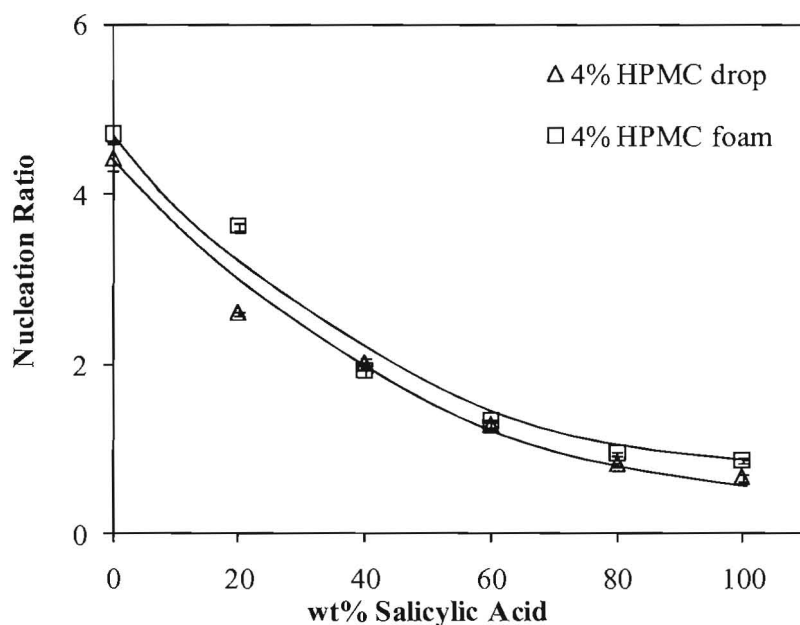


Figure 7-7 Foam and drop nucleation ratios as a function of wt% salicylic acid.

Figure 7-8 and Figure 7-9 show that the nuclei appear to be weaker and smaller as the proportion of salicylic acid increases in the powder mixture.



Figure 7-8 Nuclei produced from 6wt% HPMC foams on powder beds containing various proportions of salicylic acid. Scale indicates millimetres.

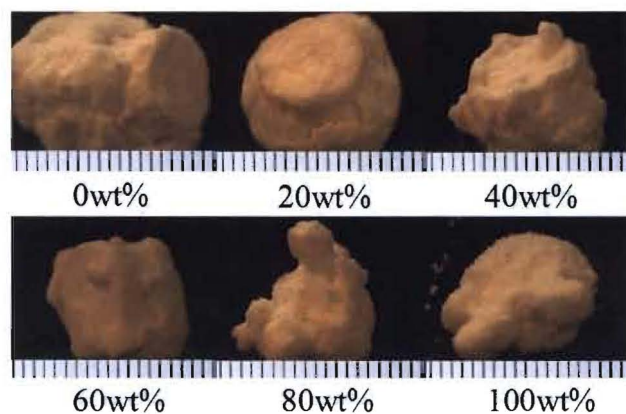


Figure 7-9 Nuclei produced from 6wt% HPMC droplets and powder beds containing various proportions of salicylic acid. Scale indicates millimetres.

Both foam and drop addition methods produced nuclei with a saturated centre ‘stalk’ surrounded by weak outer shell. The nuclei made from predominantly salicylic acid appear to be weaker than nuclei made from predominantly lactose, which is reflected in the formation of irregularly shaped nuclei due to attrition during the excavation process. No liquid marbles (Aussillous and Quere, 2001; Hapgood and Khanmohammadi, 2009) were formed even on completely hydrophobic powders (100wt% of salicylic acid in the powder bed). This is probably due to the earlier observation that the HPMC solutions are able to wet and penetrate the salicylic acid formulation.

7.3.3 Power consumption profile

Figure 7-10 and Figure 7-11 show the power consumption during foam and spray granulation of salicylic acid-200 mesh lactose (SA-L200m), and salicylic acid-100 mesh lactose (SA-L100m) respectively using a 5-litre mixer-granulator (Key International Inc., New Jersey, USA). The power consumption during the dry mix has been subtracted to show the changes after granulation. For most formulations, the progression of the power consumption profiles is similar. The power reading is stable during the dry mixing stage (first 20 seconds), begins to climb slowly after the beginning of liquid binder addition (the following 90 seconds) and becomes stable (at a higher power value) at the end of the process.

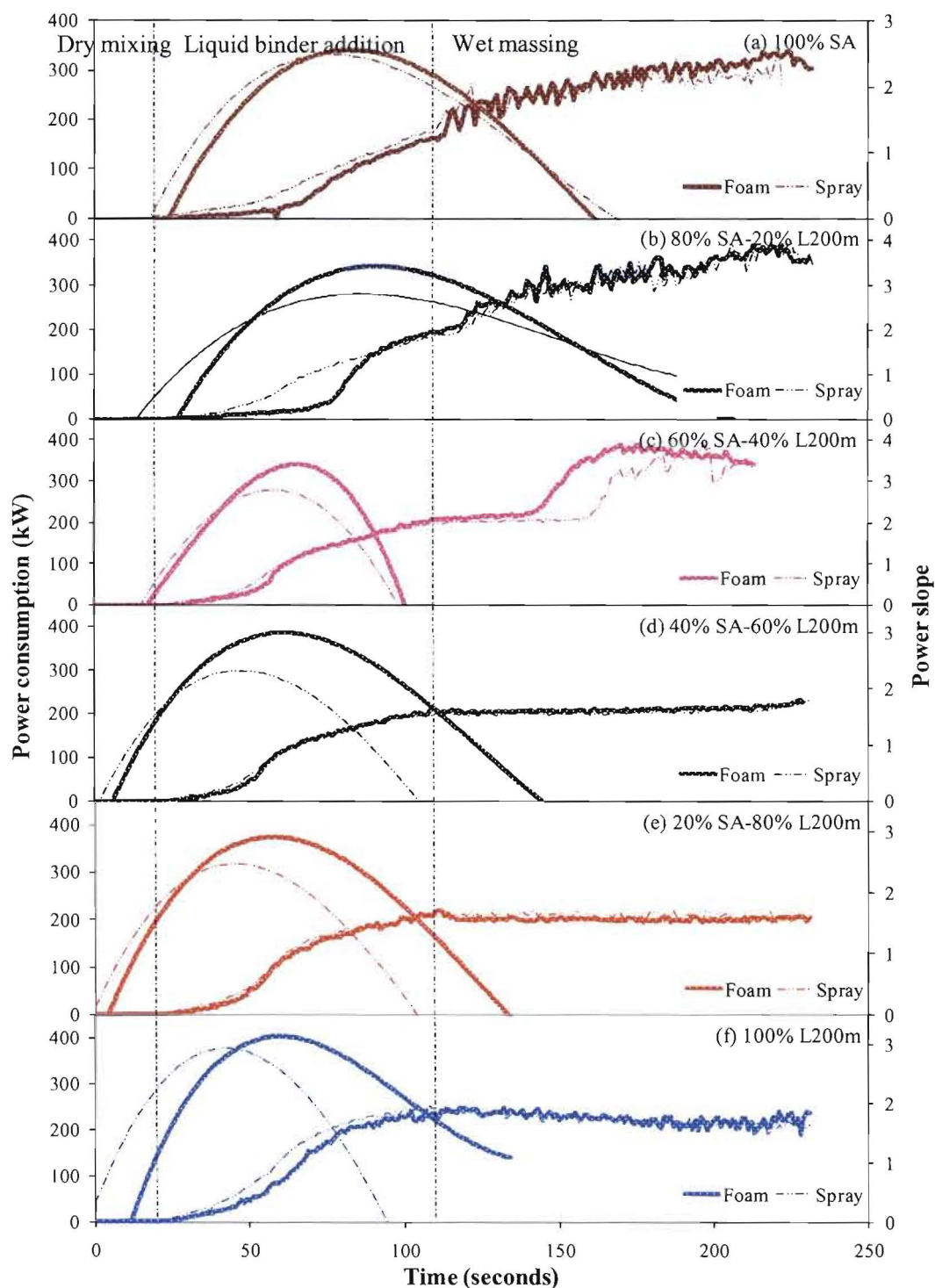


Figure 7-10 Power consumption and the slope of the profile (first derivative with respect to time) during foam and spray granulation relative to the dry mix as a function of powder composition – 4% HPMC, salicylic acid (SA) and 200 mesh lactose (L200m) powder mixtures, 285rpm.

From Figure 7-10, it is seen that the rate at which the power consumption rise is slightly different during foam and spray granulation. After the dry mixing stage, spray granulation tends to incur an earlier rise in the power consumption compared to foam granulation. This trend of power consumption was observed previously with other formulations shown in *Chapter 6*. As granulation proceeds, foam and spray granulation reach a similar power consumption end point. This can also be reflected by the derivative of the power consumption with respect to time shown on the same plot (Betz *et al.*, 2003; 2004; Laicher *et al.*, 1997; Leuenberger *et al.*, 2009), where the peak of the power derivative indicate the inflection point of the power consumption curve. According to Leuenberger (2009), the peak point should act as a reference point for the desired granulation end point where the process is more or less well-defined after the peak point. For most formulations, the peak points for foam and spray granulation are close.

From the peak detection method (Bier *et al.*, 1979; Holm *et al.*, 2001), it can be also seen that the 'point of reference' is shifted towards a lower liquid requirement for formulations containing more than 50% lactose. This implies that for a similar granulation end-point, lactose-enriched formulations will require a lower amount of liquid binder compared to salicylic acid-enriched formulations. As shown in Figure 7-11, same trends were observed for salicylic acid and 100 mesh lactose powder mixture.

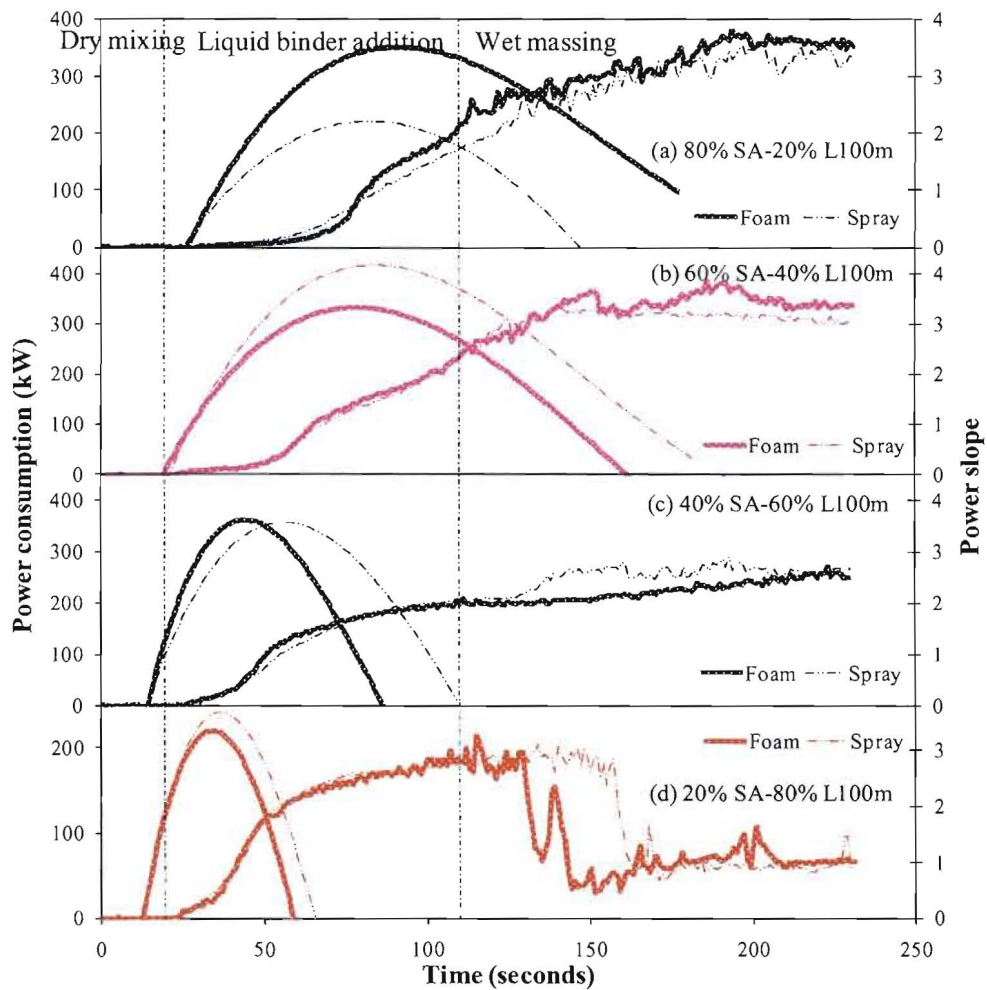


Figure 7-11 Power consumption and the slope of the profile (first derivative with respect to time) during foam and spray granulation relative to the dry mix as a function of powder composition – 4% HPMC, salicylic acid (SA) and 100 mesh lactose (L100m) powder mixture, 285rpm. The processes started with dry mixing, followed by liquid binder addition and ended with wet massing.

For the 60% SA-40% L200m batch (Figure 7-10(c)), both foam and spray granulation have generated a second rise in the power consumption during the wet massing phase. This is taken to illustrate that there is extra “free” fluid to be mixed during the last minute of wet massing. It is noted that foam granulation has generated an earlier second rise in the power consumption compared to spray granulation, which again supports the suggestion that foam granulation requires less liquid than spray granulation to produce similar granules (Keary and Sheskey, 2004). This is also observed for the 20% SA-80% L100m batch (Figure 7-11(d)), where foam

granulation has generated an earlier descent in the power consumption compared to spray granulation. This sudden descent in the power consumption indicates that foam granulation requires less liquid to overgranulate the system and form a slurry (Iveson *et al.*, 2001a) compared to spray granulation.

7.3.4 Granule size distribution

Figure 7-12 and Figure 7-13 show the granule size distribution for both foam and spray granulation on salicylic acid-200 mesh lactose (SA-L200m) and salicylic acid-100 mesh lactose (SA-L100m) respectively. For both foam and spray granulation, the granule size distributions tend to shift to the right towards the larger size range as the proportion of salicylic acid decreases. This indicates that increasing the proportion of hydrophilic lactose in the granulation mixture results in a larger average granule size of the batch. Due to the hydrophobic nature of the salicylic acid, the particles exhibit weak adherence to lactose or other salicylic acid powder particles and weak granules are created during granulation. These weak granules are more susceptible to attrition in which fragmented granules or loose aggregates are formed through breakage, reducing the average granule size of the batch as the proportion of salicylic acid increases. This trend is also supported from the nucleation ratio data (previously shown in Figure 7-7) and agrees with the data from other workers (Aulton and Banks, 1979; Belohlav *et al.*, 2007; Jaiyeoba and Spring, 1980; Lerk *et al.*, 1976; Nguyen *et al.*, 2010).

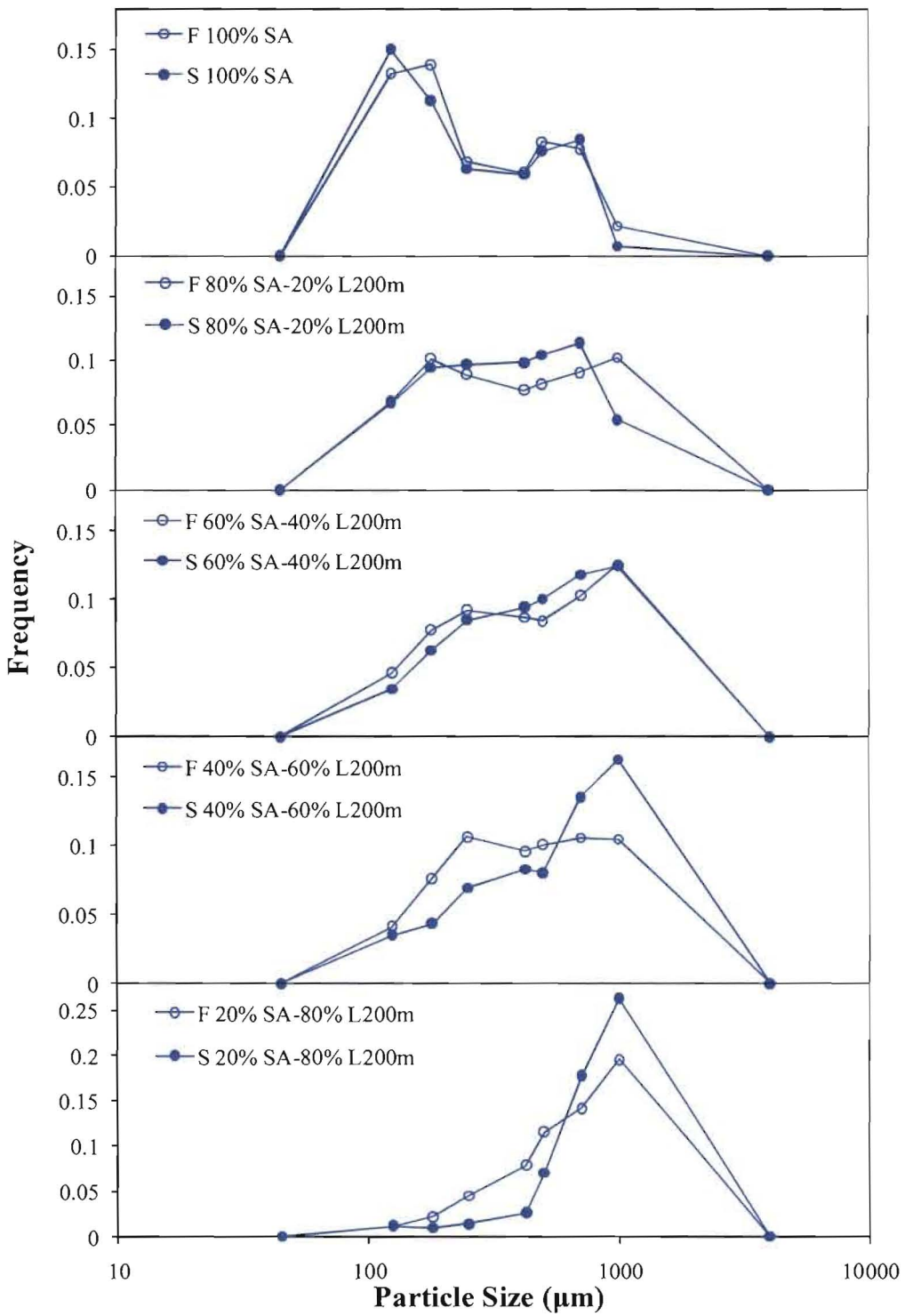


Figure 7-12 Foam (F) and spray (S) granule size distributions as a function of powder composition – 4% HPMC, salicylic acid (SA) and 200 mesh lactose (L200m) powder mixture, 285rpm.

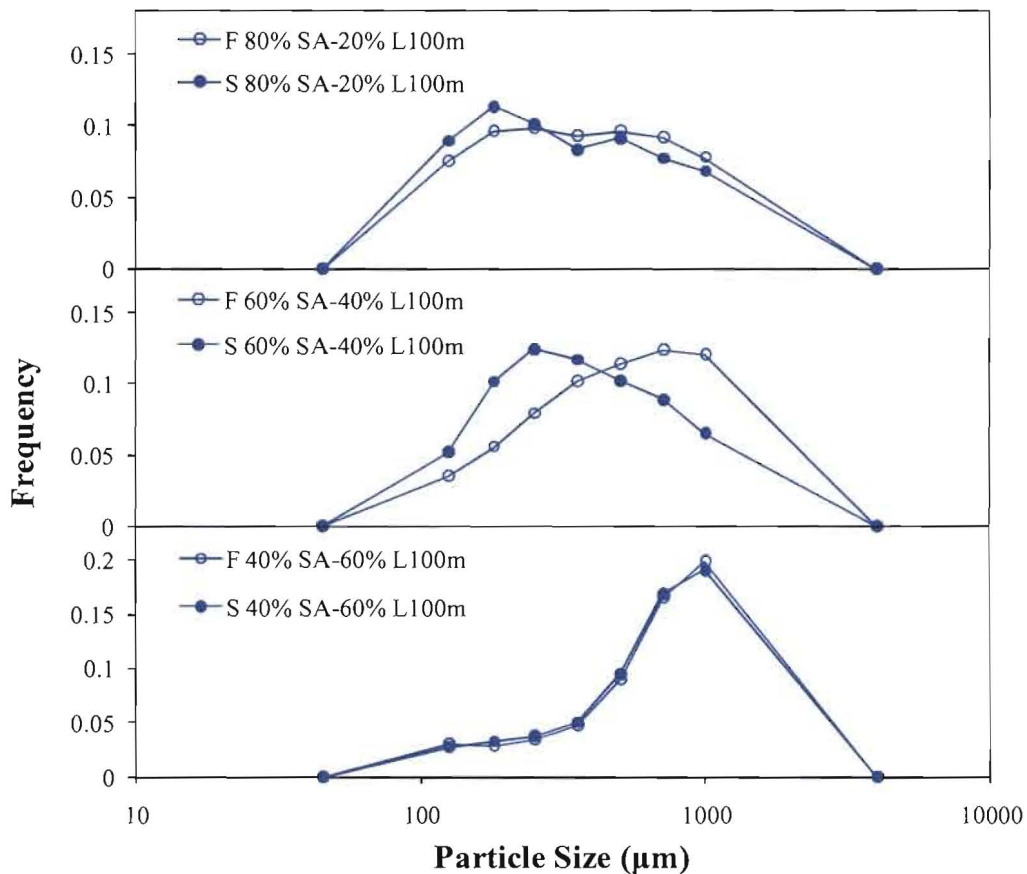


Figure 7-13 Foam (F) and spray (S) granule size distributions as a function of powder composition – 4% HPMC, salicylic acid (SA) and 100 mesh lactose (L100m) powder mixture, 285rpm.

For salicylic acid and 200 mesh lactose powder mixture (Figure 7-12), spray granulation tends to generate a larger fraction of granules greater than 500 μm for formulations containing more than 50% lactose. This trend was not observed for salicylic acid and 100 mesh lactose powder mixture (Figure 7-13). In general, foam and spray granulation show no clear trends in the differences of the granule size distributions. For some batches, foam granulation shows larger and wider granule size distributions while for other batches the granule size distributions are very similar.

7.3.5 Drug distribution

Figure 7-14, Figure 7-15, Figure 7-16 and Figure 7-17 show the percent of drug claim as a function of granule size for foam and spray granulation batches consisting of varying powder

composition. The drug claim indicates how closely the sieve fraction assay concentration matches with the theoretical drug claim for the granulation batch. A 20% theoretical drug claim would indicate that the batch contains 20% by mass of drug. The y-axis error bars represent a constant estimated error of $\pm 5\%$ in the concentration of salicylic acid.

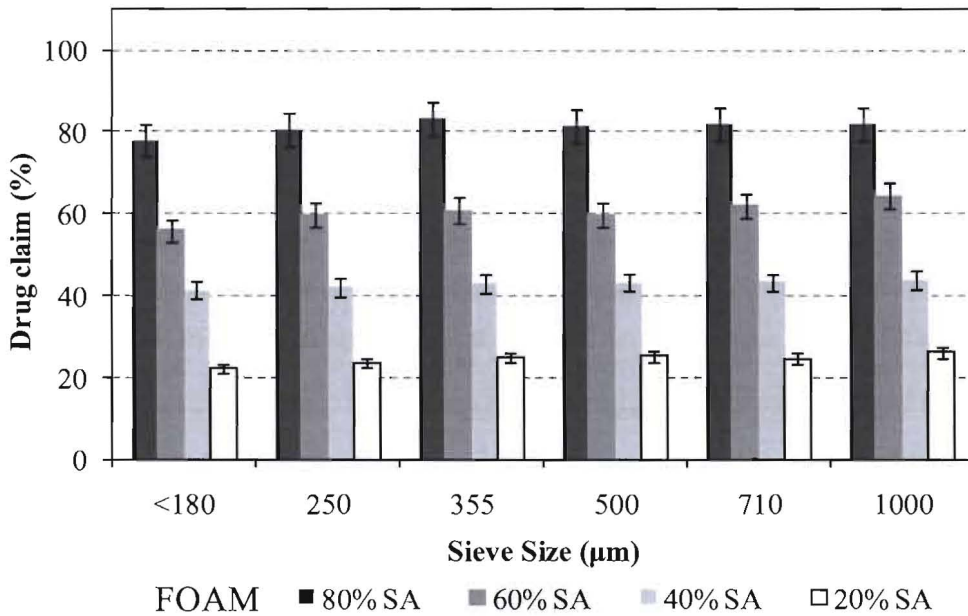


Figure 7-14 Foam granulation – % drug claim as a function of granule size for salicylic acid-200 mesh lactose formulations.

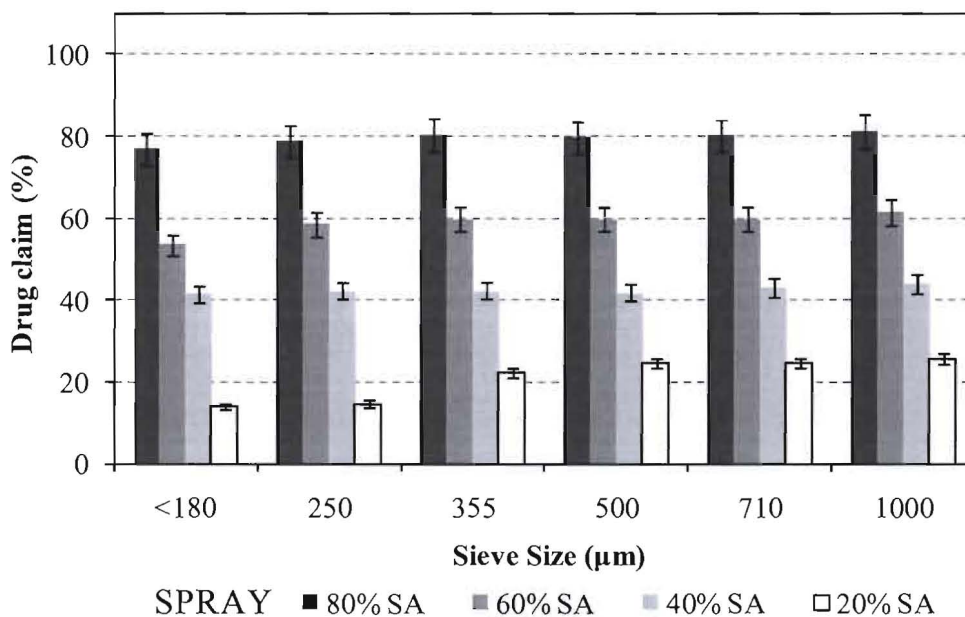


Figure 7-15 Spray granulation – % drug claim as a function of granule size for salicylic acid-200 mesh lactose formulations.

From Figure 7-14 and Figure 7-15, it is seen that foam and spray granulation on salicylic acid-200 mesh lactose formulations do not significantly affect the distribution of the salicylic acid drug component. For both foam and spray granulation, the composition of drug in the granules is remarkably consistent across all size fractions, which have resulted in a drug claim that closely matches the theoretical drug loading. There is a slight deviation in the fine size fractions (<250µm) for spray granulation of the 20% salicylic acid batch (Figure 7-15). This could be due to potential over-wetting of the lactose powder since the wetting behaviour is not as favourable for lactose and HPMC as it is between salicylic acid and HPMC (as seen previously from the study of single foam/drop penetration on static powder beds shown in *section 7.3.1*), hence leading to minor liquid pooling during wet granulation and producing a larger fraction of coarse granules. However the minor pooling effect seems to have been overcome by using foam as seen in Figure 7-14. Foam is able to distribute the liquid over a greater surface area, which could help in minimising liquid pooling and over-wetting of the predominantly lactose powder mixture.

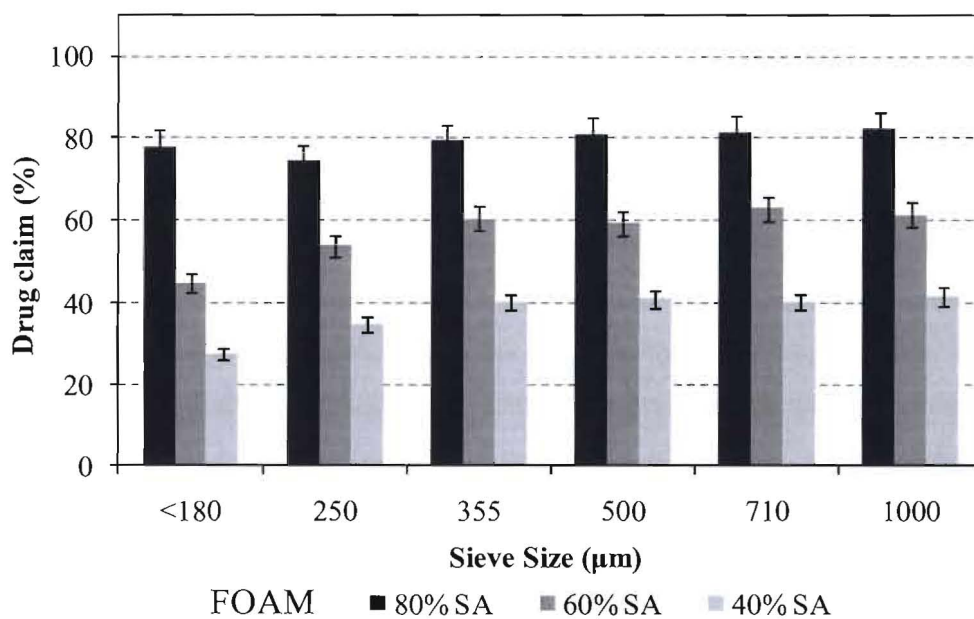


Figure 7-16 Foam granulation – % drug claim as a function of granule size for salicylic acid-100 mesh lactose formulations.

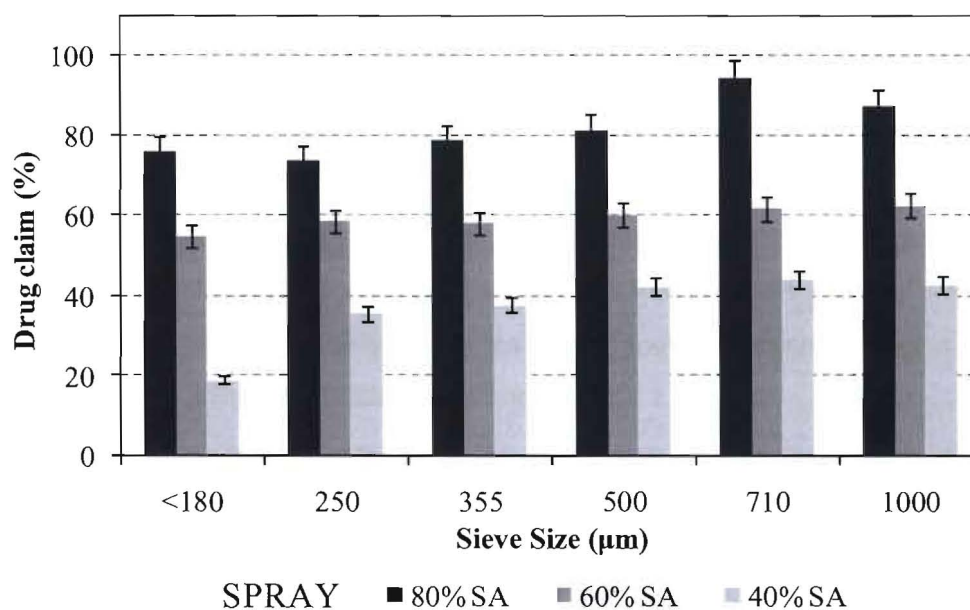


Figure 7-17 Spray granulation – % drug claim as a function of granule size for salicylic acid-100 mesh lactose formulations.

For foam and spray granulation on salicylic acid-100 mesh lactose formulations, as shown in Figure 7-16 and Figure 7-17, the percent of drug claim as a function of granule size seems to deviate away from the ideal drug claim (as shown by the dashed lines). Both foam and spray granulation performances show a relatively poor ability to evenly distribute the salicylic acid drug component compared to the previous formulations with salicylic acid-200 mesh lactose. Foam granulation seems to perform better in achieving a uniform salicylic acid drug composition in the granules for the 80% SA batch, while spray granulation shows a more uniform salicylic acid drug composition in the granules for the 60% SA batch. There is a general trend where both foam and spray show a decreasing granulation performance in achieving uniform drug composition as the proportion of salicylic acid decreases in the formulation. In particular for the 40% SA batch, the majority of the drug composition data shows a lower percent of drug claim in the fine size fraction.

7.4 Discussion

7.4.1 Monitoring granulation via power consumption measurement

The measurement of the power consumption has been widely used for monitoring wet granulation processes. The power consumption during the granulation obtained in this chapter shows a typical profile – initial steady power consumption for the dry mixing stage, steep rise with liquid binder addition, followed by a stable power consumption. Certain formulations show a decrease in the power consumption during the wet massing phase (Leuenberger, 1982; Leuenberger *et al.*, 2009). Again, we see that spray binder addition caused an earlier onset of power consumption (after the dry mixing stage) whereas the onset of the power consumption for foam binder addition was delay. This pattern of power consumption was observed previously with other formulations shown in *Chapter 6*.

It is clear that the rise in the power consumption corresponds well with the start of liquid binder addition, which signals the uptake of the added liquid binder by the powder (wetting) and the formation of liquid bridges between the particles (nucleation). During spraying, the liquid binder droplets come into contact with the powder bed penetrate and nucleate the particles. The wetting and nucleation involves liquid penetration and immersion nucleation (van den Dries and Vromans, 2004; 2009), where the liquid binder flows extensively into the powder bed to form semi-saturated powder shell surrounding the nucleus (Hapgood *et al.*,

2004). The increase in the power consumption should coincide with the increase in saturation (moisture content) as more liquid binder penetrates into the powder bed (Holm *et al.*, 1985a; Leuenberger *et al.*, 2009). For foamed binder that first comes into contact with the powder bed, the delay in the power consumption rise implies that liquid penetration is relatively insignificant in this case. Alternatively, the foamed binder tends to spread rather than to penetrate locally into the powder bed during foam granulation. This is also supported by the study of single foam penetration on static powder beds, where the foam penetration time was found to be less dependent on the powder hydrophobicity. This implies that liquid penetration is not a controlling factor during foam induced nucleation (which is also supported by the study of single foam/drop penetration previously shown in *section 7.3.1*). For spraying, liquid penetration nucleation is the predominant mechanism (van den Dries and Vromans, 2009).

As granulation proceeds, foam becomes well-incorporated into the powder mix in which the power consumption continues to increase to a similar stable power level with the spray. The increase in the power consumption suggests that the energetic collisions between the granules increases with increasing granule concentration, and energy dissipated by inter-particle movements is much superior with increasing liquid content compared to that of dry powders. For foam and spray granulation, the power consumption reached an equilibrium at a similar end-point when the liquid binder is fully dispersed. The plateau value of the power consumption suggests that there is a balance between granule coalescence and breakage. The number of collisions reduces as a result of granule coalescence due to reduced number of granules while the energy dissipation due to granule-granule collisions increases as the average granule size increases (Iveson *et al.*, 2001a). For formulations that incur a sharp decrease in the power consumption during the wet massing phase, the process has possibly reached an overgranulated state where the saturation level is higher than 100%. After the over-wetting point, the power consumption rapidly decreases as the excess liquid acts as a lubricant in the inter-particle movement (Betz *et al.*, 2003).

The peak detection method using the first derivative of the power consumption curve can provide a useful guideline to the critical liquid binder requirement (Bier *et al.*, 1979; Holm *et al.*, 1985b; Holm *et al.*, 2001). It is sensible that the liquid binder requirement decreases with increasing proportion of lactose component in the formulation before the powder became overwetted, and this was 'detected' by the peak of the power derivative.

Although the correlation of power consumption with the granulation state may not always be linear in the entire range, and the power consumption may possibly be confounded by the friction losses in the motor bearings, the data shows consistent trends in different foam and spray granulation batches. From the data shown in this chapter and in *Chapter 6*, monitoring of foam and spray granulation processes via the measurement of the power consumption of the impeller motor was shown to be a potential method.

7.4.2 Drug distribution

In this chapter, salicylic acid was used as the drug model and lactose was used as the main excipient in the formulations. Comparing the ability of foam and spray granulation to evenly distribute the drug component in the granules, it was shown that both foam and spray granulation have led to reasonably even drug distribution across all the granule size fractions in the salicylic acid-200 mesh lactose batches (Figure 7-14 and Figure 7-15). There are three possible reasons for this result:

1. *The HPMC liquid binder is partially wettable to the powder.* As shown in section 7.3.1, the penetration of HPMC liquid binder into the salicylic acid powder bed indicates that salicylic acid exhibits a contact angle of less than 90° with the HPMC liquid binder. A core-saturated nucleus was formed which also indicates that immersion wetting of the salicylic acid occurs with the HPMC foam/droplet. For liquid binders that is partially hydrophobic to the drug particles, granulation allow more of the liquid binder to be able to adhere to the drug rather than being self-associated, which consequently leads to homogeneous drug distribution in the granular materials (Crooks and Schade, 1978; Miyamoto *et al.*, 1998; Rossetti *et al.*, 2004; Schæfer *et al.*, 2004).
2. *The primary particles of salicylic acid and lactose 200mesh are similar in size.* Preferential granulation of the smaller particles is limited in this case (Johansen and Schaefer, 2001; Scott *et al.*, 2000), which means all particles are evenly granulated.
3. *The granulation extent has possibly reached an optimum due to excess amount of liquid binder used.* In general, the amount of liquid binder used has possibly been pushed to the limit. Increasing the amount of granulating liquid increases the granulation extent which allows all particles to be fully granulated, leaving no un-granulated drug

(Horisawa *et al.*, 1995; Wan *et al.*, 1992). A larger amount of liquid binder could also improve the ability of the excipients to encase the drug during the granule growth stage, leading to uniform drug distribution in the granular materials.

At the same granulating conditions, the granulation performance in the salicylic acid-100 mesh lactose batches shows a relatively poor ability to achieve a uniform composition in the granules. The drug distribution is less uniform, with the coarse fractions tend to be enriched with salicylic acid that is granulated with the 100 mesh lactose powder. The primary cause for this granule heterogeneity in drug content in this case is due to *the feed powder particle size difference between the drug and excipient particles*. Salicylic acid particles are smaller in the average size ($\sim 50\mu\text{m}$) than the 100 mesh lactose particles ($\sim 150\mu\text{m}$). The liquid binder is taken up more by the smaller salicylic acid particles, causing preferential granulation of small sized drug components. This potentially gives rise to a higher content of drug particles in the coarse (drug-enriched) granules (Scott *et al.*, 2000).

Overall, foam and spray granulation show strong performances in achieving uniform drug distribution in the salicylic acid-200 mesh lactose batches. In the cases where salicylic acid and lactose primary particle sizes are not similar, the drug distribution appears to have deviated from the target drug claim. Foam granulation gave rise to a more uniform drug distribution in the 80% SA-20% L100M batch and the 40% SA-60% L100M batch, whereas spray granulation seems to perform better in the 60% SA-40% L100M batch. We are unable to conclusively determine whether foam or spray granulation is more robust in achieving uniform drug distribution. Perhaps the processing conditions, including liquid binder amount, impeller speed and wet massing, and the wettability properties of the formulation are the dominant factors in this case in which the binder addition method has little influence. These parameters could have more of an influence than liquid binder addition method, causing both foam and spray granulation to show strong performances in delivering homogeneous granules.

7.5 Conclusions

This chapter investigated foam granulation of heterogeneous-wetting formulations, and comparison was made with spray granulation. Single nucleus formation via single foam/drop

penetration, power consumption during granulation, granule size distribution and drug distribution in the granules were analysed and compared.

Investigations into single nucleus formation found that the nucleus size decreases as the concentration of hydrophobic component increases in the formulation. For glass ballotini powder mixtures, foam binder addition appears to create nuclei with a more uniform size and structure. For salicylic acid and lactose powder mixtures, the nuclei size and structure were less uniform in formulations enriched with salicylic acid for both foam and spray binder addition methods. It was also shown that foam penetration is relatively insensitive to the properties (physical and/or interfacial) of the powder bed compared to spray penetration.

The power consumption profiles obtained during granulation also suggest that foam and spray granulation involve different wetting and nucleation mechanisms – spray tends to incur early liquid penetration whereas liquid penetration is relatively insignificant during foam granulation. The peak estimation method (peak of the power derivative) can be useful to provide a sensible guide to the critical liquid binder requirement for different granulation batches.

For the cases where salicylic acid and lactose primary particles are similar in size, the drug distribution is fairly uniform across all the size fractions in the granulation batches regardless of the binder addition method. In this case, a combination effect of primary particle size, liquid binder amount, granulation extent and the wettability properties of the formulation appears to be the dominant parameters that affect the drug distribution during granulation. When salicylic acid was granulated with 100 mesh lactose, the drug distribution results deviated due to the effect of primary particle size difference. The ability of foam granulation to achieve uniform drug distribution was enhanced in the 80% SA-20% L100M batch and the 40% SA-60% L100M batch, but was relatively poor in the 60% SA-40% L100M batch.

CHAPTER 8
CONCLUSIONS

8 CONCLUSIONS

8.1 A Summary of Major Findings

This PhD thesis is the first thesis to report an independent research investigation on foam granulation. The investigation begins with a literature review on the scientific understanding of foam as well as its application in various industrial processes, the developments in wet granulation, and the understanding gap between both the foam and wet granulation disciplines (*Chapter 2 Literature Review*). Experimental studies were divided into a few different scales, starting with small scale experiments investigating single nucleus formation by foam/drop penetration on static powder beds (*Chapter 3 Single Nucleus Formation*), followed by the study of nuclei formation on moving powder beds while limiting the granulation to the nucleation state only (*Chapter 4 Binder Dispersion and Nucleation*), and full scale foam granulation experiments where nucleation, growth and breakage are all occurring (*Chapter 5 Foam Granulation*). The studies ended with two case studies investigating the uniformity of moisture distribution (*Chapter 6 A Case Study of Liquid Distribution*) and drug distribution (*Chapter 7 A Case Study of Drug Distribution*) in granules.

8.1.1 Single nucleus formation

In *Chapter 3*, we have established a good understanding of the interactions between a layer of foam and a bed of powder, how the foamed binder is distributed/penetrated through the powder, and the effect on the size and morphology of the nuclei formed. We have also characterised the essential material properties for good wetting and nucleation on static powder beds. The major findings include:

- Foam specific penetration time increases with increasing foam mass, increasing foam concentration, and decreasing powder size.
- Nuclei size increases with increasing foam mass, decreasing foam concentration, and increasing powder size.
- Comparisons between foam and drop nucleation ratios have indicated that the nucleation of powder via foams provides better liquid usage and improved liquid distribution efficiency compared to the nucleation via drops on lactose powder.
- Visual observations of foam displaced on the powder bed have suggested that bubble movement and liquid drainage are critical to the foam penetration process, which is the rate limiting step in foam penetration.

- A transformation map illustrating the effect of liquid binder and powder properties on the penetration time and nucleation ratio has been proposed, which provides a guideline to the materials selection for foam granulation process.

8.1.2 Binder Dispersion and Nucleation

In *Chapter 4*, we have identified the essential conditions for good wetting and nucleation conditions during “nucleation-only” granulation. Initial developments on the mechanisms controlling foam induced wetting and nucleation have also been proposed, which acts as a foundation for the next stage of study. The major findings include:

- A narrower nuclei size distribution can be obtained by adding the liquid binder as a foam.
- Nucleation by the foam addition method was found to be influenced by the interacting effects of foam quality and the powder flow condition (bumping or roping).
- Two wetting and nucleation mechanisms for foam granulation have been proposed: “foam drainage” and “mechanical dispersion”. For “foam drainage” controlled mechanism, binder dispersion and nucleation are driven by liquid penetration (due to foam drainage), where the controlling property is foam quality. For “mechanical dispersion” controlled mechanism, powder mixing dominates the foam quality effect in the formation of nuclei.

8.1.3 Foam Granulation

In *Chapter 5*, we have characterised both the material and process properties for good wetting and nucleation conditions during full scale granulation, and have verified the proposition of the mechanisms controlling foam wetting and nucleation. The major findings include:

- Increasing the liquid to solid ratio, decreasing the foam quality, granulating at powder bumping flow conditions, increasing the primary particle size and/or decreasing the binder concentration have an equivalent effect in increasing the average granule size and the spread of the granule size distribution.
- “Foam drainage” controlled and “mechanical dispersion” controlled wetting and nucleation mechanisms pose strong effects on the initial nuclei size distribution, and the effects are retained through to the final granule size distribution.

- Transformation maps have been proposed to illustrate the changes in granule size (distribution) as a function of the relative interaction of process/material parameters on the basis of “foam drainage” and “mechanical dispersion” controlled wetting and nucleation mechanisms.

8.1.4 A Case Study of Liquid Distribution

In *Chapter 6*, we identified the differences in the wetting and nucleation mechanisms controlling foam and spray granulation, and the major contribution to the uniformity of moisture distribution in granules. The major findings include:

- For spray granulation operated outside of the drop-controlled regime, the spray droplets tend to involve early uneven liquid penetration nucleation. Decreasing the foam quality during foam granulation has a similar effect.
- For both foam and spray granulation, mechanical mixing is successfully used to redisperse the coarse granules and redistribute the moisture, creating homogeneous granules, although the granulation initially falls outside of the ideal drop-controlled nucleation regime.
- A regime map is presented by plotting impeller speed, foam quality and liquid to solid ratio to illustrate the granulation behaviour for the systems investigated.

8.1.5 A Case Study of Drug Distribution

In *Chapter 7*, we have identified the differences in the wetting and nucleation mechanisms controlling foam and spray granulation, and the major contributions to the uniformity of drug distribution in granules. The major findings include:

- Nucleus size decreases as the concentration of hydrophobic component increases in the formulation.
- Foam penetration is relatively insensitive to the properties (physical and/or interfacial) of the powder bed compared to drop penetration.
- The power consumption profiles obtained during granulation appears to be useful for monitoring foam and spray granulation processes. The peak estimation method (peak of the power derivative) can be used to provide a sensible guide to the critical liquid binder requirement for different granulation batches.

- The drug distribution in granules showed deviation when salicylic acid was granulated with coarser lactose powder. In the cases where salicylic acid and lactose primary particles are similar in size, the drug distribution is fairly uniform across all of the size fractions in the granulation batches regardless of the binder addition method, due to a combination effect of primary particle size, liquid binder amount, granulation extent and the wettability properties of the formulation.
- Both foam and spray granulation showed strong performances in achieving uniform drug distribution in granules.

8.2 Recommendations for Future Research

There are some potential future research that would further improve the understanding on foam nucleation and granulation. The recommendations from this thesis include:

- Further experiments with other formulations in several different granulators to validate the transformation and regime maps
- Further experiments on moisture distribution at various liquid levels, especially at low liquid content
- A micro-scale study on the subject of foam flow in powder bed to understand the interaction between the foam and the powder particle in the granulator
- Fundamental study on the structure and the rheology behaviour of foam
- Develop a model for foam penetration time
- Studies on scale-up

8.3 Concluding Comments

The subjects of wet granulation and foam have attracted significant scientific interest in the academic sector as well as in various industrial sectors for more than a decade. The use of foam in wet granulation process has emerged in the last 5 years as a potential development that brings with it many advantages. Among a list of wet granulation methods, foam granulation appears to be the latest development, and remains a developing area.

This thesis studies foam nucleation and granulation in between the meso and macro scales, by establishing the general regularities, qualifying the behaviour at the meso scales in terms of

rates processes, and producing a description of the macro behaviour. We quantify the drainage properties of foam and relate them to the nuclei size (distribution), which also linked with the liquid to solid ratio, impeller speed, and powder and liquid binder properties to describe the granulation behaviour and predict the final granule size (distribution). Although we have yet to fully describe the growth and breakage mechanisms, we now know the key formulation properties and process parameters that control foam nucleation and granulation. The interacting effects of these material and process properties are given in the proposed transformation and regime maps, which should prove to be useful in identifying the dominant mechanism controlling the nucleation and granulation processes and in rationalising the nuclei granule size distribution via characterisation of the key material and process properties.

REFERENCES

Altmann, M., (2008). *Dow foam granulation technology™ for innovative tablet manufacture used in second drug candidate at bristol-myers squibb.* viewed <http://www.dow.com/dowwolff/en/news/2008/20081120a.htm>

Arzhavitina, A., Steckel, H., (2010). *Foams for pharmaceutical and cosmetic application.* International Journal of Pharmaceutics. In Press, Uncorrected Proof.

Aulton, M.E., Banks, M., (1979). *Influence of the hydrophobicity of the powder mix on fluidised bed granulation.* International conference on powder technology in pharmacy Powder Advisory Centre, Basel, Switzerland.

Aussillous, P., Quere, D., (2001). *Liquid marbles.* Nature 411: 924-927.

Ax, K., Feise, H., Sochon, R., Hounslow, M., Salman, A., (2008). *Influence of liquid binder dispersion on agglomeration in an intensive mixer.* Powder Technology 179: 190-194.

Bardin, M., Knight, P.C., Seville, J.P.K., (2004). *On control of particle size distribution in granulation using high-shear mixers.* Powder Technology 140: 169-175.

Barigou, M., Davidson, J.F., (1994). *Soap film drainage: Theory of experiment.* Chemical Engineering Science 49: 1807-1819.

Barigou, M., Deshpande, N.S., Wiggers, F.N., (2001). *An enhanced electrical resistance technique for foam drainage measurement.* Colloids and Surfaces A: Physicochemical and Engineering Aspects 189: 237-246.

Belohlav, Z., Brenkov, L., Hanika, J., Durdil, P., Rapek, P., Tomasek, V., (2007). *Effect of drug active substance particles on wet granulation process.* Chemical Engineering Research and Design 85: 974-980.

Bergeron, V., Walstra, P., Lyklema, J., (2005). *Chapter 7 foams.* In: Lyklema, J. (Eds.), Fundamentals of interface and colloid science, Academic Press, 1-38.

Betz, G., Bürgin, P.J., Leuenberger, H., (2003). *Power consumption profile analysis and tensile strength measurements during moist agglomeration.* International Journal of Pharmaceutics 252: 11-25.

Betz, G., Bürgin, P.J., Leuenberger, H., (2004). *Power consumption measurement and temperature recording during granulation.* International Journal of Pharmaceutics 272: 137-149.

Bhakta, A., Ruckenstein, E., (1997). *Decay of standing foams: Drainage, coalescence and collapse.* Advances in Colloid and Interface Science 70: 1-124.

Bier, H.P., Leuenberger, H., Sucker, H., (1979). *Determination of the uncritical quantity of granulating liquid by power measurements on planetary mixers.* Pharm. Ind. 41: 375-380.

Bindal, S.K., Sethumadhavan, G., Nikolov, A.D., Wasan, D.T., (2002). *Foaming mechanisms in surfactant free particle suspensions*. *AIChE Journal* 48: 2307-2314.

Binks, B.P., (2002). *Particles as surfactants--similarities and differences*. *Current Opinion in Colloid & Interface Science* 7: 21-41.

Bouwman, A.M., Visser, M.R., Meesters, G.M.H., Frijlink, H.W., (2006). *The use of stokes deformation number as a predictive tool for material exchange behaviour of granules in the 'equilibrium phase' in high shear granulation*. *International Journal of Pharmaceutics* 318: 78-85.

Boys, C.V., (1959). *Soap bubbles*. Dover Publications, Inc, New York, USA.

Brenner, J.W., Richmond, V., Engle, J.P., Okla, T., *Foam cleaning of surfaces*. United States Patent Office, Patent no.: 3,037,887, filed on 5 June 1962.

Bryant, G.M., (1979). *Chapter 12 energy and related savings from controlled low wet pick-up application of textile chemicals and dyes via semistable foams*. In: Tyrone, L.V. and Louis, J.N. (Eds.), *Energy conservation in textile and polymer processing*, American Chemical Society, 145-154.

Butensky, M., Hyman, D., (1971). *Rotary drum granulation. An experimental study of the factors affecting granule size*. *Industrial & Engineering Chemistry Fundamentals* 10: 212-219.

Calvert, J.R., Nezhati, K., (1987). *Bubble size effects in foams*. *International Journal of Heat and Fluid Flow* 8: 102-106.

Cantor, S.L., Kothari, S., Koo, O.M.Y., (2009). *Evaluation of the physical and mechanical properties of high drug load formulations: Wet granulation vs. Novel foam granulation*. *Powder Technology* 195: 15-24.

Carrier, V., Destouesse, S., Colin, A., (2002). *Foam drainage: A film contribution?* *Physical Review E* 65: 061404.

Chang, D., Chang, R.-K., (2007). *Review of current issues in pharmaceutical excipients (excipients)*. *Pharmaceutical Technology* 31: 56-66.

Chang, K.-S., Lemlich, R., (1980). *A study of the electrical conductivity of foam*. *Journal of Colloid and Interface Science* 73: 224-232.

Churaev, N.V., (2005). *Aqueous wetting films in contact with a solid phase*. *Advances in Colloid and Interface Science* 114-115: 3-7.

Cole, H.W., Taylo, S.E., *Method for controlling dust in grain*. United States Patent Office, Patent no.: 5,069,72, filed on 3 December 1991.

Crooks, M.J., Schade, H.W., (1978). *Fluidized bed granulation of a microdose pharmaceutical powder*. *Powder Technology* 19: 103-108.

-
- Datye, A.K., Lemlich, R., (1983). *Liquid distribution and electrical conductivity in foam*. International Journal of Multiphase Flow 9: 627-636.
- Denesuk, M., Smith, G. L., Zelinski, B. J. J., Kreidl, N. J., Uhlmann, D. R., (1993). *Capillary penetration of liquid droplets into porous materials*. Journal of Colloid and Interface Science 158: 114-120.
- Dholkawala, Z.F., Sarma, H.K., Kam, S.I., (2007). *Application of fractional flow theory to foams in porous media*. Journal of Petroleum Science and Engineering 57: 152-165.
- Ding, J., Tsaur, F.W., Lips, A., Akay, A., (2007). *Acoustical observation of bubble oscillations induced by bubble popping*. Physical Review E 75: 041601.
- Drenckhan, W., Hutzler, S., Weaire, D., (2005). *Foam physics: The simplest example of soft condensed matter*. 748: 22-28.
- Durand, M., Langevin, D., (2002). *Physicochemical approach to the theory of foam drainage*. The European Physical Journal E: Soft Matter and Biological Physics 7: 35-44.
- Eliassen, H., Kristensen, H.G., Schæfer, T., (1999). *Growth mechanisms in melt agglomeration with a low viscosity binder*. International Journal of Pharmaceutics 186: 149-159.
- Eliassen, H., Schæfer, T., Gjelstrup Kristensen, H., (1998). *Effects of binder rheology on melt agglomeration in a high shear mixer*. International Journal of Pharmaceutics 176: 73-83.
- Engels, T., von Rybinski, W., Schmiedel, P., (1998). *Structure and dynamics of surfactant-based foams*. In: Kremer, F. and Lagaly, G. (Eds.), Structure, dynamics and properties of disperse colloidal systems, 117-126.
- Ennis, B.J., (1996). *Agglomeration and size enlargement session summary paper*. Powder Technology 88: 203-225.
- Ennis, B.J., Litster, J.D., (1997). *Chapter 20 size reduction and size enlargement*. In: Perry, R.H. and Green, D.W. (Eds.), Perry's chemical engineers' handbook (7th edition), McGraw-Hill, 61-73.
- Ennis, B.J., Tardos, G., Pfeffer, R., (1991). *A microlevel-based characterization of granulation phenomena*. Powder Technology 65: 257-272.
- Fains, A., Bertrand, D., Baniel, A., Popineau, Y., (1997). *Stability and texture of protein foams: A study by video image analysis*. Food Hydrocolloids 11: 63-69.
- Gandolfo, F.G., Rosano, H.L., (1997). *Interbubble gas diffusion and the stability of foams*. Journal of Colloid and Interface Science 194: 31-36.
- Gardiner, B.S., Dlugogorski, B. Z., Jameson, G. J., (1998). *Rheology of fire-fighting foams*. Fire Safety Journal 31: 61-75.

-
- Garrett, P.R., (1979). *The effect of polytetrafluoroethylene particles on the foamability of aqueous surfactant solutions*. Journal of Colloid and Interface Science 69: 107-121.
- Gauglitz, P.A., Friedmann, F., Kam, S.I., Rossen, W.R., (2002). *Foam generation in homogeneous porous media*. Chemical Engineering Science 57: 4037-4052.
- Goldszal, A., Bousquet, J., (2001). *Wet agglomeration of powders: From physics toward process optimization*. Powder Technology 117: 221-231.
- Gottlieb, A., Ford, R.O., Spellman, M., (2003). *The efficacy and tolerability of clobetasol propionate foam 0.05% in the treatment of mild to moderate plaque-type psoriasis of nonscalp regions*. Journal of Cutaneous Medicine and Surgery: Incorporating Medical and Surgical Dermatology 7: 185-192.
- Hapgood, K.P., Hartman, H.E., Kaur, C., Plank, R., (2002a). *A case study of drug distribution in wet granulation*. World Congress of Particle Technology 4. Sydney, Australia.
- Hapgood, K.P., Khanmohammadi, B., (2009). *Granulation of hydrophobic powders*. Powder Technology 189: 253-262.
- Hapgood, K.P., Litster, J.D., Biggs, S.R., Howes, T., (2002b). *Drop penetration into porous powder beds*. Journal of Colloid and Interface Science 253: 353-366.
- Hapgood, K.P., Litster, J.D., Smith, R., (2003). *Nucleation regime map for liquid bound granules*. AIChE Journal 49: 350-361.
- Hapgood, K.P., Litster, J.D., White, E.T., Mort, P.R., Jones, D.G., (2004). *Dimensionless spray flux in wet granulation: Monte-carlo simulations and experimental validation*. Powder Technology 141: 20-30.
- Hapgood, K.P., Iveson, S.M., Litster, J.D., Liu, L.X., (2007). *Chapter 20 granulation rate processes*. In: Salman, A.D., Hounslow, M.J. and Seville, J.P.K. (Eds.), Handbook of powder technology, Elsevier Science B.V., 897-977.
- Hilgenfeldt, S., Koehler, S.A., Stone, H.A., (2001). *Dynamics of coarsening foams: Accelerated and self-limiting drainage*. Physical Review Letters 86: 4704.
- Holm, P., Schaefer, T., Kristensen, H.G., (1985a). *Granulation in high-speed mixers part v. Power consumption and temperature changes during granulation*. Powder Technology 43: 213-223.
- Holm, P., Schaefer, T., Kristensen, H.G., (1985b). *Granulation in high-speed mixers part vi. Effects of process conditions on power consumption and granule growth*. Powder Technology 43: 225-233.
- Holm, P., Schaefer, T., Larsen, C., (2001). *End-point detection in a wet granulation process*. Pharmaceutical Development and Technology 6: 181 - 192.

-
- Hoornaert, F., Wauters, P.A.L., Meesters, G.M.H., Pratsinis, S.E., Scarlett, B., (1998). *Agglomeration behaviour of powders in a lödige mixer granulator*. Powder Technology 96: 116-128.
- Horisawa, E., Komura, A., Danjo, K., Otsuka, A., (1995). *Effect of binder characteristics on the strength of agglomerates prepared by the wet method ii*. Chem. Pharm. Bull. 43: 488-492.
- Huang, X., Tanojo, H., Lenn, J., Deng, C.H., Krochmal, L., (2005). *A novel foam vehicle for delivery of topical corticosteroids*. Journal of the American Academy of Dermatology 53: S26-S38.
- Hudales, J.B.M., Stein, H.N., (1990). *The influence of solid particles on foam and film drainage*. Journal of Colloid and Interface Science 140: 307-313.
- Hunter, T.N., Pugh, R. J., Franks, G. V., Jameson, G. J., (2008). *The role of particles in stabilising foams and emulsions*. Advances in Colloid and Interface Science 137: 57-81.
- Iveson, S.M., Litster, J.D., (1998a). *Fundamental studies of granule consolidation part 2: Quantifying the effects of particle and binder properties*. Powder Technology 99: 243-250.
- Iveson, S.M., Litster, J.D., (1998b). *Growth regime map for liquid-bound granules*. AIChE journal 44: 1510-1518.
- Iveson, S.M., Litster, J.D., Ennis, B.J., (1996). *Fundamental studies of granule consolidation part 1: Effects of binder content and binder viscosity*. Powder Technology 88: 15-20.
- Iveson, S.M., Litster, J.D., Hapgood, K.P., Ennis, B.J., (2001a). *Nucleation, growth and breakage phenomena in agitated wet granulation processes: A review*. Powder Technology 117: 3-39.
- Iveson, S.M., Wauters, P.A.L., Forrest, S., Litster, J.D., Meesters, G.M.H., Scarlett, B., (2001b). *Growth regime map for liquid-bound granules: Further development and experimental validation*. Powder Technology 117: 83-97.
- Jaiyeoba, K.T., Spring, M.S., (1980). *The granulation of ternary mixtures: The effect of the solubility of the excipients*. Journal of Pharmacy and Pharmacology 32: 1-5.
- Johansen, A., Schaefer, T., (2001). *Effects of interactions between powder particle size and binder viscosity on agglomerate growth mechanisms in a high shear mixer*. European Journal of Pharmaceutical Sciences 12: 297-309.
- Kaptay, G., (2003). *Interfacial criteria for stabilization of liquid foams by solid particles*. Colloids and Surfaces A: Physicochemical and Engineering Aspects 230: 67-80.
- Kapur, P.C., (1978). *Balling and granulation*. In: (Eds.), Advances in chemical engineering, Academic Press, 55-123.
- Kealy, T., Abram, A., Hunt, B., Buchta, R., (2008). *The rheological properties of pharmaceutical foam: Implications for use*. International Journal of Pharmaceutics 355: 67-80.

-
- Keary, C., Sheskey, P., (2004). *Preliminary report of the discovery of a new pharmaceutical granulation process using foamed aqueous binders*. Drug Development & Industrial Pharmacy 30: 831-845.
- Keningley, S.T., Knight, P.C., Marson, A.D., (1997). *An investigation into the effects of binder viscosity on agglomeration behaviour*. Powder Technology 91: 95-103.
- Knight, P.C., (1993). *An investigation of the kinetics of granulation using a high shear mixer*. Powder Technology 77: 159-169.
- Knight, P.C., Instone, T., Pearson, J.M.K., Hounslow, M.J., (1998). *An investigation into the kinetics of liquid distribution and growth in high shear mixer agglomeration*. Powder Technology 97: 246-257.
- Knight, P.C., Johansen, A., Kristensen, H.G., Schæfer, T., Seville, J.P.K., (2000). *An investigation of the effects on agglomeration of changing the speed of a mechanical mixer*. Powder Technology 110: 204-209.
- Kobubo, H., Sunada, H., (1996). *Effect of process variables on the properties and binder distribution of granules prepared by a high shear mixer*. Chem. Pharm. Bull. 44: 1546-1549.
- Koehler, S.A., Hilgenfeldt, S., Stone, H.A., (2000). *A generalized view of foam drainage: Experiment and theory*. Langmuir 16: 6327-6341.
- Koehler, S.A., Hilgenfeldt, S., Weeks, E.R., Stone, H.A., (2002). *Drainage of single plateau borders: Direct observation of rigid and mobile interfaces*. Physical Review E - Statistical, Nonlinear, and Soft Matter Physics 66: 040601/1-040601/4.
- Koehler, S.A., Hilgenfeldt, S., Weeks, E.R., Stone, H.A., (2004). *Foam drainage on the microscale ii. Imaging flow through single plateau borders*. Journal of Colloid and Interface Science 276: 439-449.
- Kristensen, H.G., Schaefer, T., (1987). *Granulation: A review on pharmaceutical wet-granulation*. Drug Development & Industrial Pharmacy 13: 803-872.
- Laicher, A., Profitlich, T., Schwitzer, K., Ahlert, D., (1997). *A modified signal analysis system for end-point control during granulation*. European Journal of Pharmaceutical Sciences 5: 7-14.
- Lerk, C.F., Schoonen, A.J.M., Fell, J.T., (1976). *Contact angles and wetting of pharmaceutical powders*. Journal of Pharmaceutical Sciences 65: 843-847.
- Leuenberger, H., (1982). *Granulation, new techniques*. Pharmaceutica acta Helvetiae 57: 72-82.
- Leuenberger, H., (2001). *New trends in the production of pharmaceutical granules: The classical batch concept and the problem of scale-up*. European Journal of Pharmaceutics and Biopharmaceutics 52: 279-288.

Leuenberger, H., Puchkov, M., Krausbauer, E., Betz, G., (2009). *Manufacturing pharmaceutical granules: Is the granulation end-point a myth?* Powder Technology 189: 141-148.

Levin, M., (2006). *Wet granulation: End-point determination and scale-up*. Encyclopedia of Pharmaceutical Technology: Third Edition 4078 - 4098.

Litster, J., Ennis, B., (2004). *The science and engineering of granulation processes*. Kluwer Academic Publishers, Dordrecht, The Netherlands.

Litster, J.D., (2003). *Scaleup of wet granulation processes: Science not art*. Powder Technology 130: 35-40.

Litster, J.D., Hapgood, K.P., Michaels, J.N., Sims, A., Roberts, M., Kameneni, S.K., (2002). *Scale-up of mixer granulators for effective liquid distribution*. Powder Technology 124: 272-280.

Litster, J.D., Hapgood, K.P., Michaels, J.N., Sims, A., Roberts, M., Kameneni, S.K., Hsu, T., (2001). *Liquid distribution in wet granulation: Dimensionless spray flux*. Powder Technology 114: 32-39.

Liu, L., Levin, M., Sheskey, P., Yihong, Q., Yisheng, C., Geoff, G.Z.Z., Lirong, L., William, R.P., (2009). *Process development and scale-up of wet granulation by the high shear process*. In: (Eds.), Developing solid oral dosage forms, Academic Press, 667-699.

Liu, L.X., Litster, J.D., Iveson, S.M., Ennis, B.J., (2000). *Coalescence of deformable granules in wet granulation processes*. AIChE Journal 46: 529-539.

Louvet, N., Rouyer, F., Pitois, O., (2009). *Ripening of a draining foam bubble*. Journal of Colloid and Interface Science 334: 82-86.

Müller, W., Meglio, J.-M.d., (1999). *Avalanches in draining foams*. Journal of Physics: Condensed Matter 11: L209.

Mackaplow, M.B., Rosen, L.A., Michaels, J.N., (2000). *Effect of primary particle size on granule growth and endpoint determination in high-shear wet granulation*. Powder Technology 108: 32-45.

Magrabi, S.A., Dlugogorski, B.Z., Jameson, G.J., (2000). *Performance of aged aqueous foams for mitigation of thermal radiation*. Developments in Chemical Engineering and Mineral Processing 8: 93-112.

Magrabi, S.A., Dlugogorski, B. Z., Jameson, G. J., (2002). *A comparative study of drainage characteristics in afff and ffff compressed-air fire-fighting foams*. Fire Safety Journal 37: 21-52.

Malysa, K., (1992). *Wet foams: Formation, properties and mechanism of stability*. Advances in Colloid and Interface Science 40: 37-83.

Maurdev, G., Saint-Jalmes, A., Langevin, D., (2006). *Bubble motion measurements during foam drainage and coarsening*. Journal of Colloid and Interface Science 300: 735-743.

Mengual, O., Meunier, G., Cayre, I., Puech, K., Snabre, P., (1999). *Turbiscan ma 2000: Multiple light scattering measurement for concentrated emulsion and suspension instability analysis*. Talanta 50: 445-456.

Miao, S., Janssen, J., Domburg, B., Pauvert, F., (2009). *Study of foam-assisted granulation in food model systems*. 9th International Symposium on Agglomeration. Sheffield, United Kingdom.

Middleman, S., (1995). *Capillary penetration dynamics*. In: (Eds.), Modeling axisymmetric flows, Academic Press, 211-240.

Mills, P.J.T., Seville, J.P.K., Knight, P.C., Adams, M.J., (2000). *The effect of binder viscosity on particle agglomeration in a low shear mixer/agglomerator*. Powder Technology 113: 140-147.

Miyamoto, Y., Ryu, A., Sugawara, S., Miyajima, M., Ogawa, S., Matsui, M., Takayama, K., Nagai, T., (1998). *Simultaneous optimization of wet granulation process involving factor of drug content dependency on granule size*. Drug Development and Industrial Pharmacy 24: 1055-1065.

Mody, V., Jakhete, R., (1988). *Dust control handbook*. William Andrew Publishing/Noyes, New Jersey, USA.

Mort, P., A.D. Salman, M. J. Hounslow, Seville, J.P.K., (2007). Chapter 19 *Scale-up of high-shear binder-agglomeration processes*. In: (Eds.), Handbook of powder technology, Elsevier Science B.V., 853-896.

Mort, P.R., Tardos, G., (1999). *Scale-up of agglomeration processes using transformations*. Kona 17: 64-75.

Newitt, D.M., Conway-Jones, J.M., (1958). *A contribution to the theory and practice of granulation*. Trans. I. Chem. Eng 36: 422-441.

Nguyen, T., Shen, W., Hapgood, K., (2009). *Drop penetration time in heterogeneous powder beds*. Chemical Engineering Science 64: 5210-5221.

Nguyen, T.H., Shen, W., Hapgood, K., (2010). *Effect of formulation hydrophobicity on drug distribution in wet granulation*. Chemical Engineering Journal. In Press, Corrected Proof.

Ojile, J.E., Macfarlane, C.B., Selkirk, A.B., (1982). *Drug distribution during massing and its effect on dose uniformity in granules*. International Journal of Pharmaceutics 10: 99-107.

Perkowitz, S., (2000). *Universal foam: From cappuccino to the cosmos*. Walker & Company, New York, USA.

-
- Perri, J., Conway, C., (1956). *Foam as a fire exposure protection medium - evaluating effectiveness of wetting and protein agents*. *Industrial & Engineering Chemistry* 48: 2021-2023.
- Phelan, R., Weairey, D., Petersz, E.A.J.F., Verbist, G., (1996). *The conductivity of a foam*. *Journal of Physics: Condensed Matter* 8: L475.
- Plank, R., Diehl, B., Grinstead, H., Zega, J., (2003). *Quantifying liquid coverage and powder flux in high-shear granulators*. *Powder Technology* 134: 223-234.
- Prud'homme, R.K., Khan, S.A., (1996). *Foams: Theory, measurements, and applications*. Marcel Dekker Inc., New York, USA.
- Pugh, R.J., (1996). *Foaming, foam films, antifoaming and defoaming*. *Advances in Colloid and Interface Science* 64: 67-142.
- Pugh, R.J., (2005). *Experimental techniques for studying the structure of foams and froths*. *Advances in Colloid and Interface Science* 114-115: 239-251.
- Purdon, C.H., Haigh, J.M., Surber, C., Smith, E.W., (2003). *Foam drug delivery in dermatology: Beyond the scalp*. *American Journal of Drug Delivery* 1: pp. 71-75.
- Ralph, A.L., Robert, L., (1965). *A study of interstitial liquid flow in foam. Part i. Theoretical model and application to foam fractionation*. 11: 18-25.
- Ralston, J., (1983). *Thin films and froth flotation*. *Advances in Colloid and Interface Science* 19: 1-26.
- Ramaker, J.S., Jelgersma, M.A., Vonk, P., Kossen, N.W.F., (1998). *Scale-down of a high-shear pelletisation process: Flow profile and growth kinetics*. *International Journal of Pharmaceutics* 166: 89-97.
- Ren, X., (2000). *Development of environmental performance indicators for textile process and product*. *Journal of Cleaner Production* 8: 473-481.
- Reynolds, G.K., Biggs, C.A., Salman, A.D., Hounslow, M.J., (2004). *Non-uniformity of binder distribution in high-shear granulation*. *Powder Technology* 140: 203-208.
- Reynolds, G.K., Fu, J.S., Cheong, Y.S., Hounslow, M.J., Salman, A.D., (2005). *Breakage in granulation: A review*. *Chemical Engineering Science* 60: 3969-3992.
- Rios, M., (2008). *Foam granulation technology update and future applications*. viewed <http://pharmtech.findpharma.com/pharmtech/Article/Foam-Granulation-Technology-Update-and-Future-App/ArticleStandard/Article/detail/514845>
- Robert, D.L., (1982). *Low wet pick-up processing for the 80s*. *Journal of the Society of Dyers and Colourists* 98: 422-429.
- Roe, D.C., Chen, J.C., *Methods for suppressing dust emissions*. United States Patent Office, Patent no.: 5,648,116, filed on 15 July 1997.

Rossetti, D., Simons, Stefaan J.R., Pagliai, P., Ward, R., Fitzpatrick, S., (2004). *Predicting the performance of granulation binders through micro-mechanistic observations*. Particle & Particle Systems Characterization 21: 284-292.

Rough, S.L., Wilson, D.I., Bayly, A.E., York, D.W., (2005a). *Mechanisms in high-viscosity immersion-granulation*. Chemical Engineering Science 60: 3777-3793.

Rough, S.L., Wilson, D.I., York, D.W., (2005b). *A regime map for stages in high shear mixer agglomeration using ultra-high viscosity binders*. Advanced Powder Technology 16: 373-386.

Saha, S., Bhaumik, S., Roy, A., (2009). *Coupling between drainage and coarsening in wet foam*. Pramana 72: 1037-1044.

Saint-Jalmes, A., (2006). *Physical chemistry in foam drainage and coarsening*. Soft Matter 2: 836-849.

Saint-Jalmes, A., Langevin, D., (2002). *Time evolution of aqueous foams: Drainage and coarsening*. Journal of Physics: Condensed Matter 14: 9397.

Saleh, K., Vialatte, L., Guigon, P., (2005). *Wet granulation in a batch high shear mixer*. Chemical Engineering Science 60: 3763-3775.

Salman, A.D., Hounslow, M.J., Seville, J.P.K., (2007a). *Granulation handbook*. Elsevier Science B.V., UK.

Salman, A.D., Reynolds, G.K., Tan, H.S., Gabbott, I., Hounslow, M.J., (2007b). *Chapter 21 breakage in granulation*. In: Salman, A.D., Hounslow, M.J. and Seville, J.P.K. (Eds.), Handbook of powder technology, Elsevier Science B.V., 979-1040.

Schaafsma, S.H., Vonk, P., Kossen, N.W.F., (2000). *Fluid bed agglomeration with a narrow droplet size distribution*. International Journal of Pharmaceutics 193: 175-187.

Schaafsma, S.H., Vonk, P., Segers, P., Kossen, N. W. F., (1998). *Description of agglomerate growth*. Powder Technology 97: 183-190.

Schaefer, T., (1992). *Melt pelletization in a high shear mixer. I. Effects of process variables and binder*. Acta pharmaceutica Nordica 4: 133-140.

Schaefer, T., Johnsen, D., Johansen, A., (2004). *Effects of powder particle size and binder viscosity on intergranular and intragranular particle size heterogeneity during high shear granulation*. European Journal of Pharmaceutical Sciences 21: 525-531.

Schaefer, T., Mathiesen, C., (1996). *Melt pelletization in a high shear mixer. Viii. Effects of binder viscosity*. International Journal of Pharmaceutics 139: 125-138.

Schramm, L.L., (1994a). *Foams: Fundamentals and applications in the petroleum industry*. American Chemical Society, Washington, DC.

-
- Schramm, L.L., (1994b). *Foams: Fundamentals and applications in the petroleum industry*. American Chemical Society, Washington D.C., USA.
- Schramm, L.L., (2006). *Introduction to practical and industrial applications*. In: Schramm, L.L. (Eds.), *Emulsions, foams, and suspensions*, 223-230.
- Schramm, L.L., Novosad, J.J., (1990). *Micro-visualization of foam interactions with a crude oil*. *Colloids and Surfaces* 46: 21-43.
- Schramm, L.L., Novosad, J.J., (1992). *The destabilization of foams for improved oil recovery by crude oils: Effect of the nature of the oil*. *Journal of Petroleum Science and Engineering* 7: 77-90.
- Scott, A.C., Hounslow, M.J., Instone, T., (2000). *Direct evidence of heterogeneity during high-shear granulation*. *Powder Technology* 113: 205-213.
- Sheskey, P., Garcia-Todd, P., Holbrook, D.L., Balwinski, K., Kenny, R., (2009). *Foam coating: Initial investigation of a novel tablet coating technology*. 2009 AAPS Annual Meeting. Los Angeles, California, USA.
- Sheskey, P., Keary, C., Clark, D., (2006). *Foam granulation technology: Scale-up of immediate release and controlled release formulations from laboratory scale to manufacturing scale*. 2006 AAPS Annual Meeting. San Antonio, Texas, USA.
- Sheskey, P., Keary, C., Clark, D., Balwinski, K., (2007). *Scale-up trials of foam-granulation technology--high shear*. *Pharmaceutical Technology* 31: 94-108.
- Sheskey, P., Keary, C., Inbasekaran, P., Deyarmond, V., Balwinski, K., (2003). *Foam technology: The development of a novel technique for the delivery of aqueous binder systems in high-shear and fluid-bed wet-granulation applications*. 2003 AAPS Annual Meeting. Salt Lake City, Utah, USA.
- Sheskey, P., Keary, C., Inbasekaran, P., Shrestha, U., Balwinski, K., (2004a). *Foamed aqueous binders as carriers of low-dose drugs*. 31st Annual Meeting of the Controlled Release Society. Honolulu, Hawaii.
- Sheskey, P., Keary, C., Shrestha, U., Becker, J., (2004b). *Use of a novel foam granulation technique to incorporate low drug loading into intermediate release tablet formulations*. 2004 AAPS Annual Meeting. Baltimore, Maryland, USA.
- Simmons, B.G., Tulsa Okla, E., *Method for recycling foamed solvents*. United States Patent Office, Patent no.: 4,849,027, filed on 18 July 1989.
- Smirani-Khayati, N., Falk, V., Bardin-Monnier, N., Marchal-Heussler, L., (2009). *Binder liquid distribution during granulation process and its relationship to granule size distribution*. *Powder Technology* 195: 105-112.
- Smith, P.G., Nienow, A.W., (1983). *Particle growth mechanisms in fluidised bed granulation--i: The effect of process variables*. *Chemical Engineering Science* 38: 1223-1231.

Snow, R.H., Allen, T., Ennis, B.J., Litster, J.D., (1997). *Chapter 20 size reduction and size enlargement*. In: Perry, R.H. and Green, D.W. (Eds.), *Perry's chemical engineers' handbook* (7th edition), McGraw-Hill, 56-89.

Tamarkin, D., Eini, M., Friedman, D., (2006a). *Foam: The future of effective cosmeceuticals*. *Cosmetics Toiletries* 121(11): 75-84.

Tamarkin, D., Friedman, D., Shemer, A., (2006b). *Emollient foam in topical drug delivery*. *Expert Opinion on Drug Delivery* 3: 799-807.

Tang, F.-Q., Xiao, Z., Tang, J.-A., Jiang, L., (1989). *The effect of sio2 particles upon stabilization of foam*. *Journal of Colloid and Interface Science* 131: 498-502.

Tardos, G.I., Hapgood, K.P., Ipadeola, O.O., Michaels, J.N., (2004). *Stress measurements in high-shear granulators using calibrated "Test" Particles: Application to scale-up*. *Powder Technology* 140: 217-227.

Tardos, G.I., Khan, M.I., Mort, P.R., (1997). *Critical parameters and limiting conditions in binder granulation of fine powders*. *Powder Technology* 94: 245-258.

Thomas, J.F., Dawn, A.P., Judith, A.M., John, F.H., (2000). *Clobetasol propionate foam 0.05%: A novel vehicle with enhanced delivery*. *International Journal of Dermatology* 39: 535-538.

Turner, G.R., (1981). *Foam technology: What's it all about?* *Text. Chem. Color* 13: 28-33.

van den Dries, K., de Vegt, O.M., Girard, V., Vromans, H., (2003). *Granule breakage phenomena in a high shear mixer; influence of process and formulation variables and consequences on granule homogeneity*. *Powder Technology* 133: 228-236.

van den Dries, K., Vromans, H., (2002). *Relationship between inhomogeneity phenomena and granule growth mechanisms in a high-shear mixer*. *International Journal of Pharmaceutics* 247: 167-177.

van den Dries, K., Vromans, H., (2003). *Experimental and modelistic approach to explain granulate inhomogeneity through preferential growth*. *European Journal of Pharmaceutical Sciences* 20: 409-417.

van den Dries, K., Vromans, H., (2004). *Qualitative proof of liquid dispersion and penetration-involved granule formation in a high shear mixer*. *European Journal of Pharmaceutics and Biopharmaceutics* 58: 551-559.

van den Dries, K., Vromans, H., (2009). *Quantitative proof of liquid penetration-involved granule formation in a high shear mixer*. *Powder Technology* 189: 165-171.

Vandewalle, N., Lentz, J.F., Dorbolo, S., Brisbois, F., (2001). *Avalanches of popping bubbles in collapsing foams*. *Physical Review Letters* 86: 179.

Vemavarapu, C., Surapaneni, M., Hussain, M., Badawy, S., (2009). *Role of drug substance material properties in the processibility and performance of a wet granulated product*. International Journal of Pharmaceutics 374: 96-105.

Vera, M.U., Durian, D.J., (2002). *Enhanced drainage and coarsening in aqueous foams*. Physical Review Letters 88: 088304.

Vera, M.U., Saint-Jalmes, A., Durian, D.J., (2001). *Scattering optics of foam*. Appl. Opt. 40: 4210-4214.

Vromans, H., Poels-Janssen, H.G.M., Egermann, H., (1999). *Effects of high-shear granulation on granulate homogeneity*. 4: 297-303.

Waldie, B., (1991). *Growth mechanism and the dependence of granule size on drop size in fluidized-bed granulation*. Chemical Engineering Science 46: 2781-2785.

Waldie, B., Wilkinson, D., Zachra, L., (1987). *Kinetics and mechanisms of growth in batch and continuous fluidized bed granulation*. Chemical Engineering Science 42: 653-665.

Wan, L.S.C., Heng, P.W.S., Muhuri, G., (1992). *Incorporation and distribution of a low dose drug in granules*. International Journal of Pharmaceutics 88: 159-163.

Wauters, P.A.L., Jakobsen, R.B., Litster, J.D., Meesters, G.M.H., Scarlett, B., (2002). *Liquid distribution as a means to describing the granule growth mechanism*. Powder Technology 123: 166-177.

Weaire, D., Findlay, S., Verbisq, G., (1995). *Measurement of foam drainage using ac conductivity*. Journal of Physics: Condensed Matter 7: L217.

Weaire, D., Phelan, R., (1996). *The physics of foam*. Journal of physics. Condensed matter 8: 9519-9524.

Wilde, P.J., (1996). *Foam measurement by the microconductivity technique: An assessment of its sensitivity to interfacial and environmental factors*. Journal of Colloid and Interface Science 178: 733-739.

Wildeboer, W.J., Koppendraaier, E., Litster, J.D., Howes, T., Meesters, G., (2007). *A novel nucleation apparatus for regime separated granulation*. Powder Technology 171: 96-105.

Wildeboer, W.J., Litster, J.D., Cameron, I.T., (2005). *Modelling nucleation in wet granulation*. Chemical Engineering Science 60: 3751-3761.

Wilson, A.J., (1989). *Chapter 6 cryo-microscopical methods for the investigation of foam structure*. In: Wilson, A.J. (Eds.), *Foams: Physics, chemistry and structure*, Springer-Verlag Berlin Heidelberg, 69-88.

Woodford, R., Barry, B.W., (1977). *Bioavailability and activity of topical corticosteroids from a novel drug delivery system, the aerosol quick-break foam*. Journal of Pharmaceutical Sciences 66: 99-103.

Wyles, D.H., (1978). *Energy in relation to textile coloration*. Review of Progress in Coloration and Related Topics 9: 35-47.

Yan, W., Miller, C.A., Hirasaki, G.J., (2006). *Foam sweep in fractures for enhanced oil recovery*. Colloids and Surfaces A: Physicochemical and Engineering Aspects 282-283: 348-359.

Zhang, D., Flory, J.H., Panmai, S., Batra, U., Kaufman, M.J., (2002). *Wettability of pharmaceutical solids: Its measurement and influence on wet granulation*. Colloids and Surfaces A: Physicochemical and Engineering Aspects 206: 547-554.

Zhang, Y., Johnson, K.C., (1997). *Effect of drug particle size on content uniformity of low-dose solid dosage forms*. International Journal of Pharmaceutics 154: 179-183.

Zhao, Y., Brown, M.B., Jones, S.A., (2010). *Pharmaceutical foams: Are they the answer to the dilemma of topical nanoparticles?* Nanomedicine: Nanotechnology, Biology and Medicine 6: 227-236.

ADDENDUM

CHAPTER 1

P1: **Delete** 1st and 2nd paragraph and read:

“Wet granulation has been the subject of research and application interest for almost 50 years. A rewarding investigation of a broad range of wet granulation topics could be carried out in terms of a succession of length scales, which is usually termed as micro for the granules, meso for ensembles of granules and macro for whole process behaviour – establishing the general regularities, quantifying the micro and meso behaviour in terms of rates laws and producing a description of the macro behaviour (Litster and Ennis, 2004; Salman *et al.*, 2007a). These investigations have made a significant step forward over the past decade, and these advances in wet granulation are now at the point where they can be directly applied in many industrial processes for scale-up and formulation and process characterisation.”

“Great progress has been made in the understanding of foam science as well as the development of many new foam technologies. A broad range of research on surface phenomena could be carried out in terms of foam and foam films, qualifying the various interfaces, establishing the general regularities of foam formation, foam stability and foam properties, which are equally relevant to biology, ecology, geology and a number of other technological domains, such as the chemical, cosmetic, food or other industries. Foam is widely applied in a large variety of industries, and the emergence of foam systems appears to gradually replace water systems in many applications. This broad range of practical and industrial applications has precipitated a wealth of publications dedicated to foams, of which only a few are cited here (Bergeron *et al.*, 2005; Perkowitz, 2000; Prud'homme and Khan, 1996; Schramm, 1994b).”

CHAPTER 2

p45 line 13: **Delete** “have” and read “Cantor *et al.* (2009) has...”

p45 line 14: **Delete** “using a” and read “(where the binder was added using a peristaltic pump)...”

p46 line 3: **Delete** “exhibited” and read “...formulations exhibiting different...”

p47 line 9: **Delete** “...from a black art to quantitative engineering.”

p47 line 16: **Delete** “are” and “areas” and read “...foams is...research area”

CHAPTER 3

p49 line 20: **Delete** “The subject of foam flow in porous media is well known, but what about when the porous media is a static powder bed”

p50 line 5: **Delete** “as the mass of the powder divided by the total volume that the powder occupies” and read “...foams is an enormous...” and read “...as the division of the powder mass over the volume occupied.”

p53 line 5: **Delete** “them” and read “...inverting the dish and the sieve together...”

p54 line 3: **Delete** “are” and read “...time is plotted ...”

p54 line 6: **Delete** “out” and read “...drained from the...”

p54 line 19: **Delete** “liquid drainage, one of the characteristic of foam” and read “...foam drainage plays...”

p55 line 3: **Add** “AC, AE and AH represents coarse, medium and fine glass ballotini respectively (see Table 3-1).”

p56 line 3: **Add** “AC, AE and AH represents coarse, medium and fine glass ballotini respectively (see Table 3-1).”

p56 line 8: **Add** “100 mesh and 200 mesh represents coarse and fine lactose (see Table 3-1).”

p57 line 3: **Add** “100 mesh and 200 mesh represents coarse and fine lactose (see Table 3-1).”

p65 line 11: **Delete** “is” and read “...data are...”

CHAPTER 4

p79 line 21: **Delete** “the either” and read “...controlled either by the...”

p80 line 5: **Add** “(see *Chapter 2 – section 2.2.1.3*)”

p80 line 31: **Delete** “which supports that” and read “...as the mixer-granulator ...”

p83 line 7: **Add** “The liquid binder was delivered at a flowrate of 0.1L/min and mixed with air supplied at a flowrate of 0.2L/min, 0.5L/min or 3.0L/min, which generated aqueous foams of foam quality (FQ) – 67% FQ, 83% FQ and 97% FQ, respectively.”

p93 line 9: **Delete** “the” and read “...although there...”

p96 line 16: **Delete** “that” and read “...shows that...”

p100 line 28: **Delete** “which is similar to “drop controlled” nucleation for spray granulation (except the nuclei size distribution with drop controlled is generally narrow).”

P101 line 11: **Delete** 1st and 2nd paragraph

P102: **Add** at the beginning of the 1st paragraph: “Note that although there are some similarities between drop controlled nucleation of sprays and foam drainage controlled nucleation, foam granulation cannot currently be “fitted” into the nucleation regime map for sprays. The nucleation mechanisms for foam versus spray are quite different and sometimes appear to contradict the existing nucleation regime map for sprays (Hapgood *et al.*, 2003). During spray granulation, the drops land on the powder and either penetrate quickly into the powder (drop controlled) or are slowly dispersed mechanically by the powder agitation.”

CHAPTER 5

p106 line 24: **Delete** “can be” and read “...binder was...”

p107 line 9: **Delete** “foamed” and read “...liquid binder...”

p126 line 14: **Delete** “the packing of the powder bed also influences on” and read “...the amount of binder fluid required to form the liquid bridges is influenced by the packing of the powder bed.”

p129 line 30: **Add** reference “(Hapgood *et al.* 2002b)”

p131 line 9: **Delete** “which” and reads “...where spraying at a high liquid delivery rate generally leads to a broad granule size distribution due to droplets coalescence...However, this...”

p142 line 17&18: **Delete** "...opposite of this system, given by high foam quality..." and read "For "mechanical dispersion" controlled wetting and nucleation, given by high foam quality and high impeller speed, the system will produce a fine GSD."

CHAPTER 6

p153 line 23: **Add** "as a function of liquid to solid ratio"

p153 line 28: **Add** "Note that the binder addition rate is constant and hence the liquid binder level is a proxy for time."

p157 line 17: **Delete** "despite that the granule size distributions are slightly different" and read "...granule size distributions."

p158 line 8: **Delete** "practically" and read "...distributions are similar..."

p161 line 16: **Delete** "before phase V" and read "...at phase IV..."

p163 line 13: **Delete** "shown in error! Reference source not found" and read "... (phase IV shown in Figure 6-9)..."

p164 line 12: **Delete** "pass through" and read "...passes through..."

p166 line 6: **Delete** "essentially" and read "Drop penetration-controlled is the ideal..."

p167 line 4: **Delete** "pure the" and read "...in the case of the pure lactose..."

p170 line 7: **Delete** "group" and read "...the two dimensionless parameters..."

p172 line 28: the sentence now read ""Mechanical dispersion" controlled wetting and nucleation is the ideal operating regime provided the system lies below a critical liquid content and any mechanical impact will not promote granule coalescence and the formation oversized agglomerates."

p173 line 5: **Add** "the" and read "...care must be taken that the..."

p173 line 27: **Add** "by" and read "...followed by foam granulation..."

p174 line 15: **Add** "," and read "...given in *Chapter 5*, have great potential ..."

CHAPTER 7

p176 line 15: **Delete** "drug active substance" and read "...size of the drug component..."

p176 line 26: **Delete** "inhomogeneity phenomena" and read "...non-homogeneous material distribution..."

p177 line 5: **Delete** "the material exchange by" and read "...when granule breakage during..."

p177 line 8: **Delete** "as a mean to promote material exchange between the particles through a liquid binding agent" and read "In wet granulation, the uniformity of binder distribution is critical for good distribution of ingredients within the granules."

p179 line 11: **Add** "the" and read "...calculation of the nucleation ratio..."

p179 line 11: **Add** “the” and read “...as the mass...”

p180 line 2: **Add** “The” and read “The overhead chopper...”

p180 line 7: **Delete** “involved conducting a series of granulation processes” and read “...were carried out using...”

p185 line 5: **Delete** “foam and drop” and read “...the foam and drop addition methods...”

p185 line 12: **Delete** “is” and read “...size are...”

p186 line 14: **Delete** “binded, forming” and read “...were strongly nucleated into...”

p188 line 12: **Add** “an encapsulation of a liquid mass with a hydrophobic powder shell...”

p198 line 23: **Delete** “delay” and read “...was delayed.”

p198 line 29: **Delete** “come into contact with the powder bed” and read “...nucleate the particles as they come into contact with the powder bed.”

P200 line 23: **Delete** “allow” and read “...granulation allows more...”

p201 line 7: **Delete** “tend to be” and read “...being enriched...”

CHAPTER 8

p203 line 3: **Delete** “thesis” and read “...is the first..”

p203 line 20&21: **Delete** “we have established” and “we have also characterized” and read “...nuclei formed was established.” and “...powder beds were also characterised.”

p204 line 7: **Delete** “we have identified” and read “...granulation were identified.”

p204 line 27: **Delete** “effect in increasing” and read “...effect of increasing..”

p205 line 9: **Delete** “we have identified” and read “...granules were identified.”

p205 line 23: **Delete** “we have identified” and read “...granules were identified.”

p206 line 25: **Delete** “The use of foam in wet granulation process” and read “Foam granulation...”